Kicking the tires on picolensing as a probe of primordial black hole DM

Dark Interactions 2024

Simon Fraser University Harbour Centre

Vancouver, BC, Canada

October 18, 2024

Ongoing work [241x.yyyzz]

M.A.F. and Sergey Sibiryakov

Michael A. Fedderke

mfedderke@perimeterinstitute.ca

PERIMETER INSTITUTE

PBH dark matter

$M_{\rm PBH} \ll M_\odot$. Formed in the early-universe.

GRAVITATIONALLY COLLAPSED OBJECTS OF VERY LOW MASS

Stephen Hawking

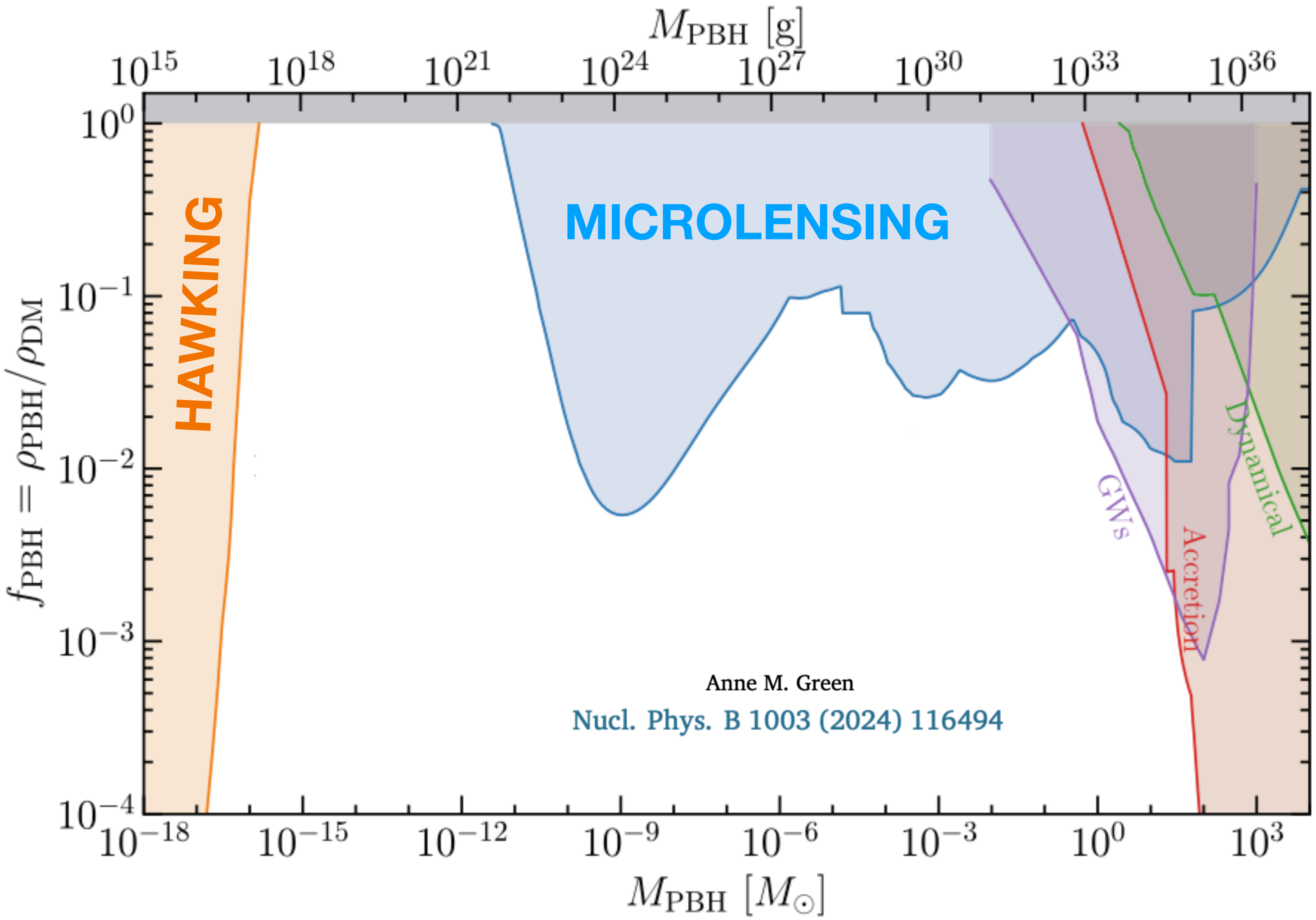

<u>This talk</u>

Agnostic to the production mechanism

Annu. Rev. Nucl. Part. Sci. 2020. 70:355–94

Bernard Carr[1] and Florian Kühnel[2]

A. M. Green and B. J. Kavanagh, *Primordial Black Holes as a dark matter candidate*, *J. Phys. G* **48** (2021) 043001 [arXiv:2007.10722].

A. Escrivà, F. Kuhnel and Y. Tada, *Primordial Black Holes*, arXiv:2211.05767.

PBH dark matter

$M_{\rm PBH} \ll M_\odot$. Formed in the early-universe.

GRAVITATIONALLY COLLAPSED OBJECTS OF VERY LOW MASS

Stephen Hawking

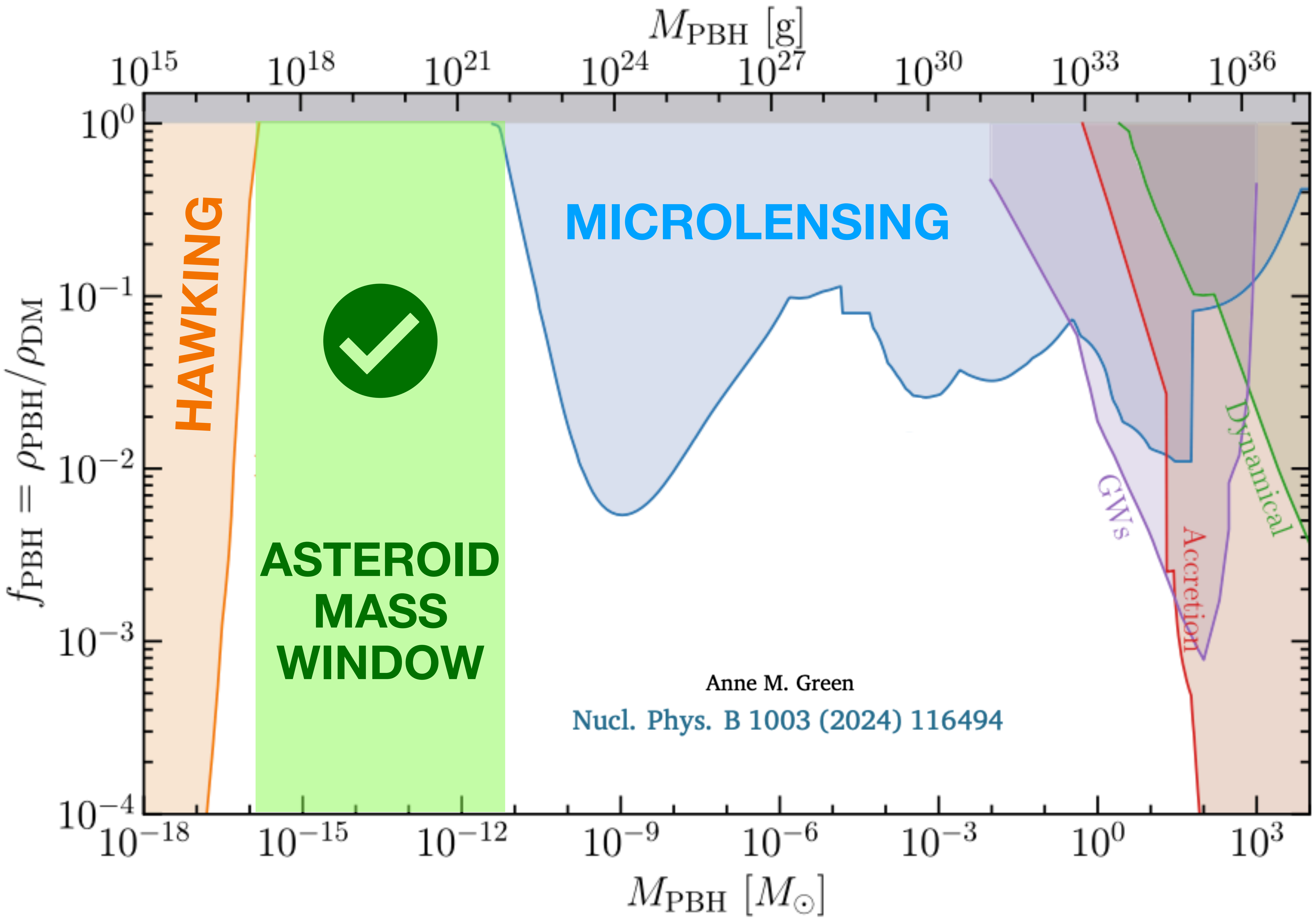

This talk

Agnostic to the production mechanism

Annu. Rev. Nucl. Part. Sci. 2020. 70:355–94

Bernard Carr[1] and Florian Kühnel[2]

A. M. Green and B. J. Kavanagh, *Primordial Black Holes as a dark matter candidate*, *J. Phys. G* **48** (2021) 043001 [arXiv:2007.10722].

A. Escrivà, F. Kuhnel and Y. Tada, *Primordial Black Holes*, arXiv:2211.05767.

Michael A. Fedderke [Perimeter]

Picolensing

NOT TO SCALE (angles similar to a basketball at the outer edge of the Oort cloud)

Picolensing

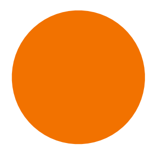

NOT TO SCALE (angles similar to a basketball at the outer edge of the Oort cloud)

Picolensing

NOT TO SCALE (angles similar to a basketball at the outer edge of the Oort cloud)

Picolensing

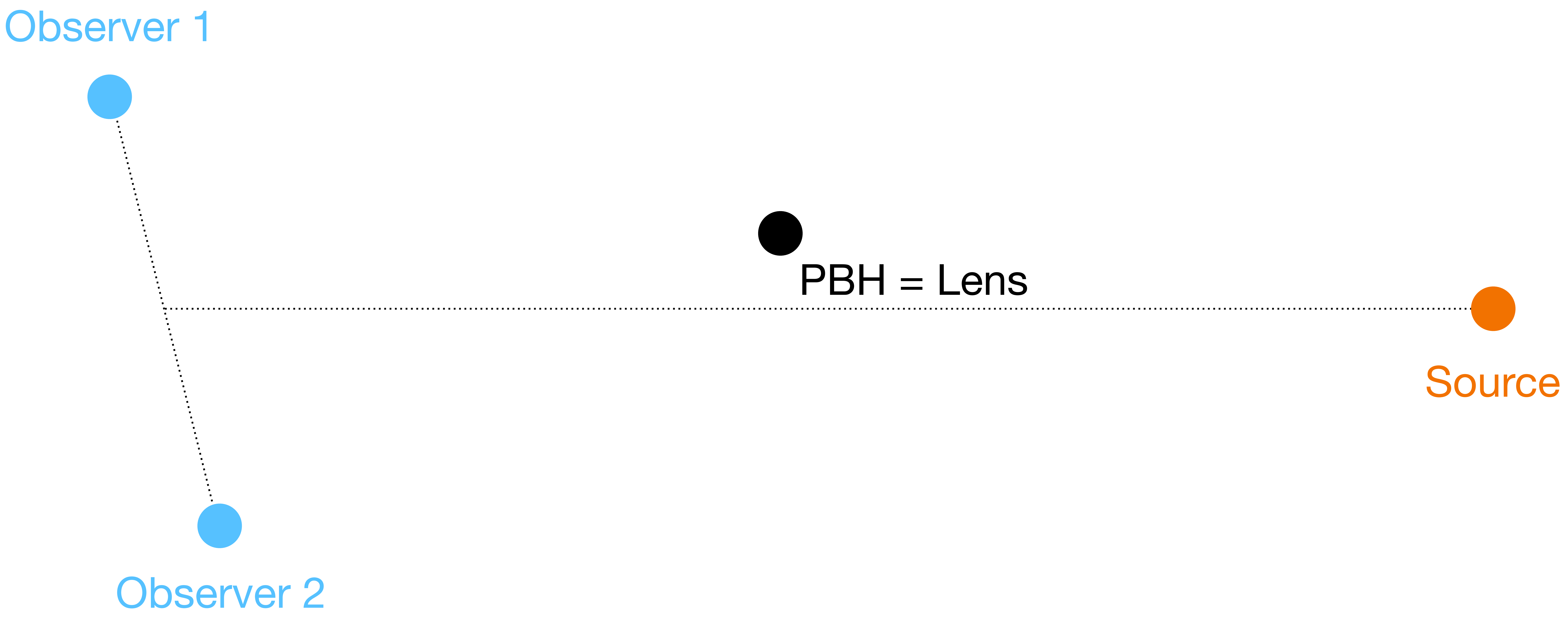

NOT TO SCALE (angles similar to a basketball at the outer edge of the Oort cloud)

Picolensing

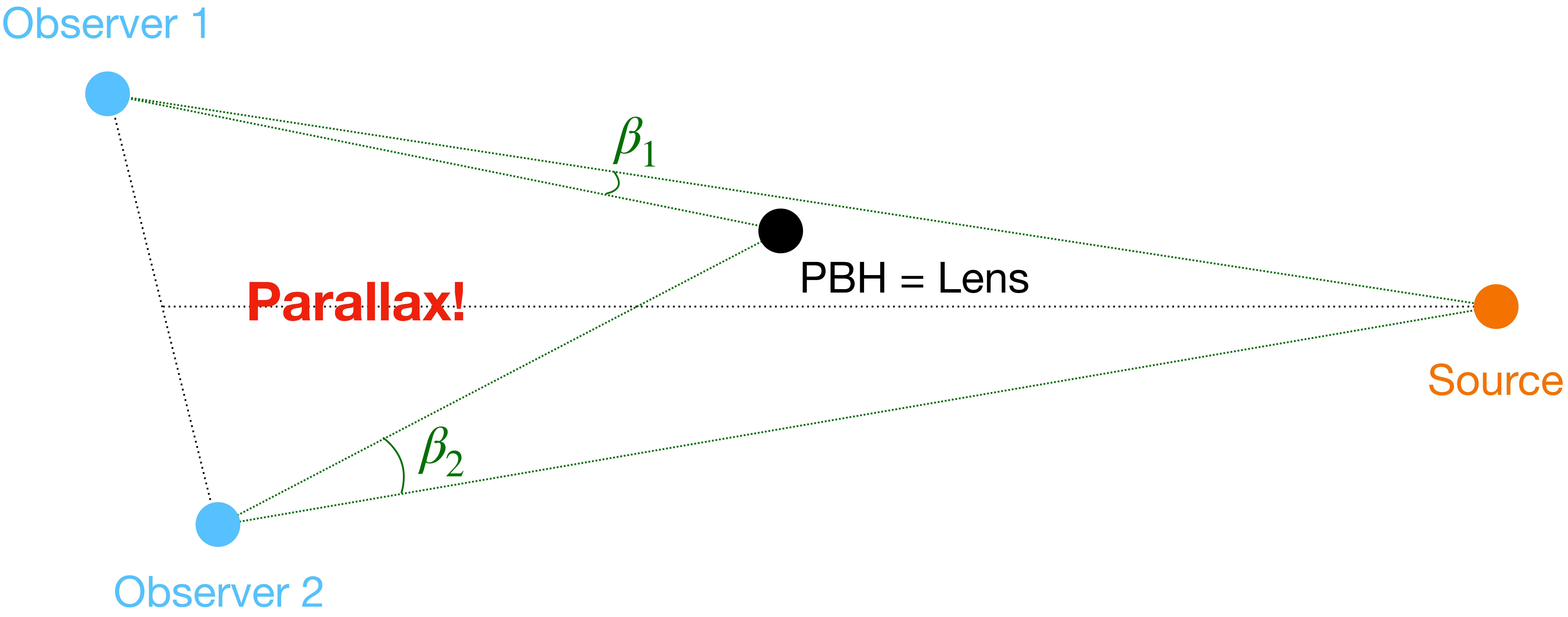

NOT TO SCALE (angles similar to a basketball at the outer edge of the Oort cloud)

Picolensing

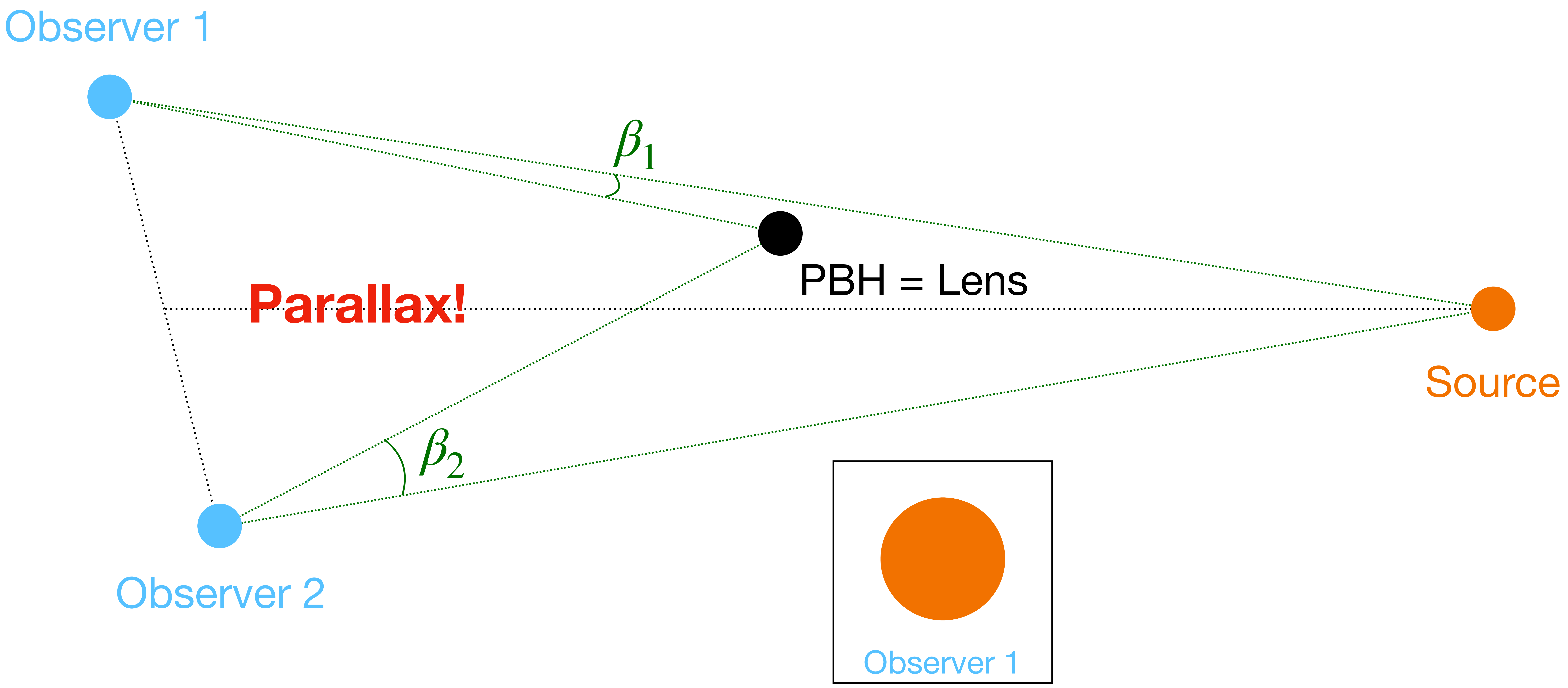

NOT TO SCALE (angles similar to a basketball at the outer edge of the Oort cloud)

Picolensing

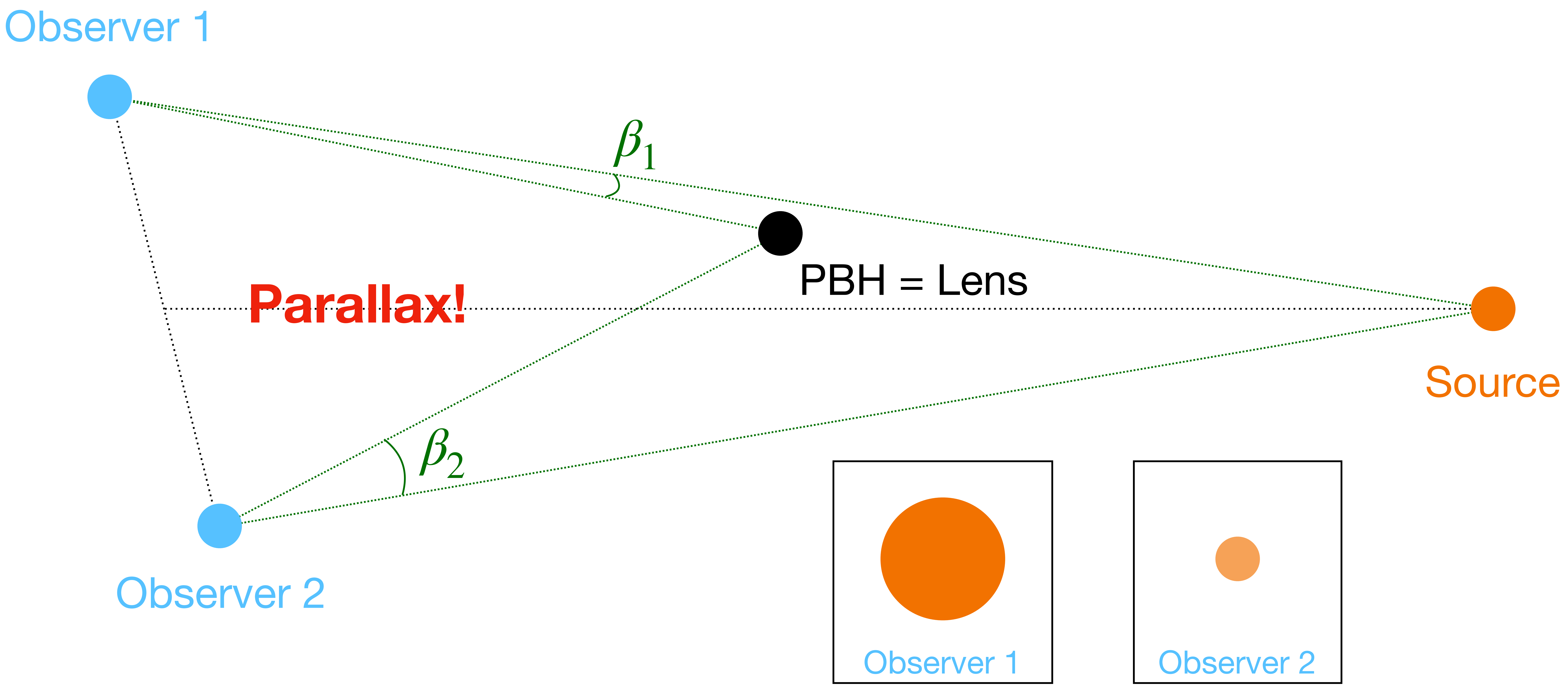

NOT TO SCALE (angles similar to a basketball at the outer edge of the Oort cloud)

Picolensing

Signal: differential observed brightness of a single source that is observed simultaneously by spatially separated detectors

Nemiroff and Gould [astro-ph/9505019]
Kolb and Tkachev [astro-ph/9510043]
Marani et al. [astro-ph/9810391]
Nemiroff [astro-ph/9806012]

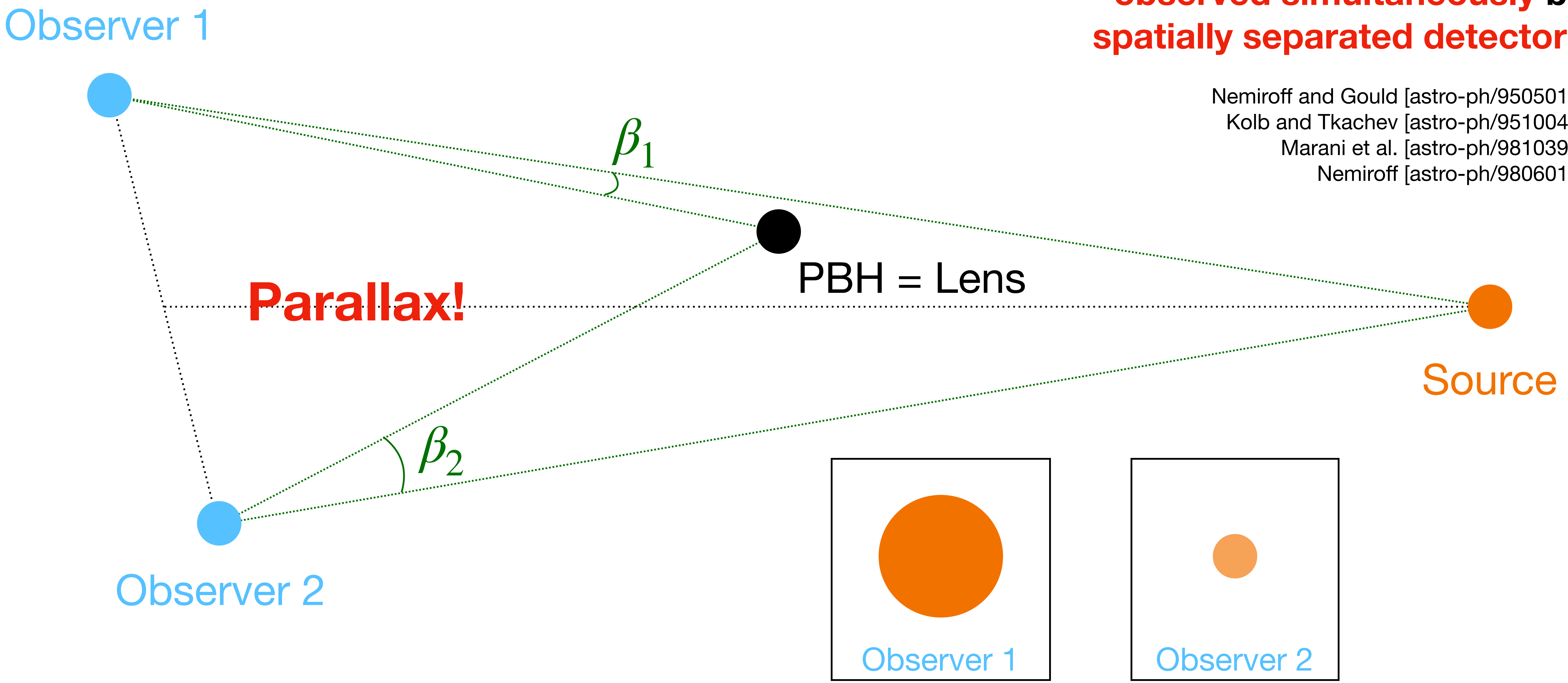

NOT TO SCALE (angles similar to a basketball at the outer edge of the Oort cloud)

Picolensing

Signal: **differential observed brightness** **of a single source** **that is observed simultaneously** **by spatially separated detectors**

Nemiroff and Gould [astro-ph/9505019]
Kolb and Tkachev [astro-ph/9510043]
Marani et al. [astro-ph/9810391]
Nemiroff [astro-ph/9806012]

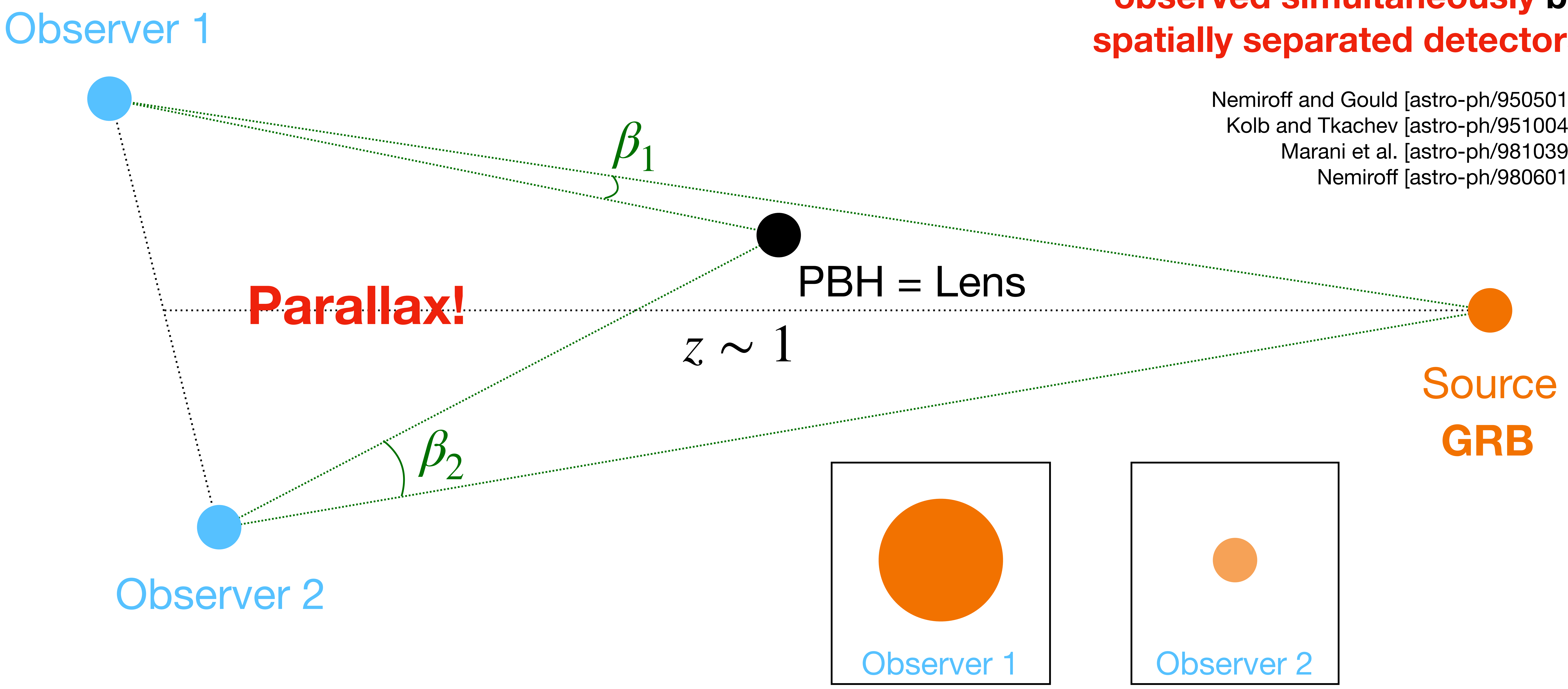

NOT TO SCALE (angles similar to a basketball at the outer edge of the Oort cloud)

Picolensing

Signal: differential observed brightness of a single source that is observed simultaneously by spatially separated detectors

Nemiroff and Gould [astro-ph/9505019]
Kolb and Tkachev [astro-ph/9510043]
Marani et al. [astro-ph/9810391]
Nemiroff [astro-ph/9806012]

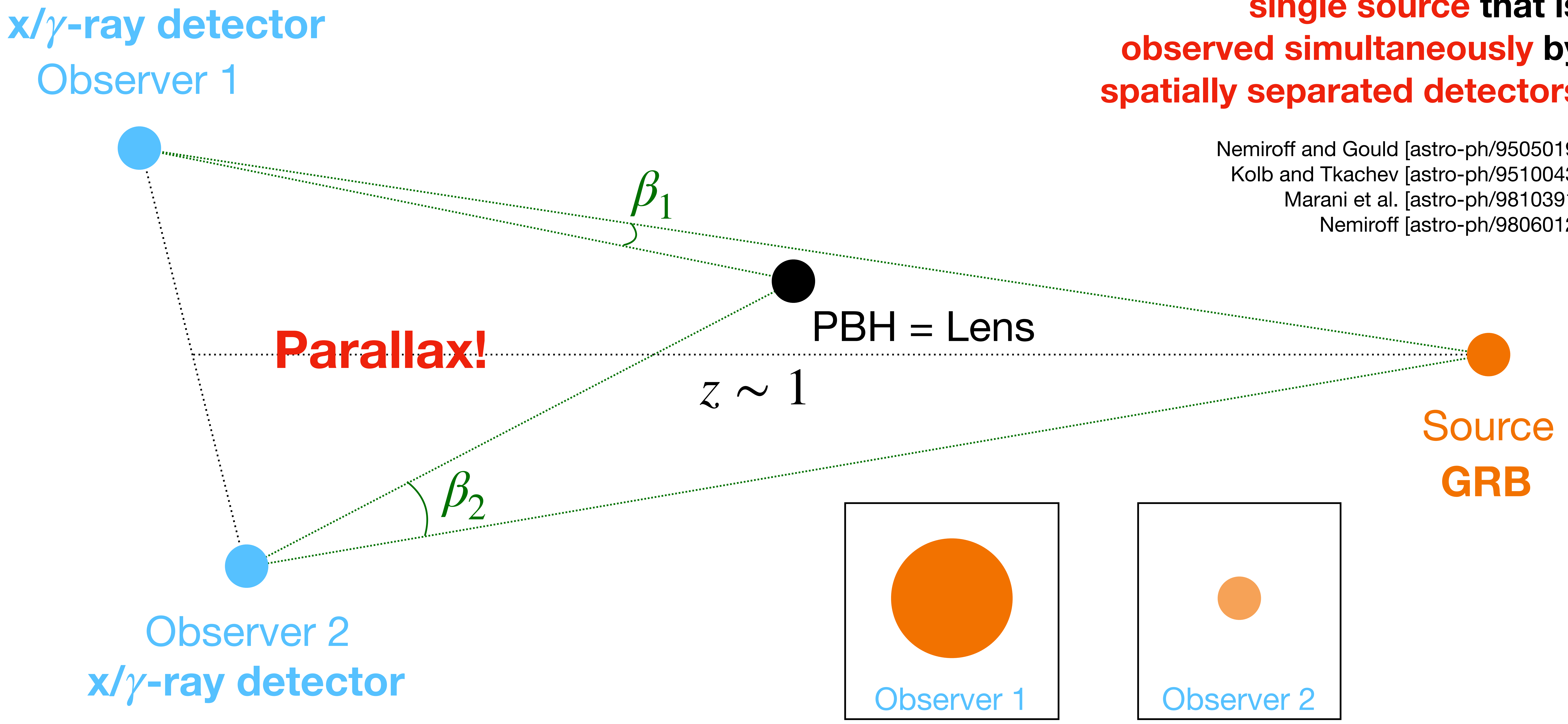

NOT TO SCALE (angles similar to a basketball at the outer edge of the Oort cloud)

Picolensing

Signal: differential observed brightness of a single source that is observed simultaneously by spatially separated detectors

Nemiroff and Gould [astro-ph/9505019]
Kolb and Tkachev [astro-ph/9510043]
Marani et al. [astro-ph/9810391]
Nemiroff [astro-ph/9806012]

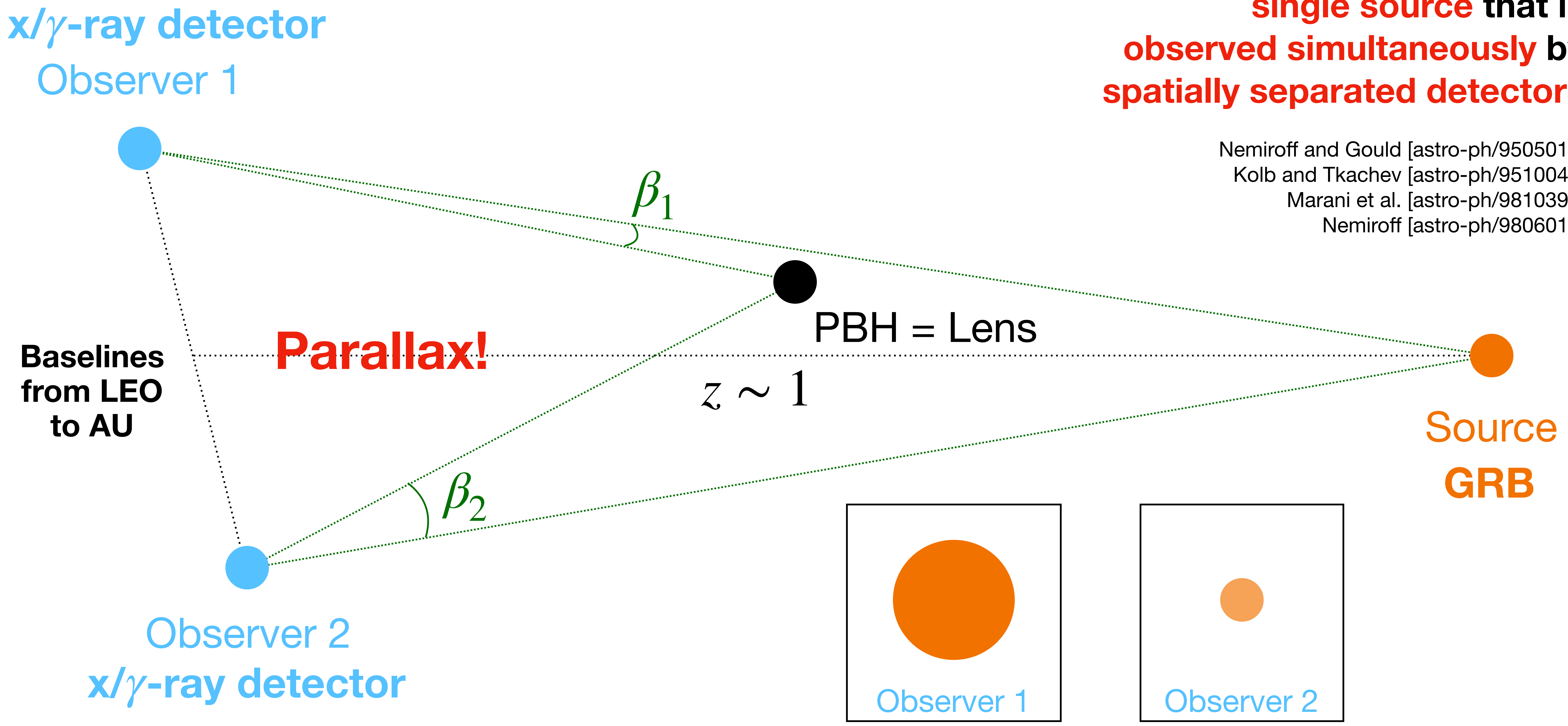

NOT TO SCALE (angles similar to a basketball at the outer edge of the Oort cloud)

Current state of the literature

(b)

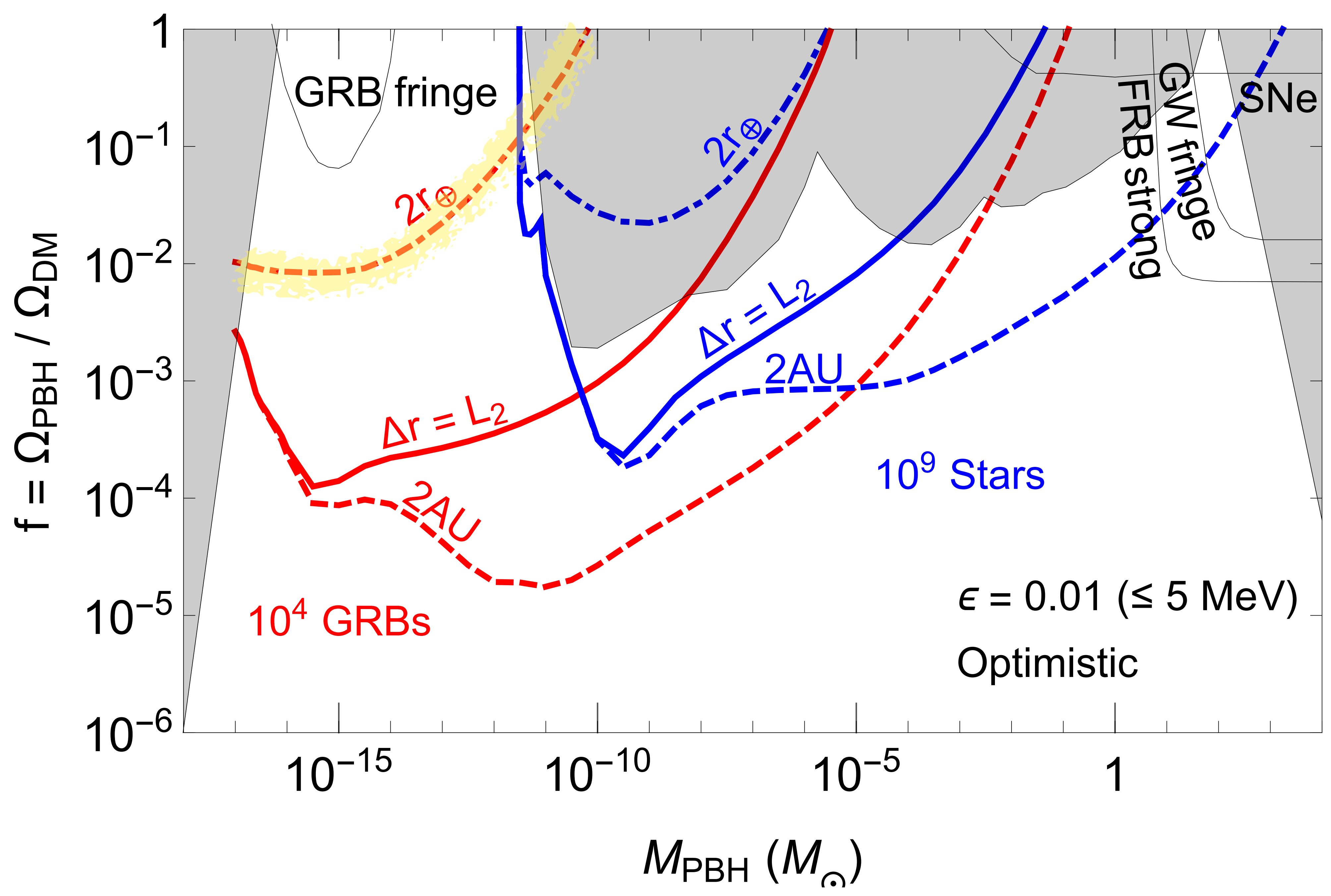

Jung and Kim [1908.00078]

Michael A. Fedderke [Perimeter]

Current state of the literature

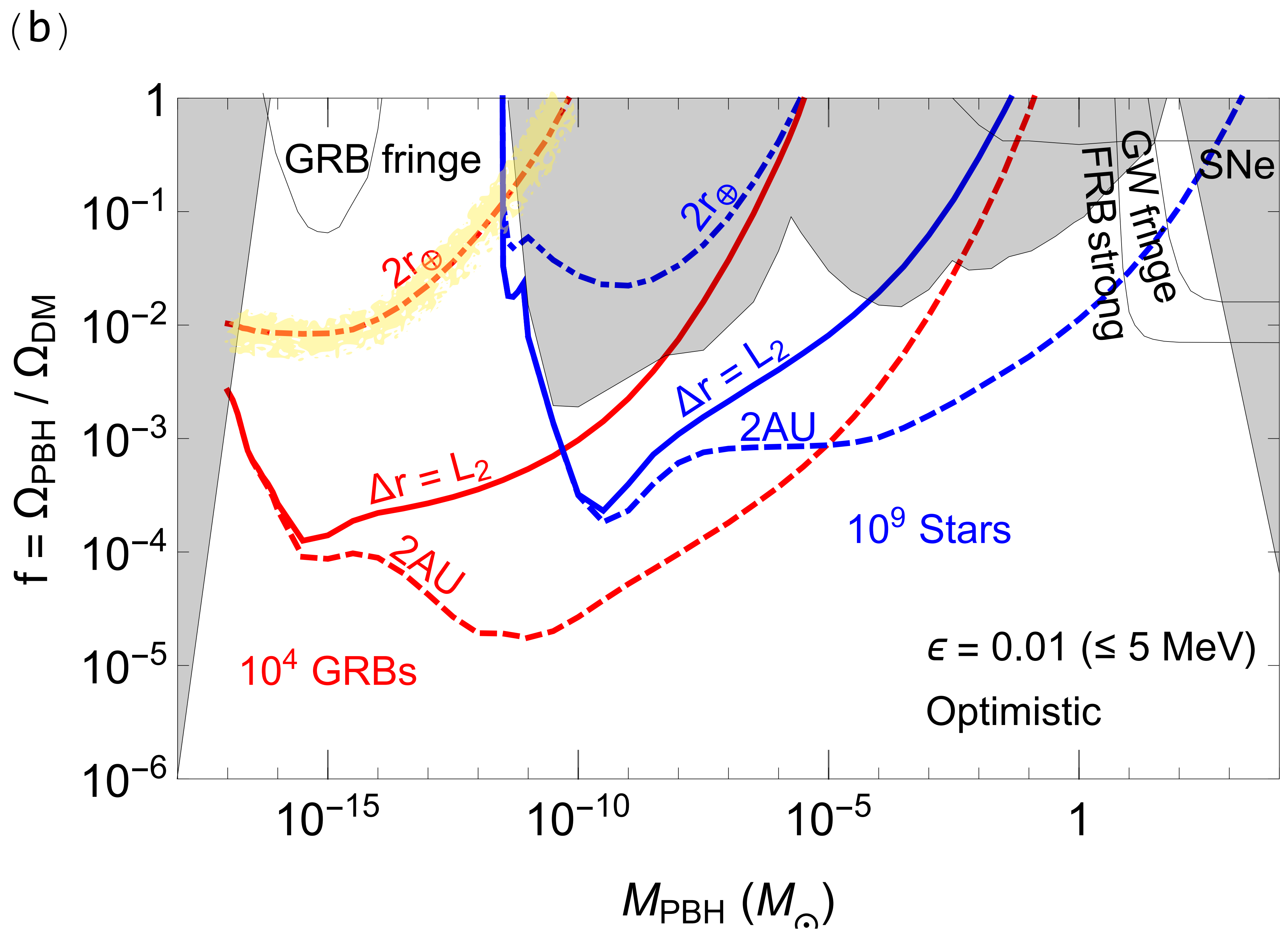

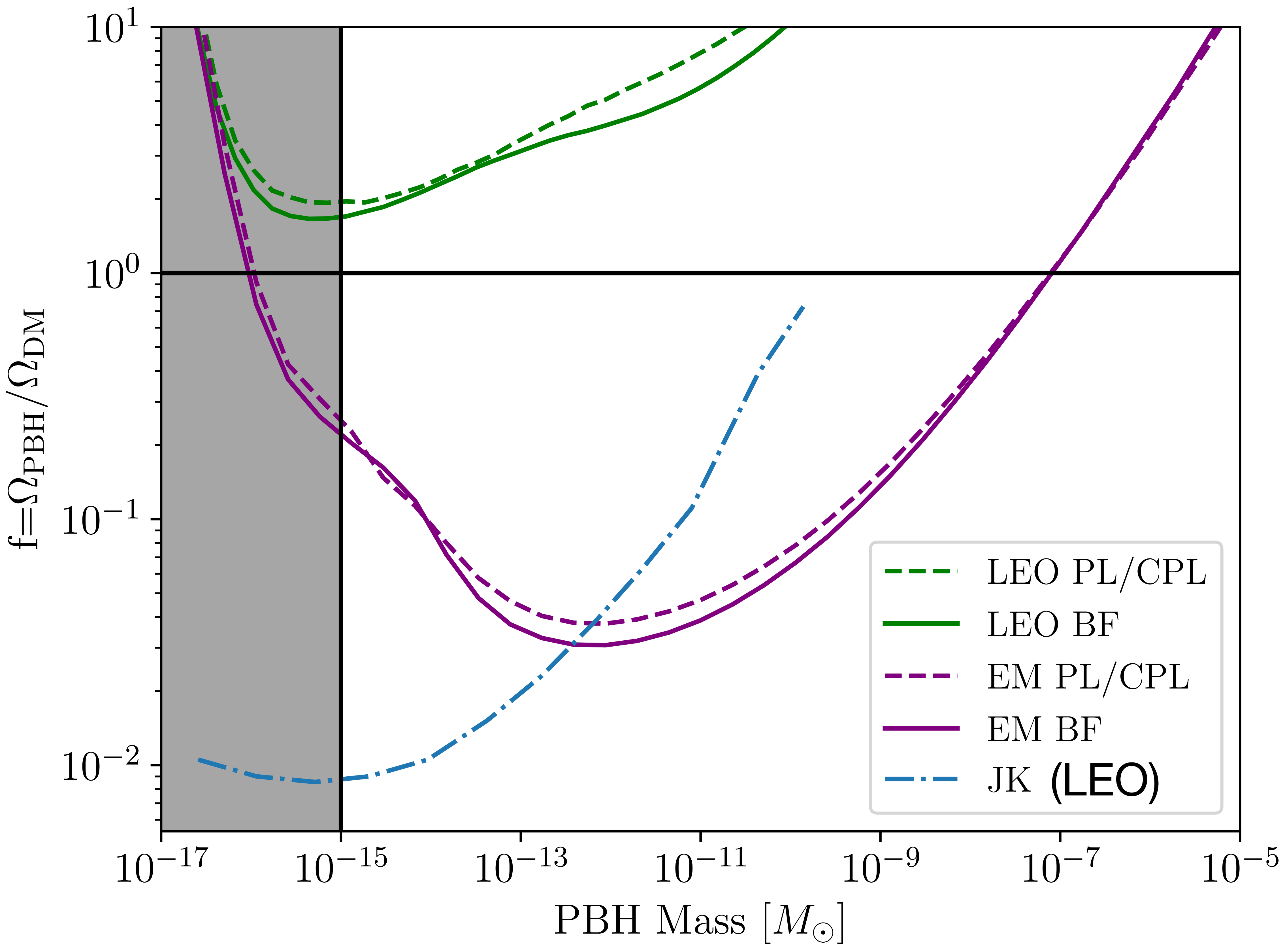

Jung and Kim [1908.00078]

Gawade, More, Bhalerao [2308.01775]

Current state of the literature

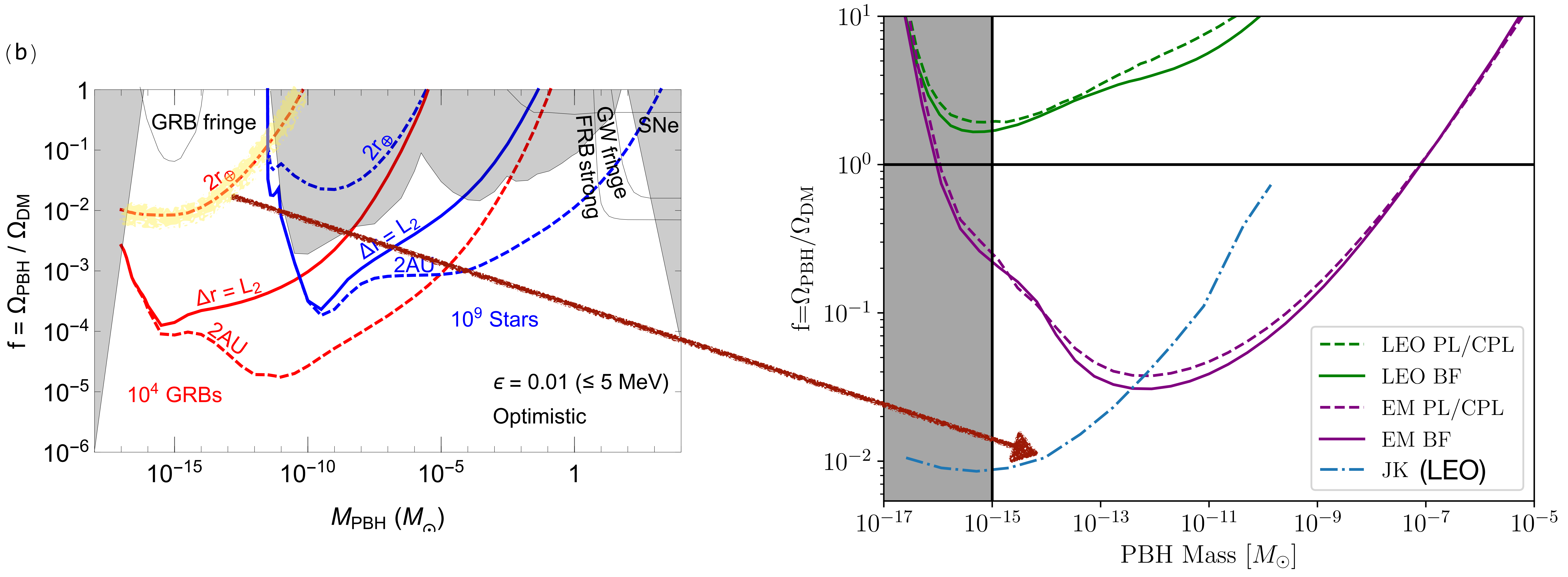

Jung and Kim [1908.00078]

Gawade, More, Bhalerao [2308.01775]

Michael A. Fedderke [Perimeter]

Current state of the literature

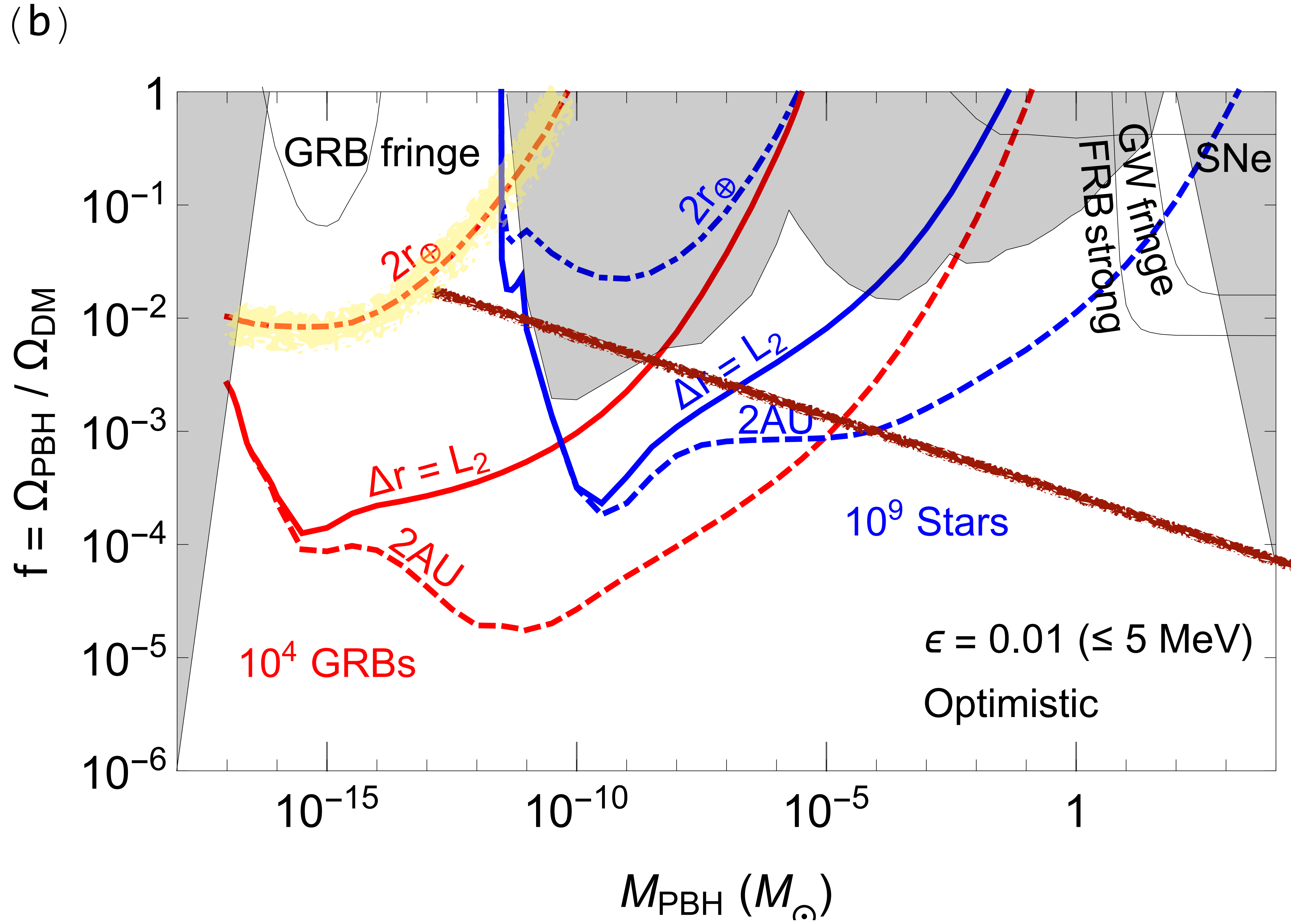

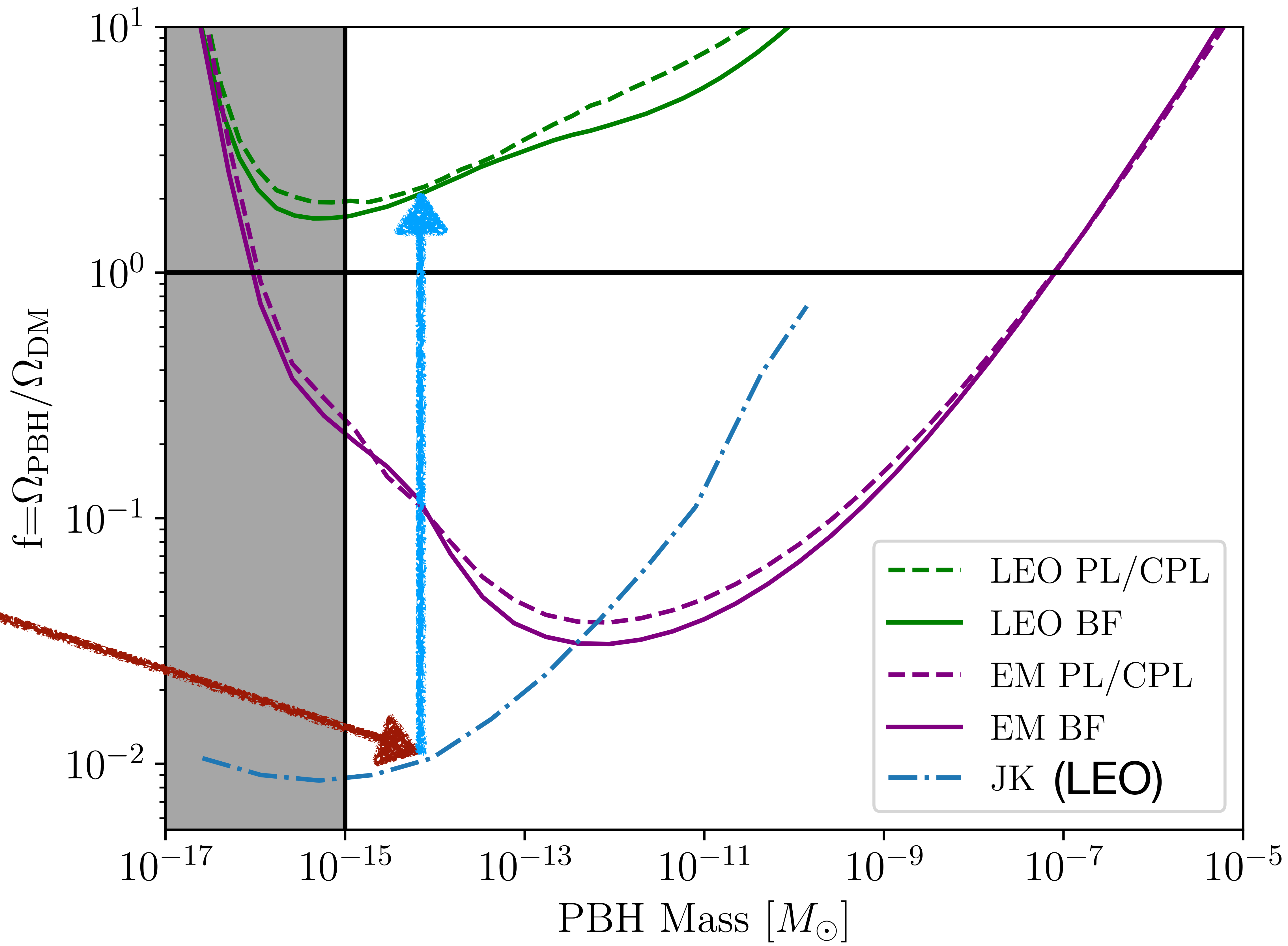

Jung and Kim [1908.00078]

Gawade, More, Bhalerao [2308.01775]

* proper statistical treatment
* more conservative detector assumptions

Current state of the literature

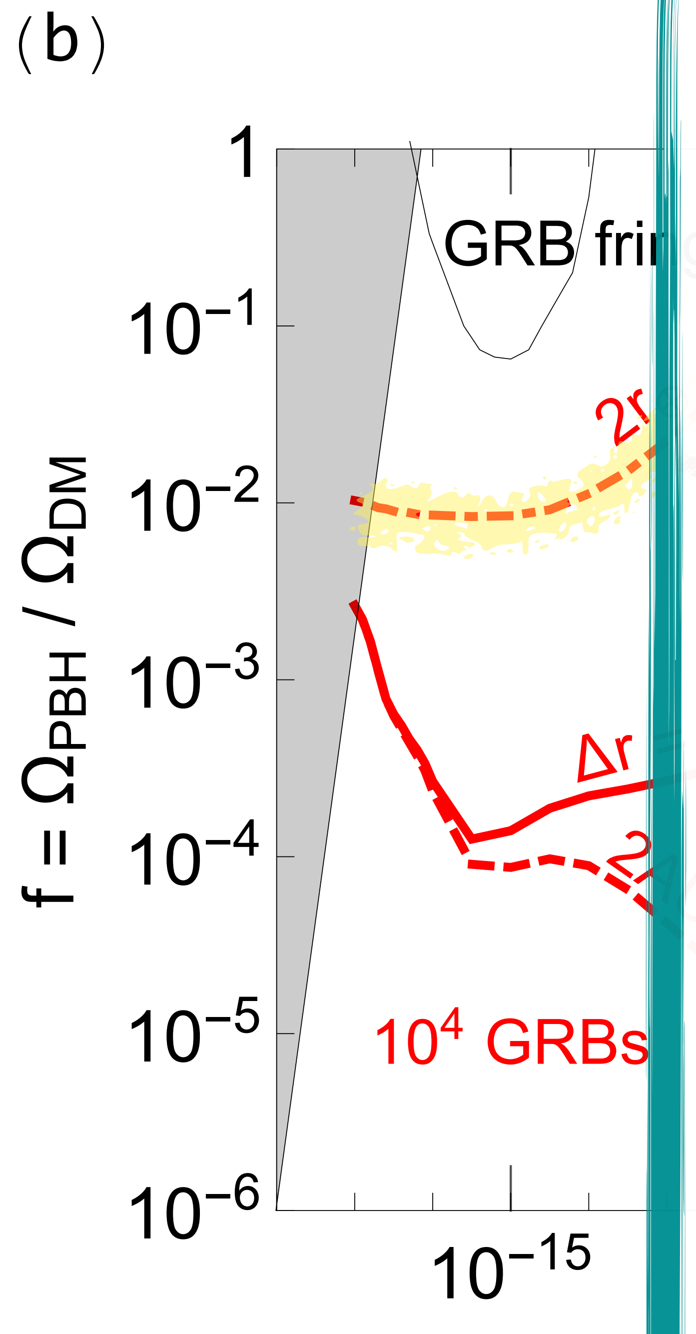

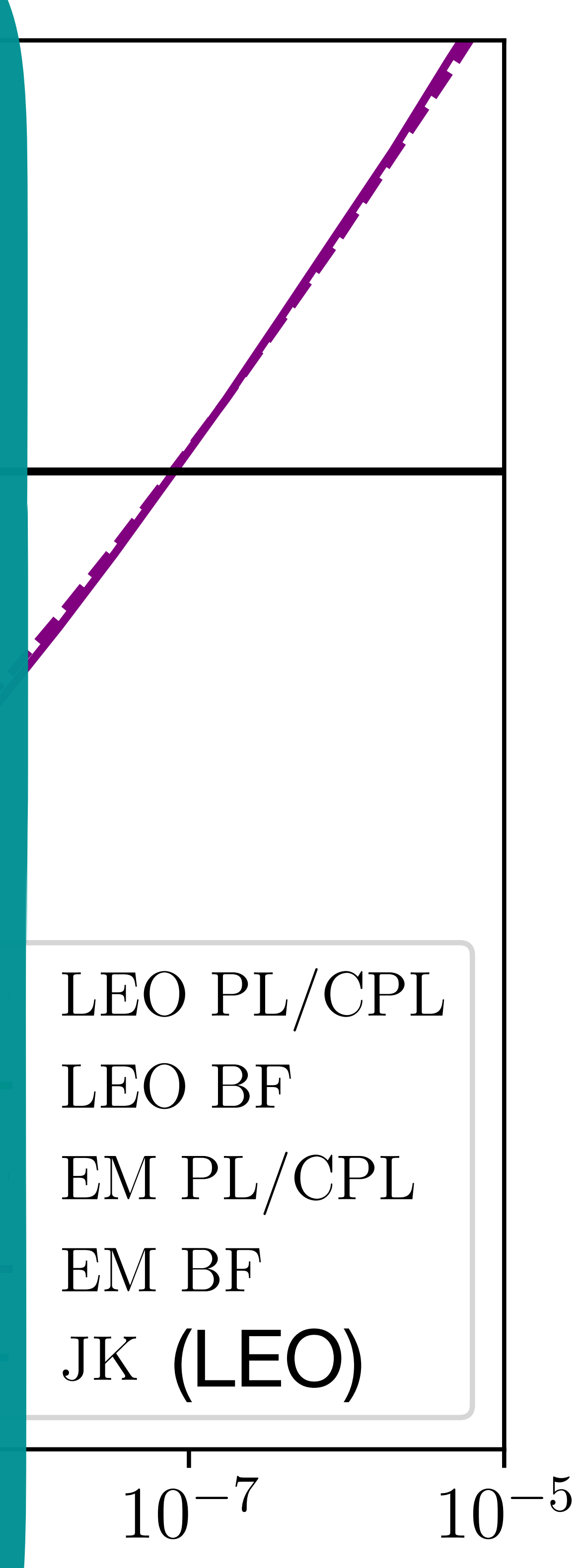

<u>HOW ROBUST IS THIS SIGNAL?</u>

SOURCE SIZE DISTRIBUTION UNCERTAINTIES

SOURCE PROFILE ON THE SKY

<u>ALSO:</u>

LARGER DETECTOR SEPARATION DONE CAREFULLY?

(And other things I won't have time to discuss here)

Jung and Kim [1908.00078]

Gawade, More, Bhalerao [2308.01775]

* proper statistical treatment
* more conservative detector assumptions

Current state of the literature

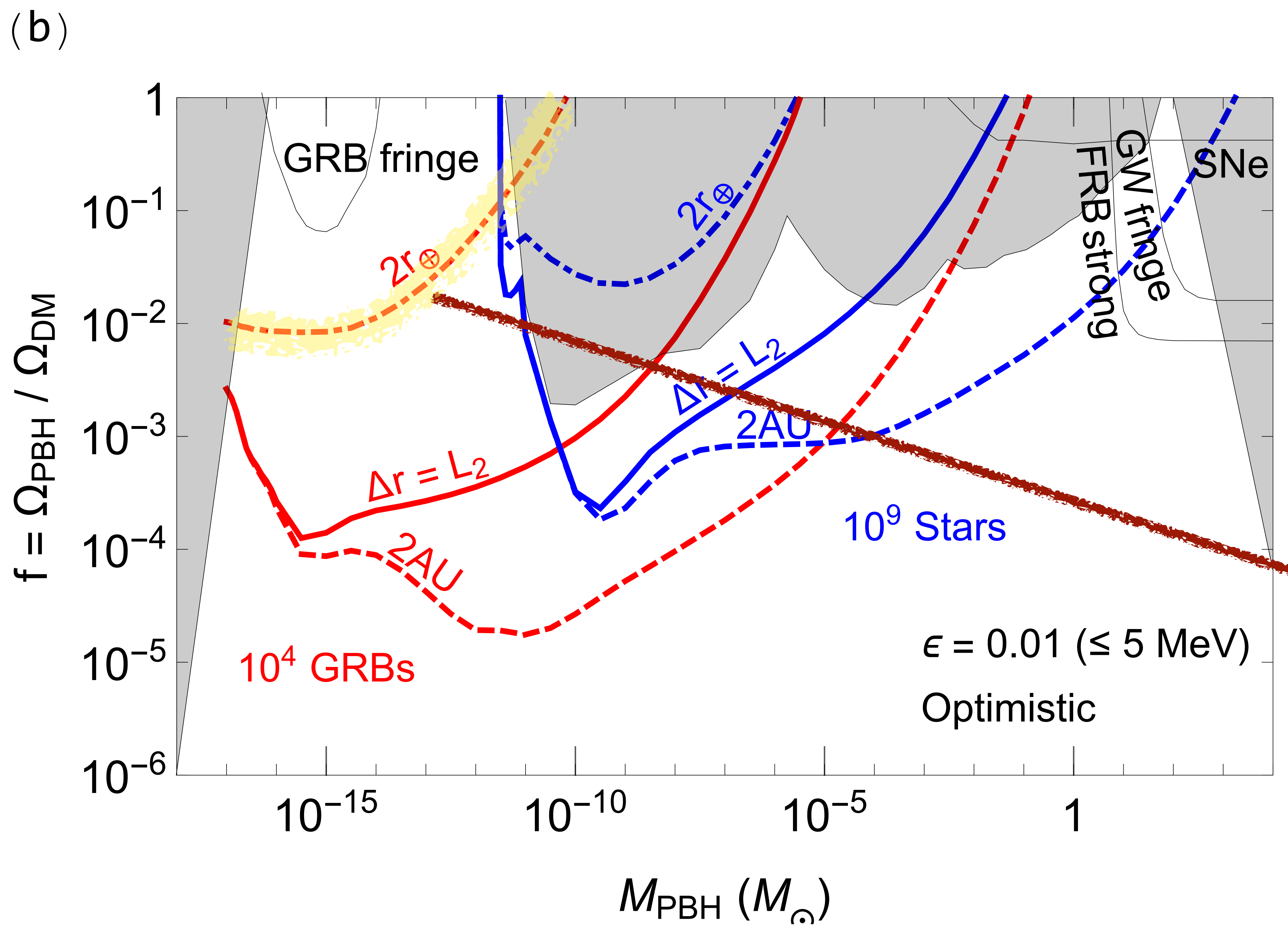

Jung and Kim [1908.00078]

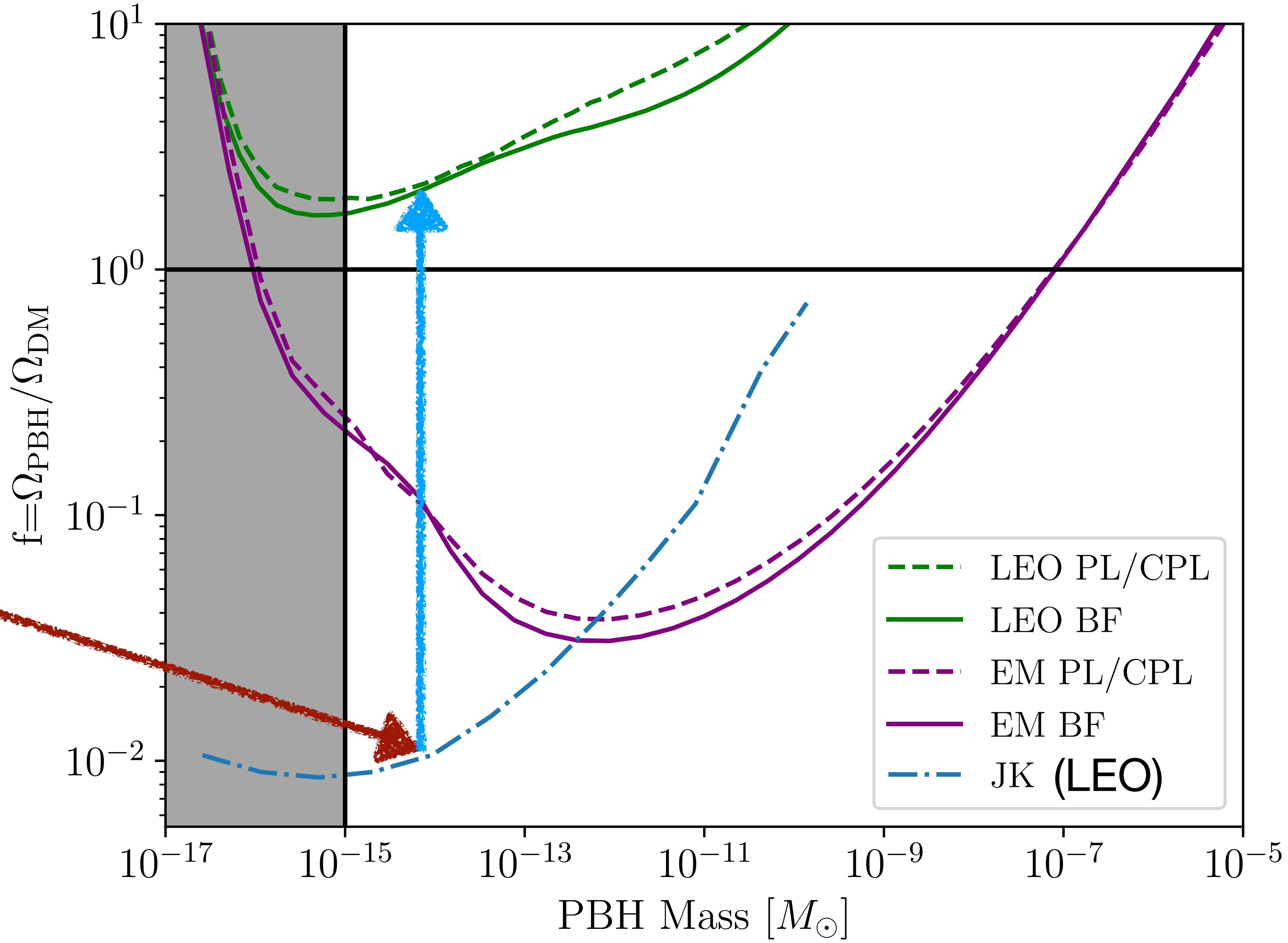

Gawade, More, Bhalerao [2308.01775]

- proper statistical treatment
- more conservative detector assumptions

Current state of the literature

We follow the methodology of this paper

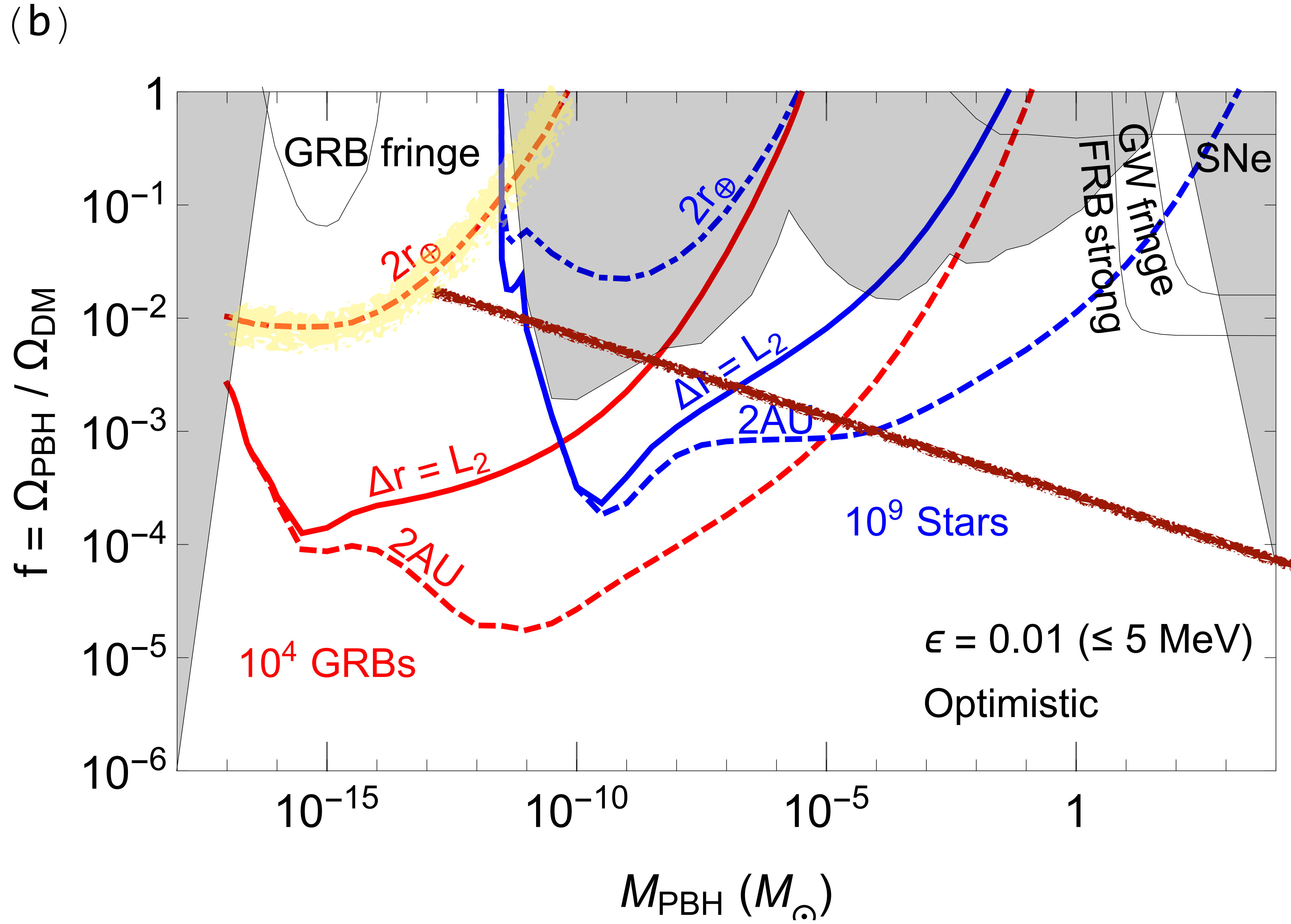

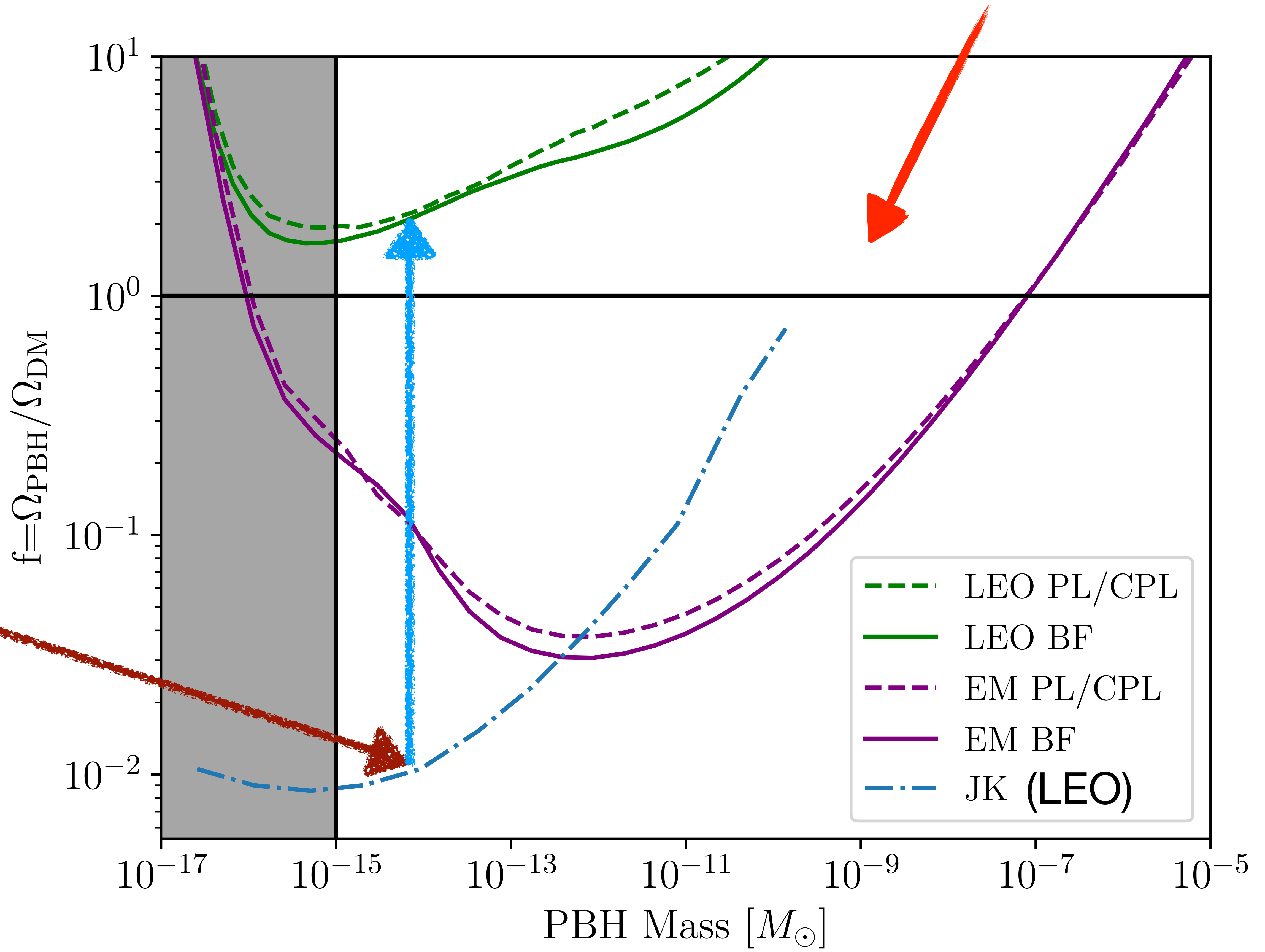

Jung and Kim [1908.00078]

Gawade, More, Bhalerao [2308.01775]

- proper statistical treatment
- more conservative detector assumptions

Gravitational Lensing 101

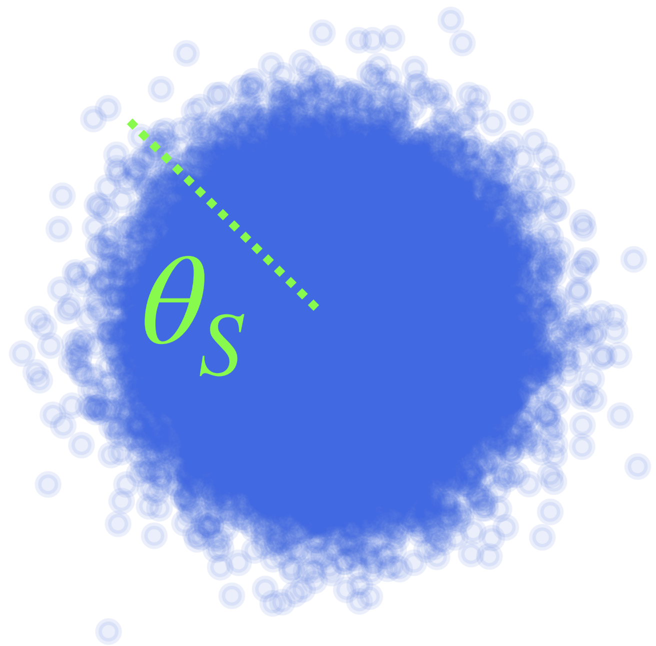

Gravitational Lensing 101

Typical angular scale associated with strong lensing: Einstein angle

$$\theta_E \equiv \sqrt{\frac{4G_N M(1+z_L)\chi_{LS}}{\chi_S \chi_L}}$$

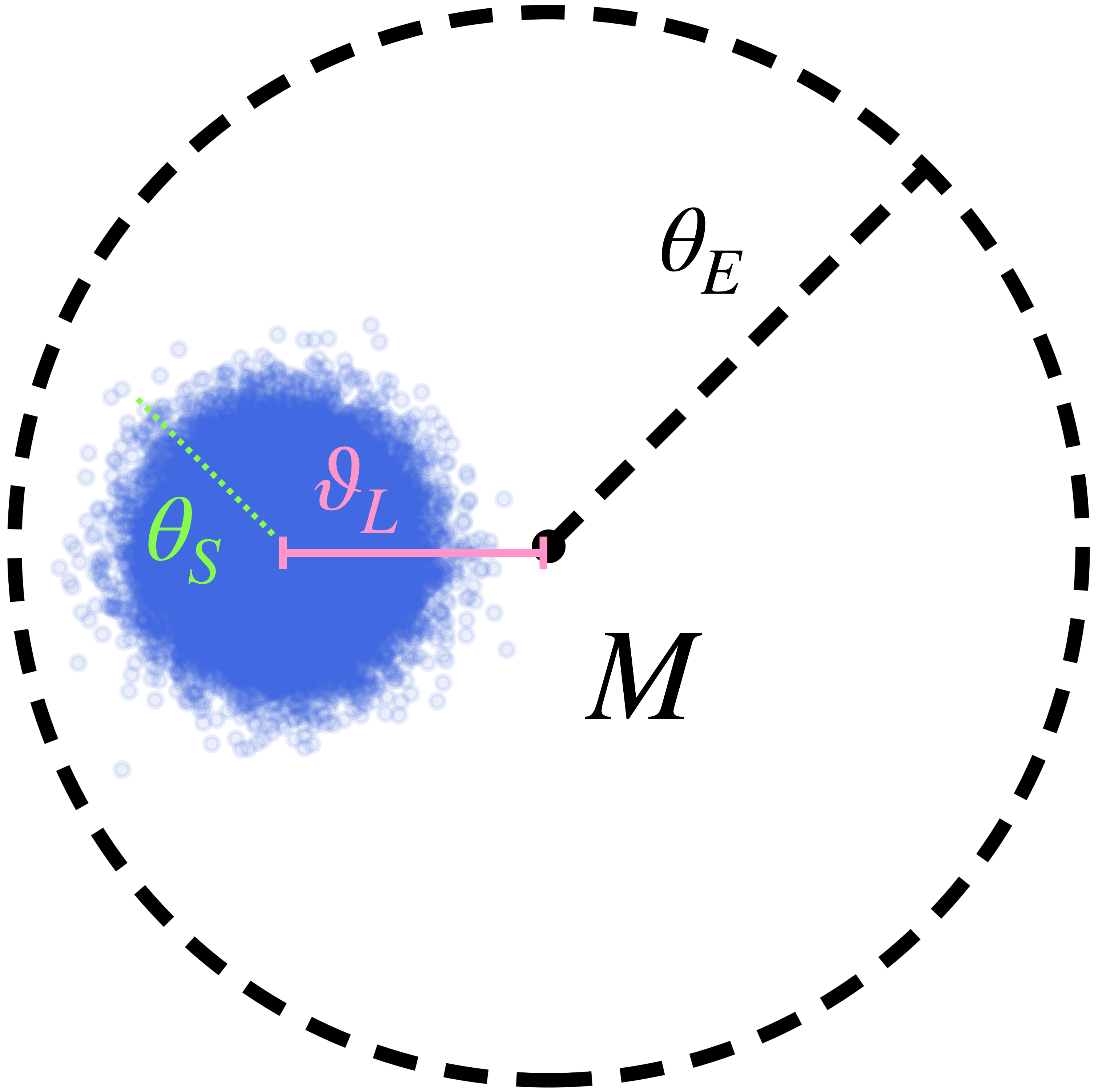

$\hbar = c = 1$

Gravitational Lensing 101

Typical angular scale associated with strong lensing: Einstein angle

$$\theta_E \equiv \sqrt{\frac{4G_N M(1+z_L)\chi_{LS}}{\chi_S \chi_L}}$$

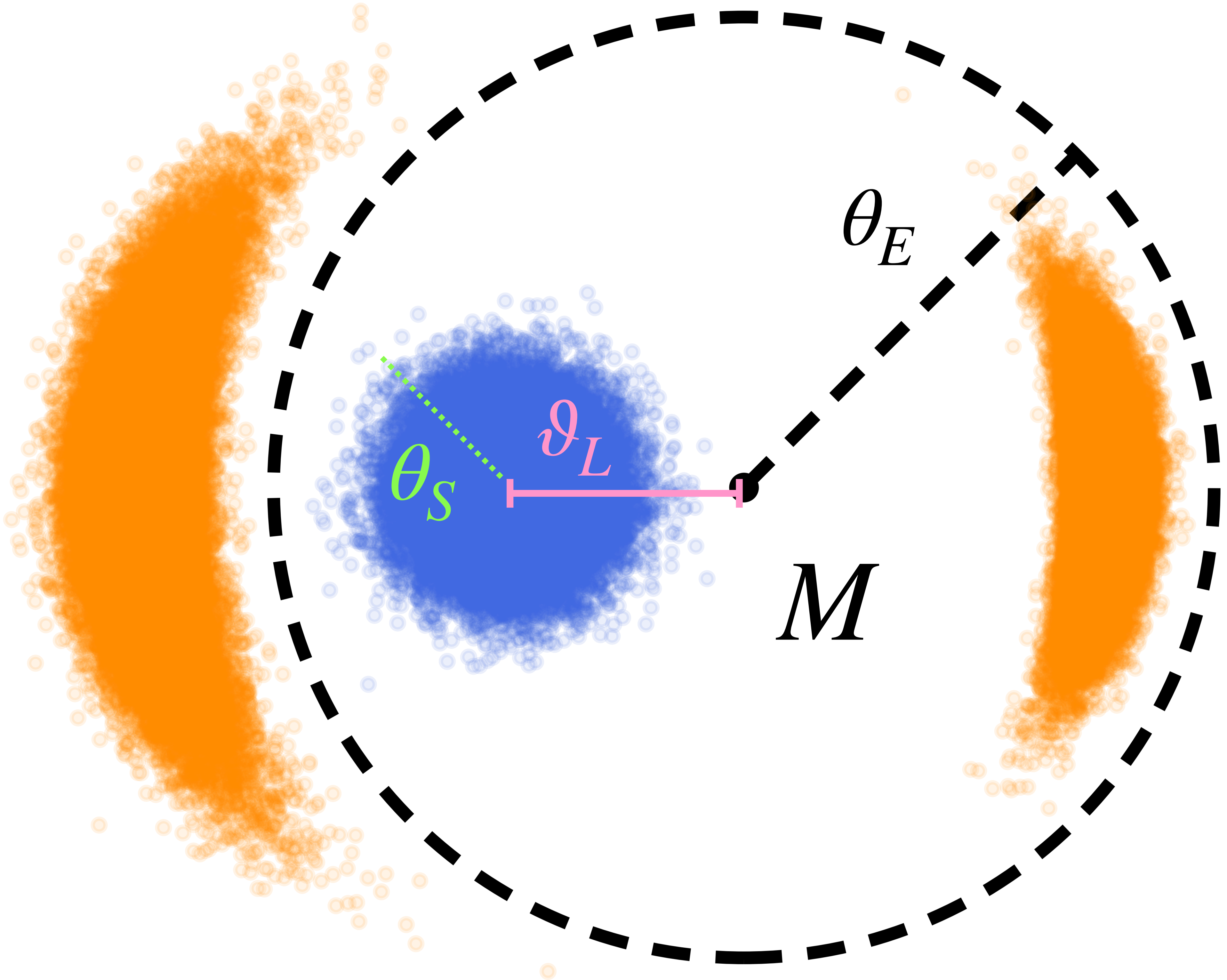

$\hbar = c = 1$

Gravitational Lensing 101

Typical angular scale associated with strong lensing: Einstein angle

$$\theta_E \equiv \sqrt{\frac{4G_N M(1+z_L)\chi_{LS}}{\chi_S \chi_L}}$$

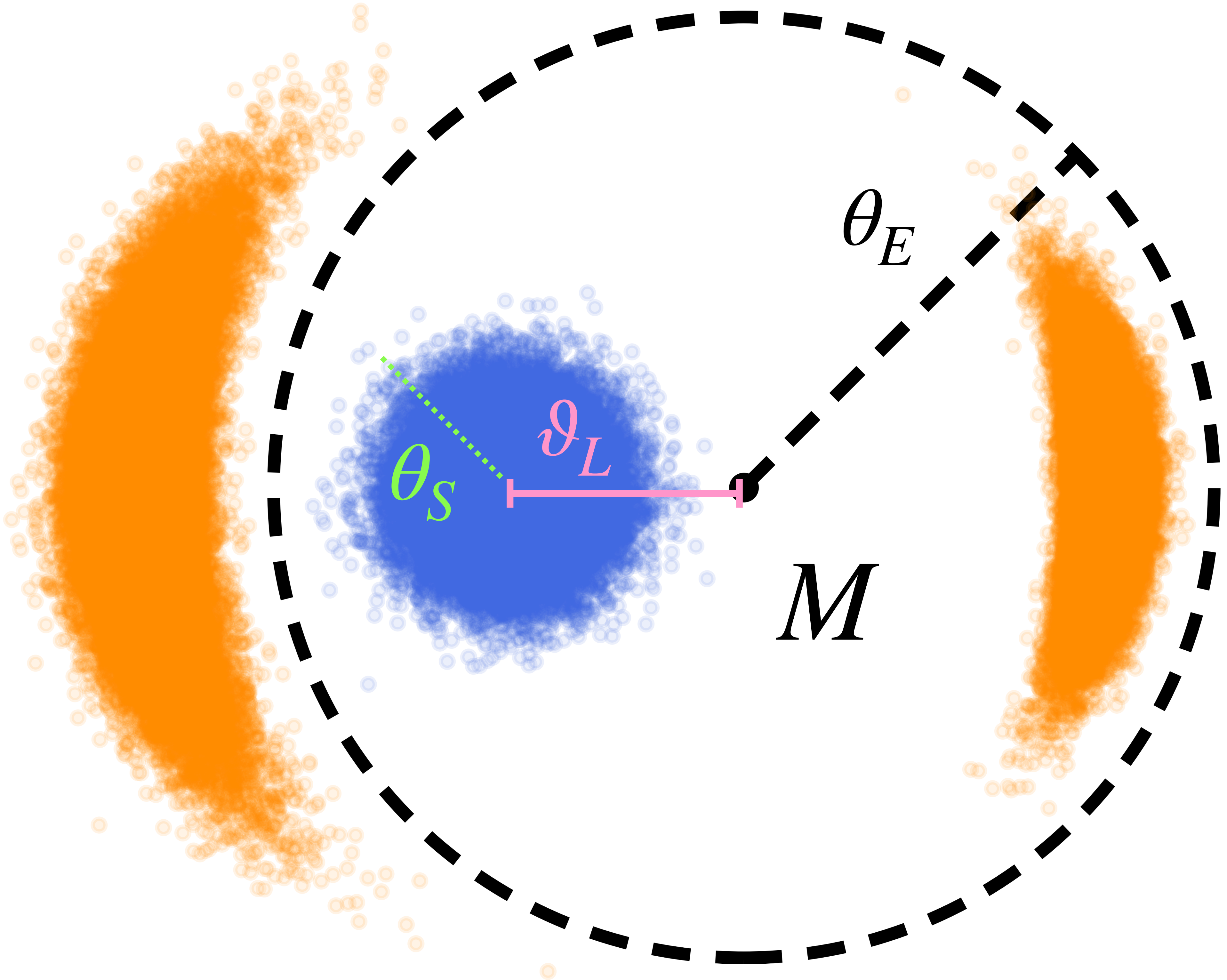

Image is magnified: $\mu \sim \dfrac{\theta_E}{\vartheta_L} \quad (\vartheta_L, \theta_S \ll \theta_E)$

$\hbar = c = 1$

Gravitational Lensing 101

Typical angular scale associated with strong lensing: Einstein angle

$$\theta_E \equiv \sqrt{\frac{4G_N M(1+z_L)\chi_{LS}}{\chi_S \chi_L}}$$

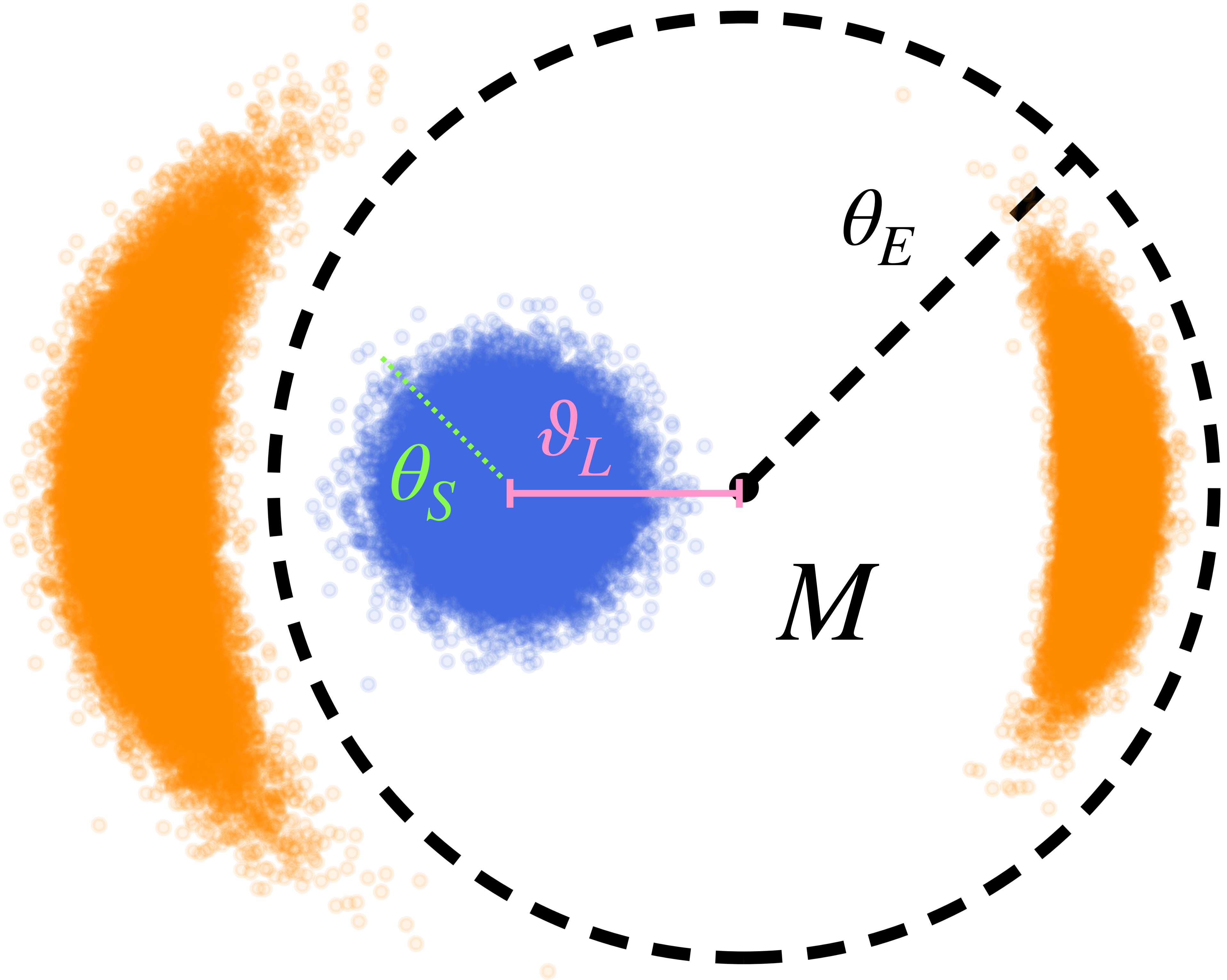

Image is magnified: $\mu \sim \frac{\theta_E}{\vartheta_L} \quad (\vartheta_L, \theta_S \ll \theta_E)$

BUT: **Finite sources** $(\theta_S \gtrsim \theta_E)$ have suppressed source-averaged magnification: $\bar{\mu} - 1 \sim \mathcal{O}(\theta_E^2/\theta_S^2)$

$\hbar = c = 1$

Gravitational Lensing 101

Typical angular scale associated with strong lensing: Einstein angle

$$\theta_E \equiv \sqrt{\frac{4G_N M(1+z_L)\chi_{LS}}{\chi_S \chi_L}}$$

$$\theta_E \sim \text{picoarcsec} \times \sqrt{\frac{M}{10^{-12}M_\odot}}$$

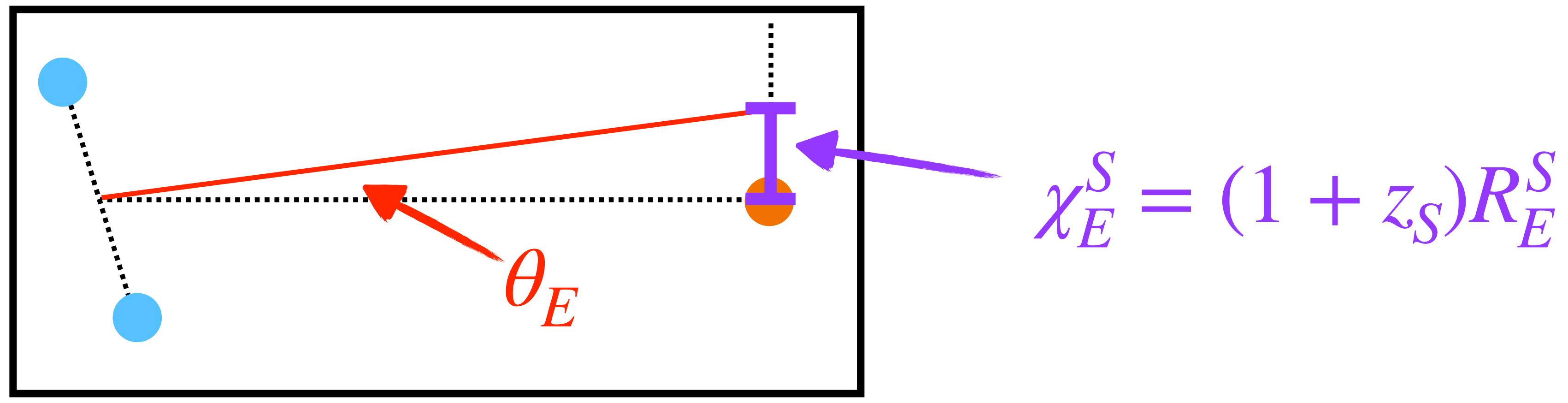

$$R_E^S = \mathscr{D}_S\theta_E \sim R_\odot \times \sqrt{\frac{M}{10^{-12}M_\odot}}$$

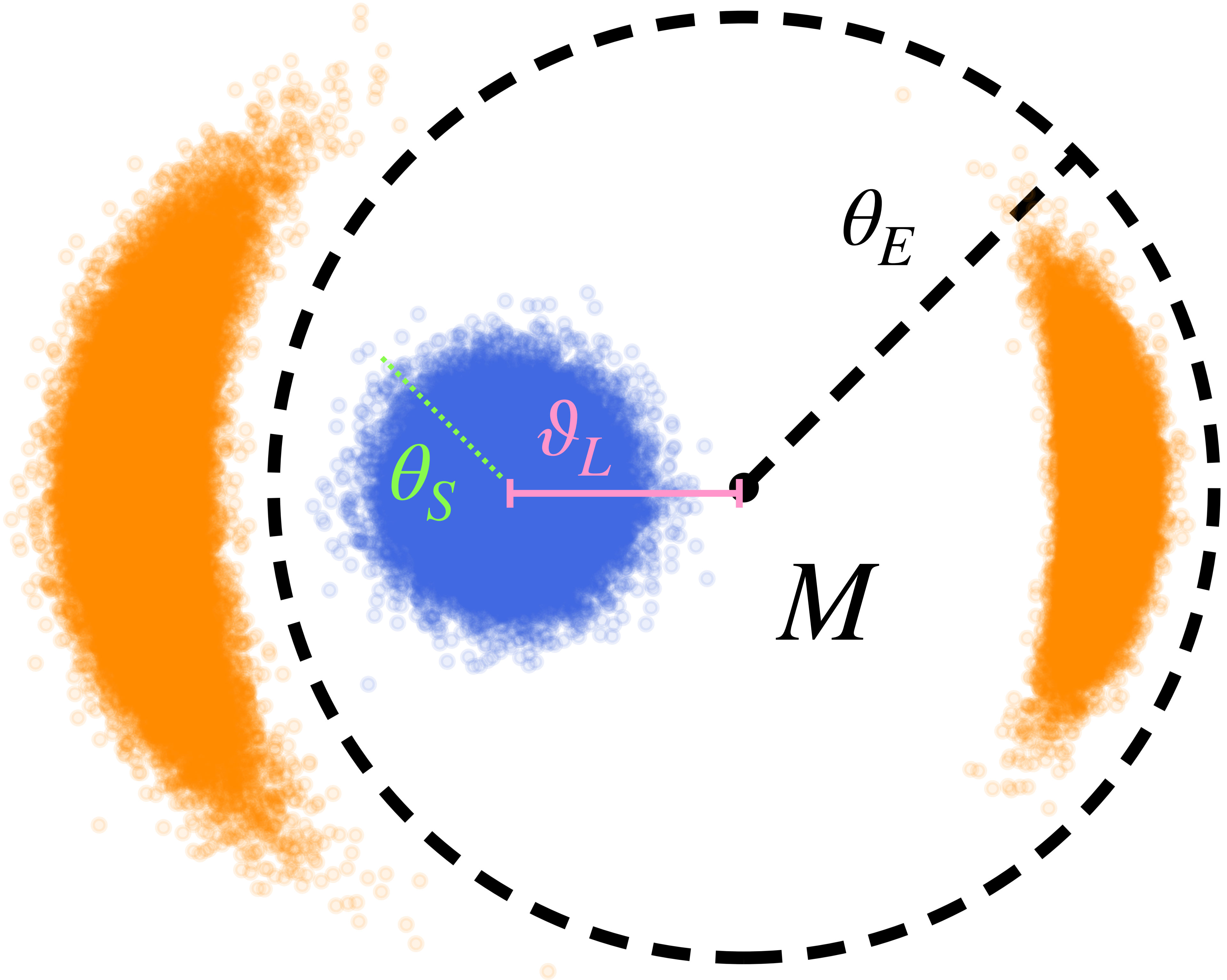

Image is magnified: $\mu \sim \dfrac{\theta_E}{\vartheta_L} \quad (\vartheta_L, \theta_S \ll \theta_E)$

BUT: Finite sources $(\theta_S \gtrsim \theta_E)$ have suppressed source-averaged magnification: $\bar{\mu} - 1 \sim \mathcal{O}(\theta_E^2/\theta_S^2)$

$\hbar = c = 1$ $[z_S = 1, \chi_L/\chi_S = 0.5\ (z_L = 0.43)]$ 1 arcsec $= 4.8 \times 10^{-6}$ rad

Gravitational Lensing 101

Typical angular scale associated with strong lensing: Einstein angle

$$\theta_E \equiv \sqrt{\frac{4G_N M(1+z_L)\chi_{LS}}{\chi_S \chi_L}}$$

$$\theta_E \sim \text{picoarcsec} \times \sqrt{\frac{M}{10^{-12} M_\odot}}$$

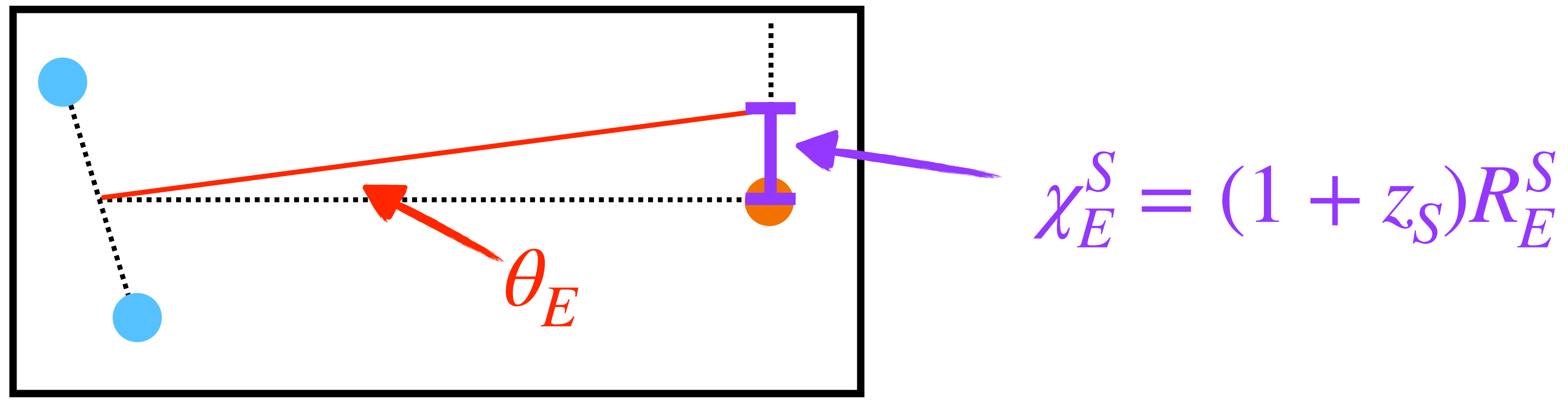

$$R_E^S = \mathscr{D}_S \theta_E \sim R_\odot \times \sqrt{\frac{M}{10^{-12} M_\odot}}$$

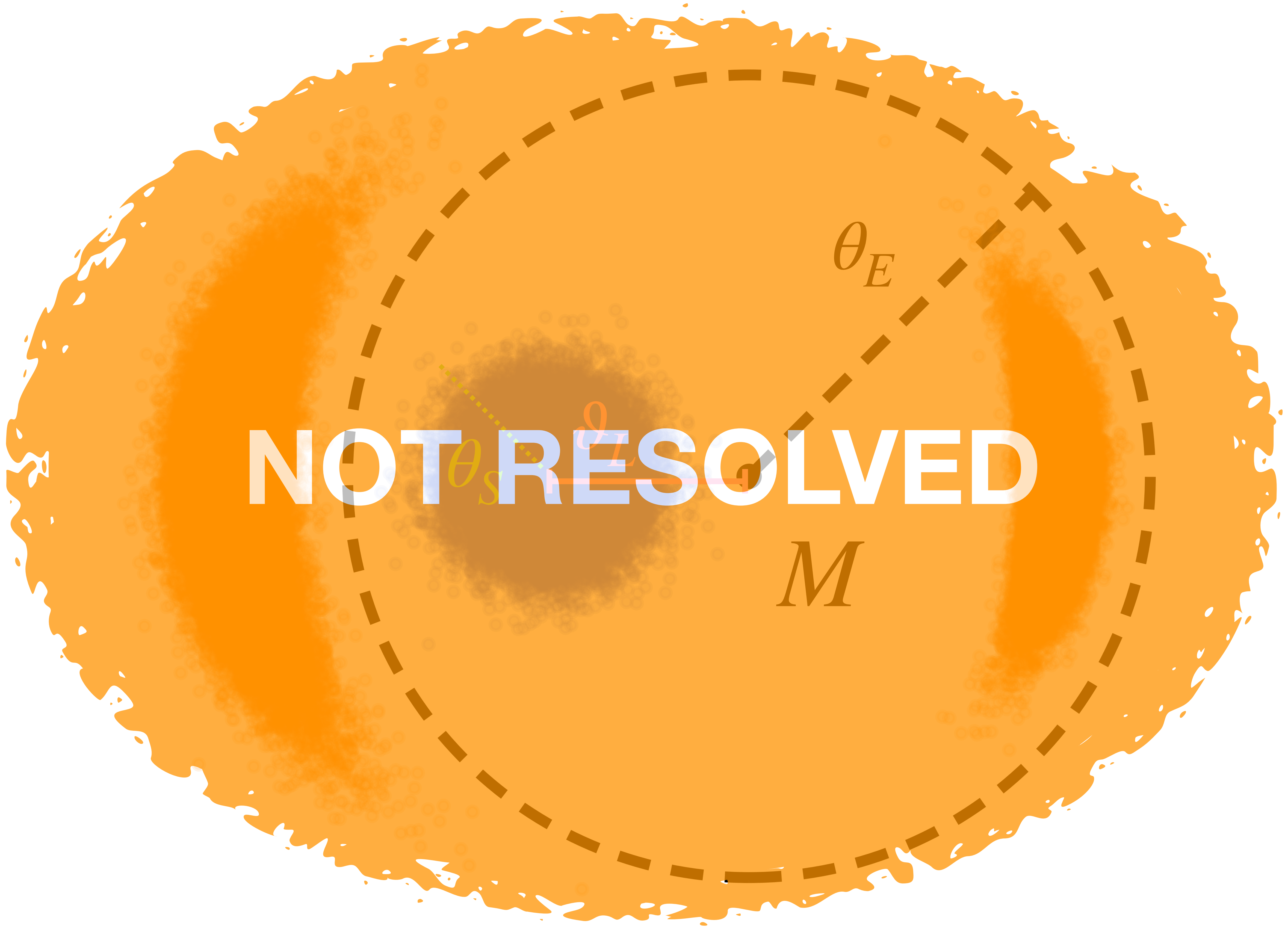

Image is magnified: $\mu \sim \frac{\theta_E}{\vartheta_L} \quad (\vartheta_L, \theta_S \ll \theta_E)$

BUT: Finite sources $(\theta_S \gtrsim \theta_E)$ have suppressed source-averaged magnification: $\bar{\mu} - 1 \sim \mathcal{O}(\theta_E^2/\theta_S^2)$

$\hbar = c = 1$ $[z_S = 1, \chi_L/\chi_S = 0.5\ (z_L = 0.43)]$ 1 arcsec $= 4.8 \times 10^{-6}$ rad

Picolensing signal

$f = \text{fluence} = \text{photons/area/time}$

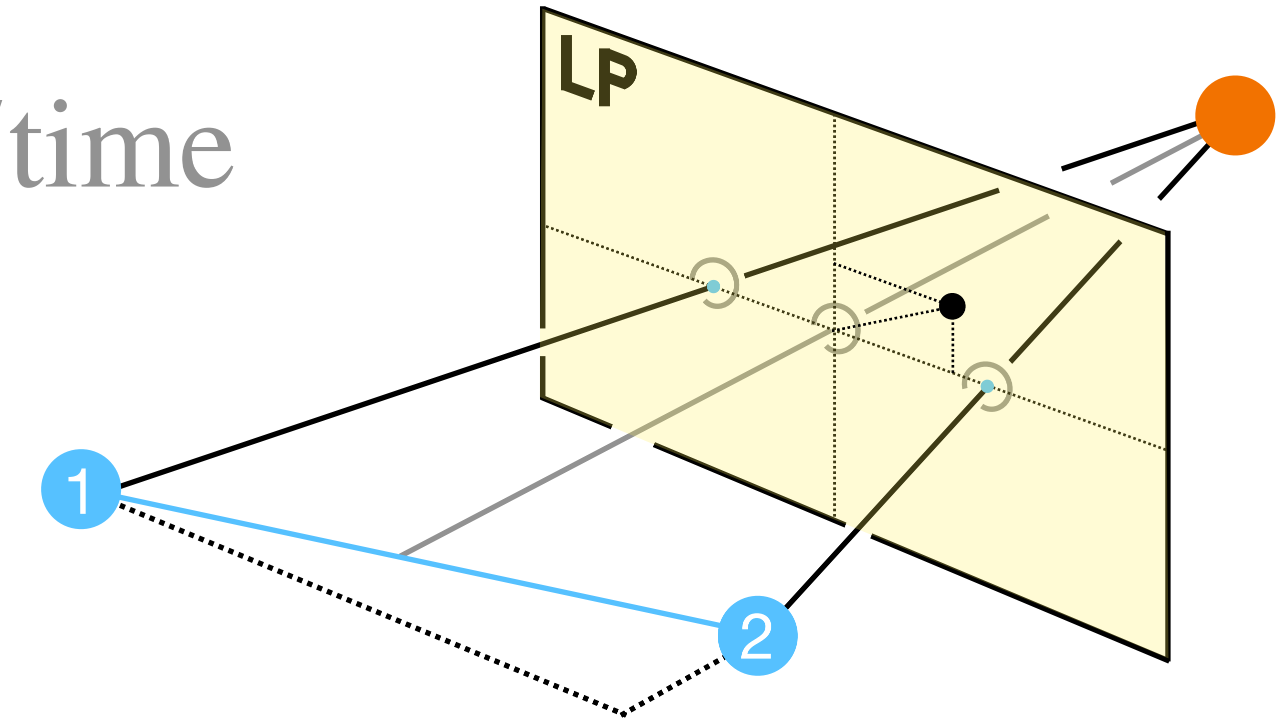

Two detectors each measure photons: $N = S + B$.

Signal: $\langle S \rangle = \bar{\mu} \cdot f_S \cdot A_S \cdot T$

Background: $\langle B \rangle = f_B \cdot A_B \cdot T$

Uncertainty: $\sqrt{\langle N \rangle}$

Assumed identical detectors, except for magnification

Could generalise

Picolensing signal: $\Delta N = | N_2 - N_1 |$.

$\langle \Delta N \rangle = | \langle S_1 \rangle - \langle S_2 \rangle |$
$\propto | \bar{\mu}_1 - \bar{\mu}_2 |$

Uncertainty: $u[\Delta N] = \sqrt{2B + S_1 + S_2}$

SNR: $\rho = \langle \Delta N \rangle \Big/ u[\Delta N]$

after: Gawade, More, Bhalerao [2308.01775]

Picolensing signal

f = fluence = photons/area/time

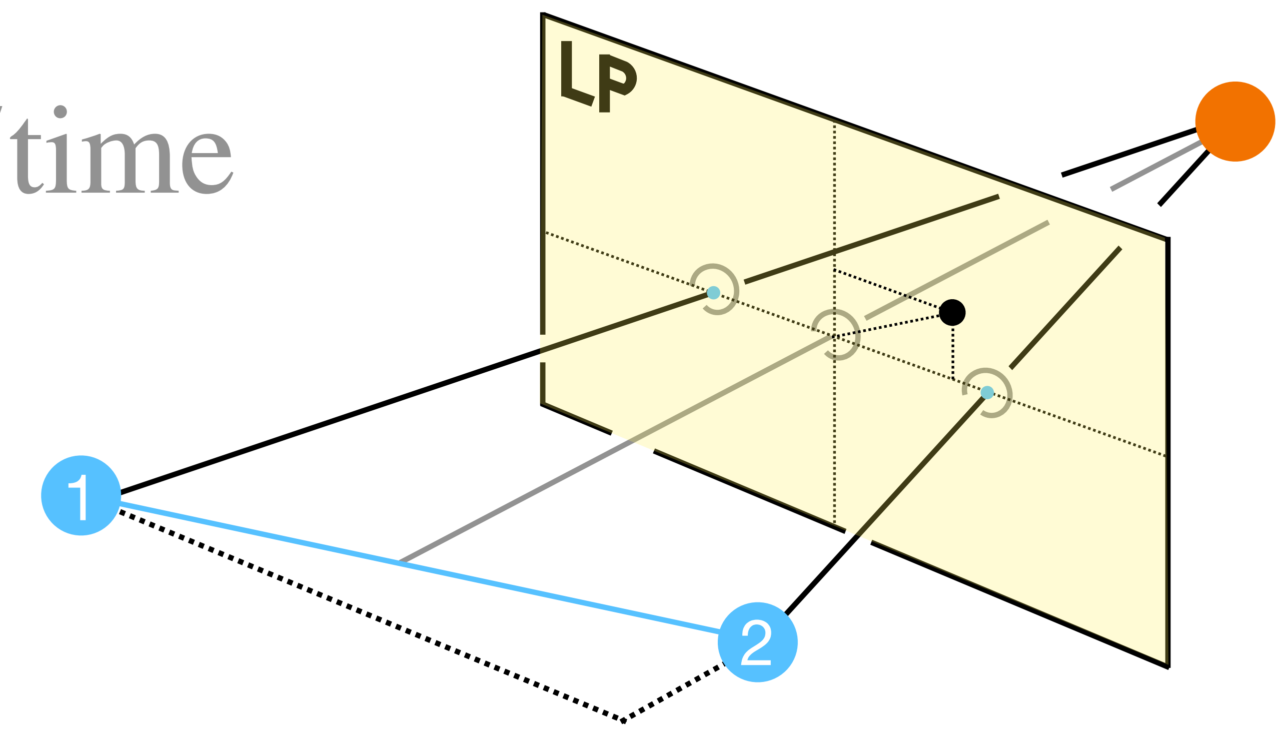

Two detectors each measure photons: $N = S + B$.

Signal: $\langle S \rangle = \bar{\mu} \cdot f_S \cdot A_S \cdot T$

Background: $\langle B \rangle = f_B \cdot A_B \cdot T$

Uncertainty: $\sqrt{\langle N \rangle}$

Assumed identical detectors, except for magnification

Could generalise

Picolensing signal: $\Delta N = |N_2 - N_1|$.

Uncertainty: $u[\Delta N] = \sqrt{2B + S_1 + S_2}$

SNR: $\rho = \langle \Delta N \rangle \big/ u[\Delta N]$

$$\langle \Delta N \rangle = |\langle S_1 \rangle - \langle S_2 \rangle|$$
$$\propto |\bar{\mu}_1 - \bar{\mu}_2|$$

after: Gawade, More, Bhalerao [2308.01775]

Michael A. Fedderke [Perimeter]

Picolensing signal

f = fluence = photons/area/time

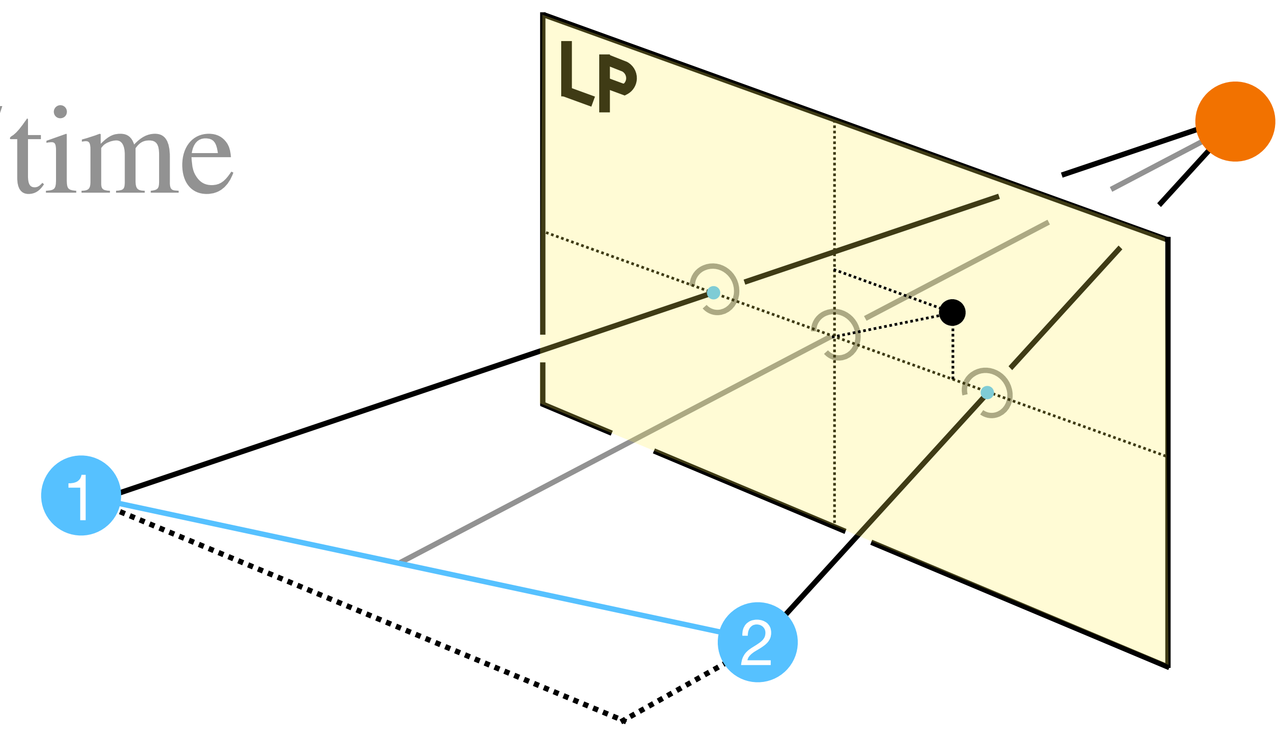

Two detectors each measure photons: $N = S + B$.

Signal: $\langle S \rangle = \bar{\mu} \cdot f_S \cdot A_S \cdot T$

Background: $\langle B \rangle = f_B \cdot A_B \cdot T$

Uncertainty: $\sqrt{\langle N \rangle}$

Assumed identical detectors, except for magnification

Could generalise

Picolensing signal: $\Delta N = | N_2 - N_1 |$.

$$\langle \Delta N \rangle = | \langle S_1 \rangle - \langle S_2 \rangle | \propto | \bar{\mu}_1 - \bar{\mu}_2 |$$

Uncertainty: $u[\Delta N] = \sqrt{2B + S_1 + S_2}$

SNR: $\rho = \langle \Delta N \rangle \big/ u[\Delta N]$

Need to convert this to a statement about number of expected picolensing events

after: Gawade, More, Bhalerao [2308.01775]

Michael A. Fedderke [Perimeter]

Picolensing Cross-section σ

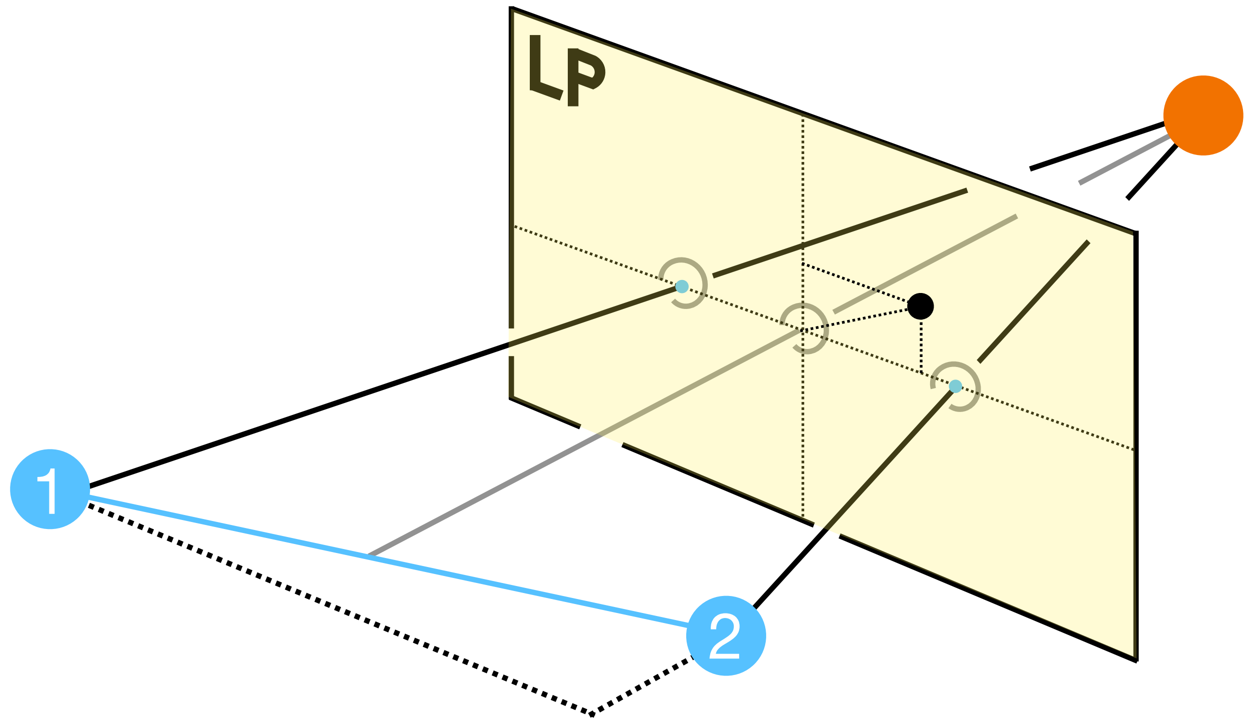

Region in lens plane where $\rho \geq \rho_*$, a threshold SNR.

Compute with Monte Carlo techniques.

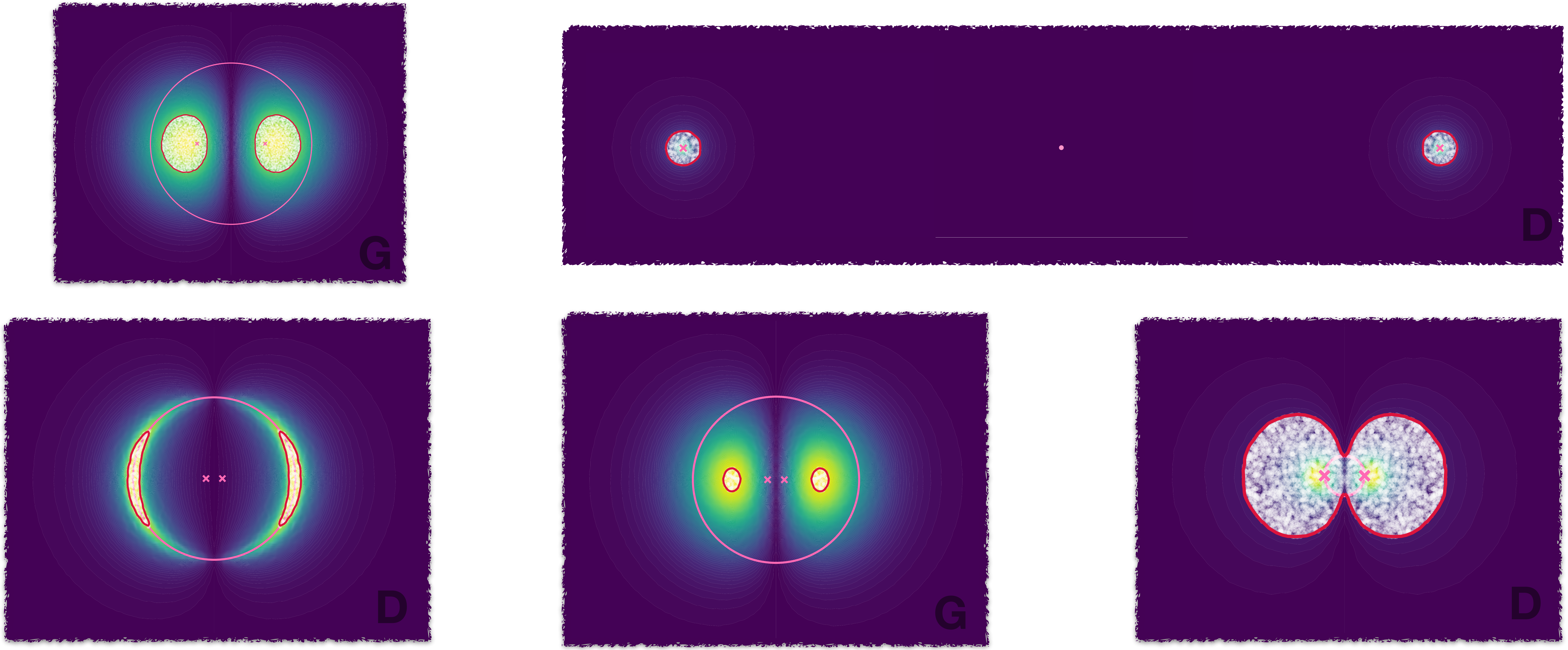

after: Gawade, More, Bhalerao [2308.01775]

Michael A. Fedderke [Perimeter]

Picolensing volume & optical depth

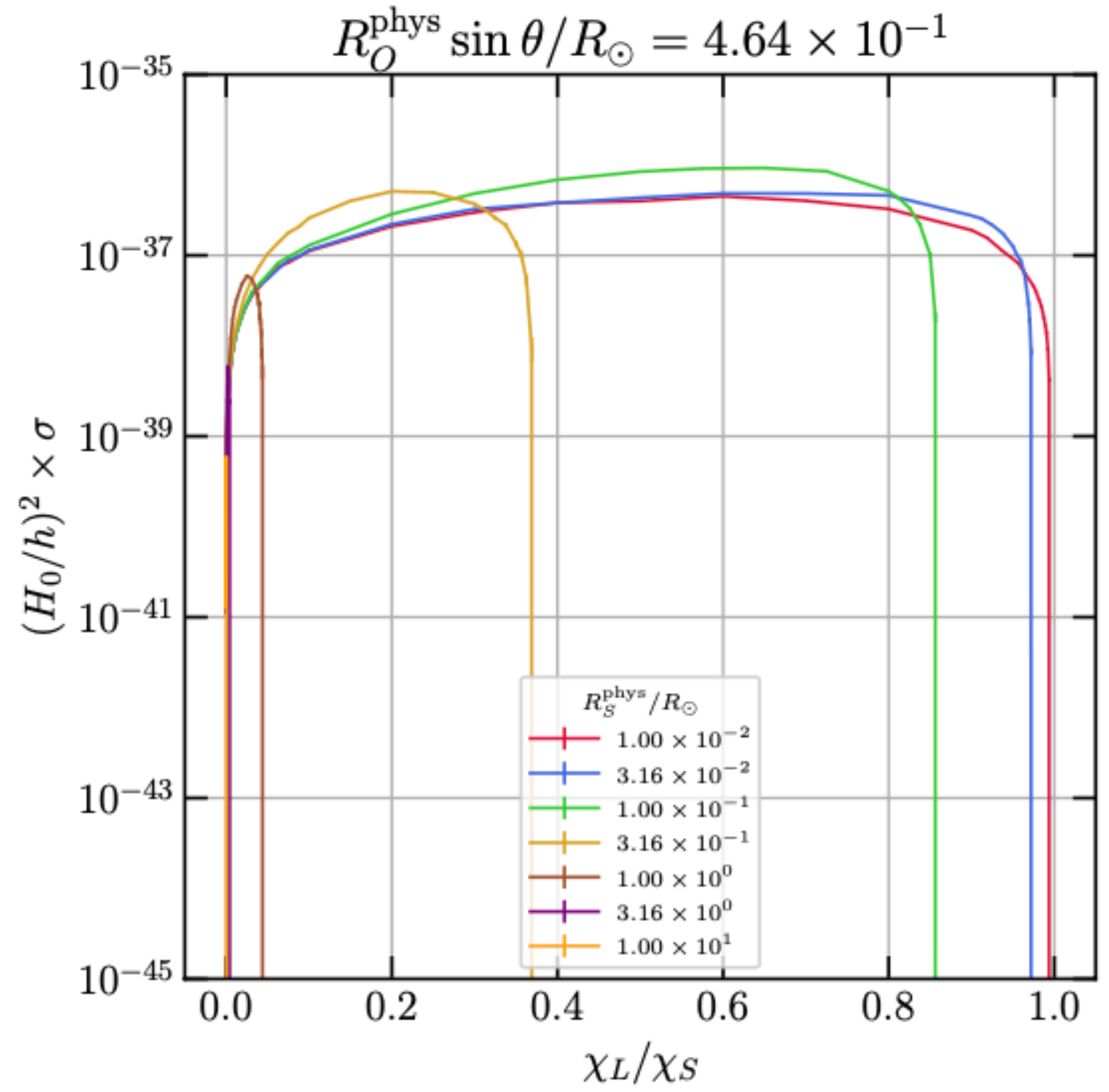

$\sigma = \sigma(\chi_L, \ldots)$ is a function of the distance to the lens plane χ_L

Co-moving picolensing volume: $\mathscr{V} = \int_0^{\chi_S} \sigma(\chi_L) d\chi_L$

PBHs: uniform* co-moving lens number density n_0

Optical depth (= expected number of lenses) to source j is $\tau_j = n_0 \mathscr{V}_j$ (need $\tau_j \ll 1$ for validity)

N sources. Average lensing volume: $\overline{\mathscr{V}} \equiv \frac{1}{N} \sum_{j=1}^{N} \mathscr{V}_j \Rightarrow \bar{\tau} = n_0 \overline{\mathscr{V}}$ average optical depth

Straightforward Poisson statistics* to then get lensing probabilities and set limits / explore discovery space

*Jung and Kim [1908.00078] looked at clustering; impact not significant for $\bar{\tau} \ll 1$. Poissonian stats OK.

after: Gawade, More, Bhalerao [2308.01775]

Picolensing volume & optical depth

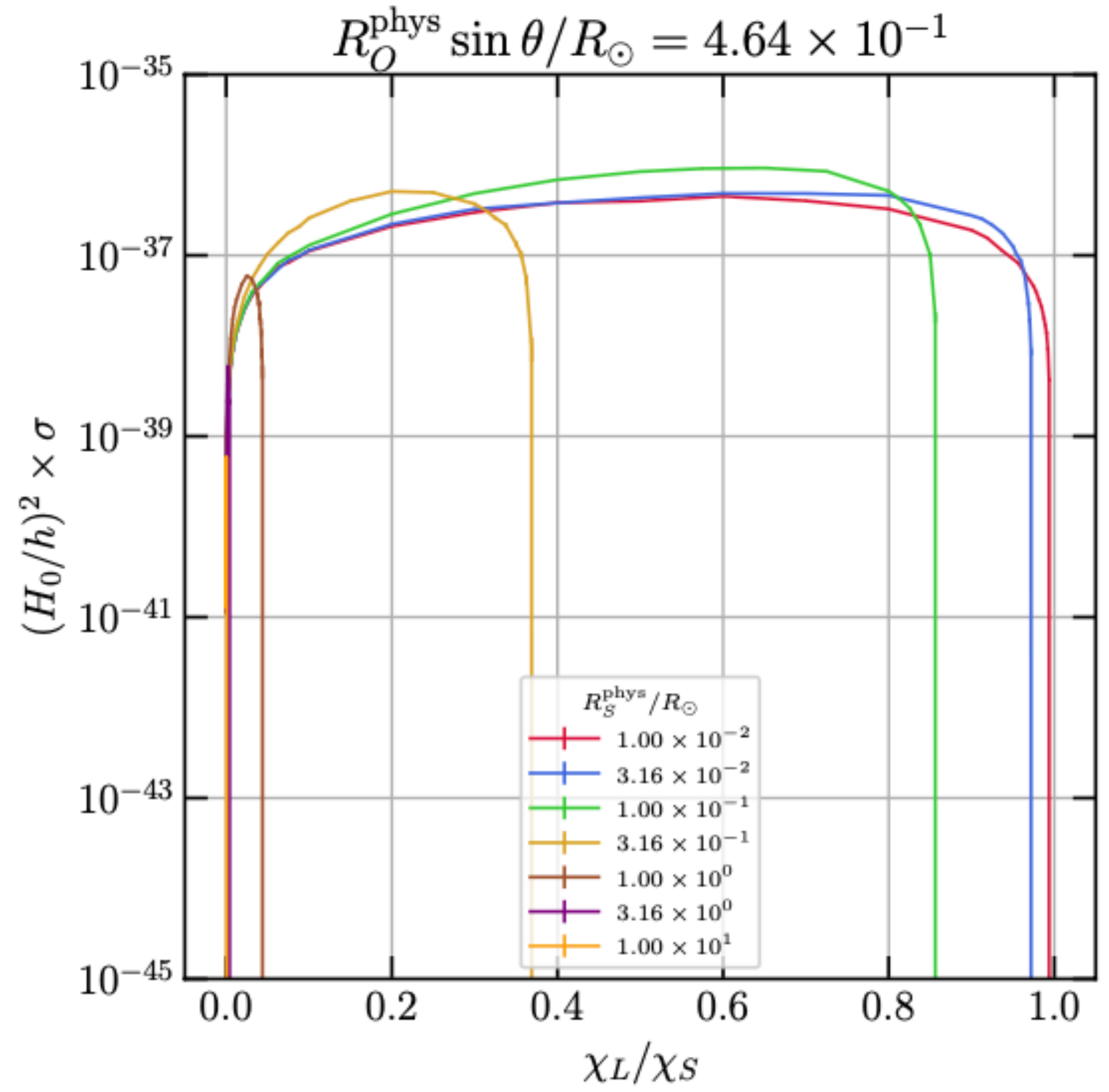

$\sigma = \sigma(\chi_L, \ldots)$ is a function of the distance to the lens plane χ_L

Co-moving picolensing volume: $$\mathscr{V} = \int_0^{\chi_S} \sigma(\chi_L) d\chi_L$$

PBHs: uniform* co-moving lens number density n_0

Optical depth (= expected number of lenses) to source j is $\tau_j = n_0 \mathscr{V}_j$ (need $\tau_j \ll 1$ for validity)

N sources. Average lensing volume: $\overline{\mathscr{V}} \equiv \frac{1}{N}\sum_{j=1}^{N} \mathscr{V}_j \Rightarrow \bar{\tau} = n_0 \overline{\mathscr{V}}$ average optical depth

Straightforward Poisson statistics* to then get lensing probabilities and set limits / explore discovery space

*Jung and Kim [1908.00078] looked at clustering;
impact not significant for $\bar{\tau} \ll 1$. Poissonian stats OK.

after: Gawade, More, Bhalerao [2308.01775]

Picolensing volume & optical depth

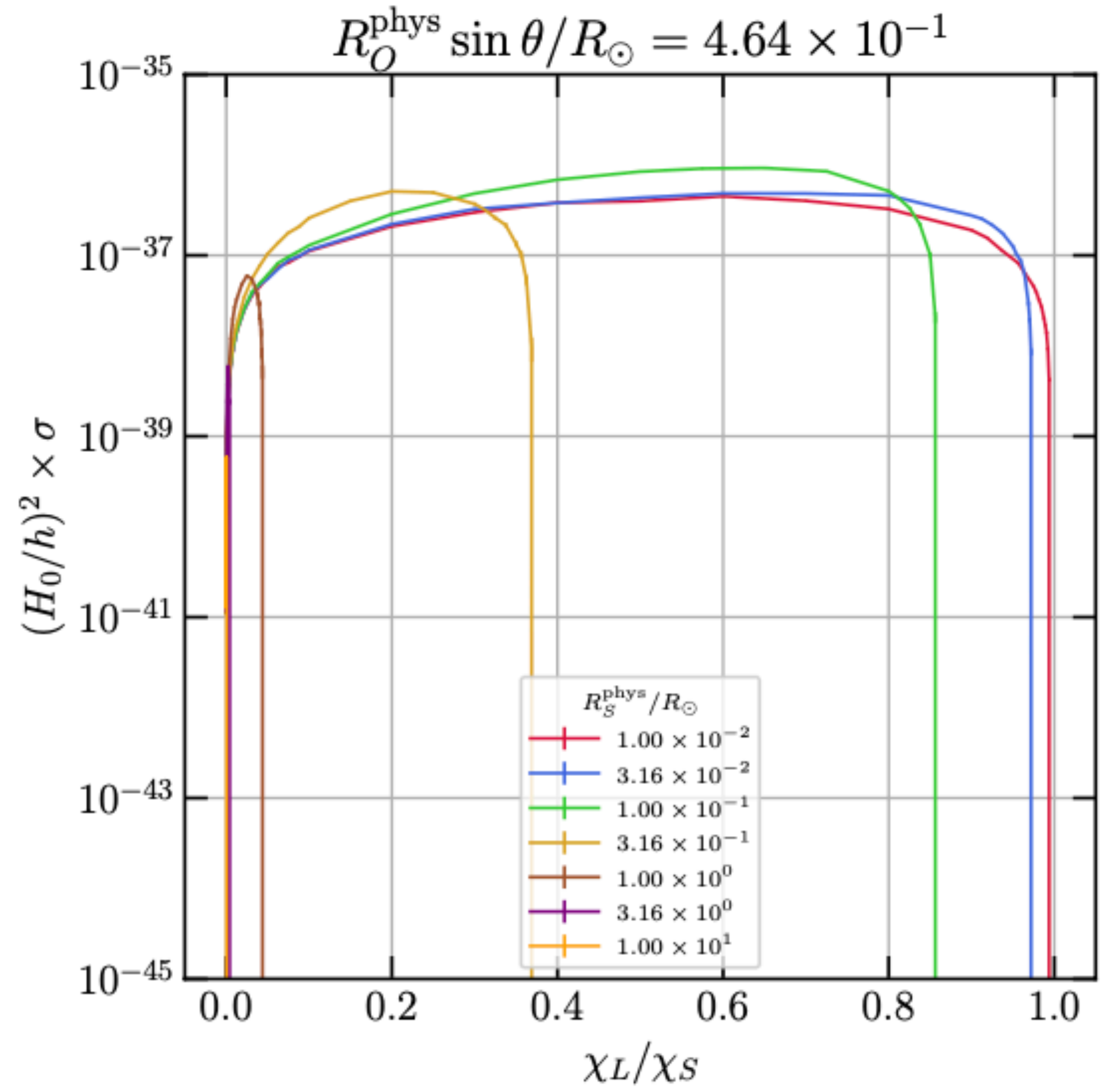

$\sigma = \sigma(\chi_L, \ldots)$ is a function of the distance to the lens plane χ_L

Co-moving picolensing volume: $\mathscr{V} = \int_0^{\chi_S} \sigma(\chi_L) d\chi_L$

PBHs: uniform* co-moving lens number density n_0

Optical depth (= expected number of lenses) to source j is $\tau_j = n_0 \mathscr{V}_j$ (need $\tau_j \ll 1$ for validity)

N sources. Average lensing volume: $\overline{\mathscr{V}} \equiv \frac{1}{N} \sum_{j=1}^{N} \mathscr{V}_j \Rightarrow \bar{\tau} = n_0 \overline{\mathscr{V}}$ average optical depth

Straightforward Poisson statistics* to then get lensing probabilities and set limits / explore discovery space

*Jung and Kim [1908.00078] looked at clustering;
impact not significant for $\bar{\tau} \ll 1$. Poissonian stats OK.

after: Gawade, More, Bhalerao [2308.01775]

Sources: Gamma-Ray Bursts (GRBs)

Transient. Two classes: long ($> 2\,\mathrm{s}$) and short ($< 2\,\mathrm{s}$)

Long: cosmologically distant ($\bar{z}_S \sim 2$) and **very** bright in x/γ-rays.

Highly beamed emission: $\Gamma \sim 10^2$ $E_{\mathrm{beam}} \sim 3 \times 10^{51}\,\mathrm{erg} \sim (2-3) \cdot E_{\mathrm{SNIa}}$

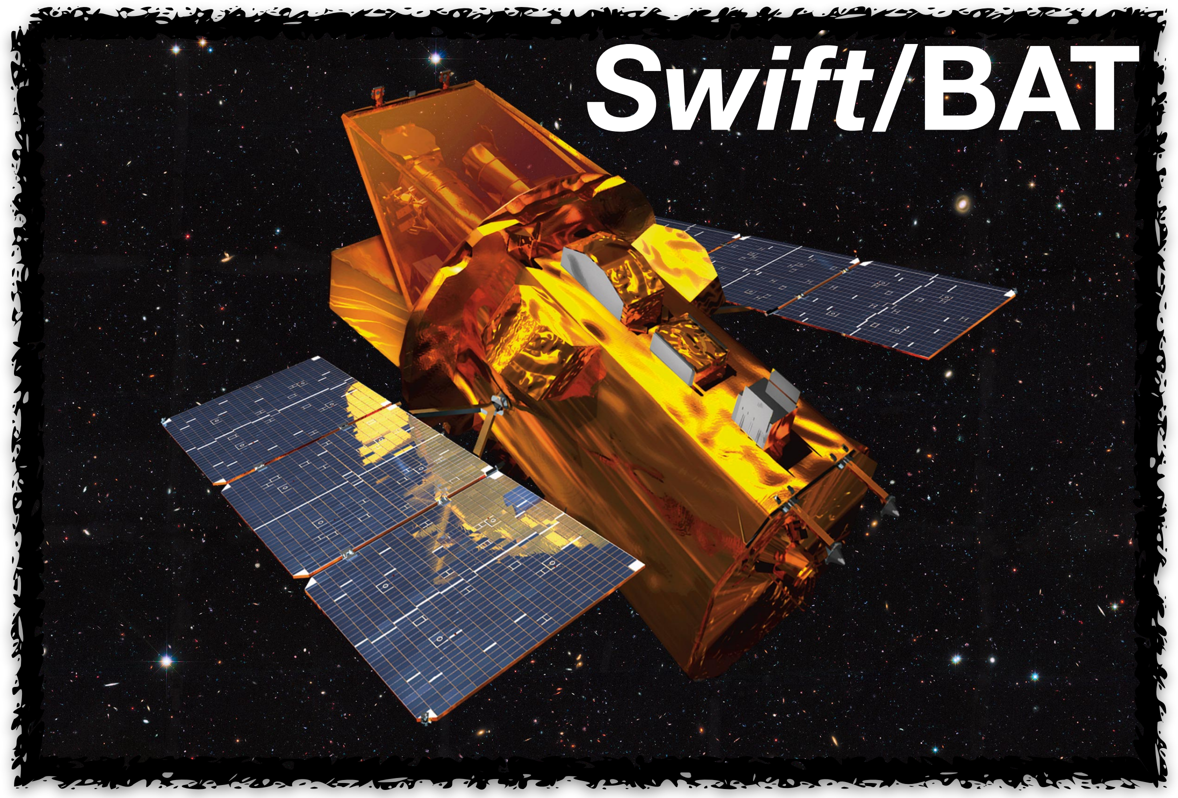

Gawade et al [2308.01775] looked at a possible future ISRO project Daksha
($2 \times \sim$ Swift/BAT-class detectors in space, but each with *Fermi*/GBM sky coverage)

For results today: **assume similar parameters to $2 \times$ *Swift*/BAT** ($\sim$ Daksha)

Sources: Gamma-Ray Bursts (GRBs)

Transient. Two classes: long ($> 2\,\mathrm{s}$) and short ($< 2\,\mathrm{s}$)

Long: cosmologically distant ($\bar{z}_S \sim 2$) and **very** bright in x/γ-rays.

Highly beamed emission: $\Gamma \sim 10^2$ $E_{\mathrm{beam}} \sim 3 \times 10^{51}\,\mathrm{erg} \sim (2-3) \cdot E_{\mathrm{SNIa}}$

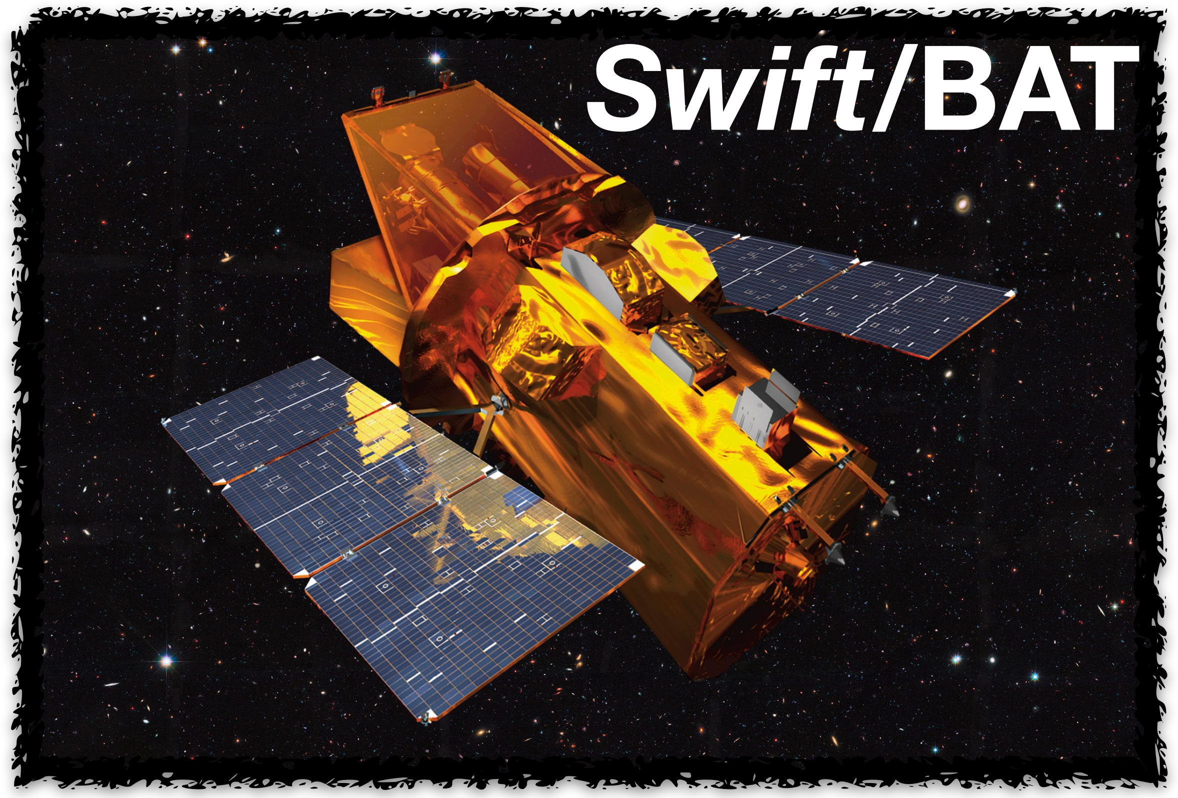

Gawade et al [2308.01775] looked at a possible future ISRO project Daksha
($2 \times \sim$ Swift/BAT-class detectors in space, but each with *Fermi*/GBM sky coverage)

For results today: **assume similar parameters to $2 \times$ *Swift*/BAT** ($\sim$ Daksha)

Source characteristics: *Swift*/BAT catalogue

Use real GRBs to make population-informed projections.

For each GRB, need:

Duration: T_{90} — time for 90% of measured intensity after trigger

Distance: z_S — known for ~ 409 GRBs in the catalogue

Brightness: power law (PL) or cut-off power law (CPL) fit to energy spectrum

Source characteristics: *Swift*/BAT catalogue

Use real GRBs to make population-informed projections.

For each GRB, need:

Duration: T_{90} — time for 90% of measured intensity after trigger

Distance: z_S — known for ~ 409 GRBs in the catalogue

Brightness: power law (PL) or cut-off power law (CPL) fit to energy spectrum

… AND: SIZE θ_S

GRB sizes

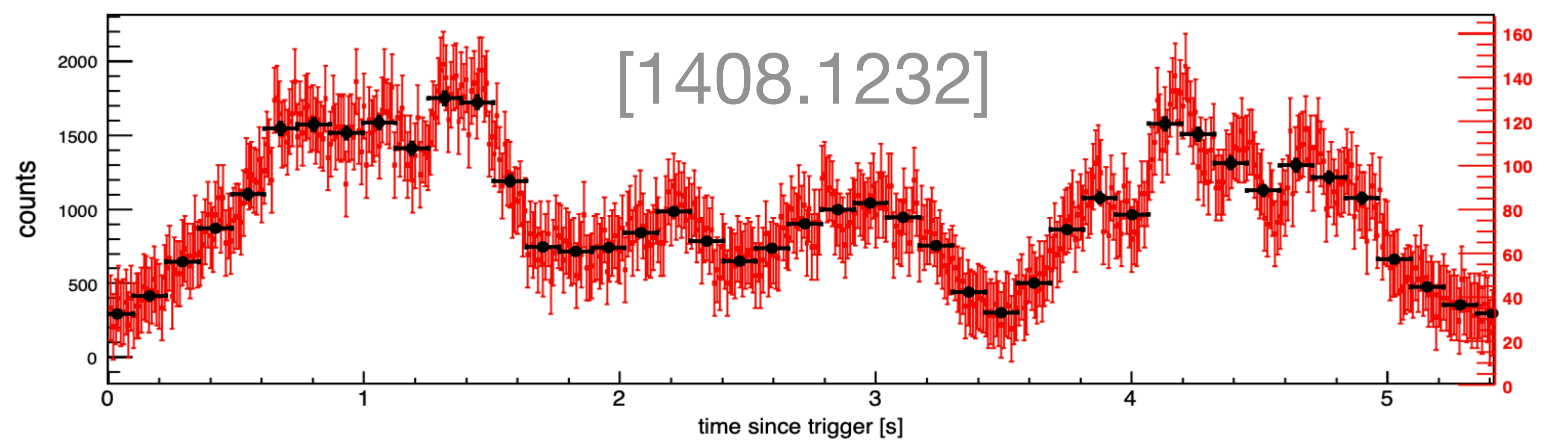

θ_S indirectly inferred from “minimum variability timescale” Δt_{var}

Gives estimate of the source light crossing time

$$D' \sim \frac{\Gamma^2 \times \Delta t_{\text{var}}}{1 + z_S}$$

Physical size of emission region

$$D_{\text{obs}} \sim \frac{D'}{\Gamma} \sim \frac{\Gamma \times \Delta t_{\text{var}}}{1 + z_S}$$

Observed size (beaming)

EMPIRICAL RELATIONSHIP: $T_{90} \sim \Gamma \Delta t_{\text{var}}$

Commonly used size estimate: $D_{\text{obs}} \sim \dfrac{T_{90}}{1 + z_S} \quad \Rightarrow \quad \theta_S = \dfrac{T_{90}}{\chi_S}$

GRB sizes

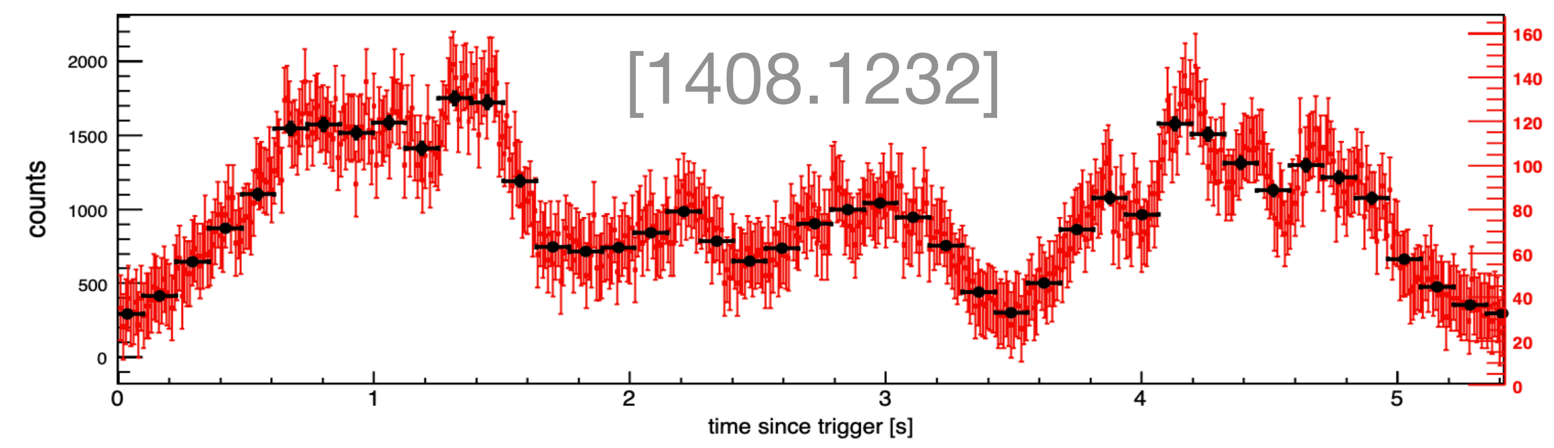

θ_S indirectly inferred from “minimum variability timescale” Δt_{var}

Gives estimate of the source light crossing time

$$D' \sim \frac{\Gamma^2 \times \Delta t_{\text{var}}}{1 + z_S}$$

Physical size of emission region

$$D_{\text{obs}} \sim \frac{D'}{\Gamma} \sim \frac{\Gamma \times \Delta t_{\text{var}}}{1 + z_S}$$

Observed size (beaming)

EMPIRICAL RELATIONSHIP: $T_{90} \sim \Gamma \Delta t_{\text{var}}$

Gawade, More, Bhalerao [2308.01775] used this

Commonly used size estimate: $D_{\text{obs}} \sim \dfrac{T_{90}}{1 + z_S} \quad \Rightarrow \quad \theta_S = \dfrac{T_{90}}{\chi_S}$

GRB size data are very uncertain

$$D_{\rm obs} \sim \frac{D'}{\Gamma} \sim \frac{\Gamma \times \Delta t_{\rm var}}{1+z_S}$$

$$D' \sim \frac{\Gamma^2 \times \Delta t_{\rm var}}{1+z_S}$$

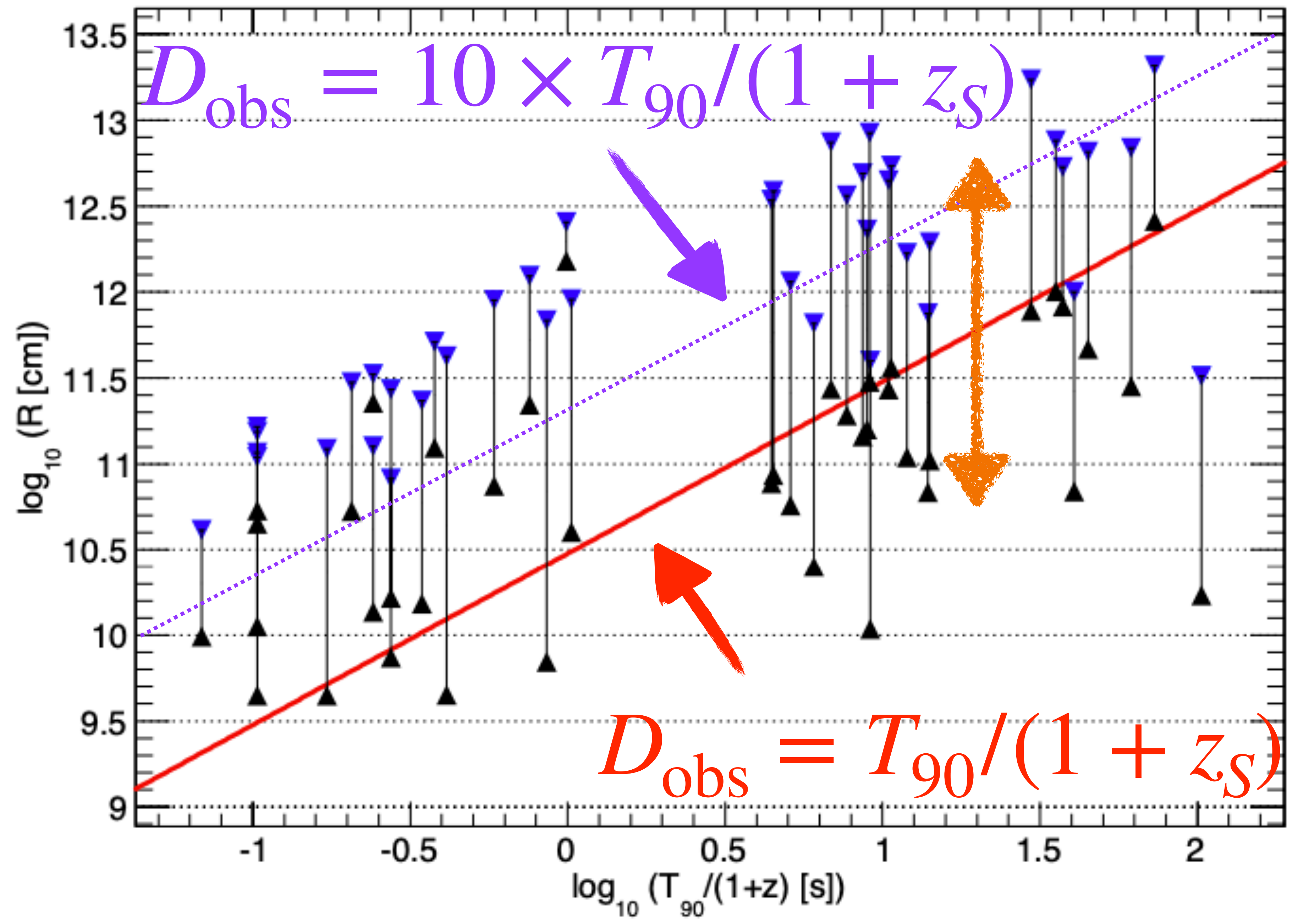

Note that this line is not attempting to fit the constraints from the data

Barnacka, Loeb [1409.1232]

-Scatter?

-Offset?

-Trend?

y-axes differ by $\Gamma \sim 10^2$

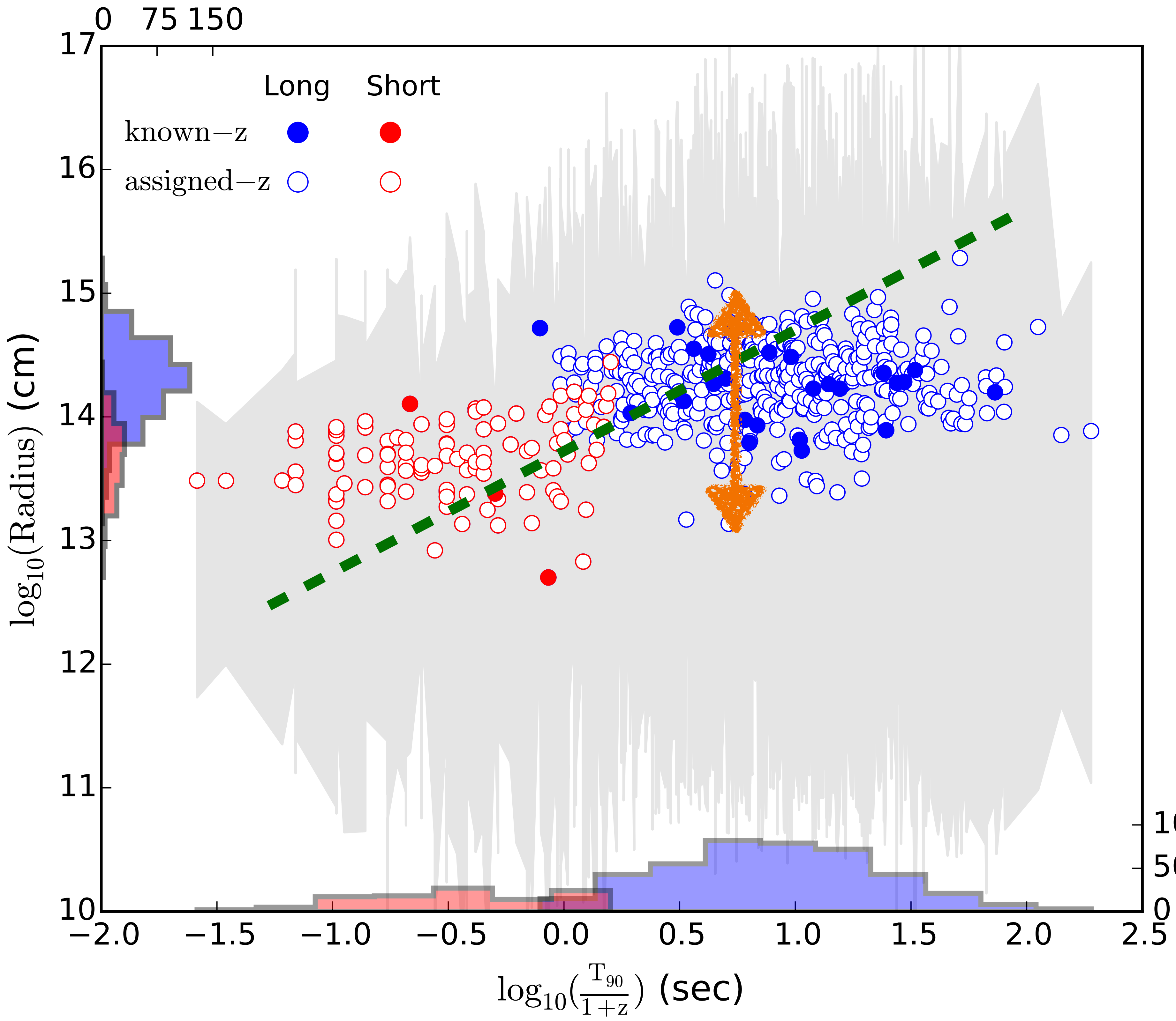

Golkhou et al [1501.05948]

Michael A. Fedderke [Perimeter]

This can matter!

$$D_{\rm obs} \equiv \frac{k_S T_{90}}{1+z_S}$$

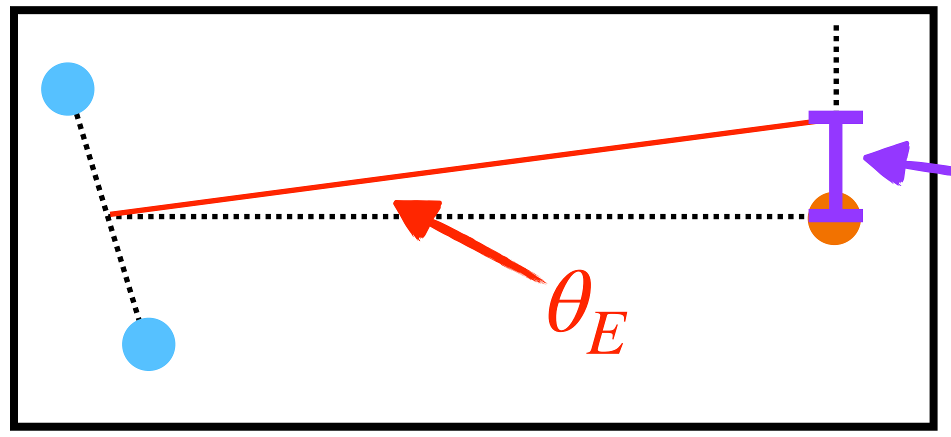

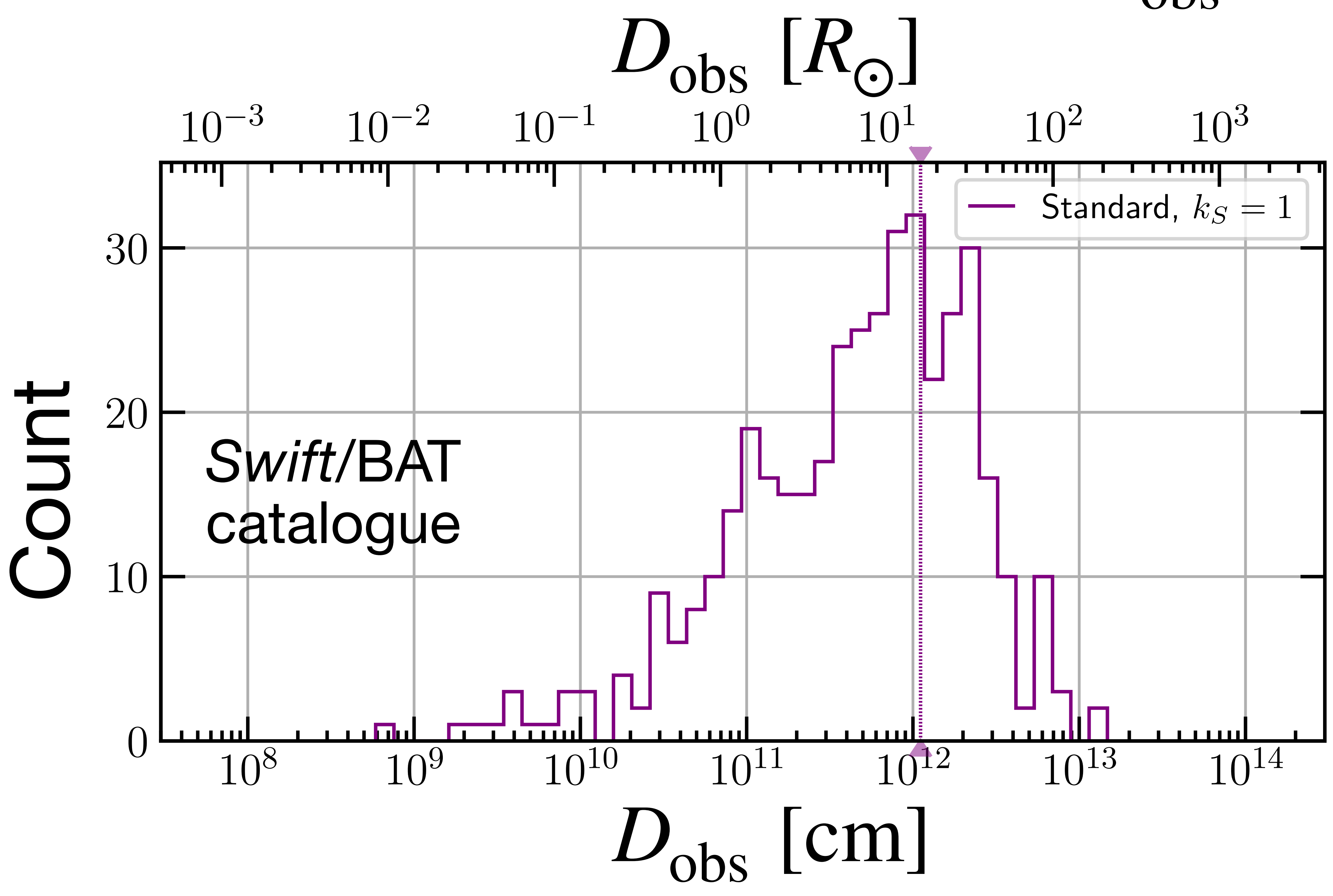

$$R_E^S = \mathscr{D}_S \theta_E \sim R_\odot \times \sqrt{\frac{M}{10^{-12} M_\odot}}$$

Source sizes can be large vs the Einstein radius in the source plane!

Magnifications are sensitive to source size uncertainties!

Enormous uncertainties, so we just bracket: $k_S = 0.1,\ 1,\ 10,\ 10^{\mathscr{U}[-1,1)}$

Michael A. Fedderke [Perimeter]

This can matter!

$$D_{\rm obs} \equiv \frac{k_S T_{90}}{1+z_S}$$

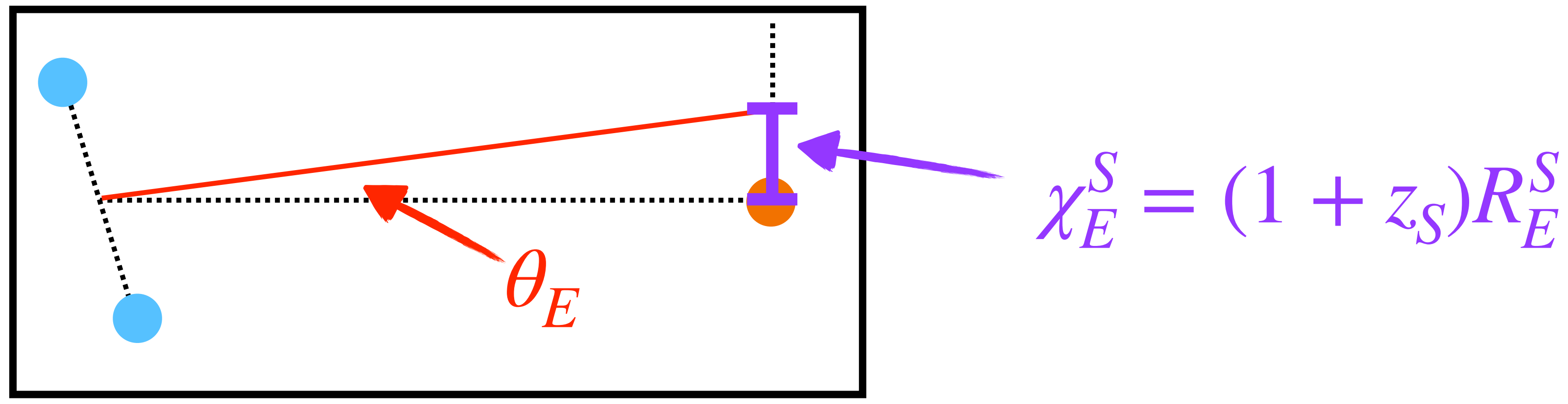

$$R_E^S = \mathscr{D}_S \theta_E \sim R_\odot \times \sqrt{\frac{M}{10^{-12} M_\odot}}$$

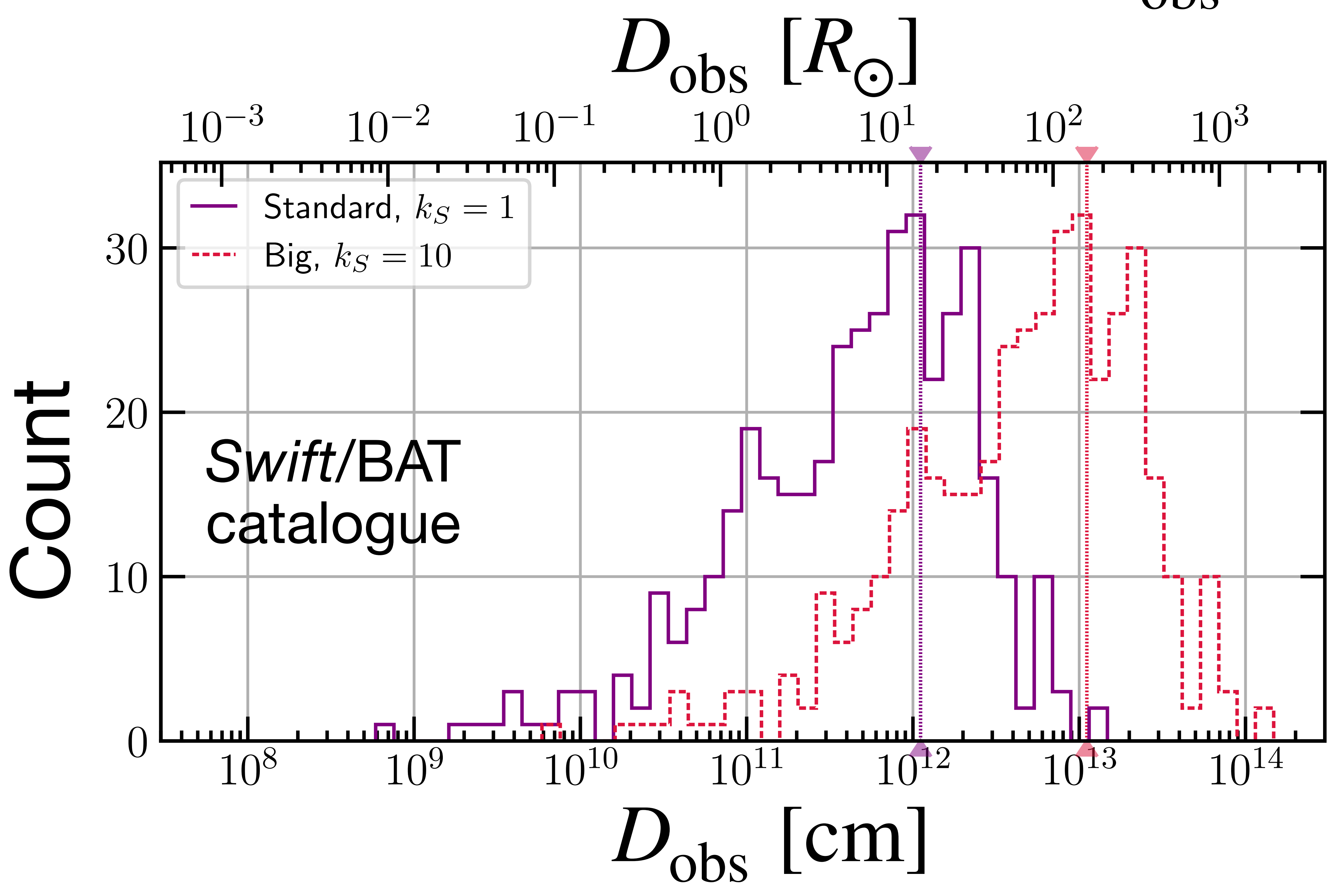

Source sizes can be large vs the Einstein radius in the source plane!

Magnifications are sensitive to source size uncertainties!

Enormous uncertainties, so we just bracket: $k_S = 0.1,\ 1,\ 10,\ 10^{\mathscr{U}[-1,1)}$

Michael A. Fedderke [Perimeter]

This can matter!

$$D_{\rm obs} \equiv \frac{k_S T_{90}}{1+z_S}$$

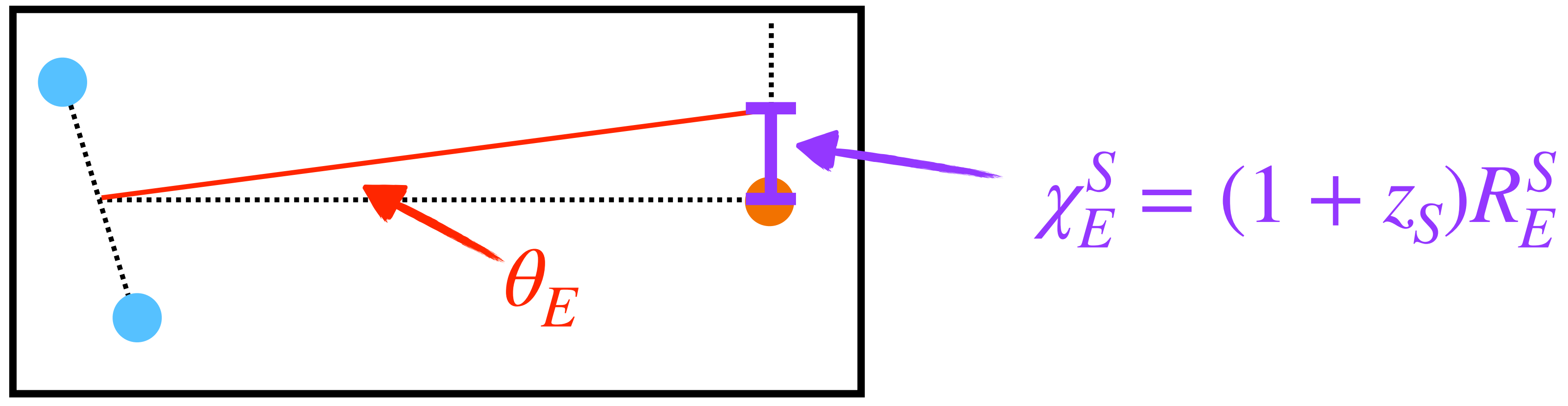

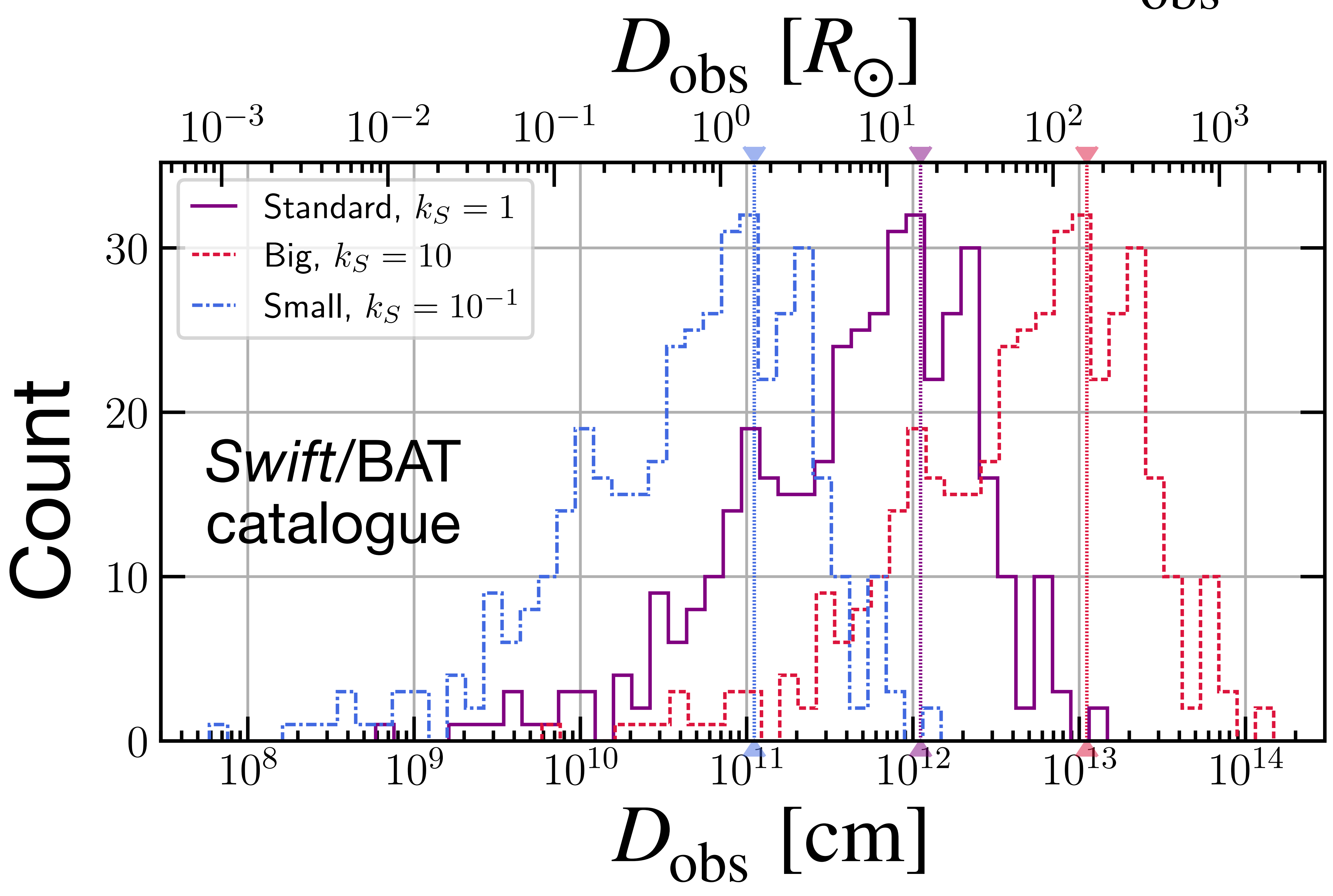

$$R_E^S = \mathscr{D}_S \theta_E \sim R_\odot \times \sqrt{\frac{M}{10^{-12} M_\odot}}$$

Source sizes can be large vs the Einstein radius in the source plane!

Magnifications are sensitive to source size uncertainties!

Enormous uncertainties, so we just bracket: $k_S = 0.1,\ 1,\ 10,\ 10^{\mathscr{U}[-1,1)}$

RESULTS

Different baselines, different source profiles

$$D_{obs} \equiv \frac{T_{90}}{1 + z_S}$$

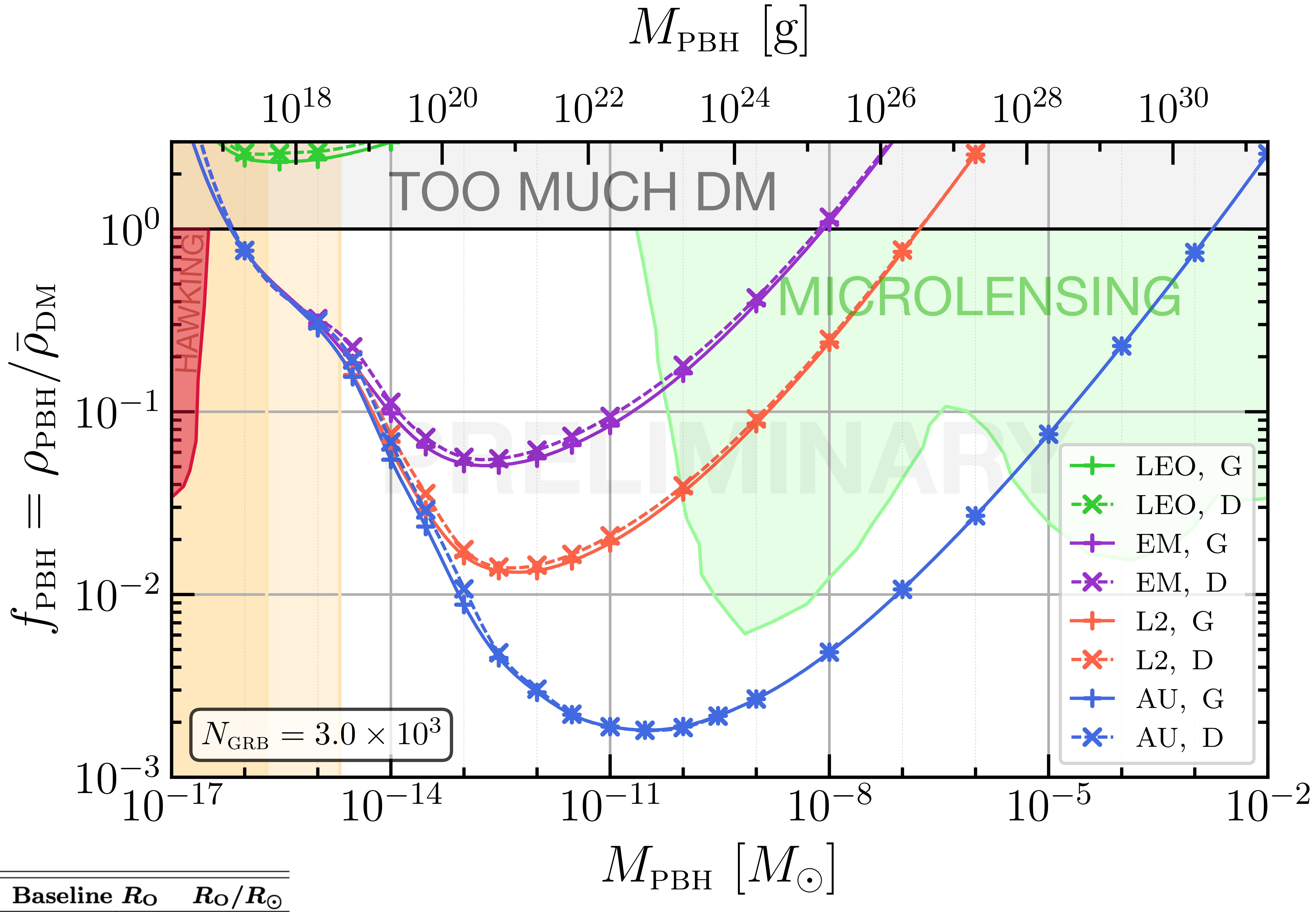

Scenario	Abbrev.	Baseline R_O	$R_O/R_\odot$
Low Earth Orbit	LEO	1.40×10^4 km	0.020
Earth–Moon	EM	3.84×10^5 km	0.55
Lagrange Point 2	L2	1.50×10^6 km	2.15
Astronomical Unit	AU	1.50×10^8 km	215

*markers are computed; lines are log-log cubic spline interpolants

Michael A. Fedderke [Perimeter]

Different baselines, different source profiles

$$D_{\text{obs}} \equiv \frac{T_{90}}{1 + z_S}$$

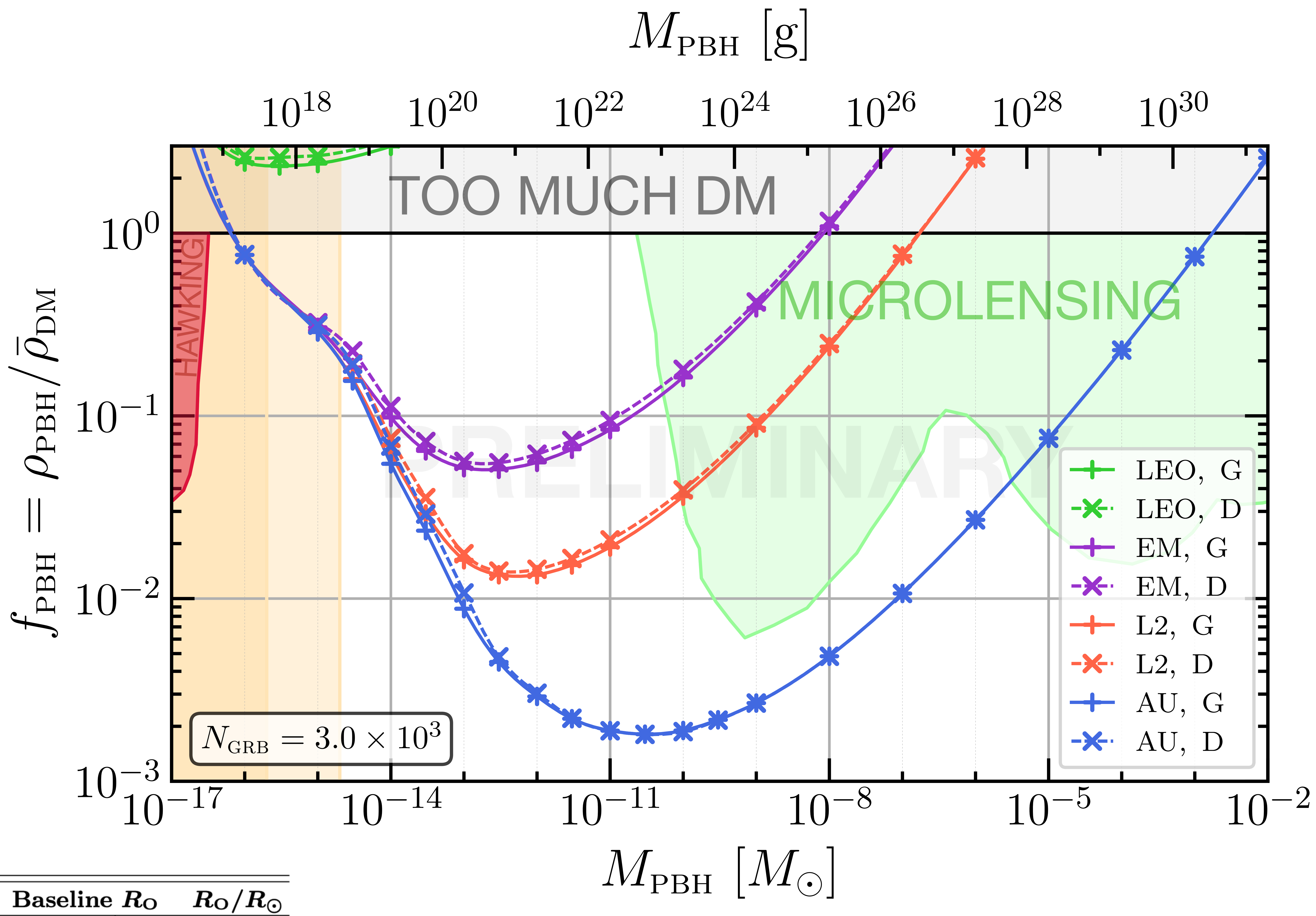

Essentially no difference in Gaussian (G) vs. Disk (D) source profiles

Scenario	Abbrev.	Baseline R_O	$R_O/R_\odot$
Low Earth Orbit	LEO	1.40×10^4 km	0.020
Earth–Moon	EM	3.84×10^5 km	0.55
Lagrange Point 2	L2	1.50×10^6 km	2.15
Astronomical Unit	AU	1.50×10^8 km	215

*markers are computed; lines are log-log cubic spline interpolants

Different baselines, different source profiles

$$D_{\text{obs}} \equiv \frac{T_{90}}{1+z_S}$$

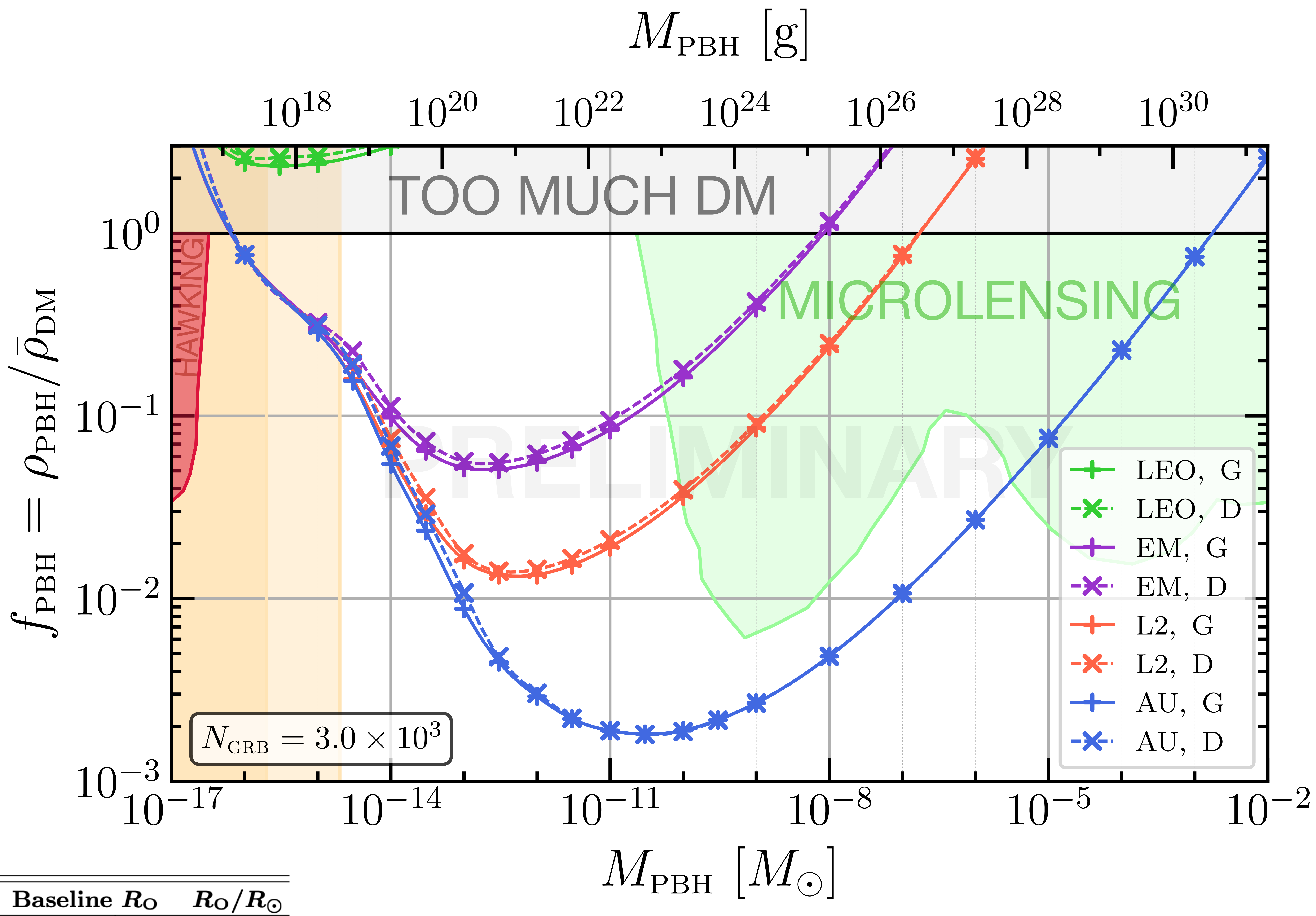

Essentially no difference in Gaussian (G) vs. Disk (D) source profiles

AU baselines can beat microlensing!

cf. Jung and Kim [1908.00078] (but for different assumptions)

Scenario	Abbrev.	Baseline R_O	$R_O/R_\odot$
Low Earth Orbit	LEO	1.40×10^4 km	0.020
Earth–Moon	EM	3.84×10^5 km	0.55
Lagrange Point 2	L2	1.50×10^6 km	2.15
Astronomical Unit	AU	1.50×10^8 km	215

*markers are computed; lines are log-log cubic spline interpolants

Different baselines, different source profiles

$$D_{\rm obs} \equiv \frac{T_{90}}{1+z_S}$$

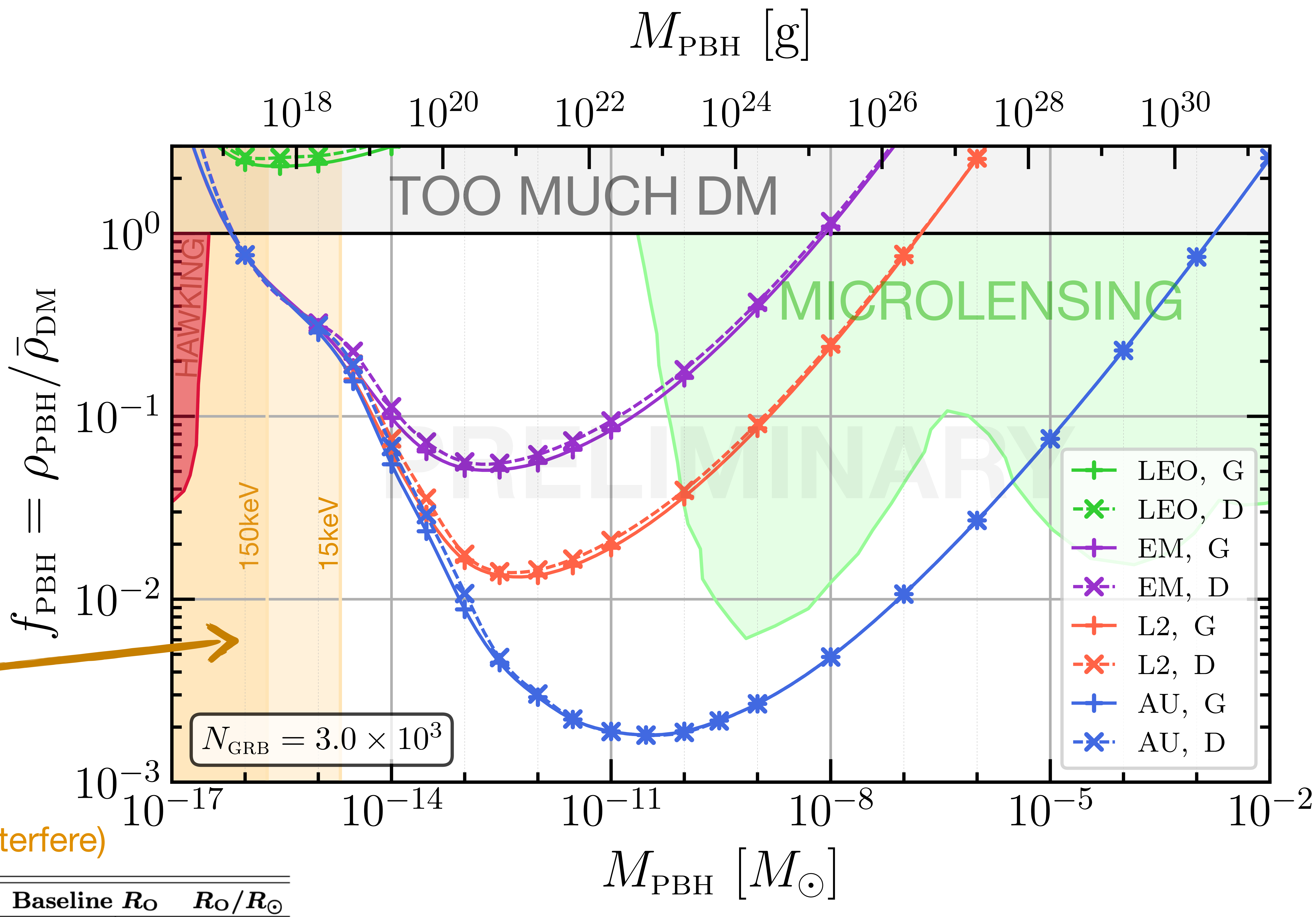

Geometrical optical fails

$\omega R_S \lesssim 1$

(two lensed images interfere)

Scenario	Abbrev.	Baseline R_O	$R_O/R_\odot$
Low Earth Orbit	LEO	1.40×10^4 km	0.020
Earth–Moon	EM	3.84×10^5 km	0.55
Lagrange Point 2	L2	1.50×10^6 km	2.15
Astronomical Unit	AU	1.50×10^8 km	215

Essentially no difference in Gaussian (G) vs. Disk (D) source profiles

AU baselines can beat microlensing!

cf. Jung and Kim [1908.00078] (but for different assumptions)

*markers are computed; lines are log-log cubic spline interpolants

Vary the source sizes

$N_{\mathrm{GRB}} = 3 \times 10^3$

$$D_{\mathrm{obs}} \equiv \frac{k_S T_{90}}{1 + z_S}$$

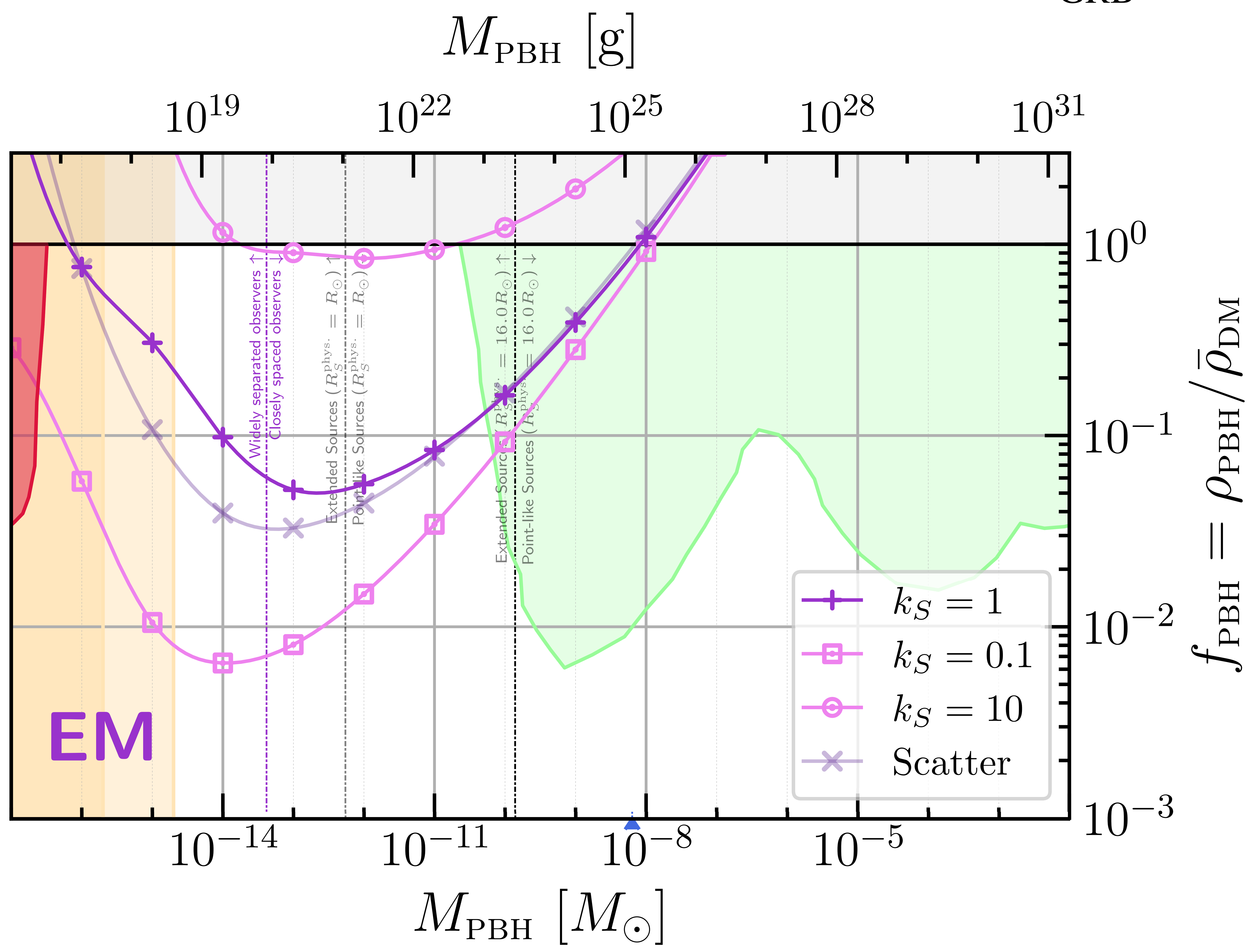

*markers are computed; lines are log-log cubic spline interpolants

Michael A. Fedderke [Perimeter]

Vary the source sizes

$N_{\mathrm{GRB}} = 3 \times 10^3$

Questionable whether you can robustly rule out $f_{\mathrm{DM}} = 1$ with this baseline if GRB sizes are systematically off

$$D_{\mathrm{obs}} \equiv \frac{k_S T_{90}}{1 + z_S}$$

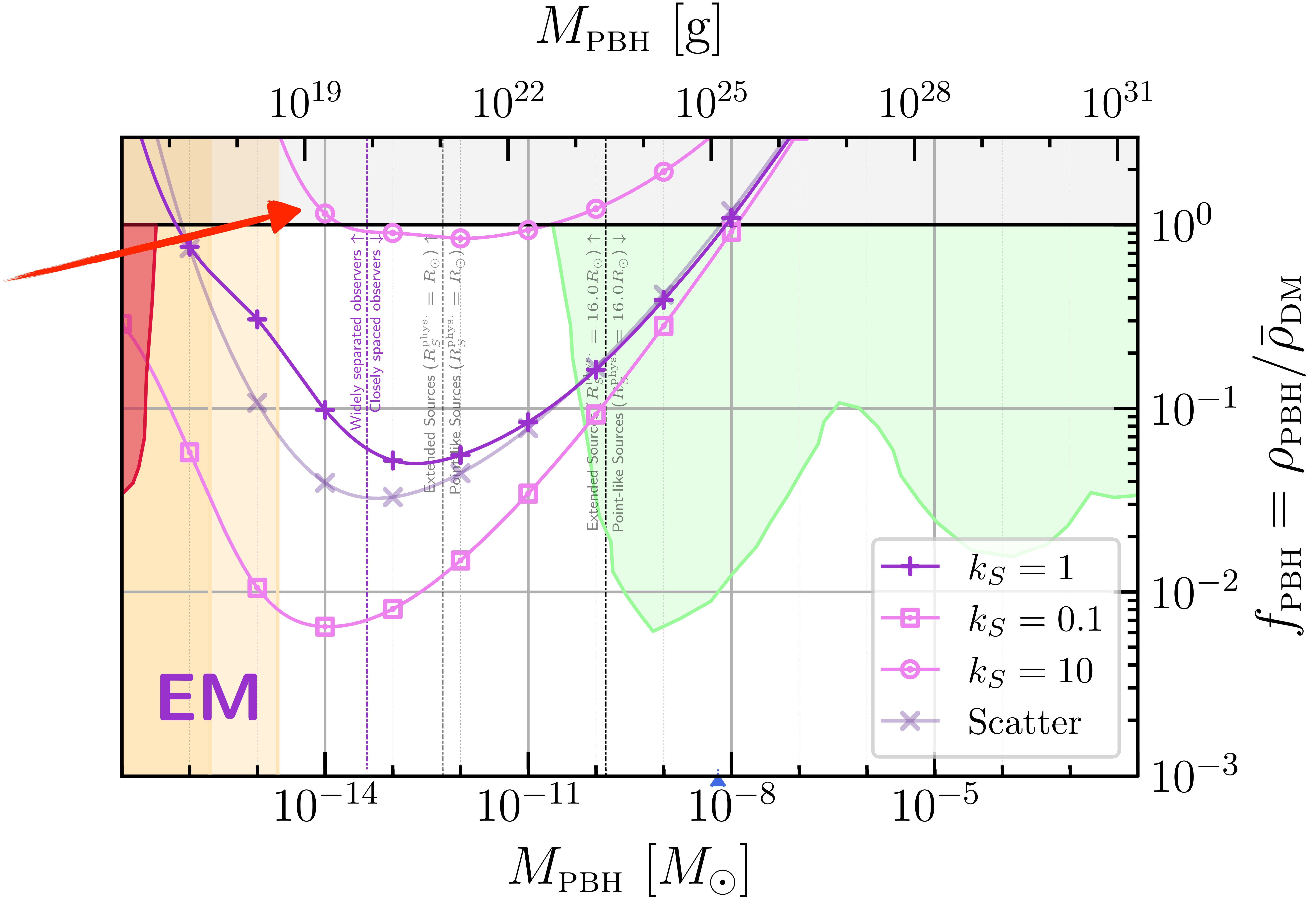

*markers are computed; lines are log-log cubic spline interpolants

Michael A. Fedderke [Perimeter]

Vary the source sizes

$N_{\mathrm{GRB}} = 3 \times 10^3$

Questionable whether you can robustly rule out $f_{\mathrm{DM}} = 1$ with this baseline if GRB sizes are systematically off

$$D_{\mathrm{obs}} \equiv \frac{k_S T_{90}}{1 + z_S}$$

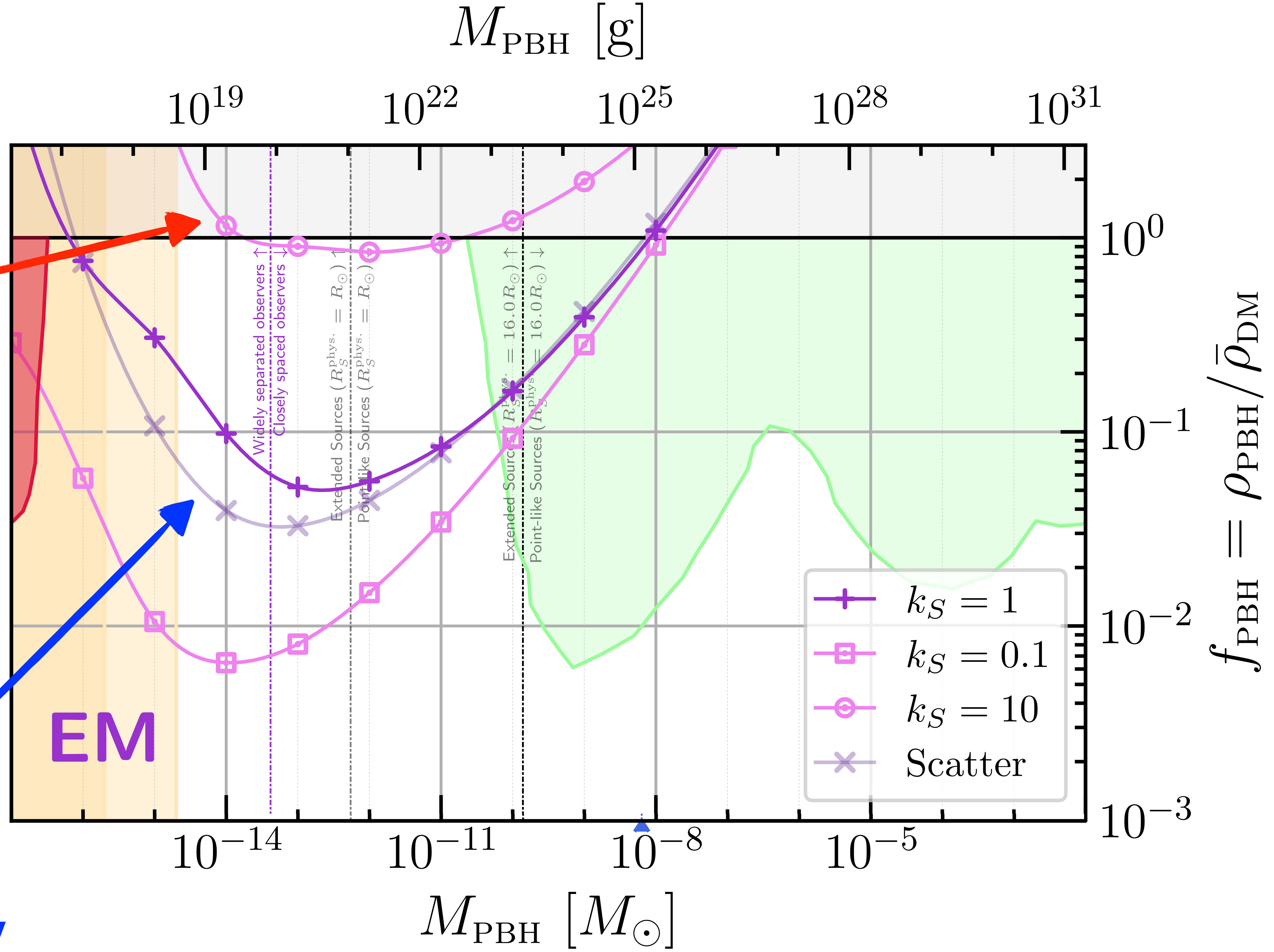

But the scatter may not be an issue

*markers are computed; lines are log-log cubic spline interpolants

Vary source sizes for each baseline

$$D_{\mathrm{obs}} \equiv \frac{k_S T_{90}}{1 + z_S}$$

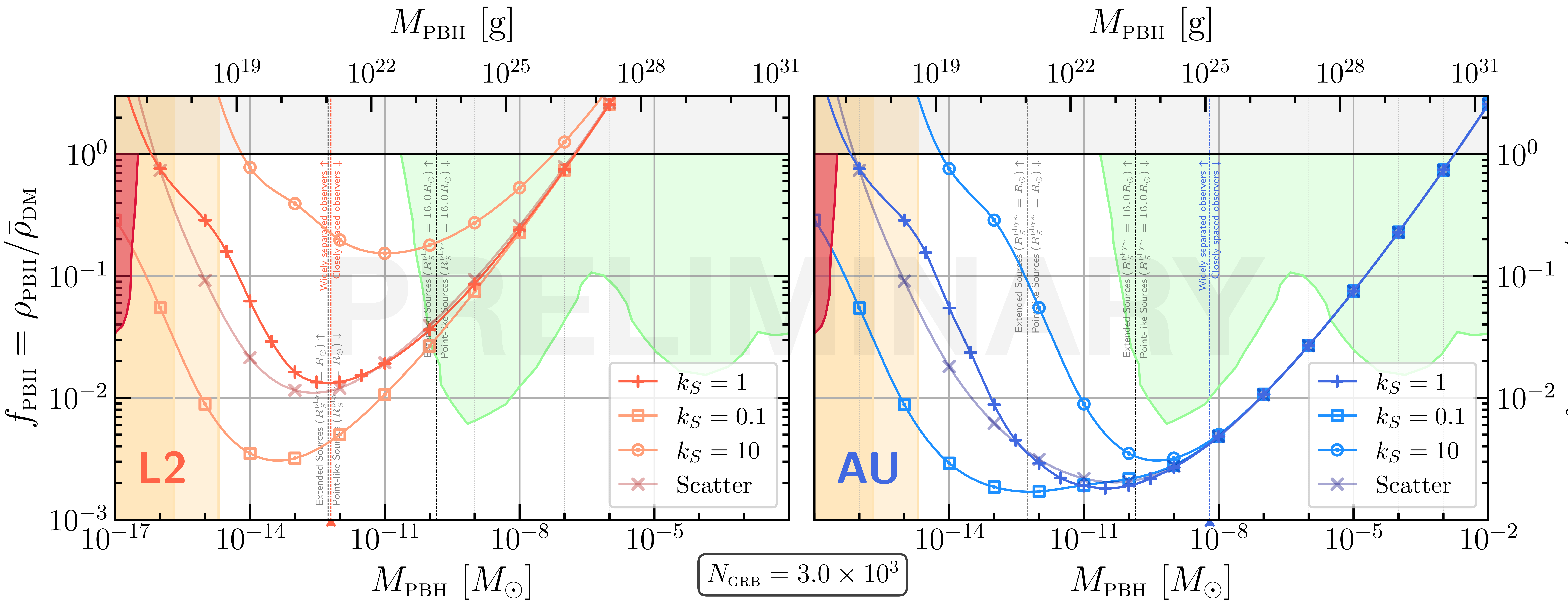

Scenario	Abbrev.	Baseline R_O	$R_O/R_{\odot}$
Low Earth Orbit	LEO	1.40×10^4 km	0.020
Earth–Moon	EM	3.84×10^5 km	0.55
Lagrange Point 2	L2	1.50×10^6 km	2.15
Astronomical Unit	AU	1.50×10^8 km	215

*markers are computed; lines are log-log cubic spline interpolants

Vary source sizes for each baseline

$$D_{\text{obs}} \equiv \frac{k_S T_{90}}{1+z_S}$$

ROBUST $f_{\text{DM}} = 1$ EXCLUSIONS FOR L2, AU

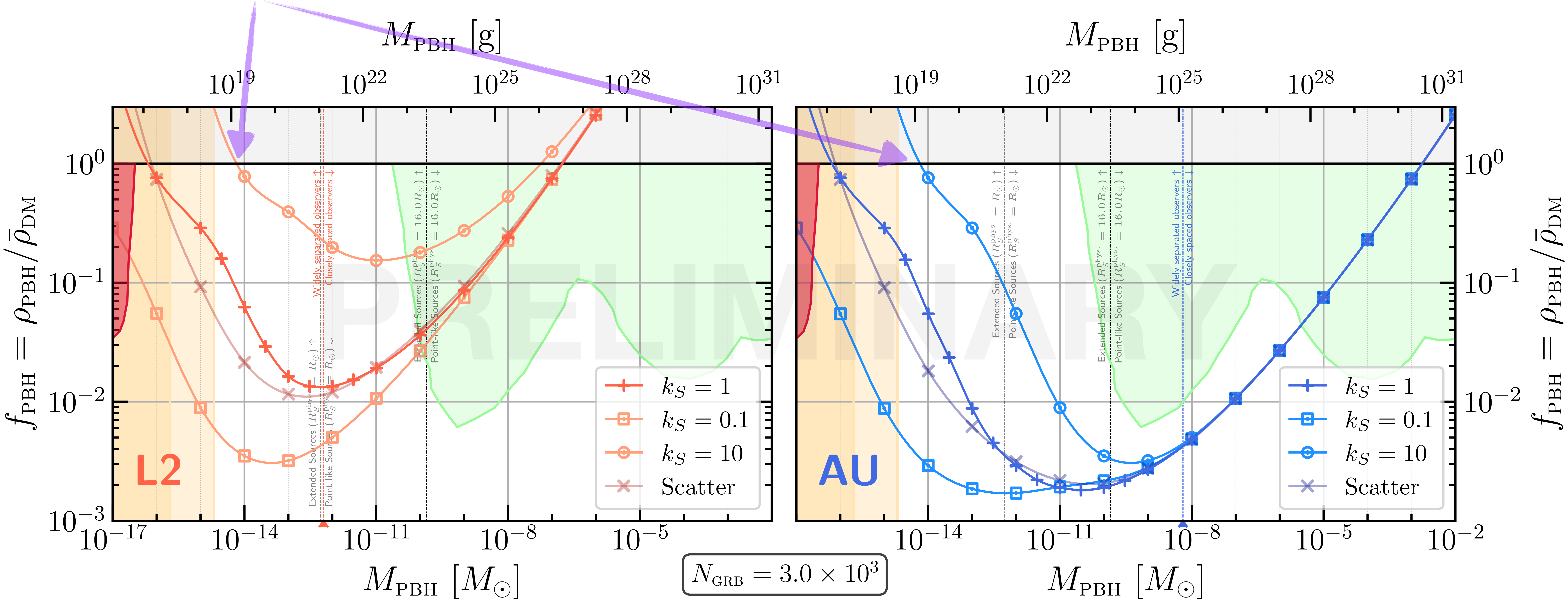

Scenario	Abbrev.	Baseline R_O	$R_O/R_\odot$
Low Earth Orbit	LEO	1.40×10^4 km	0.020
Earth–Moon	EM	3.84×10^5 km	0.55
Lagrange Point 2	L2	1.50×10^6 km	2.15
Astronomical Unit	AU	1.50×10^8 km	215

*markers are computed; lines are log-log cubic spline interpolants

Vary source sizes for each baseline

$$D_{\text{obs}} \equiv \frac{k_S T_{90}}{1+z_S}$$

ROBUST $f_{\text{DM}} = 1$ EXCLUSIONS FOR L2, AU

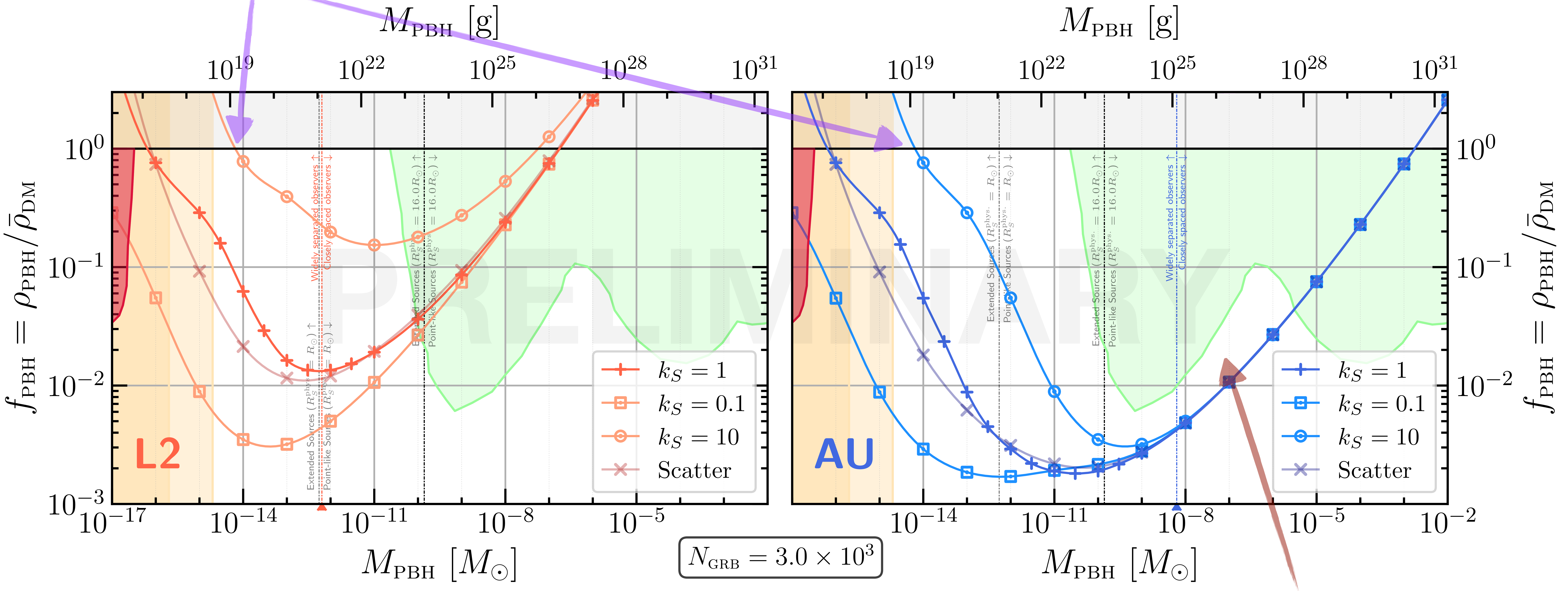

LARGE-MASS REACH AT AU INDEPENDENT OF SOURCE UNCERTAINTIES!

Scenario	Abbrev.	Baseline R_O	$R_O/R_\odot$
Low Earth Orbit	LEO	1.40×10^4 km	0.020
Earth–Moon	EM	3.84×10^5 km	0.55
Lagrange Point 2	L2	1.50×10^6 km	2.15
Astronomical Unit	AU	1.50×10^8 km	215

*markers are computed; lines are log-log cubic spline interpolants

Conclusions

Confirm that picolensing can probe asteroid mass window for PBH DM

GRB source size uncertainties are significant: most the **offset**

Previous studies slightly too optimistic with shorter baselines (e.g., EM)

Larger baselines (L2, AU) overcome systematics issues with source sizes

AU baselines would probe sub-component DM PBHs even above the window

Disk vs Gaussian source profile: not much difference

Outlook: constraints on diffuse lenses (axion stars, mini clusters etc.)?

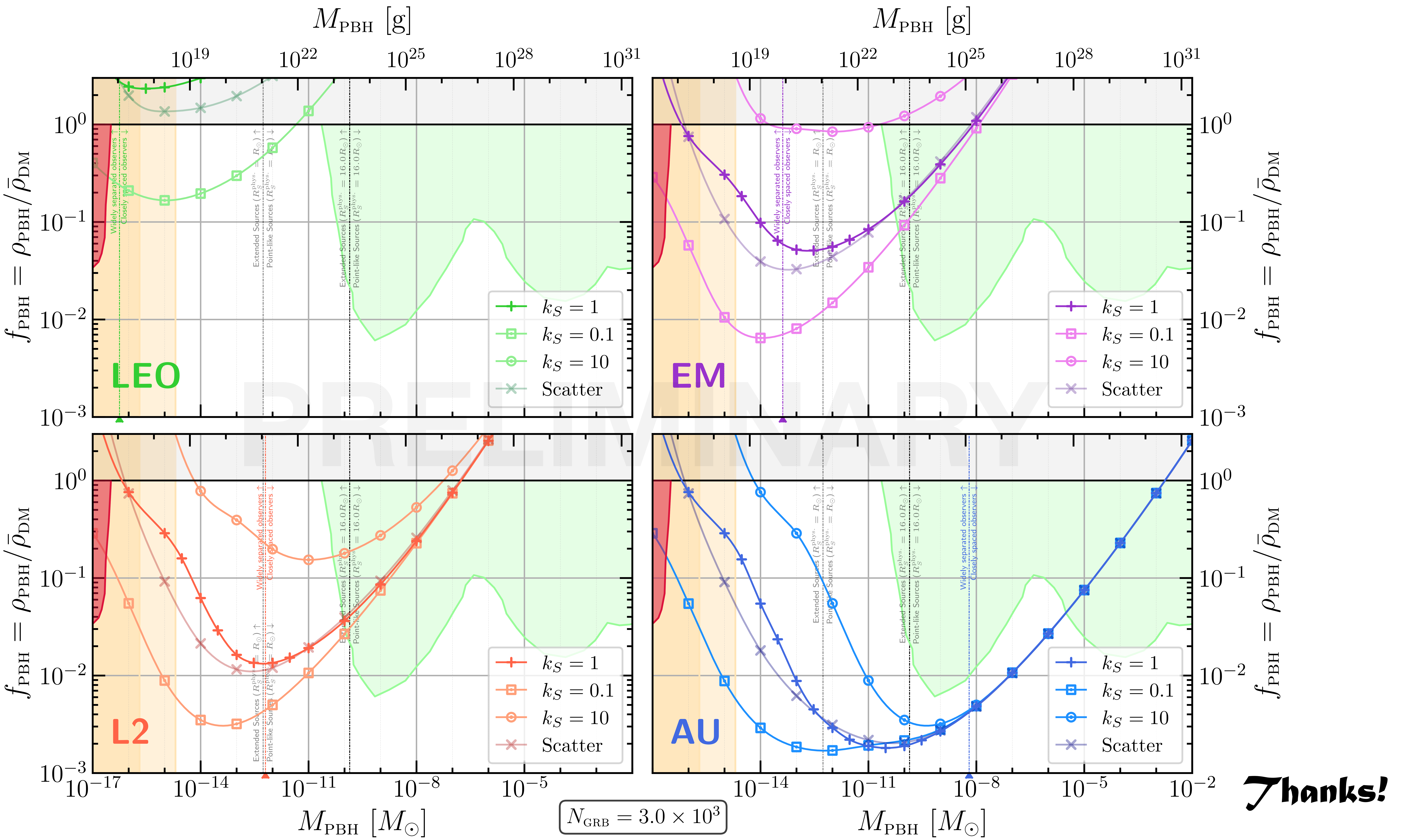

Thanks!

19

Michael A. Fedderke [Perimeter]

BACKUP

Dark Matter

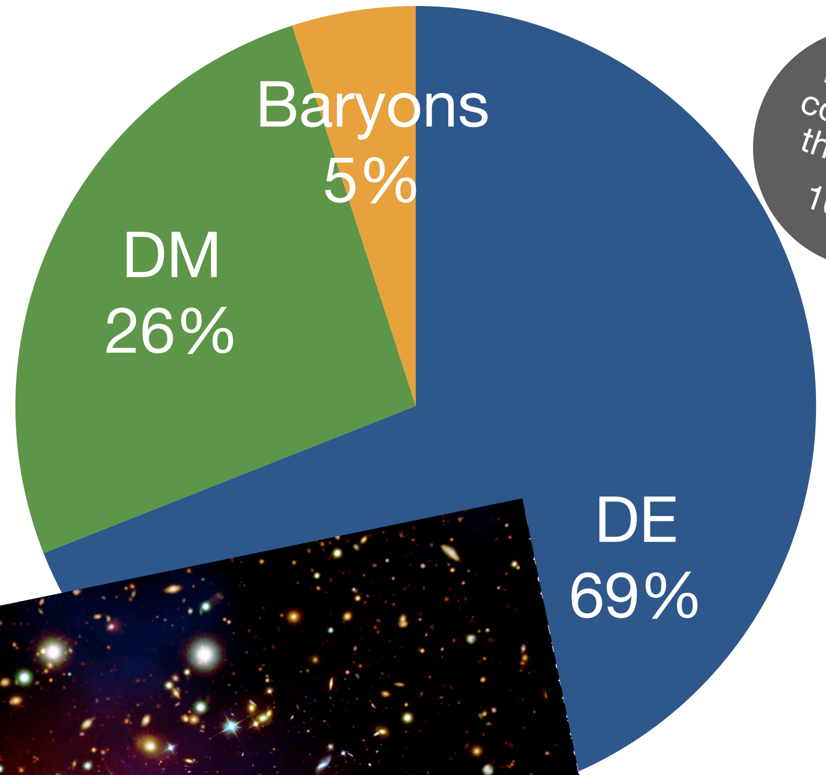

DM talks containing this slide 100%

Unambiguous gravitational evidence

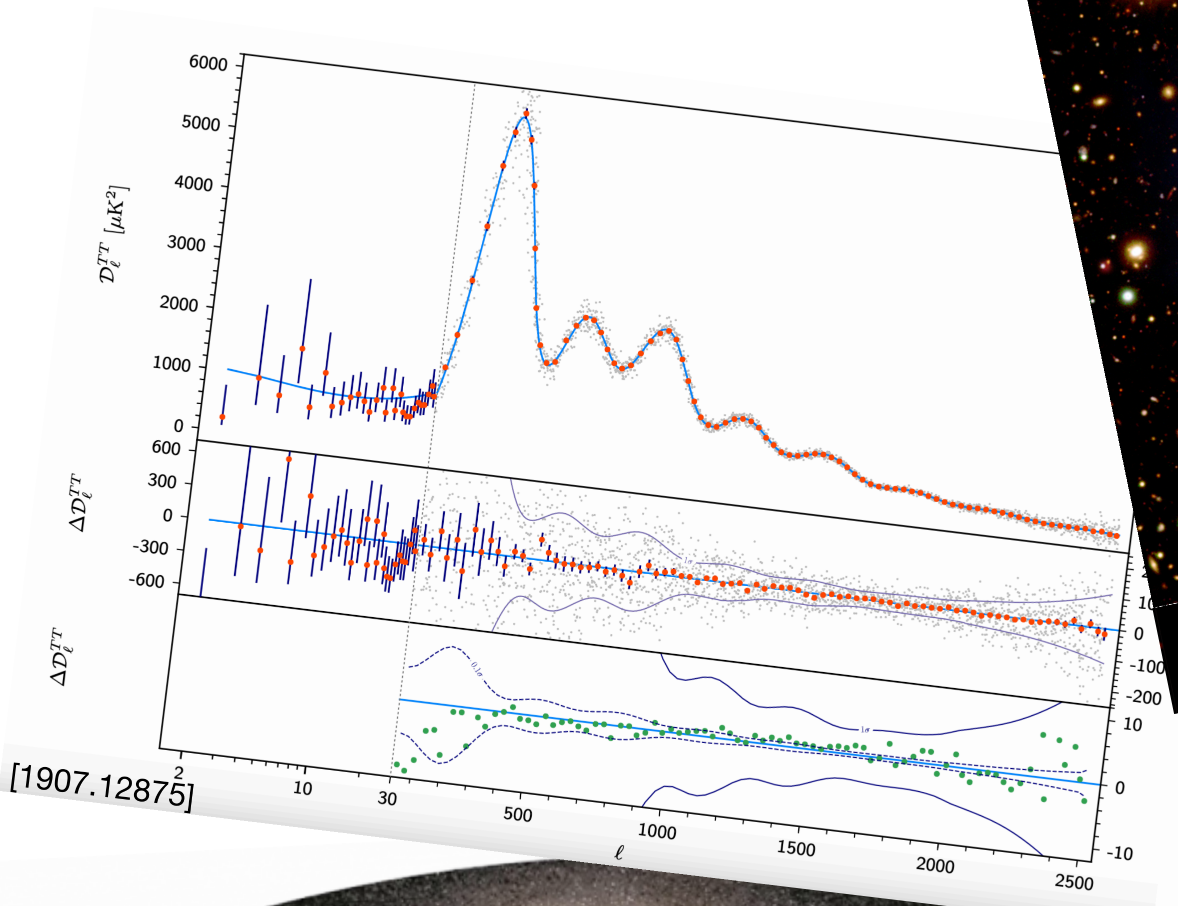

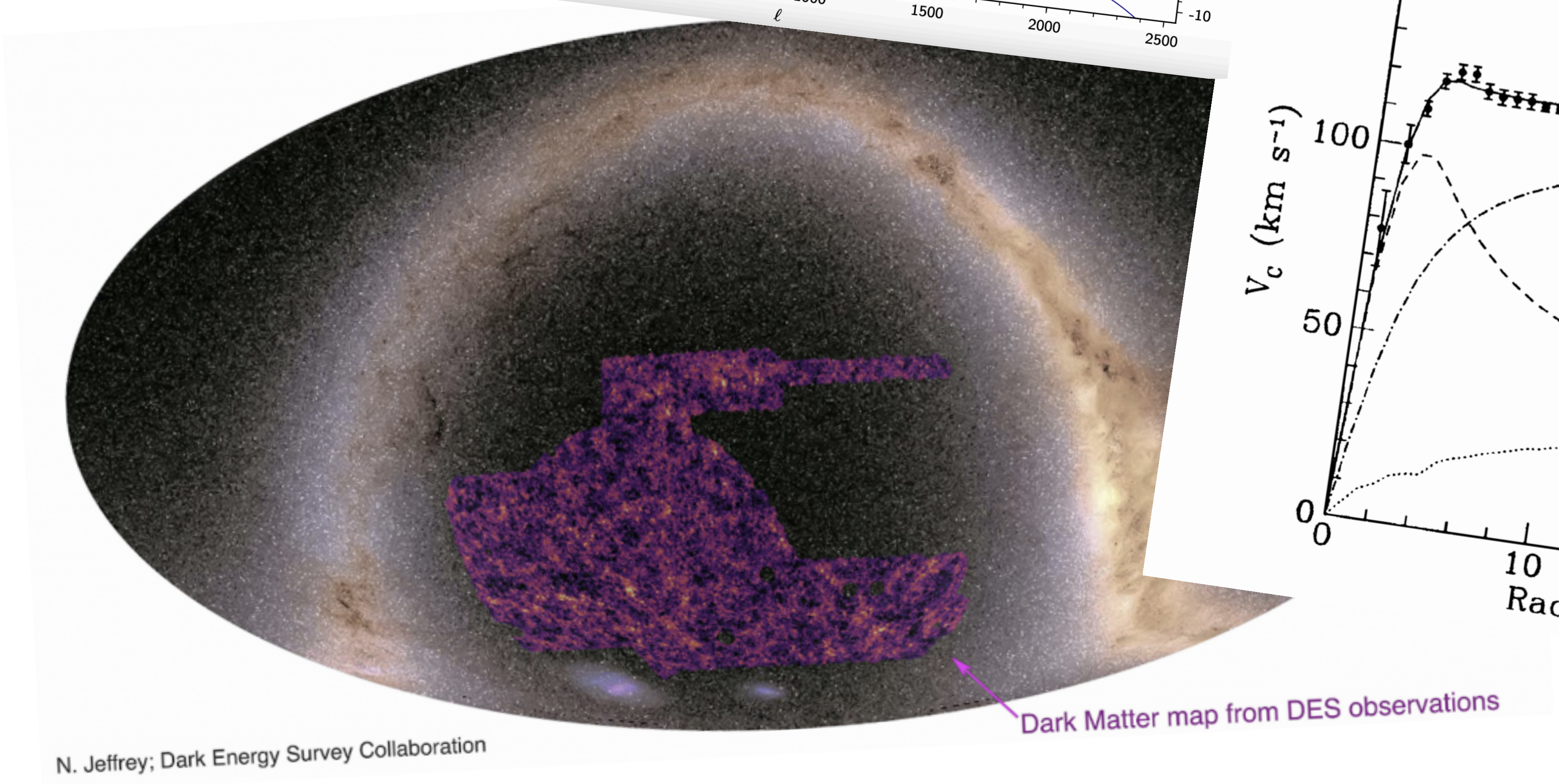

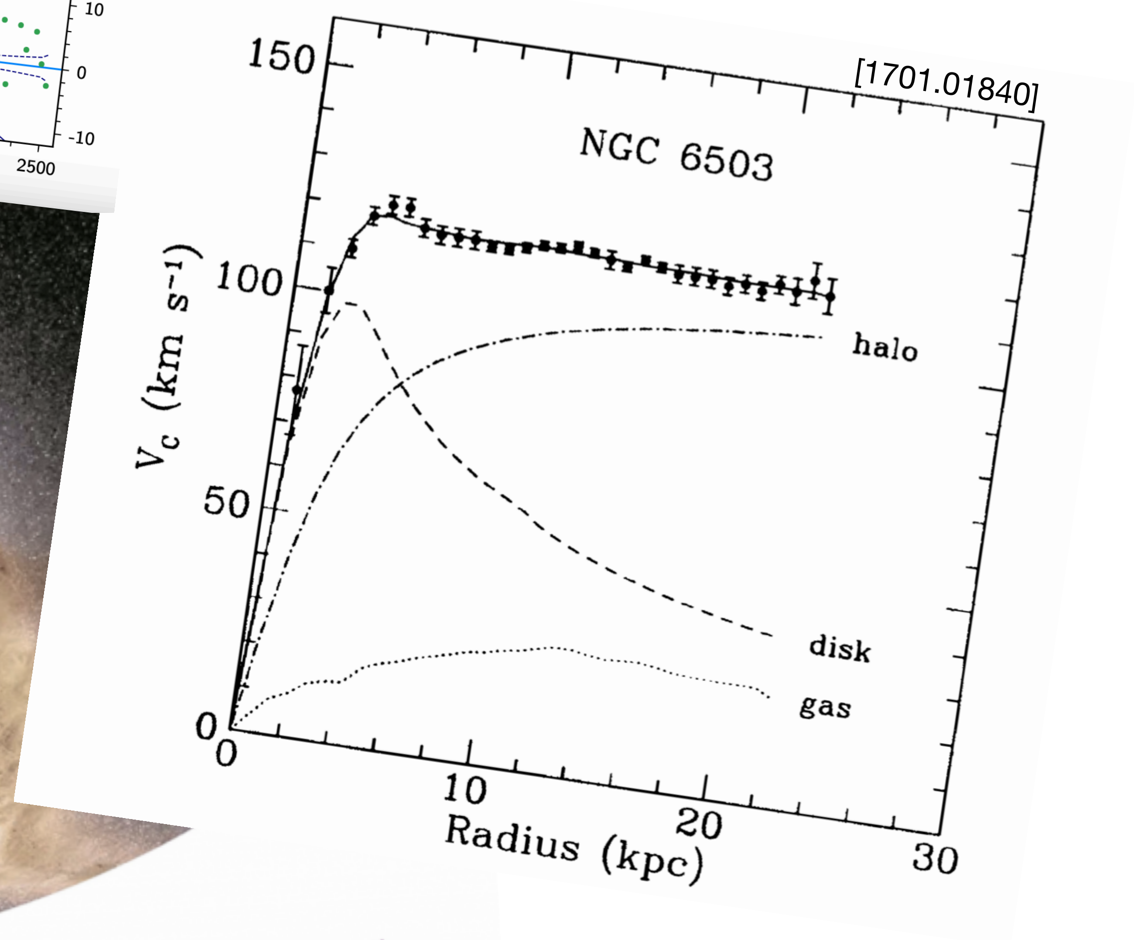

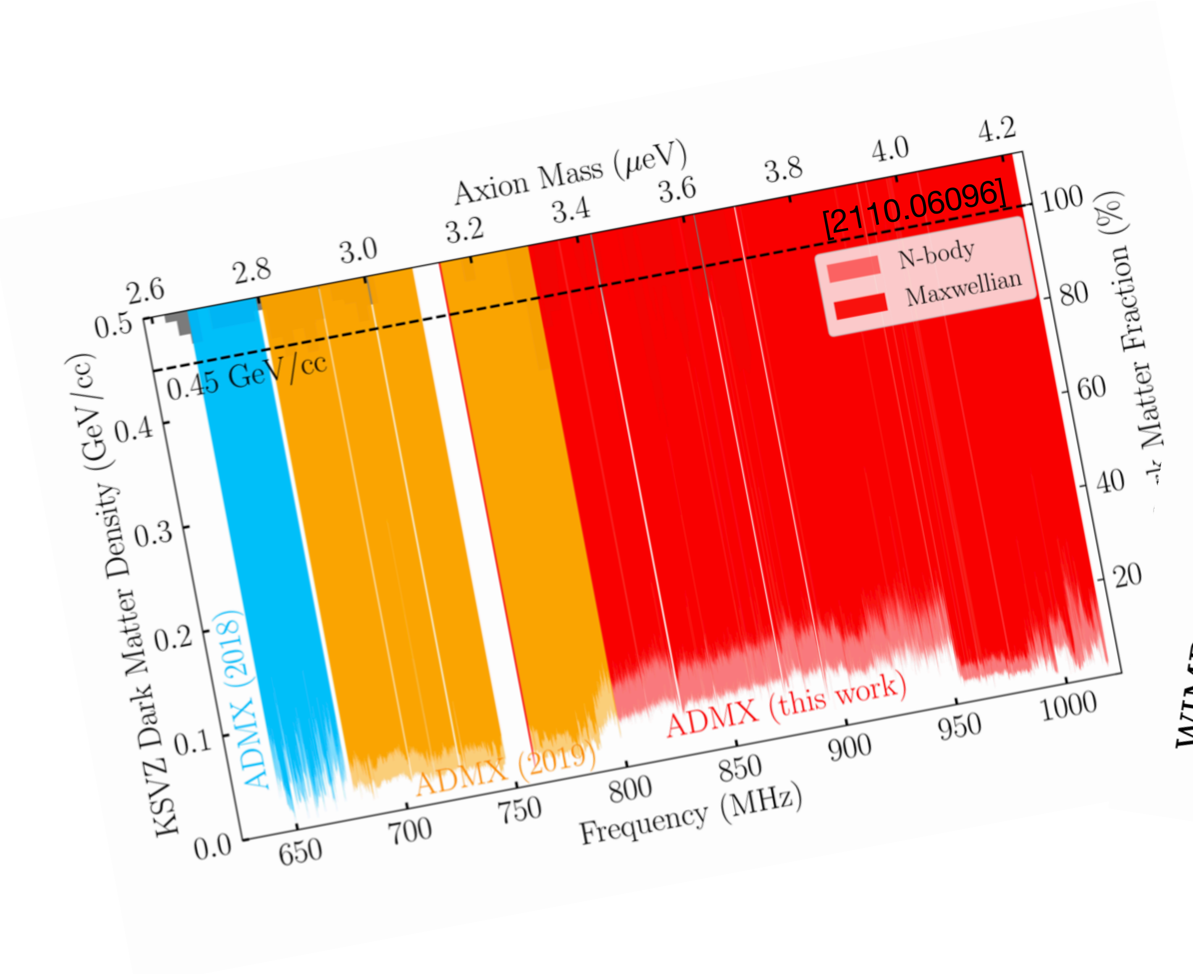

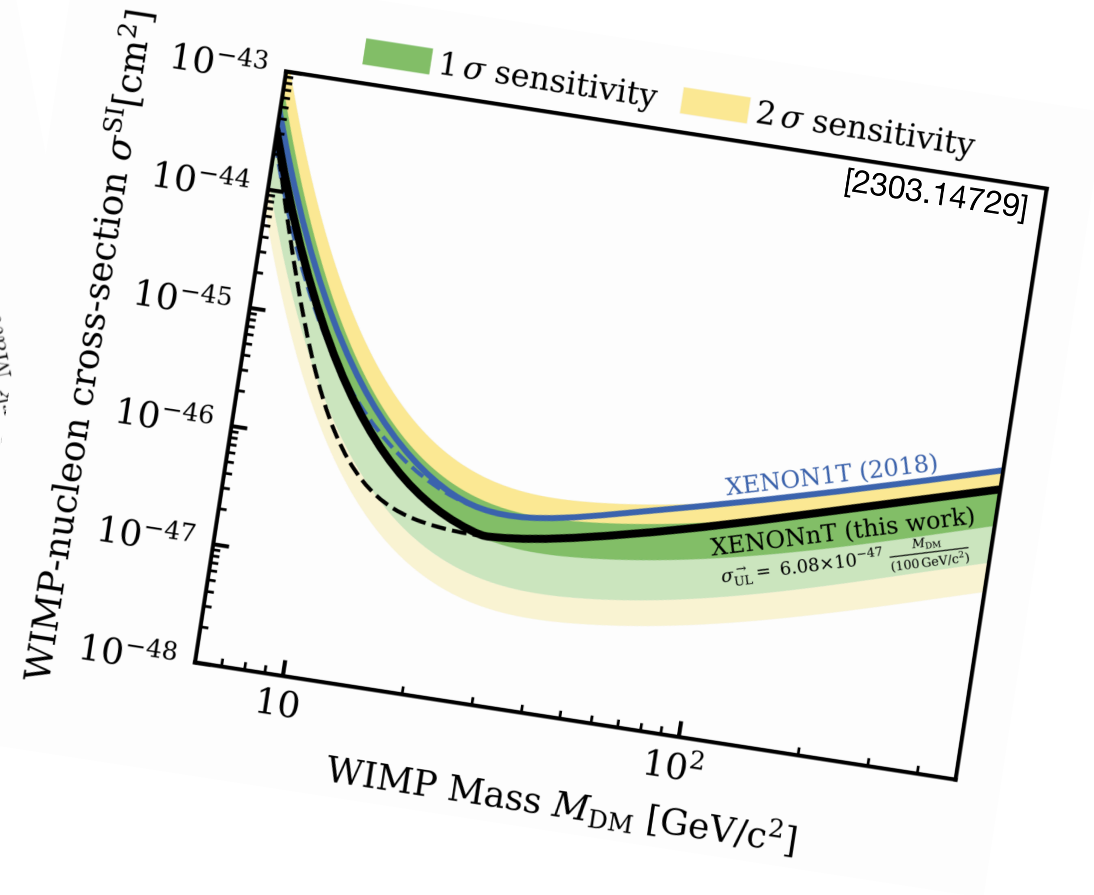

No direct, non-gravitational evidence … yet

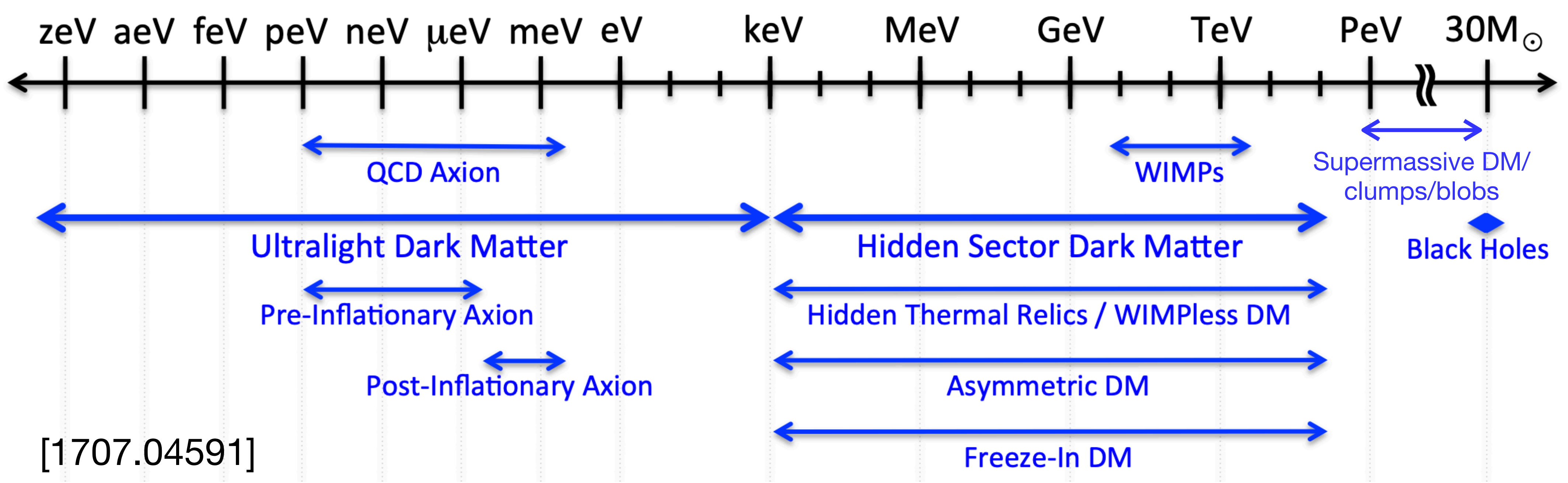

Huge number of possibilities, over many orders of magnitude in mass

Primordial black holes (PBH)

GRAVITATIONALLY COLLAPSED OBJECTS OF VERY LOW MASS

Stephen Hawking

For the purposes of this talk: sub-solar mass black holes $M_{PBH} \ll M_\odot$

Production in the early universe via:

$$M \sim \frac{c^3 t}{G} \sim 10^{15} \left(\frac{t}{10^{-23}\,\mathrm{s}}\right) \mathrm{g}.$$

- Sharp features in the inflationary power spectrum. When these re-enter, direct collapse to BH ensues if density perturbation is large enough

$$\beta \approx \mathrm{Erfc}\left[\frac{\delta_c}{\sqrt{2}\,\sigma}\right].$$

see also [2410.03451]

- Collisions of bubble walls from primordial first-order phase transitions
- … many other variations on these themes

This talk will be **agnostic to the production mechanism**.

The key point for this study is…

Annu. Rev. Nucl. Part. Sci. 2020. 70:355–94
Bernard Carr[1] and Florian Kühnel[2]

Nucl. Phys. B 1003 (2024) 116494
Anne M. Green

A. Escrivà, F. Kuhnel and Y. Tada, *Primordial Black Holes*, arXiv:2211.05767.

A. M. Green and B. J. Kavanagh, *Primordial Black Holes as a dark matter candidate*, *J. Phys. G* **48** (2021) 043001 [arXiv:2007.10722].

Primordial black hole dark matter

… these objects are dark, and are still allowed to be 100% of the DM in certain mass ranges

Hawking Evaporation

- Lifetime
- x-ray flux
- 511 keV
- etc.

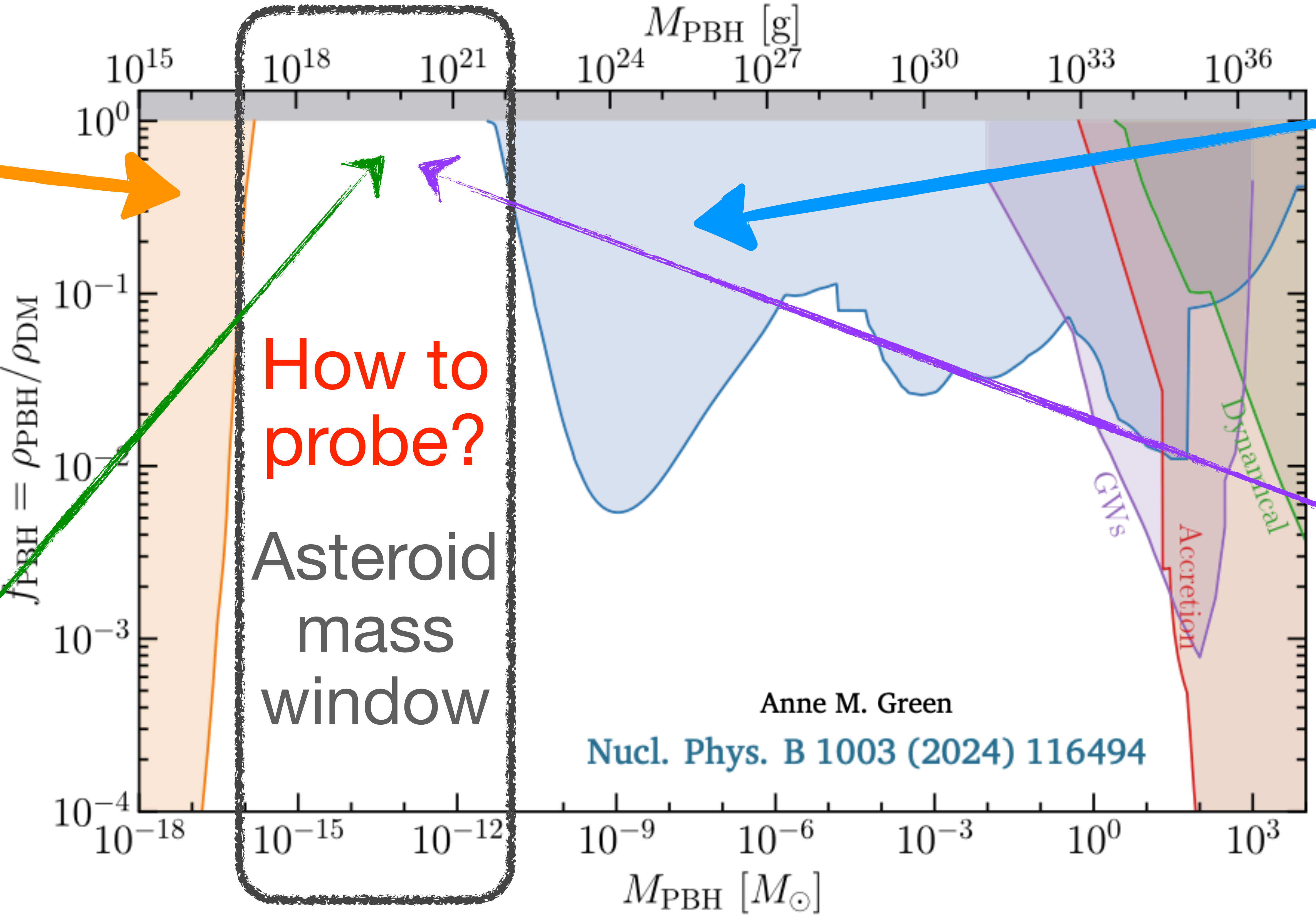

$$M_{\circledast} \sim \frac{4\pi}{3}(2.5\mathrm{g/cm^3})(10\,\mathrm{km})^3 \sim 10^{19}\,\mathrm{g} \sim 5\times 10^{-15} M_\odot$$

Microlensing

Transient brightening of distant stars by single-lensing

SNIa catalysis?

PBH dynamical heating of WD leading to SN ignition [1505.04444,1505.07464]

May not be an effective constraint [1906.05950]

Femtolensing?

Interference patterns in single-lensing spectra

Shown not to work due to source sizes

[1807.11495]

Gravitational Lensing 101

Angular diameter distance → $\mathscr{D} = a\chi = \dfrac{\chi}{1+z}$ ← comoving distance

$$b' = \chi_L \theta = (1 + z_L) b$$

$$b = \mathscr{D}_L \theta$$

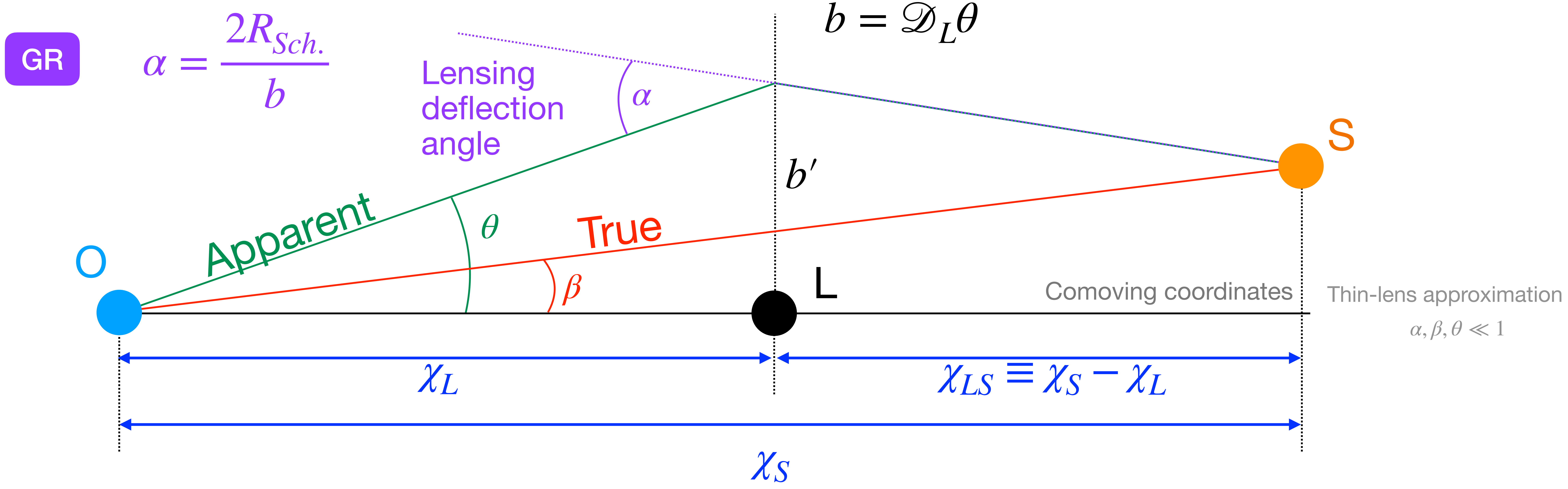

Null geodesics are straight lines in comoving coordinates

Basic geometry ⟶ Lens Equation: $\theta - \beta = \dfrac{\theta_E^2}{\theta}$, where $\theta_E \equiv \sqrt{\dfrac{4G_N M(1+z_L)\chi_{LS}}{\chi_S \chi_L}}$ Einstein angle

$R_{Sch.} = 2G_N M$

Michael A. Fedderke [Perimeter]

Gravitational Lensing 102

$$\theta_E^2 \equiv \frac{4G_N M(1+z_L)\chi_{LS}}{\chi_S \chi_L}$$

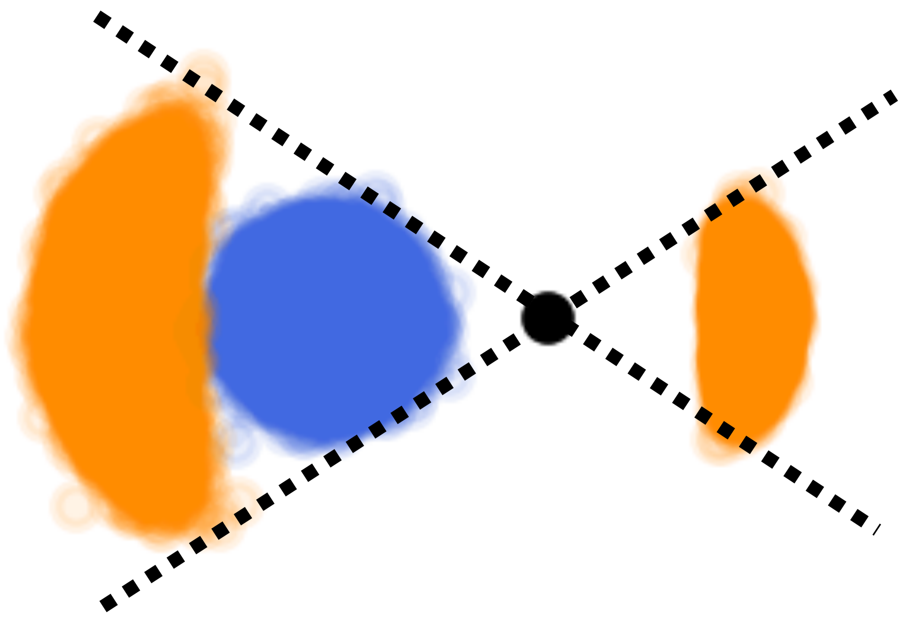

$$y \equiv \frac{\beta}{\theta_E} \quad ; \quad x \equiv \frac{\theta}{\theta_E} \quad \Rightarrow \quad x - y = \frac{1}{x} \quad \Rightarrow x_\pm = \frac{1}{2}\left[y \pm \sqrt{y^2+4}\right]$$

Magnification? Gravitational lensing preserves surface brightness, so

$$\mu \equiv \frac{d\Omega_{\text{apparent}}}{d\Omega_{\text{true}}} = \frac{d\cos\theta}{d\cos\beta} \approx \frac{\theta d\theta}{\beta d\beta} = \frac{xdx}{ydy} \quad \Rightarrow \quad \mu_\pm = \frac{1}{2}\left|1 \pm \frac{y^2+2}{y\sqrt{y^2+4}}\right|$$

Einstein angle is EXTREMELY small for a PBH: $\theta_E \sim 2\,\text{picoarcsec} \times \sqrt{\frac{M}{10^{-12}M_\odot}}$

$[z_S = 1, \chi_L/\chi_S = 0.5\ (z_L = 0.43)]$

Images are not resolved: $\mu \sim \mu_+ + \mu_- = \frac{y^2+2}{\sqrt{y^2(y^2+4)}}$

… if geometrical optics holds

$1\,\text{arcsec} = 4.8 \times 10^{-6}\,\text{rad}$

Michael A. Fedderke [Perimeter]

Finite Sources

$$\mu(y) = \frac{y^2+2}{\sqrt{y^2(y^2+4)}}$$

So far, assumed both the lens and source are point-like.

But all sources have a finite extent!

small-angle/
flat-sky approx

$$\bar{\mu}(\vec{Y}) = \iint d^2w\, \mathcal{I}(\vec{w}) \cdot \mu\left(y = |\vec{Y} - \vec{w}|\right)$$

Source-averaged magnification for lens at location $\vec{Y}$ relative to source centroid

Source brightness profile at location $\vec{w}$ relative to the source centroid

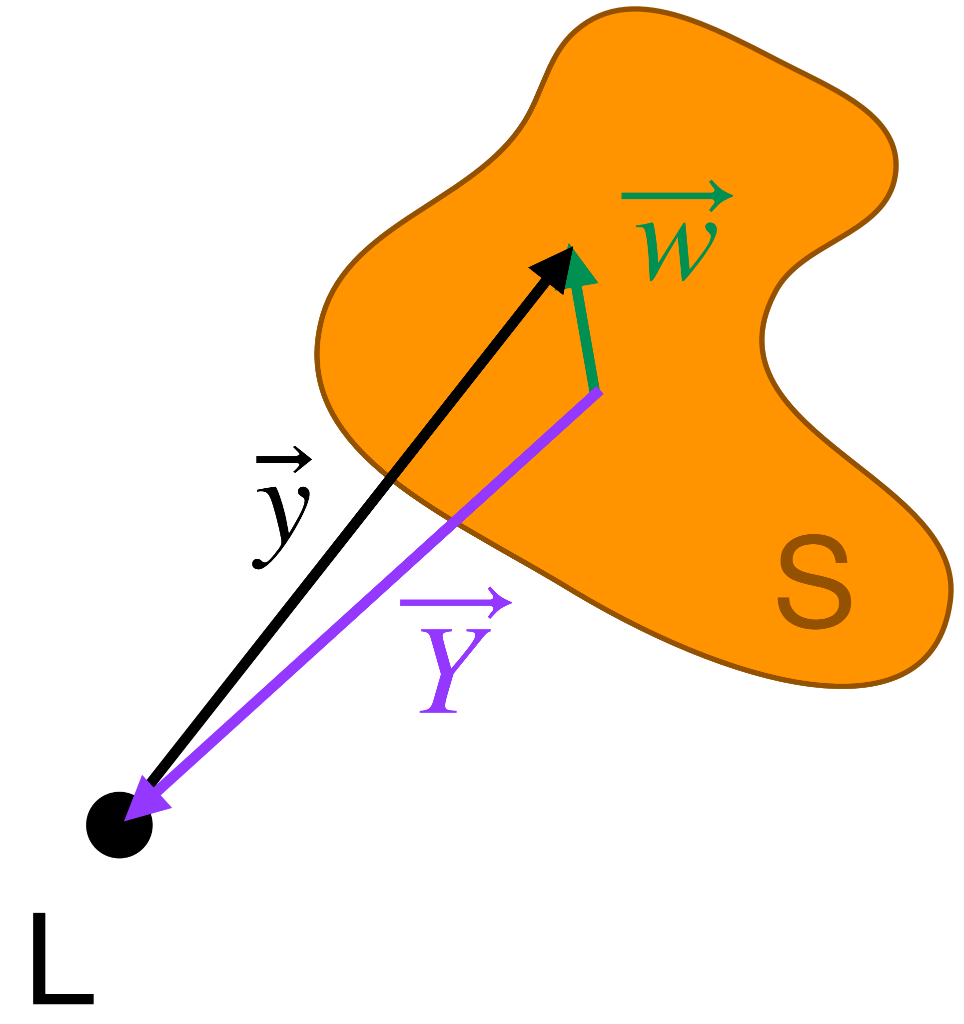

We'll consider both Gaussian and flat disk source profiles

Gaussian source

$$y' \equiv k_G \frac{\vartheta_L}{\vartheta_S} \qquad \delta \equiv \frac{1}{k_G}\frac{\vartheta_S}{\theta_E}$$

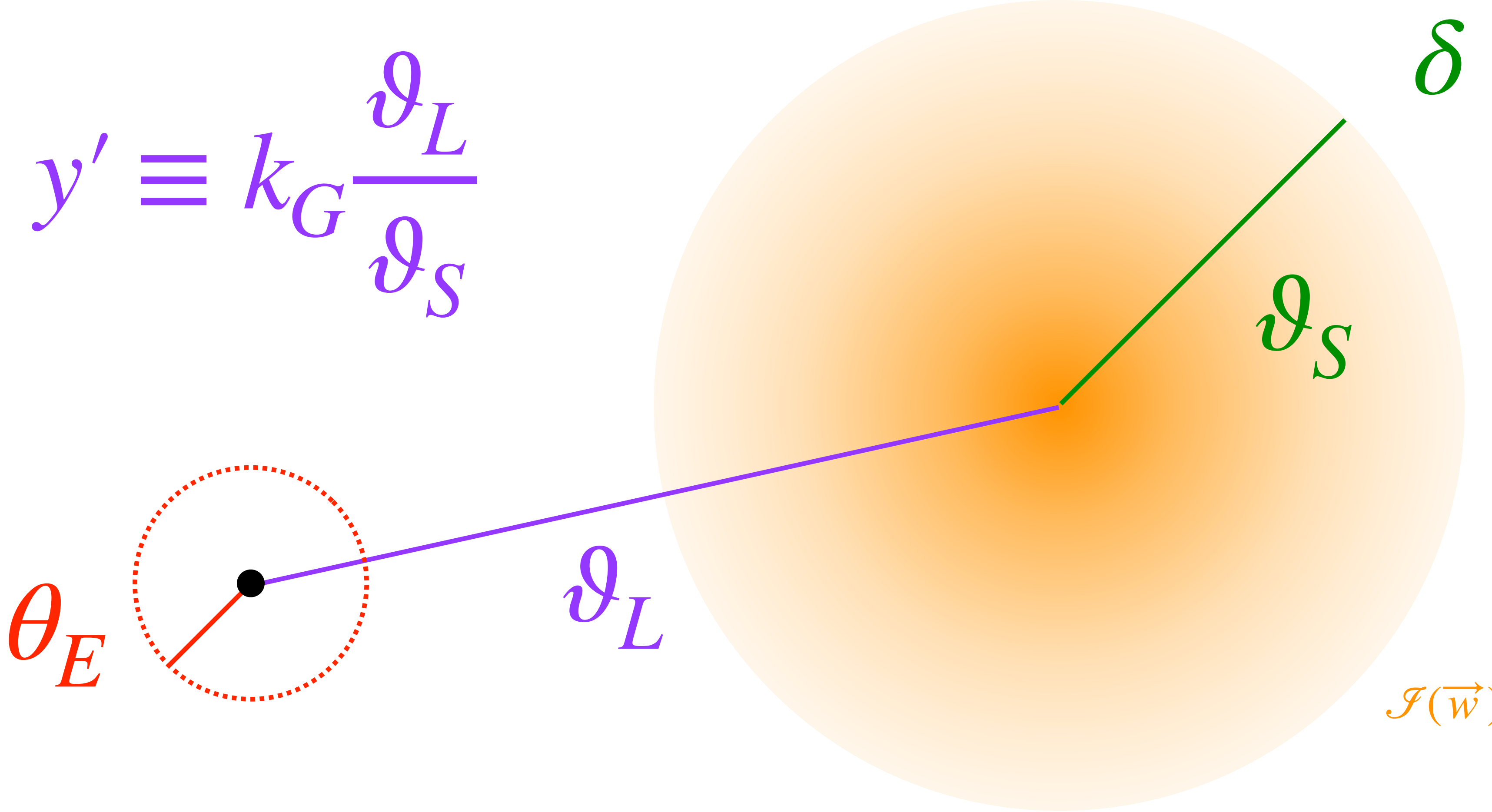

$$\mathcal{I}(\vec{w}) = \frac{1}{2\pi\delta^2}\exp\left[-\frac{|\vec{w}|^2}{2\delta^2}\right]$$

$$\bar{\mu}(y',\delta) = \frac{e^{-(y')^2/2}}{\delta}\int_0^\infty dx \frac{e^{-x^2/2}\left[2+(x\delta)^2\right] I_0(xy')}{\sqrt{4+(x\delta)^2}}$$

not tractable in closed form

Point-like behaviour $\vartheta_S \ll \theta_E$

$$\bar{\mu}(\vartheta_L \lesssim \vartheta_S) \sim 1 + \sqrt{\frac{\pi k_G^2}{2}\frac{\theta_E}{\vartheta_S}} \gg 1$$

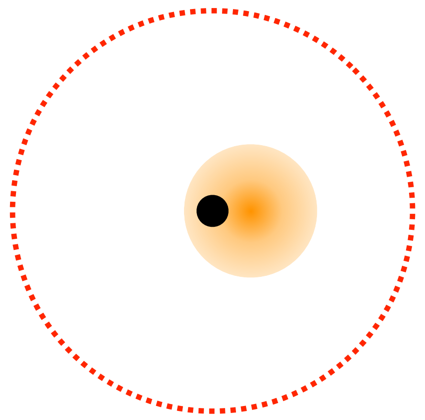

Regulated from true point-source collinear divergence $\mu \propto \frac{\theta_E}{\vartheta_L}$

$$\bar{\mu}(\vartheta_S \ll \vartheta_L \ll \theta_E) \sim 1 + \frac{\theta_E}{\vartheta_L} \gg 1$$

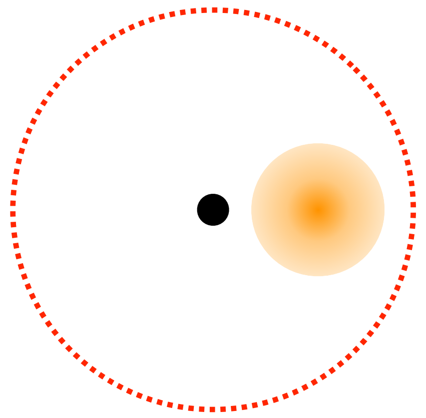

$$\bar{\mu}(\vartheta_L \gg \theta_E) \sim 1 + 2\left(\frac{\theta_E}{\vartheta_L}\right)^4 \sim 1$$

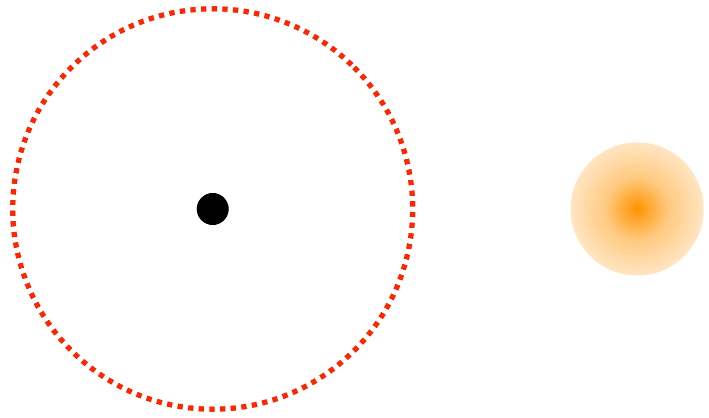

Extended source $\vartheta_S \gg \theta_E$ **

$$\bar{\mu}(\vartheta_L \lesssim \vartheta_S + \text{few} \times \theta_E) \sim 1 + \frac{k_G^2\theta_E^2}{\vartheta_S^2}\exp\left[-\frac{k_G^2\vartheta_L^2}{2\vartheta_S^2}\right]$$

~Ratio of lensed area to total area

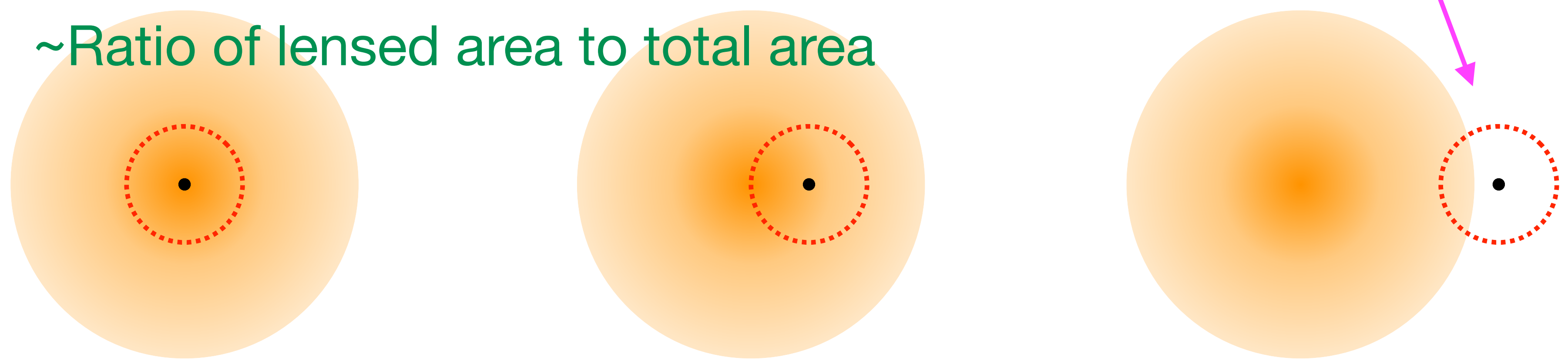

$$\bar{\mu}(\vartheta_L \gg \theta_E, \vartheta_S) \sim 1 + 2\left(\frac{\theta_E}{\vartheta_L}\right)^4 \sim 1$$

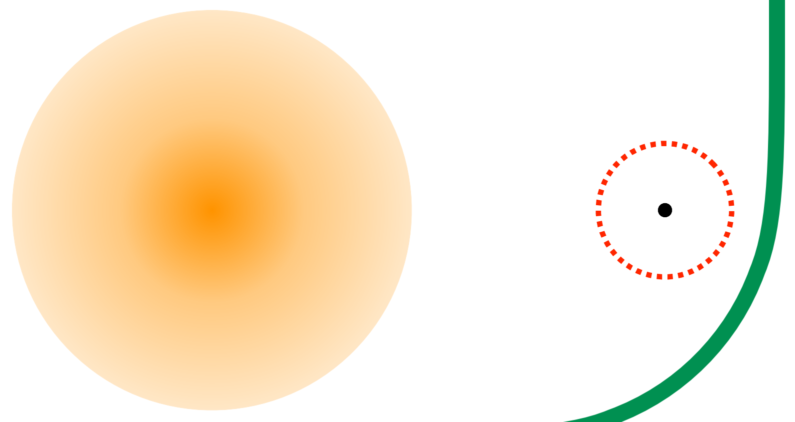

The factor $k_G = \sqrt{-2\ln(1-f_{\text{cover}})} \sim 2.1$ is a normalisation such that $2\pi\int_0^{\vartheta_S/\theta_E} w\,dw\,\mathcal{I}(w) \equiv f_{\text{cover}} \sim 0.9$

** this is a slight oversimplification

Michael A. Fedderke [Perimeter]

Picolensing cross-section

$$\rho = \rho(\{\theta_L, \phi_L, z_L, M\}, \{z_S, \theta_S, f_s\}, \{R_O, \theta_O, A_b, A_s, f_b, T\})$$

Fix: lens distance, lens mass, source parameters, observer parameters.

SNR $\rho = \rho(\theta_L, \phi_L)$.

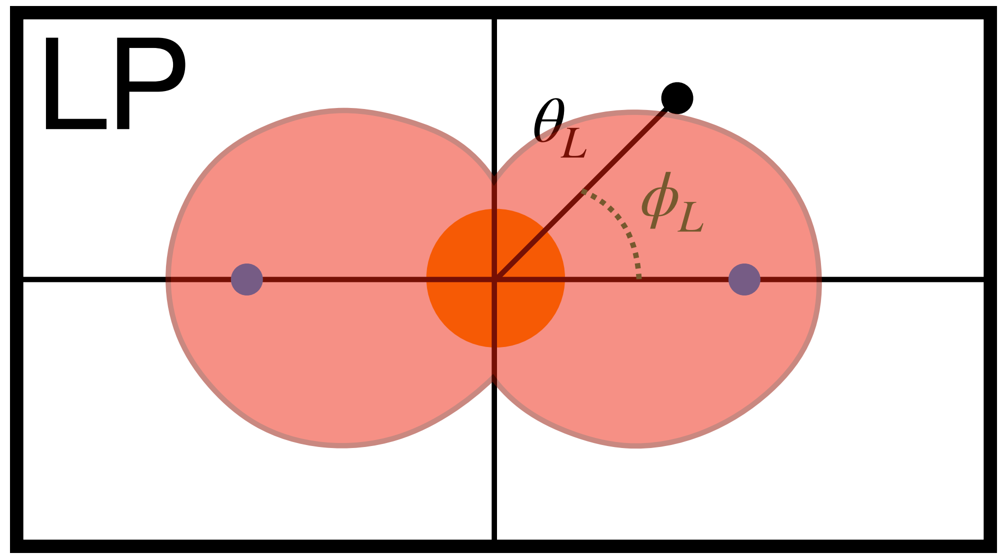

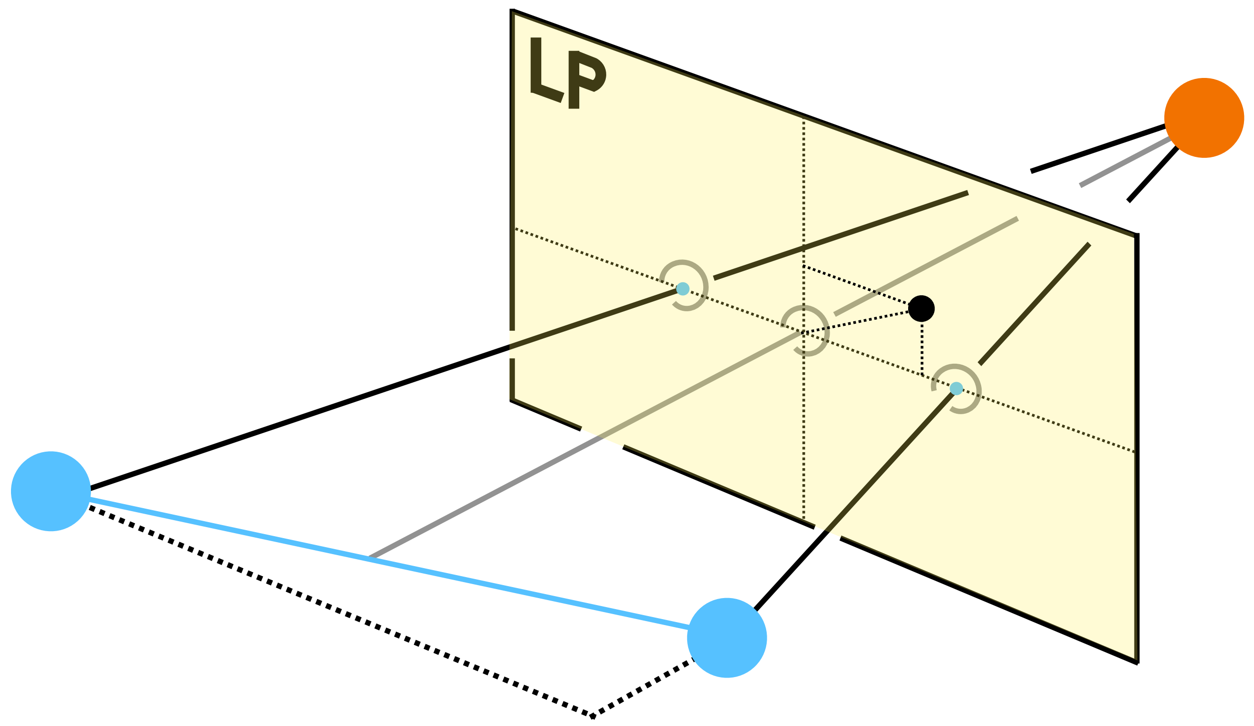

Is <u>any lens</u> detectable at some threshold SNR ρ_*?

$\rho \geq \rho_*$ defines region in the lens plane where lensing is detectable. Can be multiple disjoint regions!

Lensing cross-section σ is the area of that region (comoving): $\sigma = \sigma(\rho_*)$

Compute this using Monte Carlo methods (sample LP area with lenses randomly)

after: Gawade, More, Bhalerao [2308.01775]

Computing σ

Monte Carlo methods

Pick an appropriate sample area in the positive half-plane of the lens plane

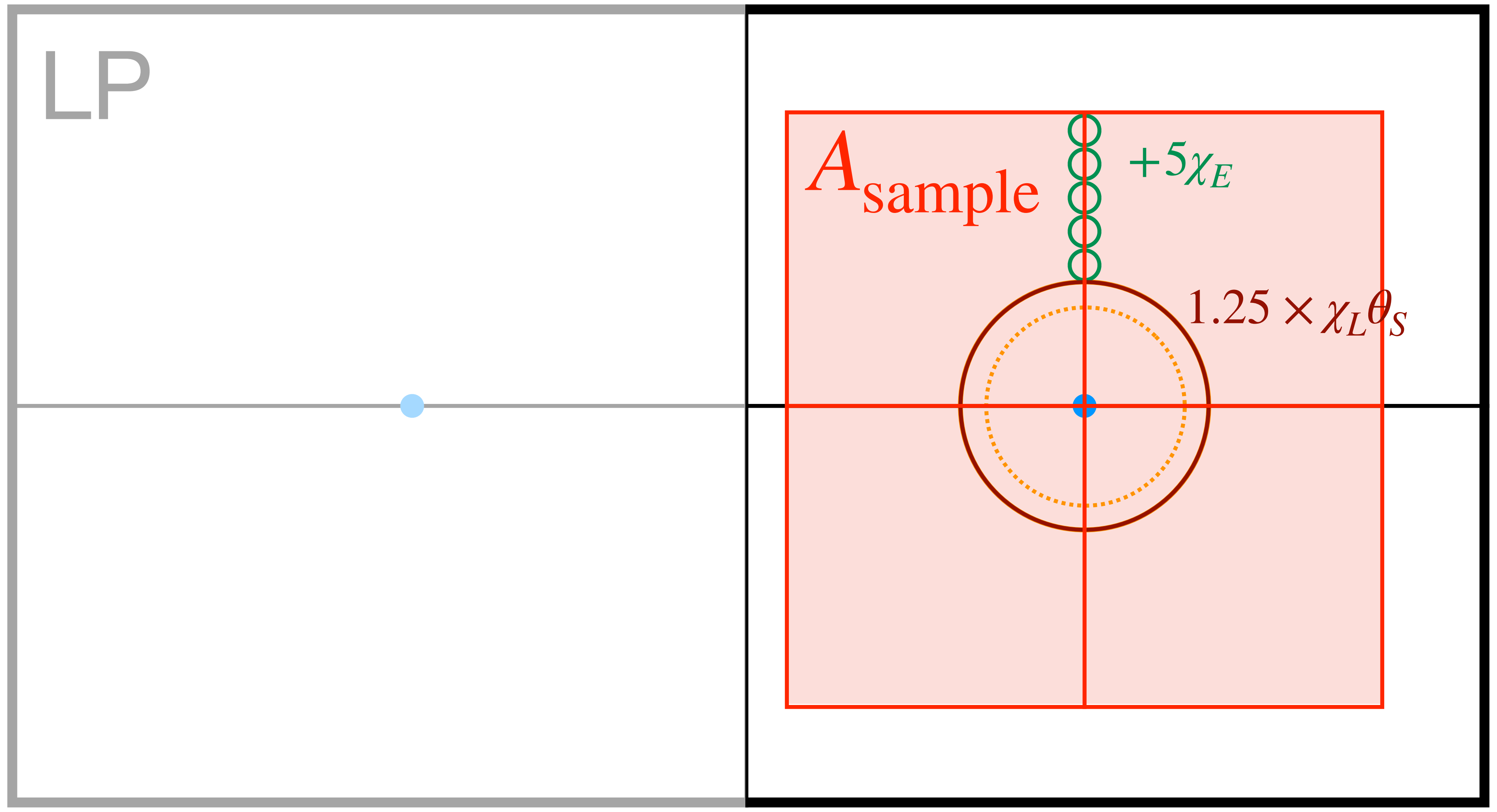

Populate with N_{lens} lenses randomly sampled in 2D; $N_{\text{lens}} = 20000$ (100000 if needed)

Compute $\bar{\mu}_i^k$ for $i = 1,2$ and ρ^k for $k = 1,\ldots,N_{\text{lens}}$. Count the fraction f_ρ with $\rho^k \geq \rho_*$

Cross-section is $\sigma = 2A_{\text{sample}} \times f_\rho$ (the 2 accounts for the reflection symmetry)

after: Gawade, More, Bhalerao [2308.01775]

Michael A. Fedderke [Perimeter]

Computing σ

Monte Carlo methods

Pick an appropriate sample area in the positive half-plane of the lens plane

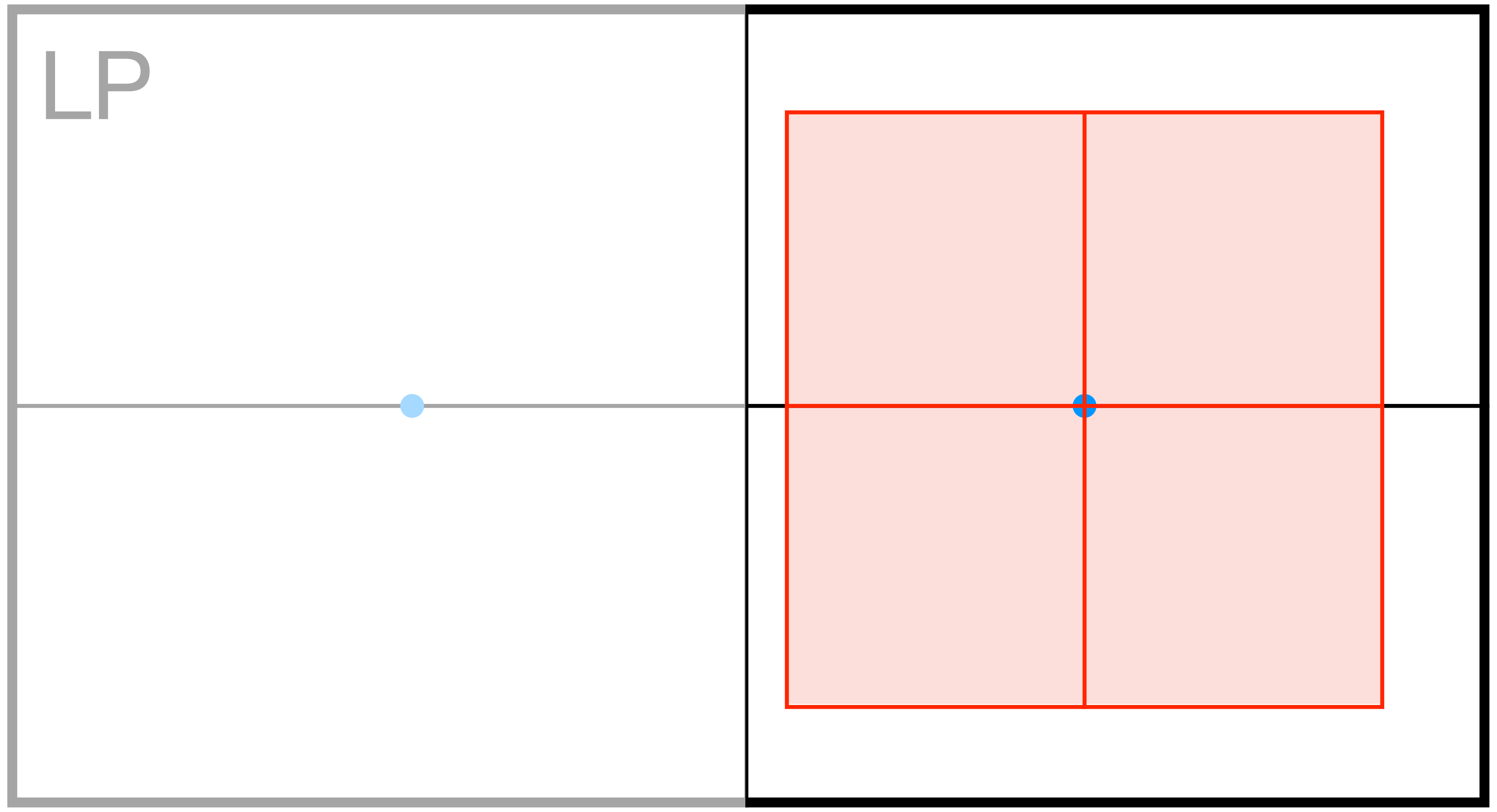

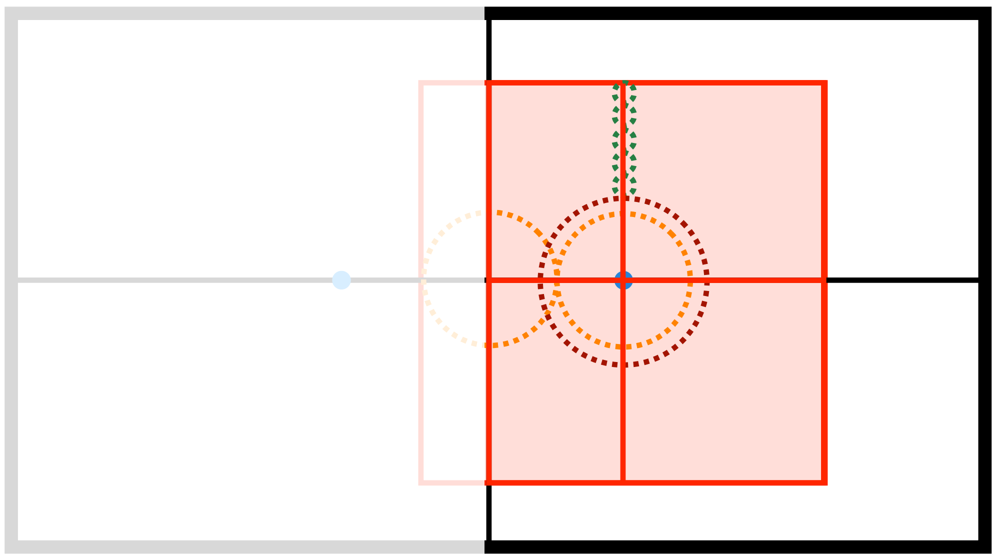

A_{sample} reduced if the box crosses the symmetry axis

Populate with N_{lens} lenses randomly sampled in 2D; $N_{\text{lens}} = 20000\ (100000 \text{ if needed})$

Compute $\bar{\mu}_i^k$ for $i = 1{,}2$ and ρ^k for $k = 1,\ldots,N_{\text{lens}}$. Count the fraction f_ρ with $\rho^k \geq \rho_*$

Cross-section is $\sigma = 2A_{\text{sample}} \times f_\rho$ (the 2 accounts for the reflection symmetry)

after: Gawade, More, Bhalerao [2308.01775]

Michael A. Fedderke [Perimeter]

Computing σ

Monte Carlo methods

Pick an appropriate sample area in the positive half-plane of the lens plane

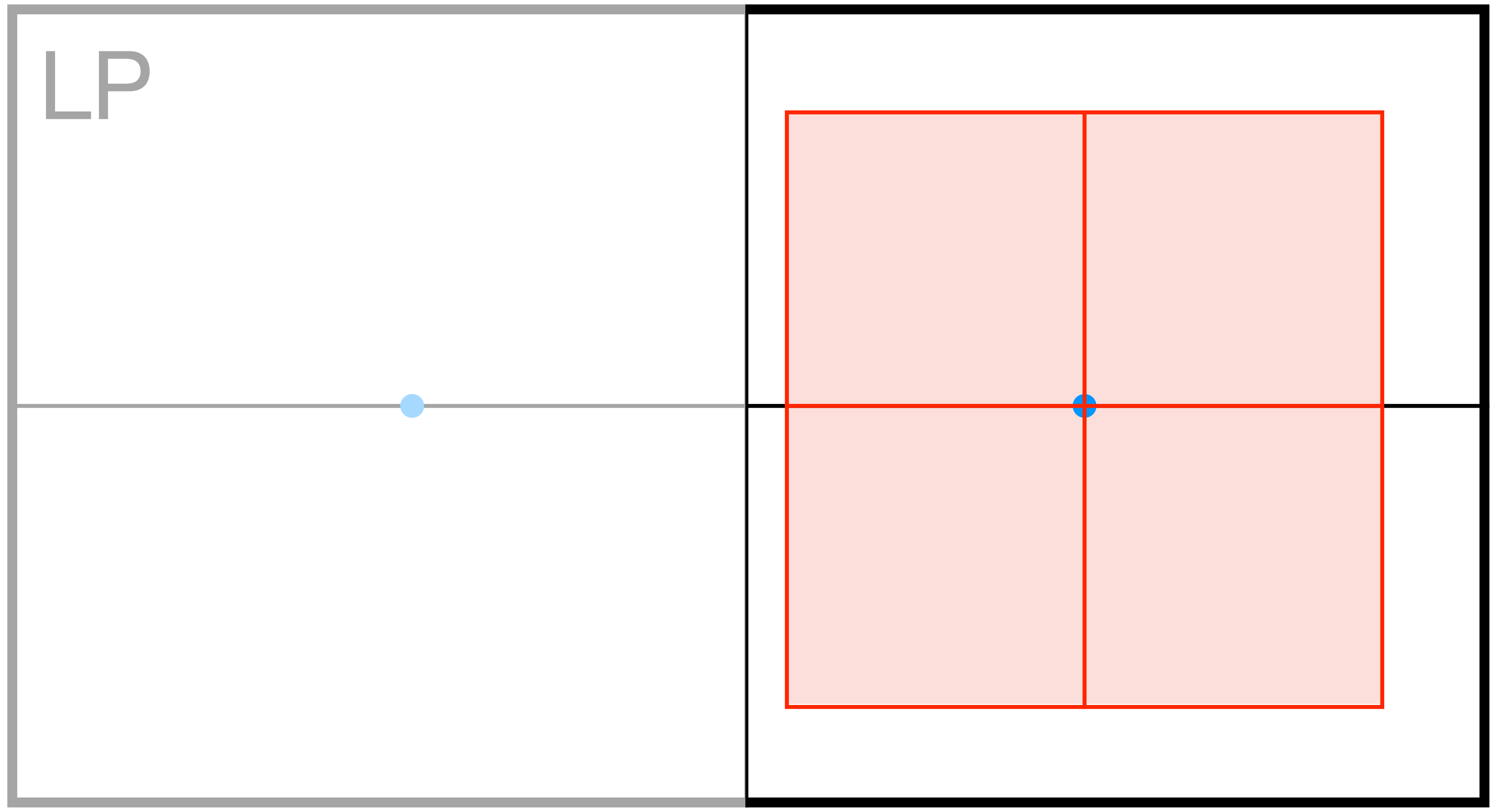

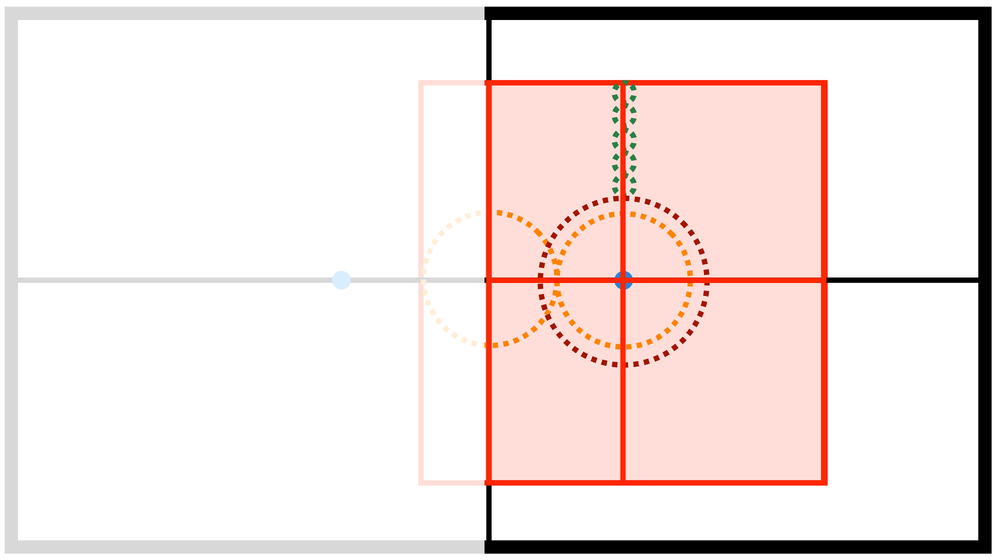

A_{sample} reduced if the box crosses the symmetry axis

Populate with N_{lens} lenses randomly sampled in 2D; $N_{\text{lens}} = 20000 \text{ (100000 if needed)}$

Compute $\bar{\mu}_i^k$ for $i = 1{,}2$ and ρ^k for $k = 1,\ldots,N_{\text{lens}}$. Count the fraction f_ρ with $\rho^k \geq \rho_*$

Cross-section is $\sigma = 2A_{\text{sample}} \times f_\rho$ (the 2 accounts for the reflection symmetry)

after: Gawade, More, Bhalerao [2308.01775]

Computing σ

Monte Carlo methods

Pick an appropriate sample area in the positive half-plane of the lens plane

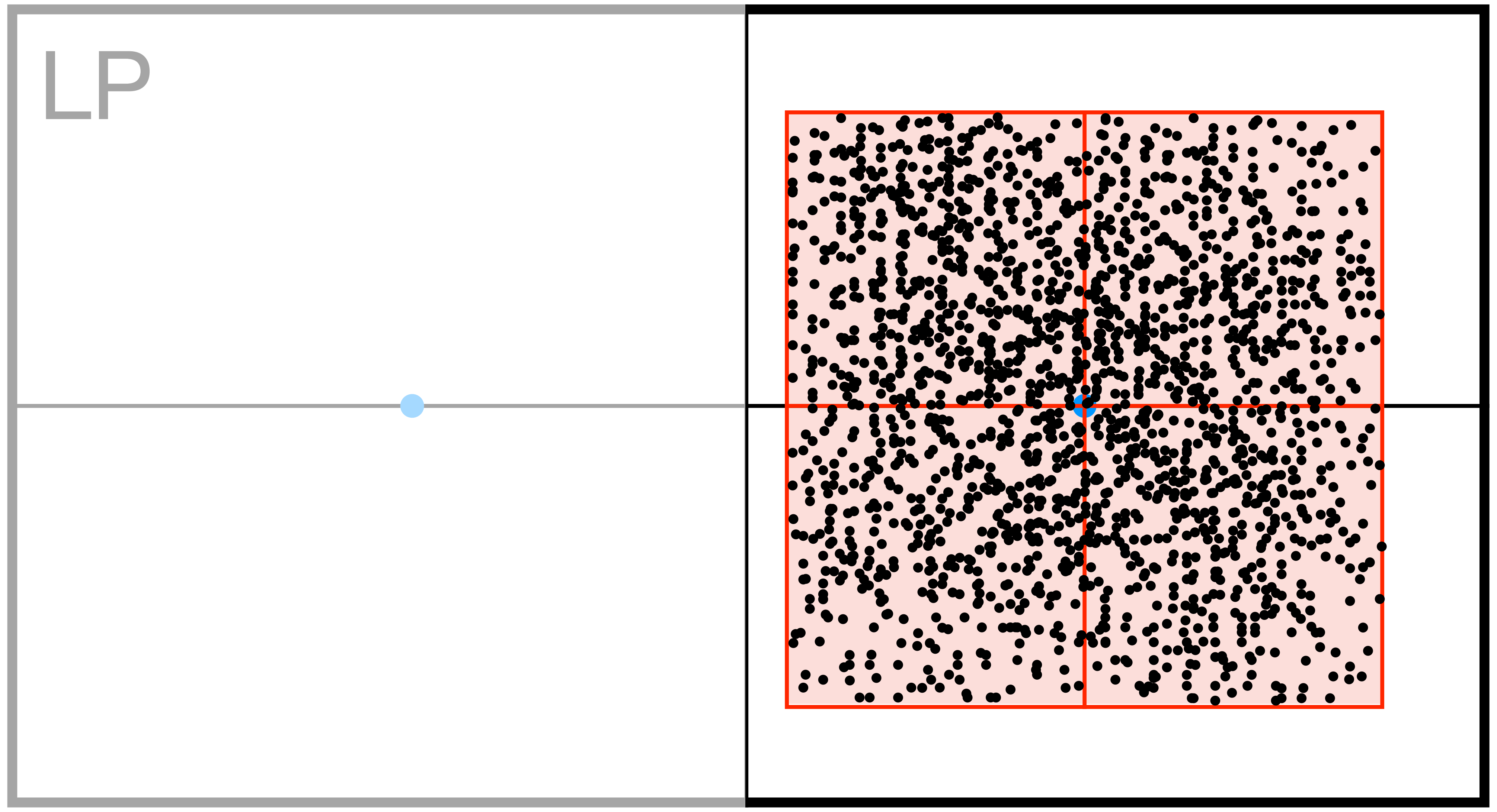

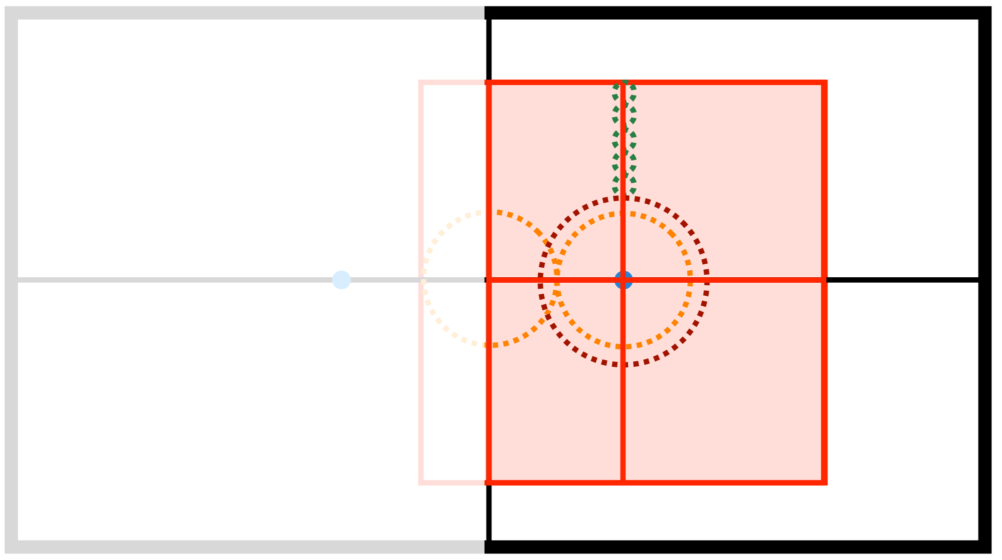

$A_{\rm sample}$ reduced if the box crosses the symmetry axis

Populate with $N_{\rm lens}$ lenses randomly sampled in 2D; $N_{\rm lens} = 20000$ (100000 if needed)

Compute $\bar{\mu}_i^k$ for $i = 1,2$ and ρ^k for $k = 1,\ldots,N_{\rm lens}$. Count the fraction f_ρ with $\rho^k \geq \rho_*$

Cross-section is $\sigma = 2A_{\rm sample} \times f_\rho$ (the 2 accounts for the reflection symmetry)

after: Gawade, More, Bhalerao [2308.01775]

Michael A. Fedderke [Perimeter]

Computing σ

Monte Carlo methods

Pick an appropriate sample area in the positive half-plane of the lens plane

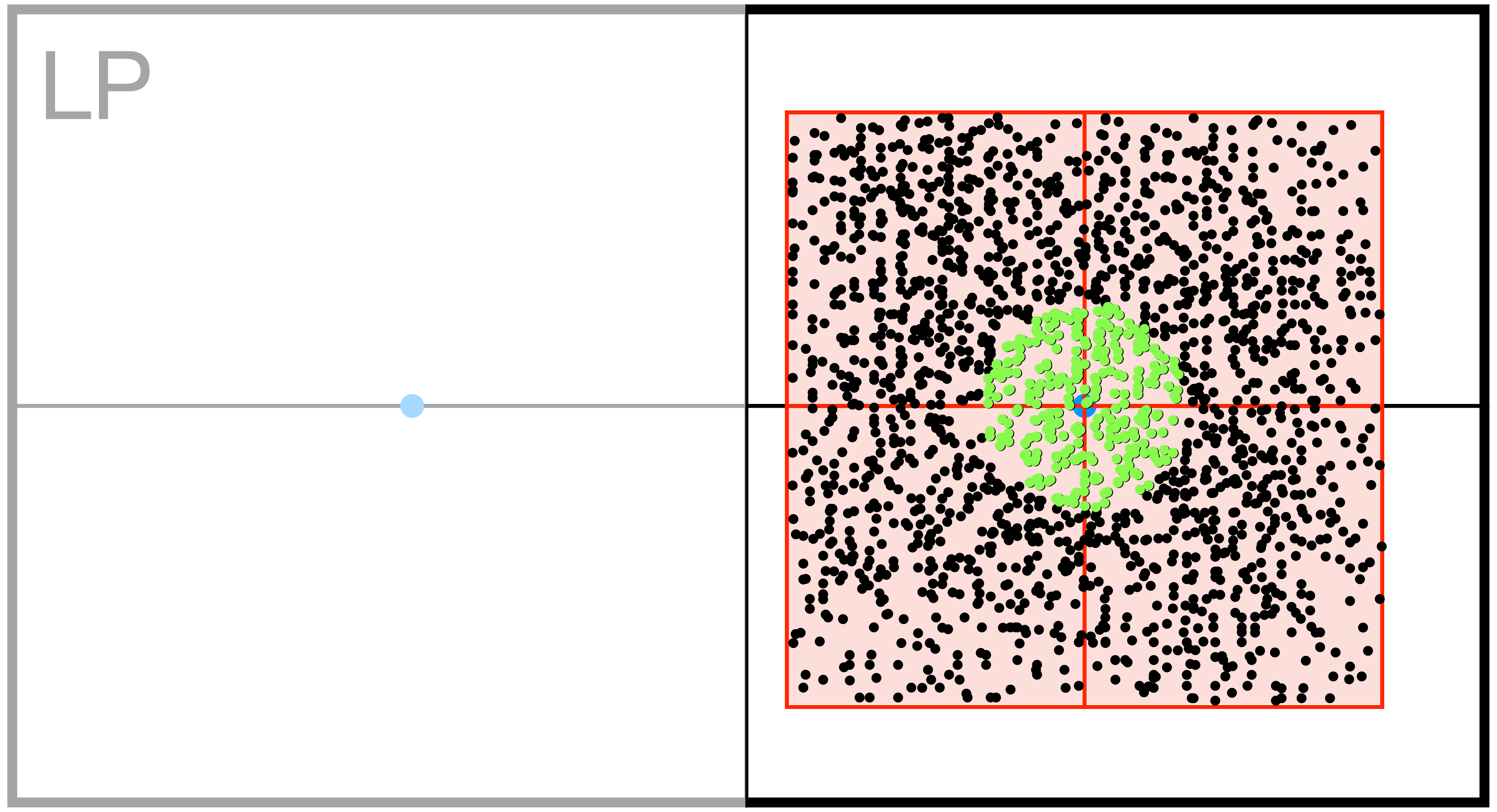

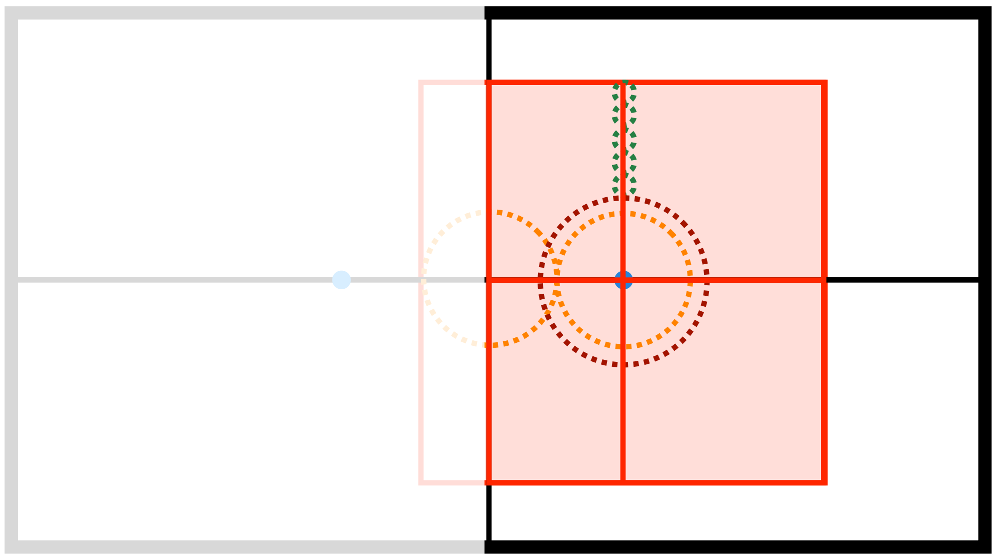

$A_{\rm sample}$ reduced if the box crosses the symmetry axis

Populate with $N_{\rm lens}$ lenses randomly sampled in 2D; $N_{\rm lens} = 20000$ (100000 if needed)

Compute $\bar{\mu}_i^k$ for $i = 1,2$ and ρ^k for $k = 1,\ldots,N_{\rm lens}$. Count the fraction f_ρ with $\rho^k \geq \rho_*$

Cross-section is $\sigma = 2A_{\rm sample} \times f_\rho$ (the 2 accounts for the reflection symmetry)

We also test that no $\rho^k \geq \rho_*$ are too close to sample box edges

after: Gawade, More, Bhalerao [2308.01775]

Computing σ

Monte Carlo methods

Pick an appropriate sample area in the positive half-plane of the lens plane

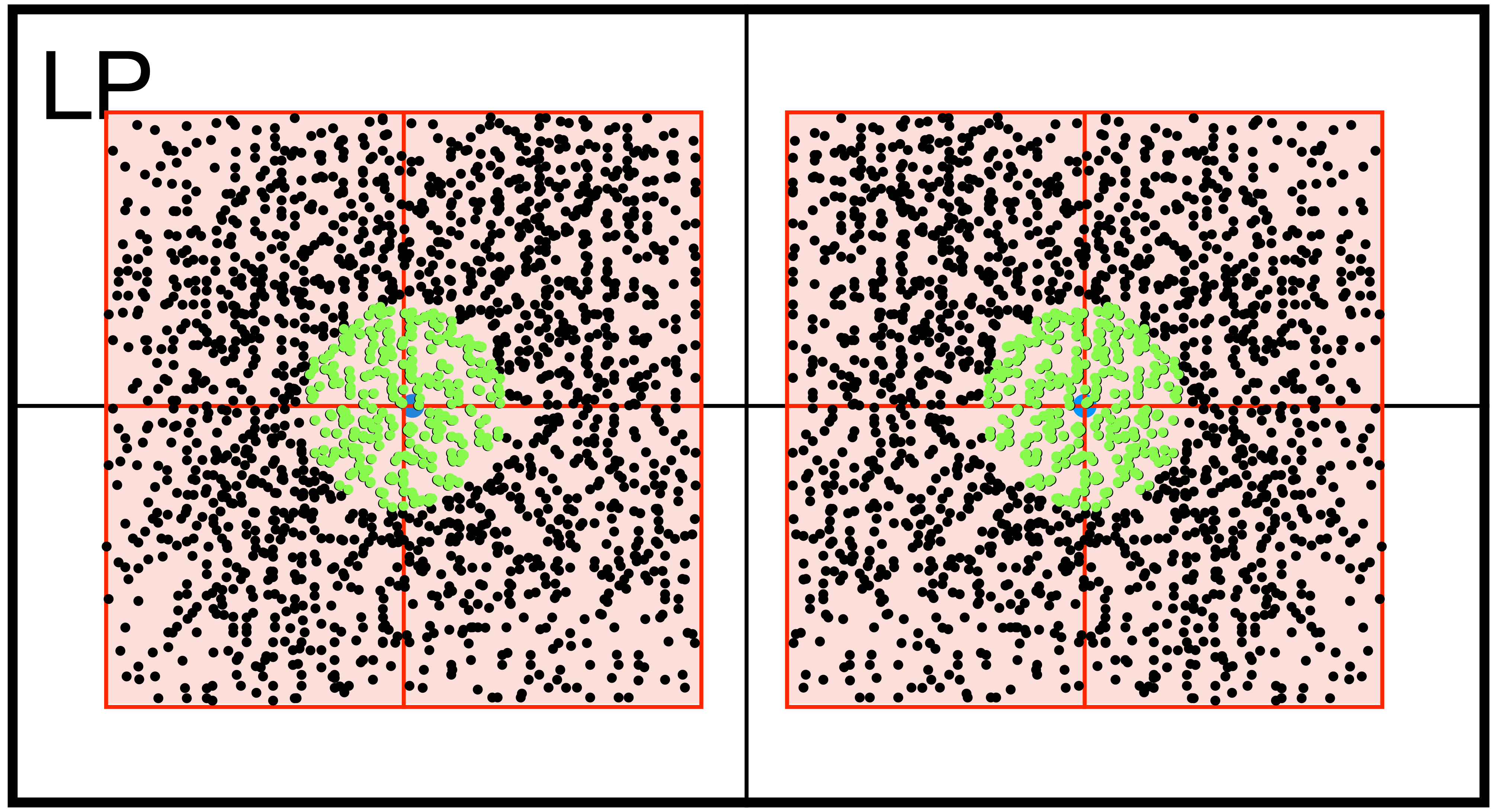

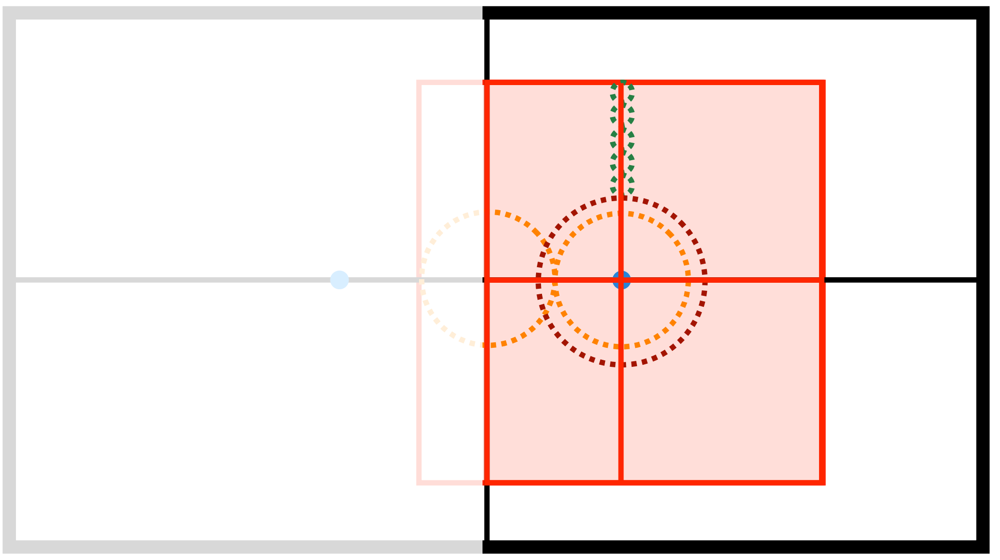

$A_{\rm sample}$ reduced if the box crosses the symmetry axis

Populate with $N_{\rm lens}$ lenses randomly sampled in 2D; $N_{\rm lens} = 20000$ (100000 if needed)

Compute $\bar{\mu}_i^k$ for $i = 1{,}2$ and ρ^k for $k = 1,\ldots,N_{\rm lens}$. Count the fraction f_ρ with $\rho^k \geq \rho_*$

Cross-section is $\sigma = 2A_{\rm sample} \times f_\rho$ (the 2 accounts for the reflection symmetry)

We also test that no $\rho^k \geq \rho_*$ are too close to sample box edges

after: Gawade, More, Bhalerao [2308.01775]

Picolensing cross-section

Gaussian

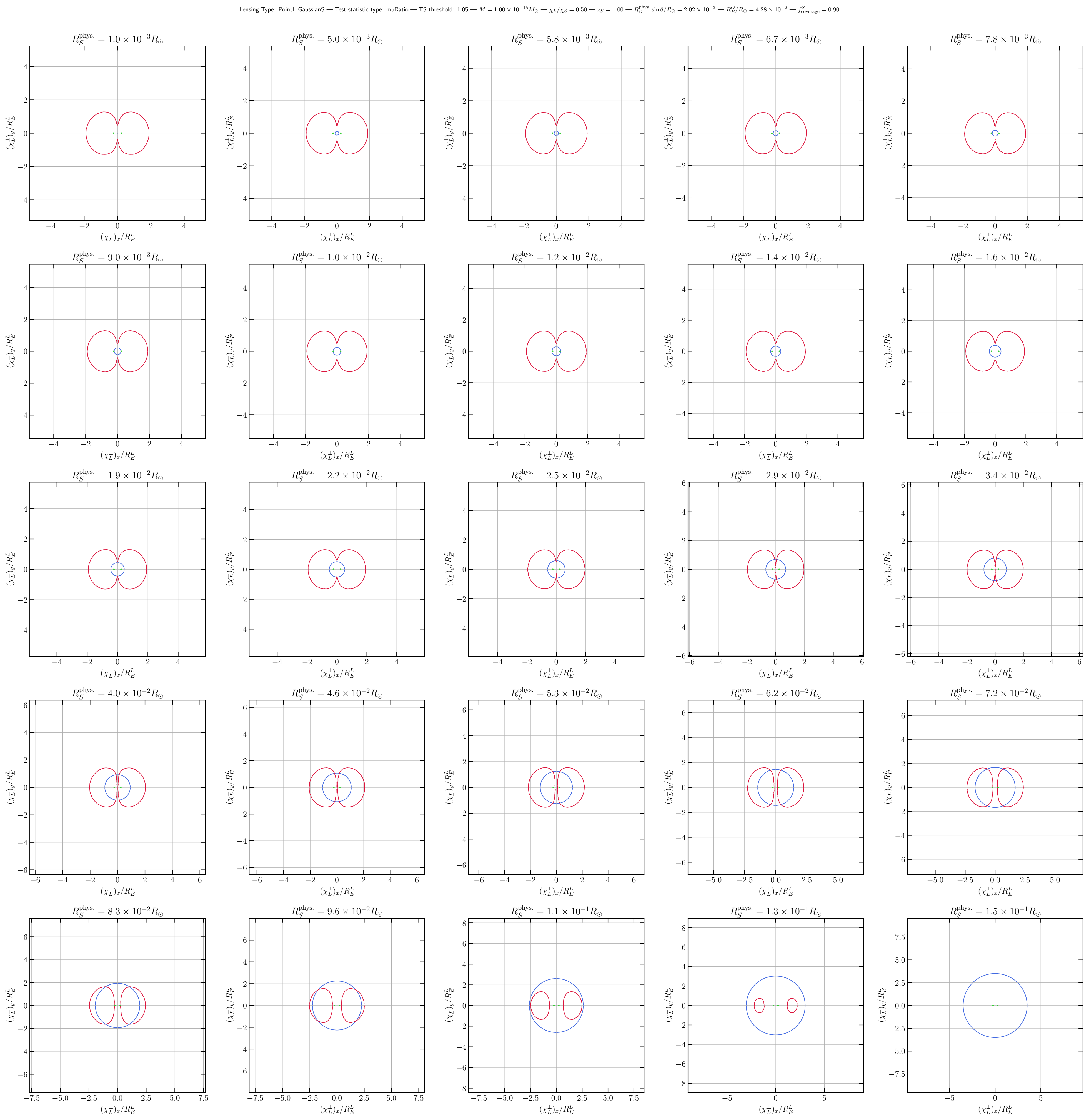

Changing source size

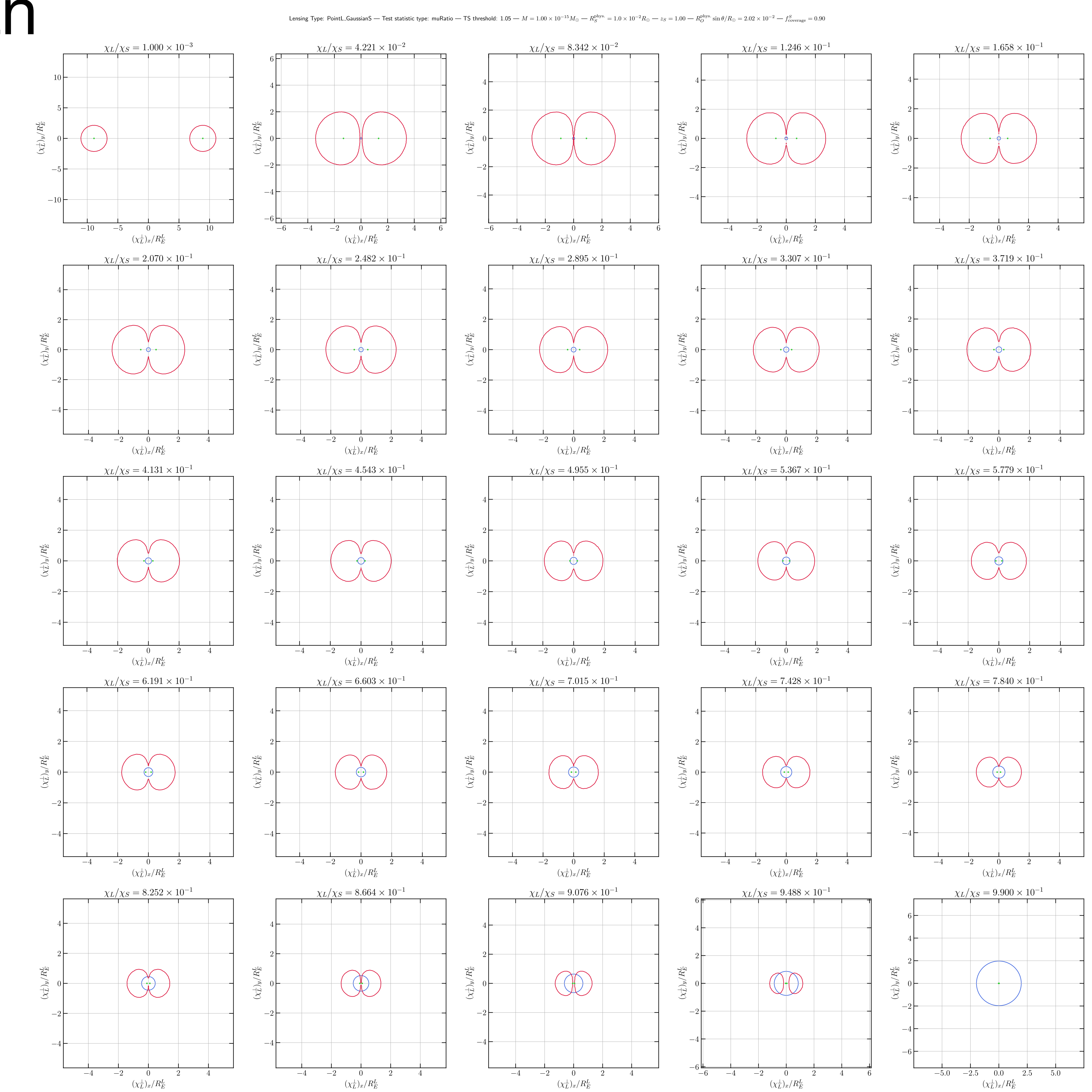

Changing lens distance

Michael A. Fedderke [Perimeter]

Picolensing cross-section

Gaussian

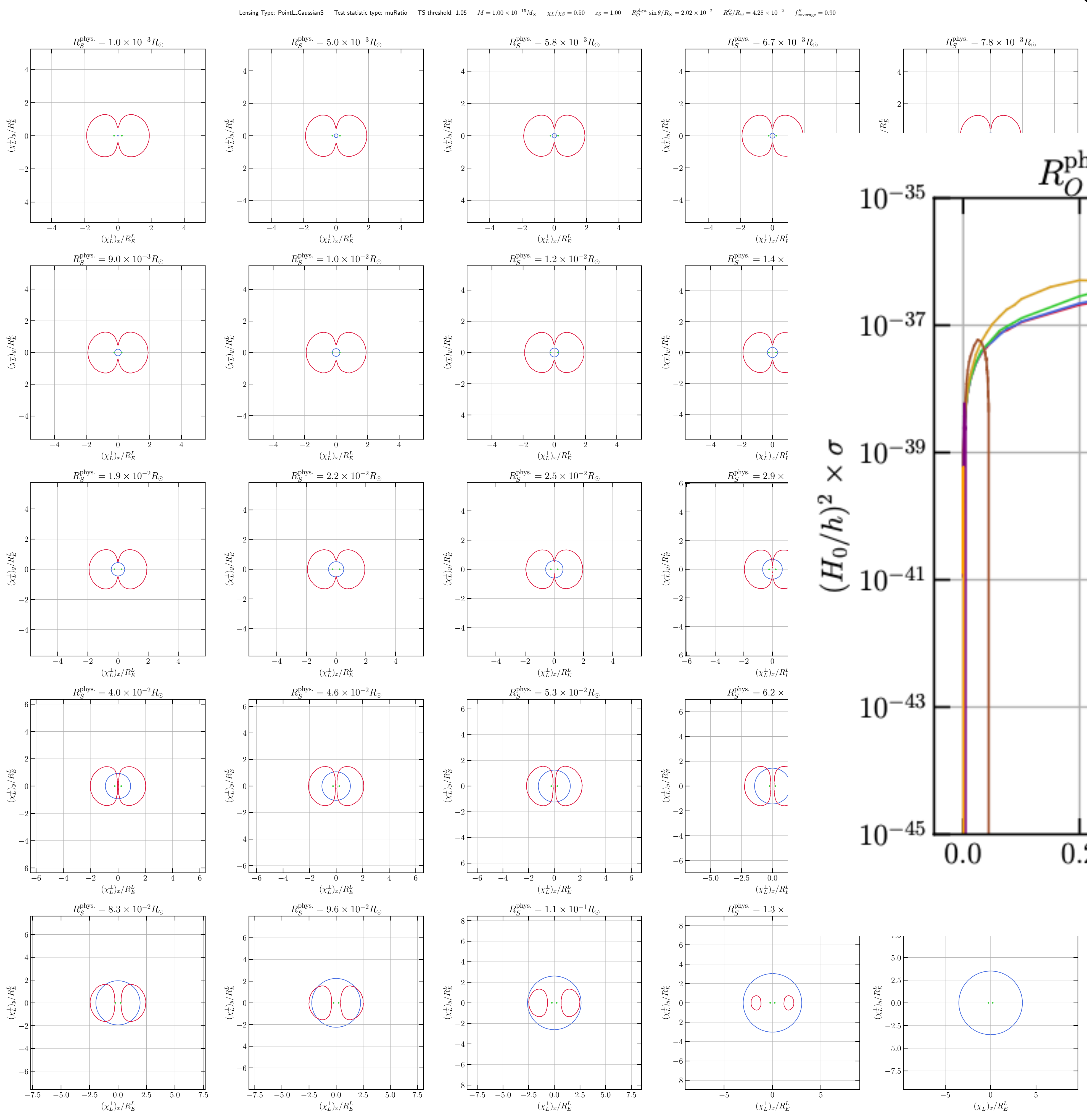

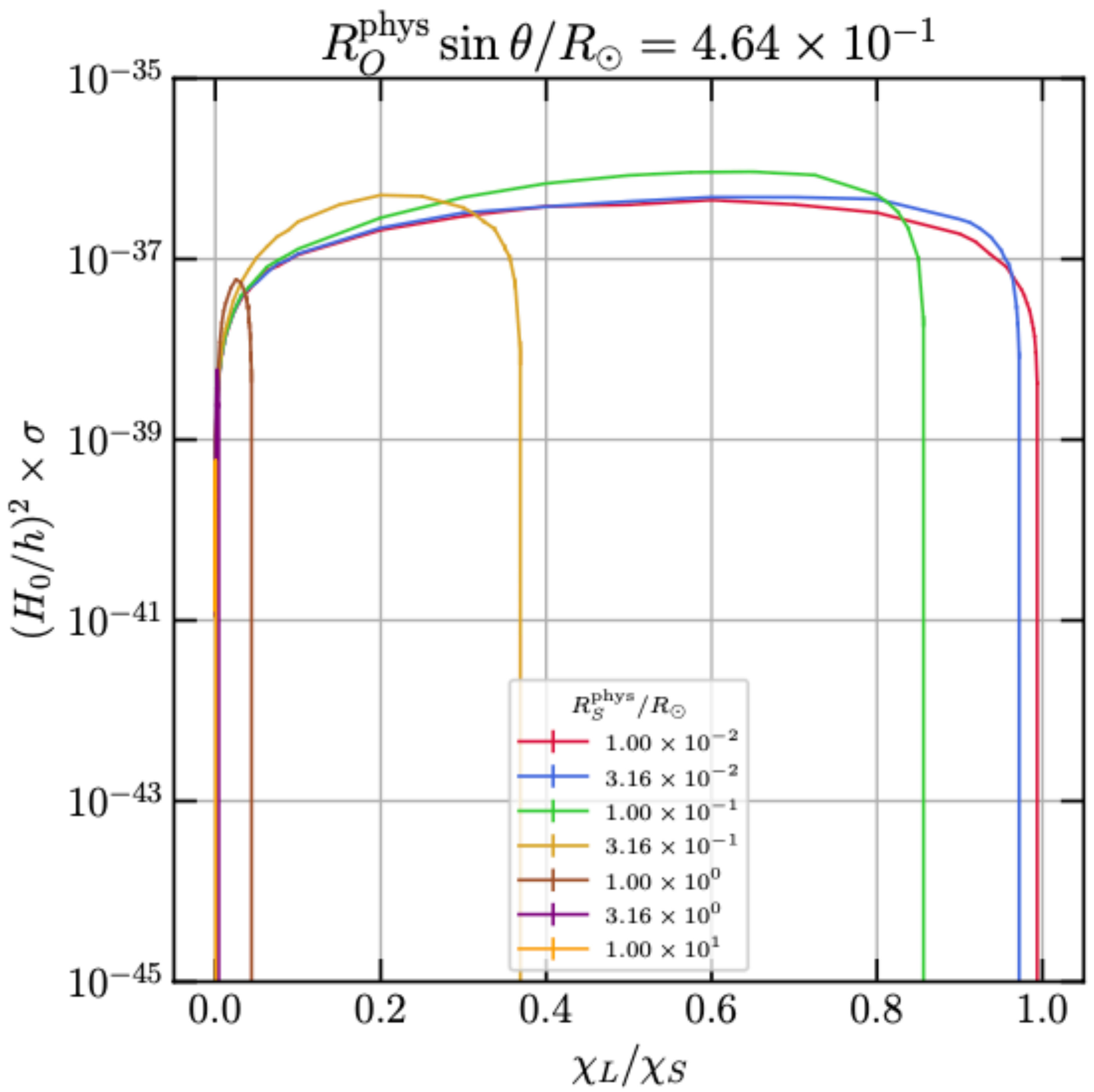

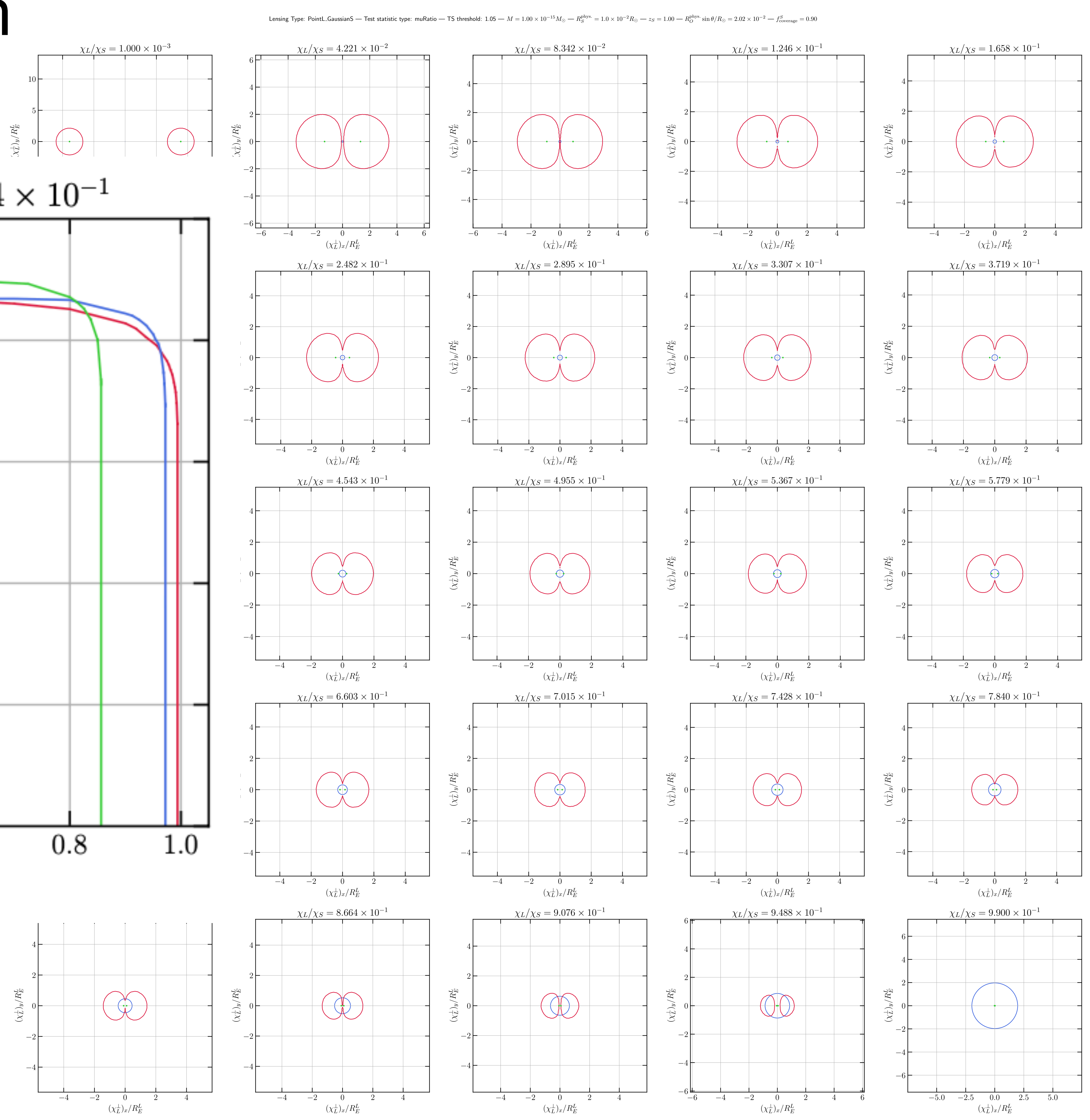

Changing source size

Changing lens distance

Michael A. Fedderke [Perimeter]

Picolensing cross-section

Disk

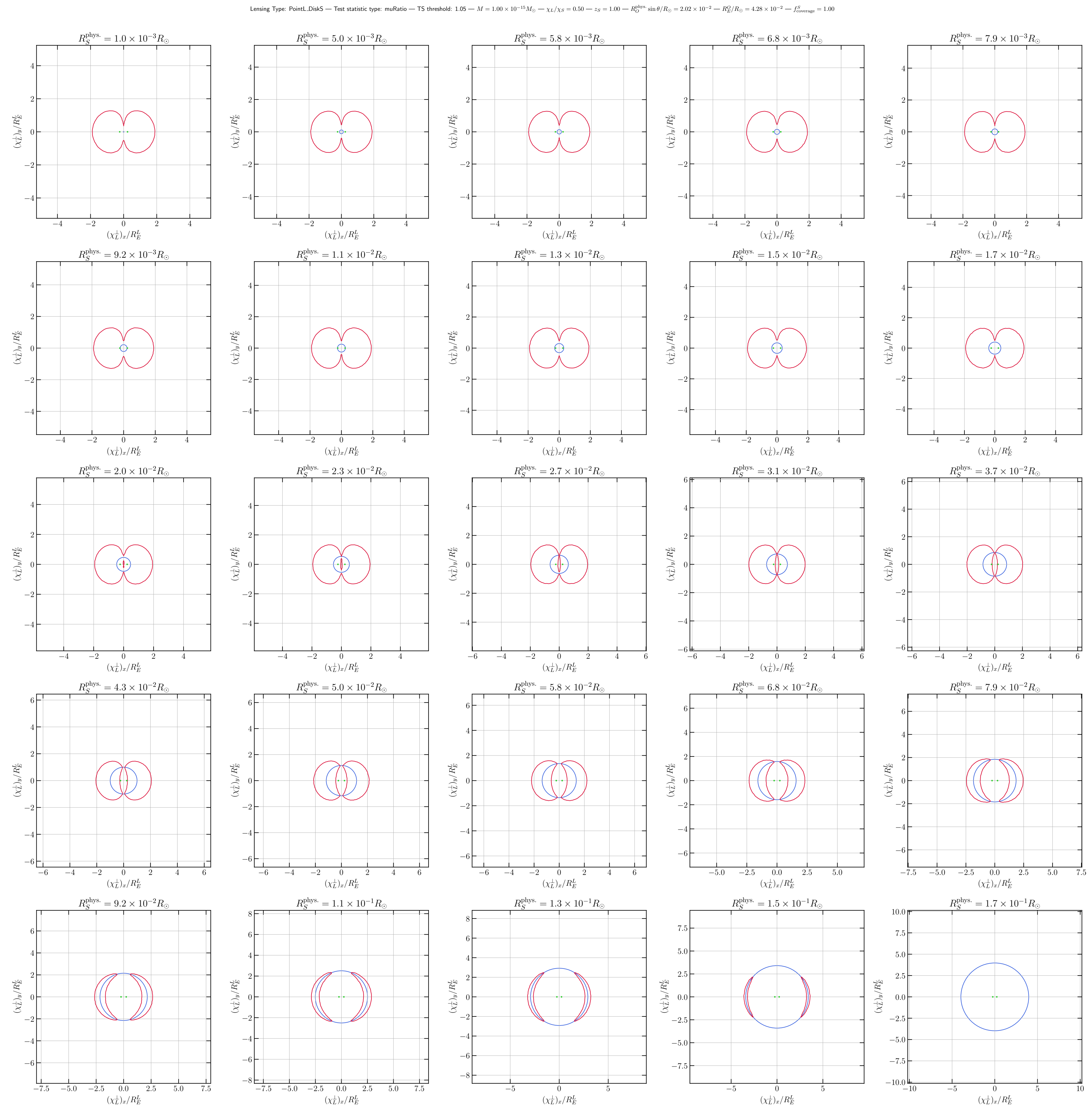

Changing source size

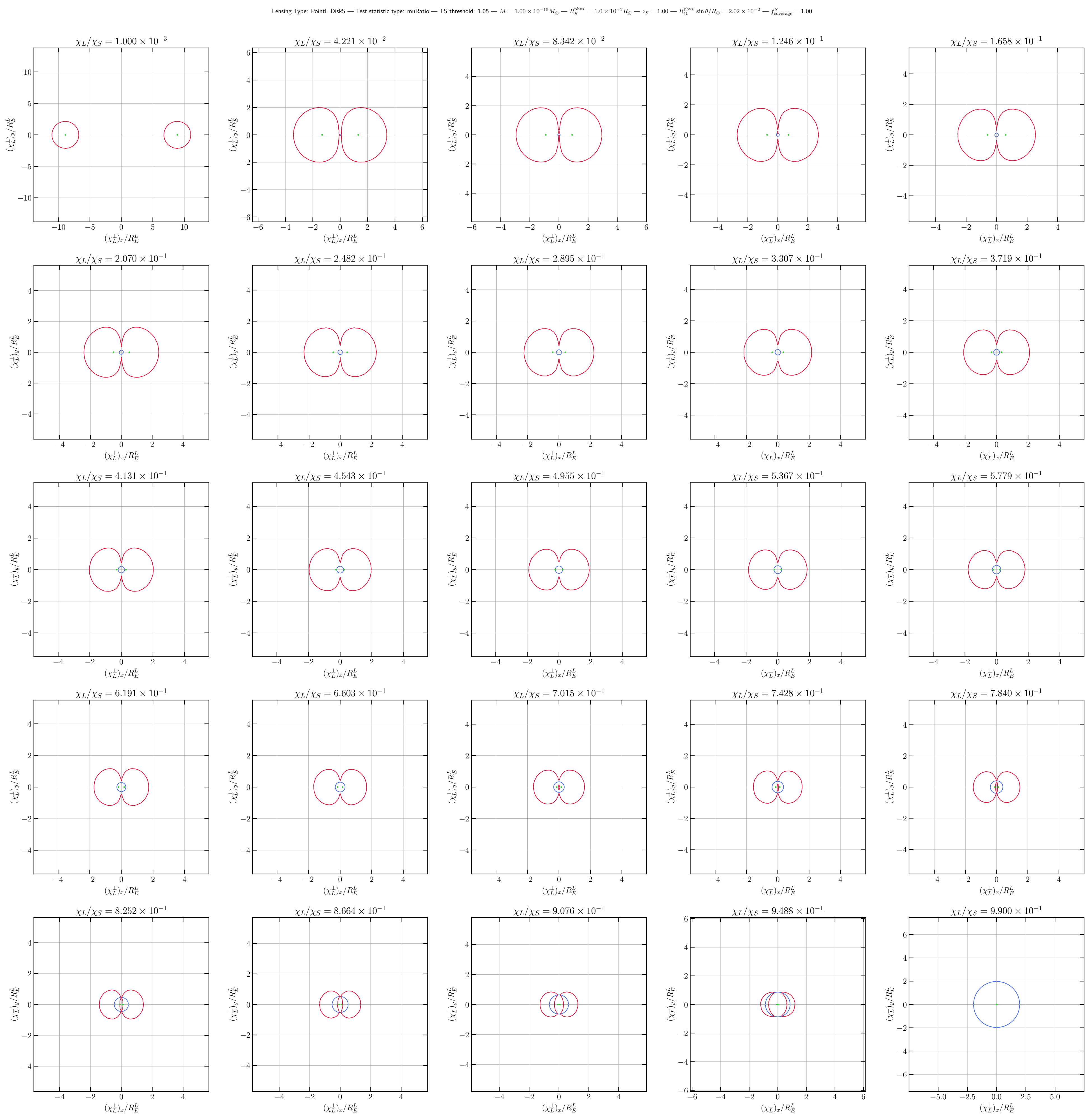

Changing lens distance

Michael A. Fedderke [Perimeter]

Picolensing cross-section

Disk

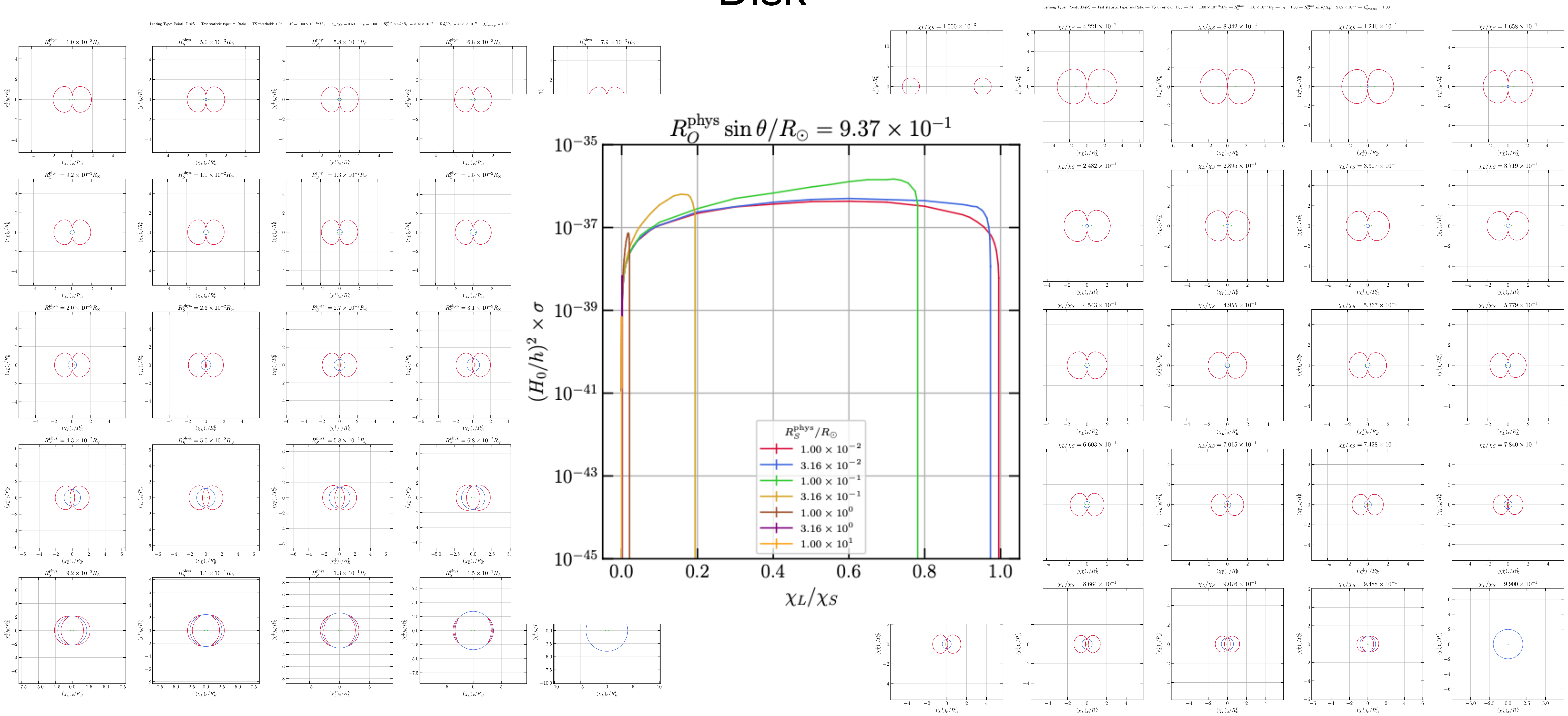

Changing source size

Changing lens distance

Michael A. Fedderke [Perimeter]

Picolensing cross-section

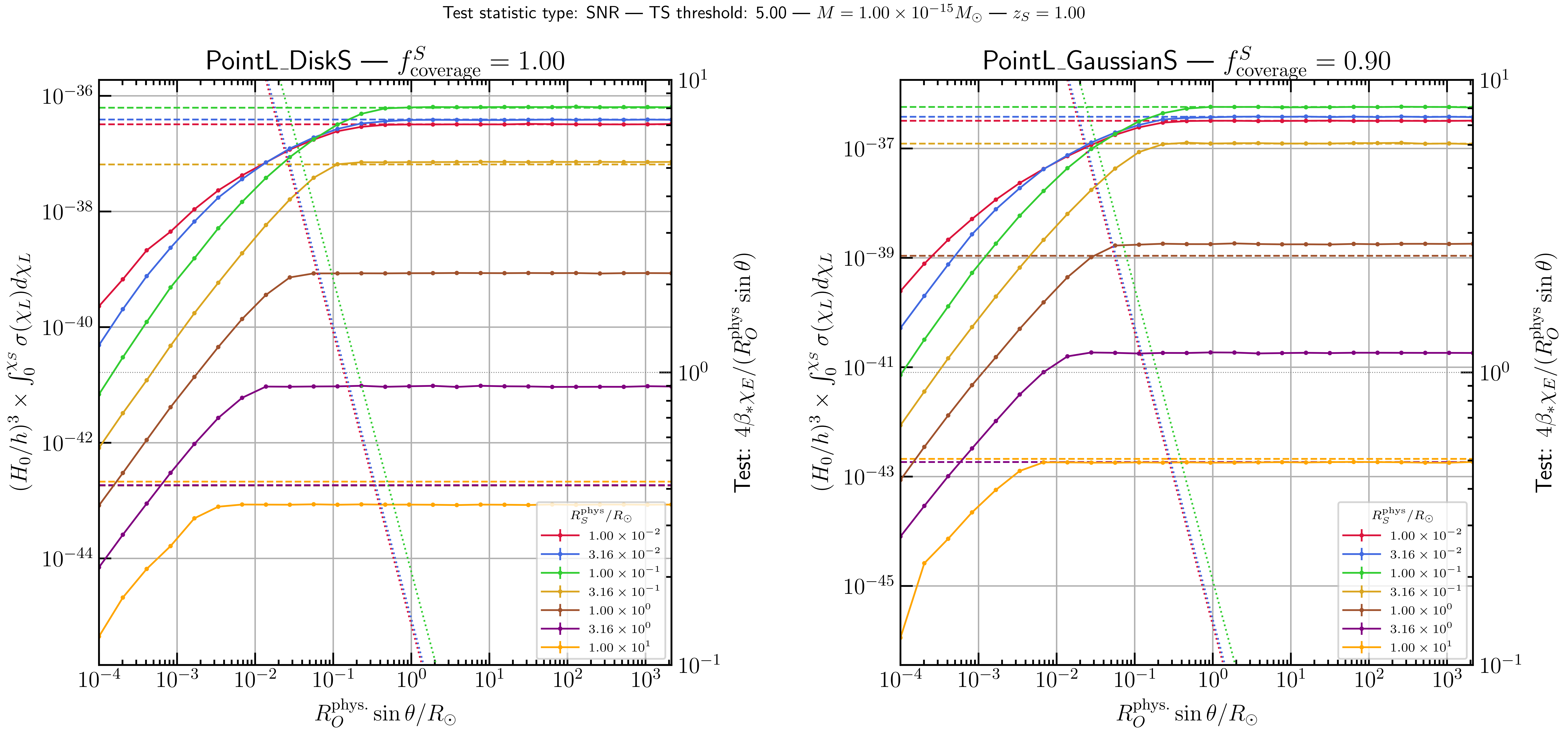

Michael A. Fedderke [Perimeter]

Picolensing cross-section

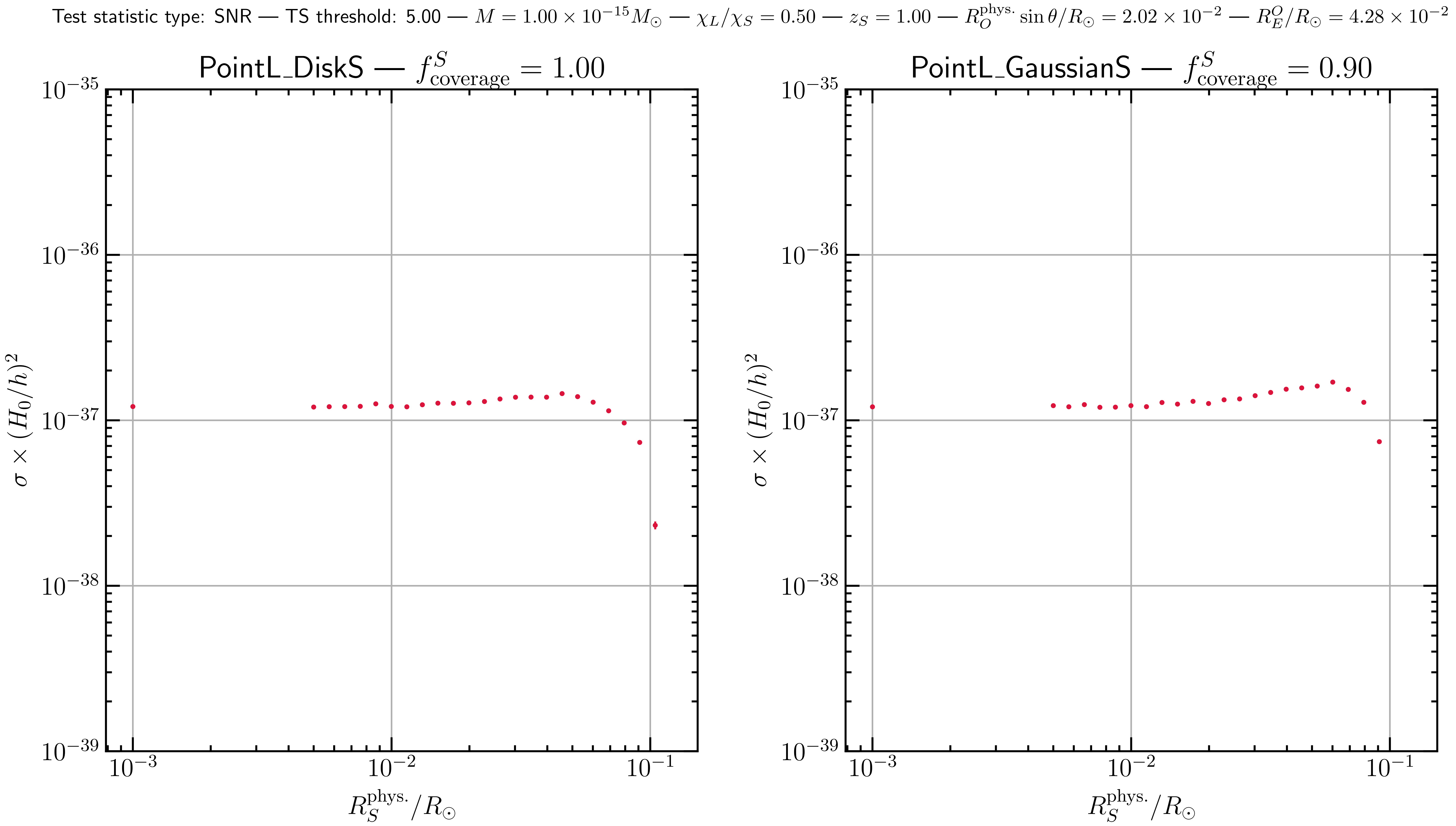

Picolensing cross-section

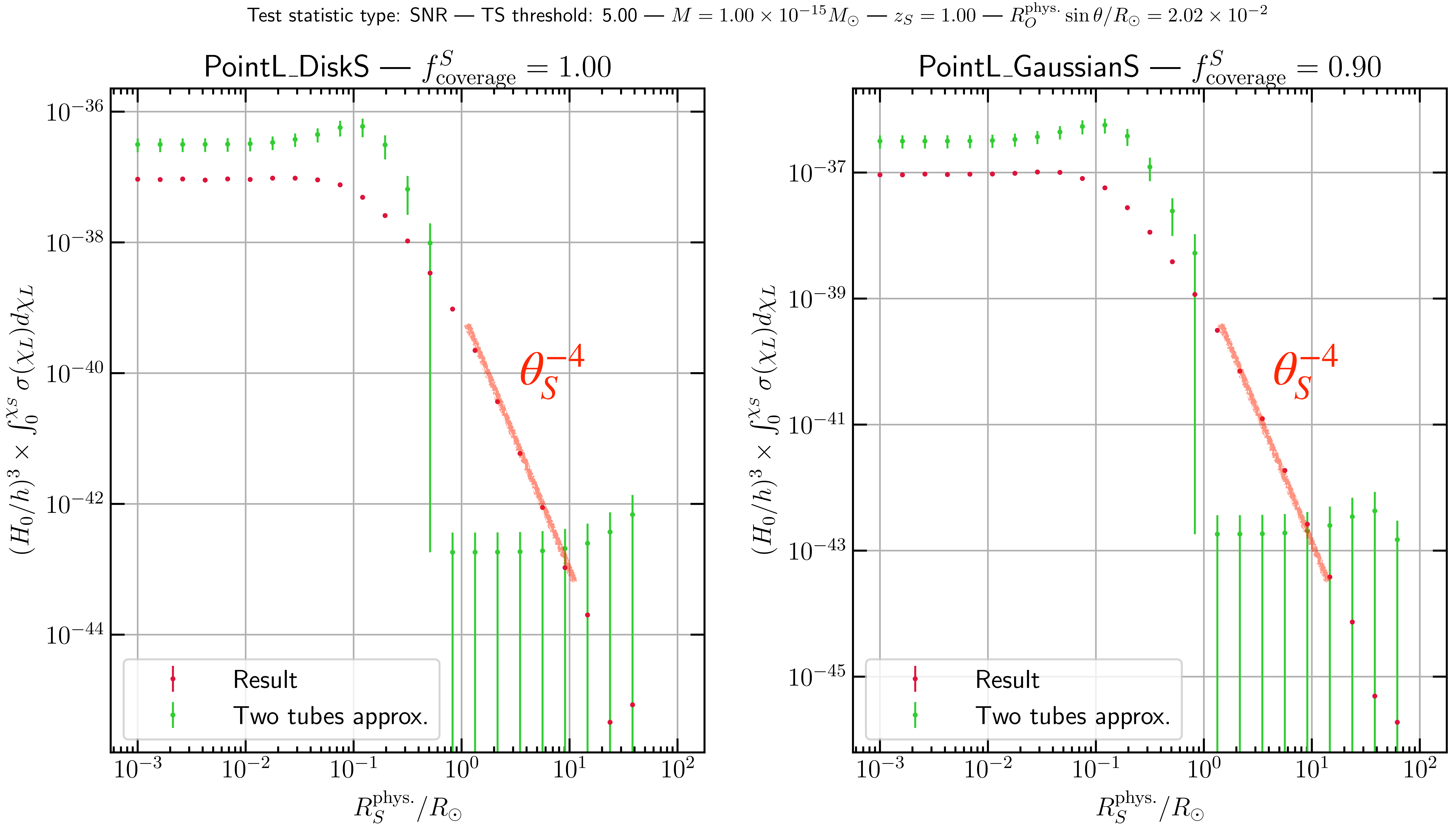

Michael A. Fedderke [Perimeter]

Picolensing cross-section

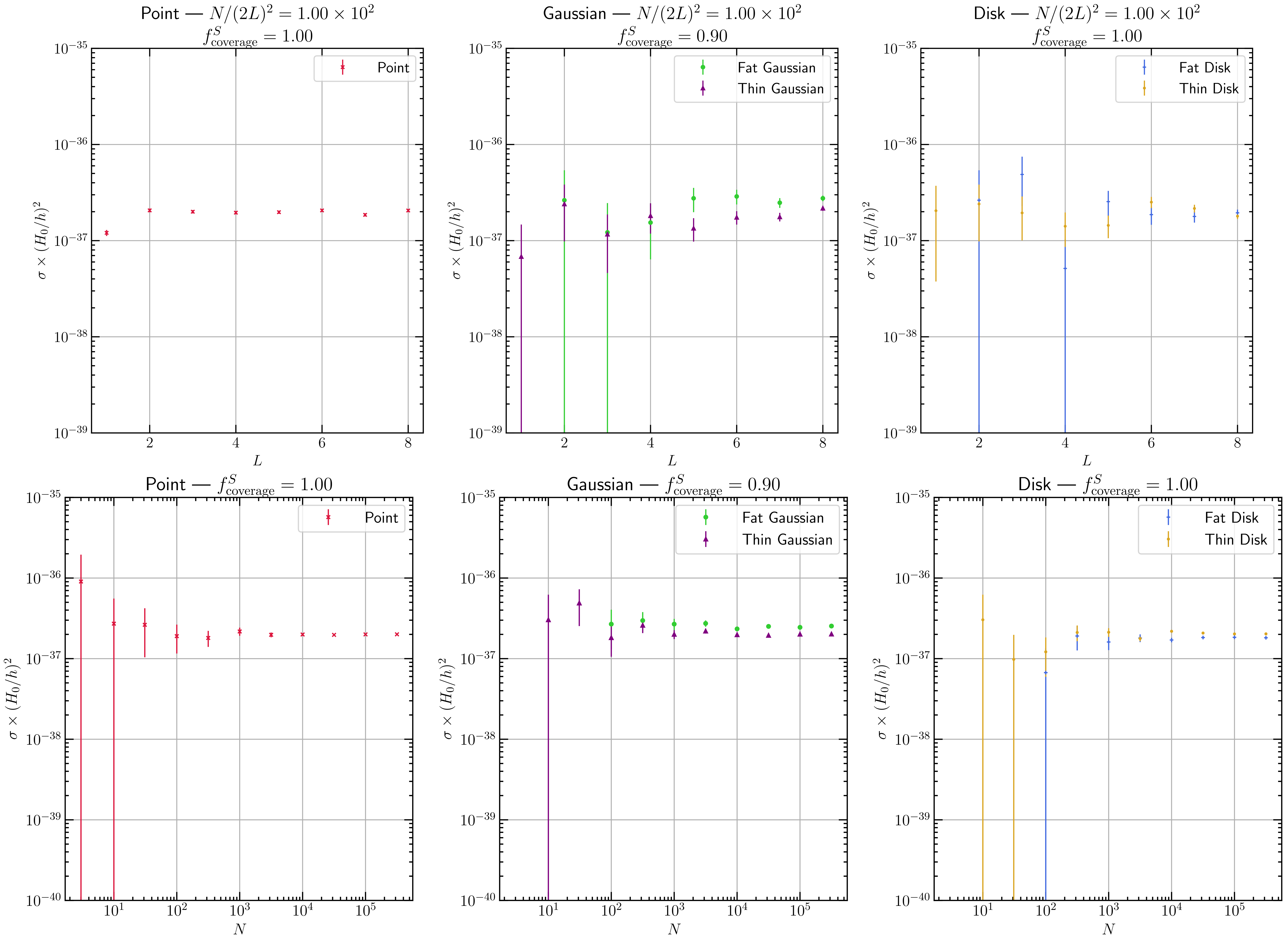

Michael A. Fedderke [Perimeter]

Source characteristics: *Swift*/BAT catalogue

Need to know: duration (T), distance (z_S), source fluence (f_s), source size (θ_S)

Duration: T_{90}, 90% of measured intensity

Distance: z_S, known for ~409 GRBs in the *Swift*/BAT catalogue

Source fluence: Band function in source frame. In detector frame, fit as a power law (PL) or cut-off power law (CPL):

$$f_{\mathrm{PL}}(E) \equiv K_{50}^{\mathrm{PL}} \left(\frac{E}{50\,\mathrm{keV}} \right)^{\alpha_{\mathrm{PL}}} \qquad f_{\mathrm{CPL}}(E) \equiv K_{50}^{\mathrm{CPL}} \left(\frac{E}{50\,\mathrm{keV}} \right)^{\alpha_{\mathrm{CPL}}} \exp\left[-\frac{E(2+\alpha_{\mathrm{CPL}})}{E_{\mathrm{CPL}}^{\mathrm{peak}}} \right]$$

$$f_s = \int_{E_{\min}}^{E_{\max}} f_{(\mathrm{C})\mathrm{PL}}(E)\, dE$$

Optically thin regime?

$$\bar{\tau}(n_0) = n_0 \bar{\mathscr{V}} = -\frac{\ln(1-\alpha)}{\aleph}\frac{n_0}{n_0^\alpha} = -\frac{\ln(1-\alpha)}{\aleph}\frac{f_{\rm DM}}{f_{\rm DM}^\alpha}$$

For $\alpha = 0.95$, $-\ln(1-\alpha) \sim 3$

If we demand $\bar{\tau} \ll 1$, at…

… the limit: $\bar{\tau}(f_{\rm DM} = f_{\rm DM}^\alpha, \alpha = 0.95) = \frac{3}{\aleph} \ll 1 \Rightarrow \aleph \gg 3$

Automatic if many sources are needed to achieve the limit

… at all of the DM: $\bar{\tau}(f_{\rm DM} = 1, \alpha = 0.95) = \frac{3}{\aleph f_{\rm DM}^{0.95}} \ll 1 \Rightarrow f_{\rm DM}^{0.95} \gg \frac{3}{\aleph}$

Need to make sure the limit is not too strong given the number of sources

Note that this is actually not dependent on $\aleph$, but really a condition on the source population

$$\frac{3}{\aleph f_{\rm DM}^{0.95}} = \omega_{\rm DM}^0 \times \frac{3\bar{\mathscr{V}}}{4\pi(H_0/h)^{-3}}\frac{(H_0/h)^{-1}}{(2G_N M)}$$

$$\mathscr{V} \lesssim \chi_S^2 G_N M$$

PBH DM

$\rho_i(z) = \rho_i^0(1+z)^{3(1+w_i)}$

Assuming we are bounding the **unclustered PBH DM component**, physical mass density would be

$$\rho_{\rm phys}(z) = f_{\rm DM} \times \rho^0_{\rm DM} \times (1+z)^3 \equiv M n_{\rm phys}(z) \Rightarrow n_{\rm phys}(z) = f_{\rm DM} \times \frac{\rho^0_{\rm DM}}{M} \times (1+z)^3 \,.$$

But comoving number density is $n_{\rm comov} = n_{\rm phys}(1+z)^{-3} = f_{\rm DM} \times \frac{\rho^0_{\rm DM}}{M} \equiv n_0 \,.$

Optimism:

DISCOVERY SPACE!

And $\rho^0_{\rm DM} = \Omega^0_{\rm DM}\rho_{\rm crit} = 3\omega^0_{\rm DM}\frac{(H_0/h)^2}{8\pi G_N}$, so… $n_0 \equiv f_{\rm DM} \times \frac{3\omega^0_{\rm DM}(H_0/h)^2}{4\pi(2G_N M)}$

Limit: $$f^\alpha_{\rm DM} = -\frac{\ln(1-\alpha)}{\omega^0_{\rm DM}\aleph}\boxed{\frac{4\pi(H_0/h)^{-3}}{3\bar{\mathscr{V}}}\frac{(2G_N M)}{(H_0/h)^{-1}}}$$

for $\aleph$ sources if I see NO picolensing at $\rho \geq \rho_*$

Ratio of Hubble volume to lensing volume (tiny!)… but you get back a single power to the Schwarzschild radius of the lens to the Hubble radius (large!)

$\mathscr{V} \sim \chi_S^2 G_N M$

$\boxed{\cdots} \propto \left(\frac{\chi_S}{H_0^{-1}}\right)^{-2}$

$\omega^0_{\rm DM} \equiv \Omega^0_{\rm DM} h^2 \sim 0.12$

after: Gawade, More, Bhalerao [2308.01775]

Lensing Probability

$\omega^0_{\mathrm{DM}} \equiv \Omega^0_{\mathrm{DM}} h^2 \sim 0.12$

No detectable lenses at $\rho \geq \rho_*$ for single source j:

$$\Pr[\text{no lensing}, j] = e^{-\tau_j}$$

Poisson statistics; also only works for $\tau_j \ll 1$, otherwise the signal SNR we computed is wrong!

Jung and Kim [1908.00078]

No lenses for $\aleph$ sources:

$$\Pr[\text{no lensing}; \aleph] = \Pi_{j=1}^{\aleph} e^{-\tau_j} = \exp\left[-\sum_{j=1}^{\aleph} \tau_j\right] = \exp\left[-\aleph \bar{\mathscr{V}} n_0\right].$$

Exclusion on n_0 at confidence level α: $\Pr[\text{no lensing}; \aleph] = (1-\alpha) \Rightarrow n_0^\alpha = -\dfrac{\ln(1-\alpha)}{\aleph \bar{\mathscr{V}}}$.

$$f^\alpha_{\mathrm{DM}} = -\frac{\ln(1-\alpha)}{\omega^0_{\mathrm{DM}}\aleph} \frac{4\pi(H_0/h)^{-2}(2G_N M)}{3\bar{\mathscr{V}}}$$

OPTIMISM: DISCOVERY SPACE!

$H_0^{-1} \sim 4.5\,\mathrm{Gpc}$ $\quad R_S(M = 10^{-12} M_\odot) = 3\,\mathrm{nm}$

after: Gawade, More, Bhalerao [2308.01775]

Clustering

Jung and Kim [1908.00078]

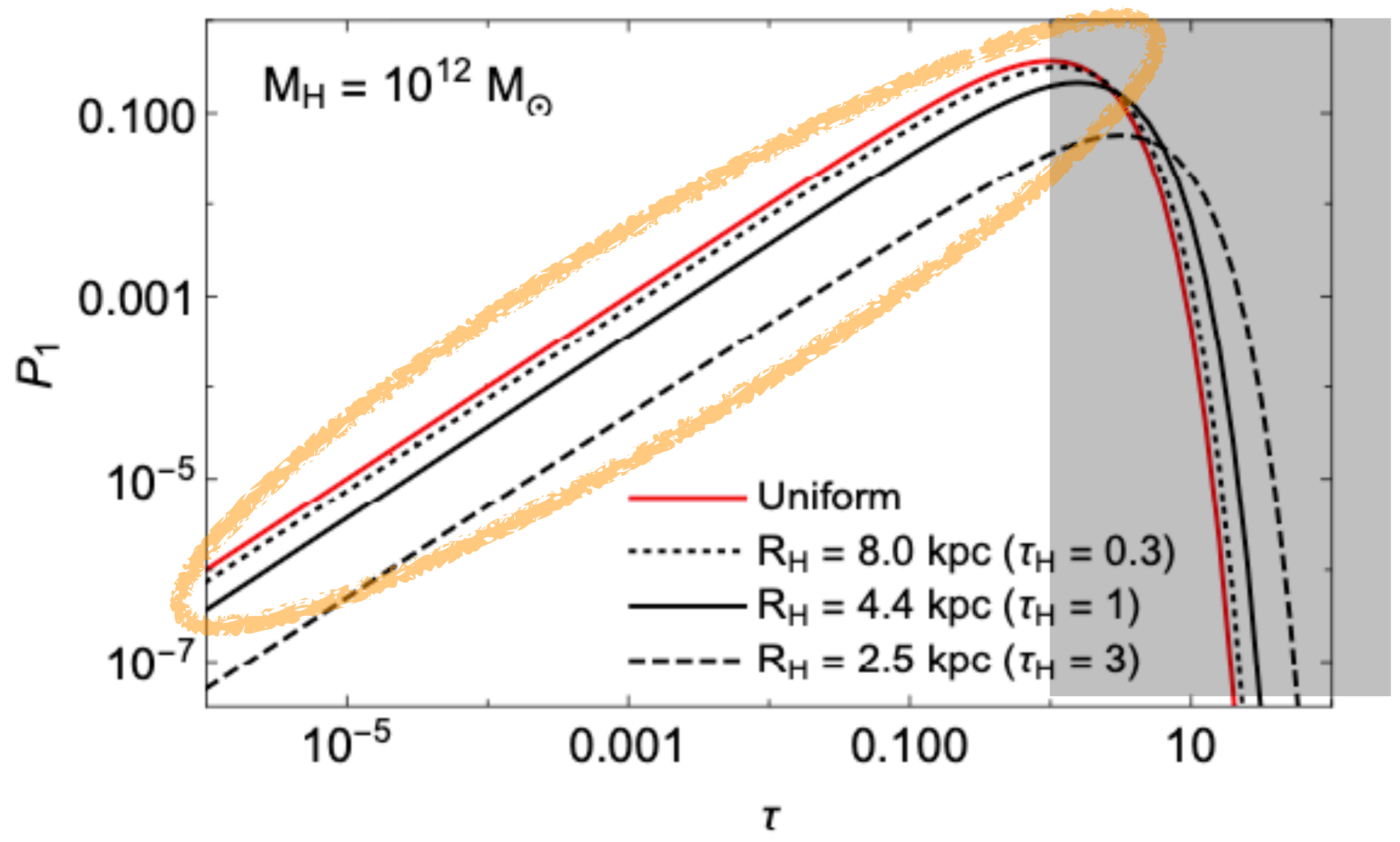

FIG. 3. Single lensing probability P_1 for selected values of R_H (equivalently, τ_H); the smaller the halo size R_H of the given mass $M_H = 10^{12} M_\odot$, the higher clustering of PBHs within the single halo yielding higher optical depth τ_H. The red line is for the uniform distribution of PBHs (no halos) giving the Poisson distribution of the number of lenses, while black lines represent clustered distributions which depart from the Poisson distribution. Note that the Milky Way has $R_H \sim 100$ kpc, yielding $\tau_H \ll 1$. $f = 10^{-2}$ and $k = 10$.

Appendix D: Effects of PBH clustering

We now demonstrate that assuming a uniform distribution of PBHs is decent in calculating lensing parallax, even though nearly half of DM is thought to be clustered around galaxies. As discussed in the paper, we (conservatively) consider only single-lensing events; multi-lensing can still lead to parallax, but is more complicated to calculate and analyze. Thus, we show that the single lensing probability P_1 does not change significantly for clustered PBHs in most regions of galaxies.

First of all, the clustering does not change the optical depth τ, as the average number of lenses within the V_L (the desired volume of PBH locations for lensing) remains the same. But P_1 may still change because once a lens is within V_L it is more likely that there are other clustered lenses within the same V_L so that multi-lensing occurs more often than single lensing. More quantitatively, the number of lenses within V_L no longer follows the Poisson distribution.

Suppose a LOS passes through N halos (the clustered PBH) and the optical depth within each halo is denoted by τ_H (the more clustered within a halo, the larger τ_H); then the expectation value of $\langle N\rangle = \tau/\tau_H$. The single-lensing probability for the case of N halos is

$$\begin{aligned} &P_{1|\text{N halos}} \\ &= (\text{number of halos}) \\ &\quad \times (\text{probability for one halo to give single lensing}) \\ &\quad \times (\text{probability for other halos to give no lensing}) \\ &= N \times \tau_H e^{-\tau_H} \times (e^{-\tau_H})^{N-1}, \end{aligned} \tag{D1}$$

where we assume that PBH DM is clustered but uniformly distributed within each halo. Summing N with its own Poisson distribution, we obtain the total probability for single lensing

$$P_1 = \sum_{N=1}^{\infty} P_{1|\text{N halos}} \times \frac{(\tau/\tau_H)^N}{N!} e^{-\tau/\tau_H}. \tag{D2}$$

Fig. 3 shows $P_1(\tau)$ for three selected values of τ_H. The deviation from the uniform distribution is sizable for $\tau_H \gtrsim 1$ irrespective of τ; this is the manifestation of non-Poissonian properties in Eq. (D2). This is understandable because $\tau_H \gtrsim 1$ directly means that clustering is so high that there are likely multiple lenses within the V_L of a single halo.

The τ_H is related to the halo radius R_H with the mass M_H. The PBH number density within the halo is $n_{|H} = (M_H f/M)/(4/3 \times \pi R_H^3)$. The V_L within the halo, denoted by $V_{L|H}$, is approximately the cylinder with a length R_H and a (Einstein) cross-section $\sigma = k \cdot \pi(D_L\theta_E)^2$, where k is determined by detection criteria and detector sensitivities (see below for realistic values of k). Thus we obtain τ_H as a function of R_H

$$\tau_H \approx 1.9 \times 10^{-22} \times kf \left(\frac{M_H}{M_\odot}\right)\left(\frac{D_L}{R_H}\right)^2 \left(\frac{1\text{ Gpc}}{D_L D_S/D_{LS}}\right). \tag{D3}$$

This allows us to interpret Fig. 3 for Milky-Way-like galaxies. For $M_H = 10^{12} M_\odot$, τ_H becomes $\gtrsim 1$ for $R_H \lesssim 4.4$ kpc. The Milky-Way is thought to have a much larger halo ~ 100 kpc. Thus, the PBH clustering is small enough not to affect our calculations based on the uniform distribution of PBH. For reference, the Milky-Way gives $\tau_H \lesssim 2 \times 10^{-3}$ with $R_H = 100$ kpc. In all these estimations, we use $k = 10$ and $f = 10^{-2}$; the values of k in our results are usually $\lesssim 10$ but grow with ϵ improvement so that the clustering and multi-lensing can become more relevant in the future.

Comparison to 2308.01775

They took

$k_S = 2$

$$A_b = 2400\,\mathrm{cm}^2 \quad A_s = 1300\,\mathrm{cm}^2$$
$$f_b = 10\,\mathrm{cm}^{-2}\mathrm{s}^{-1}$$

~Swift/BAT

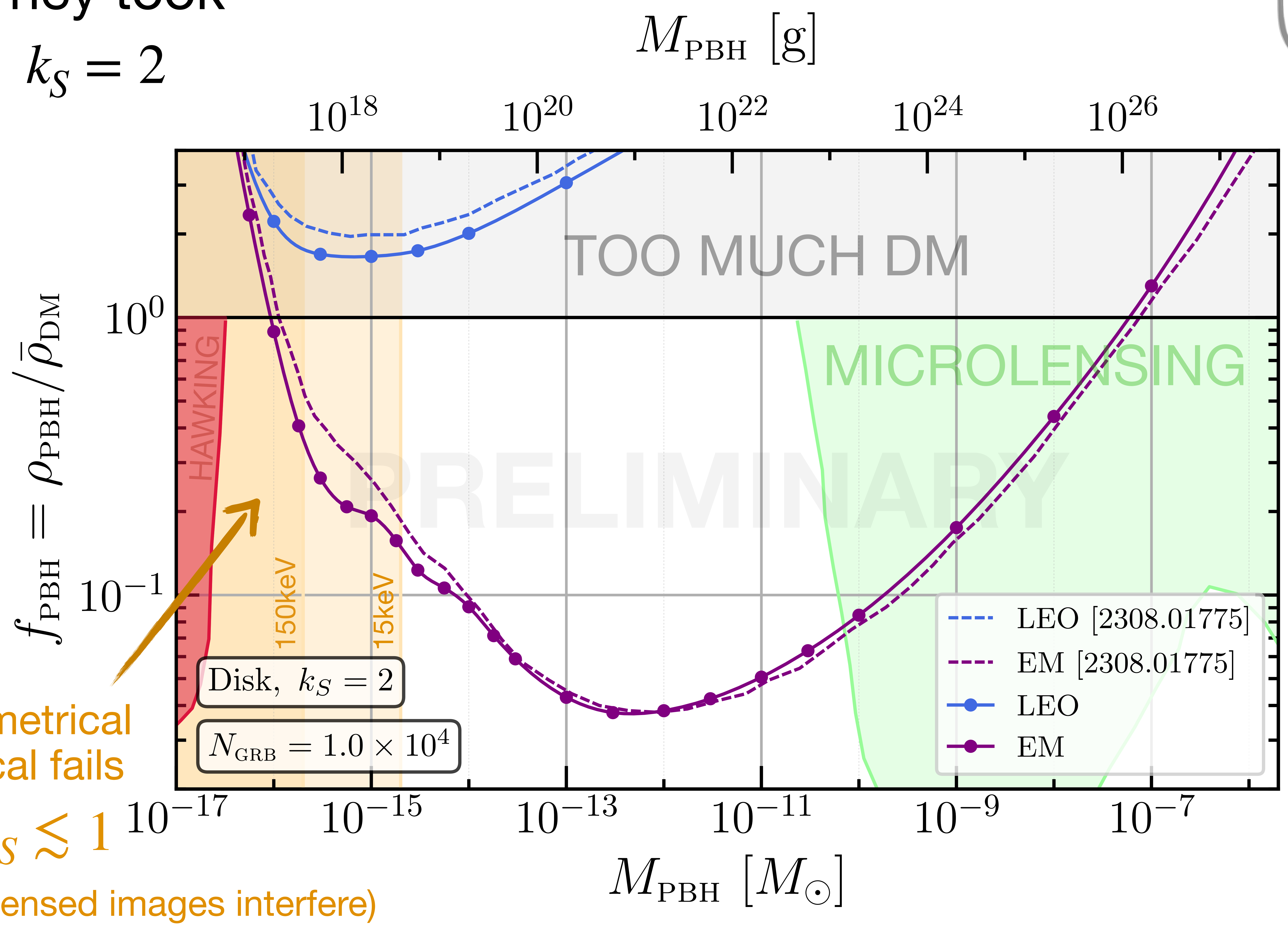

Geometrical optical fails

$\omega R_S \lesssim 1$

(two lensed images interfere)

Pretty good agreement (5-10%)

Validates our implementation

Confirms previous literature under their assumptions

Scenario	Abbrev.	Baseline R_O	$R_O/R_\odot$
Low Earth Orbit	LEO	1.40×10^4 km	0.020
Earth–Moon	EM	3.84×10^5 km	0.55

Minor difference in assumed energy range (15-150keV [us] vs. 20-200 keV [them]); makes little difference

*markers are computed; lines are log-log cubic spline interpolants

Vary minimum source size

$k_S = 1$ $\quad D_{\rm obs} \equiv \frac{k_S T_{90}}{1 + z_S}$

Recall:

$R_\odot \sim 7 \times 10^{10}\,\mathrm{cm}$

Quite robust to excluding $\lesssim R_\odot$ sources

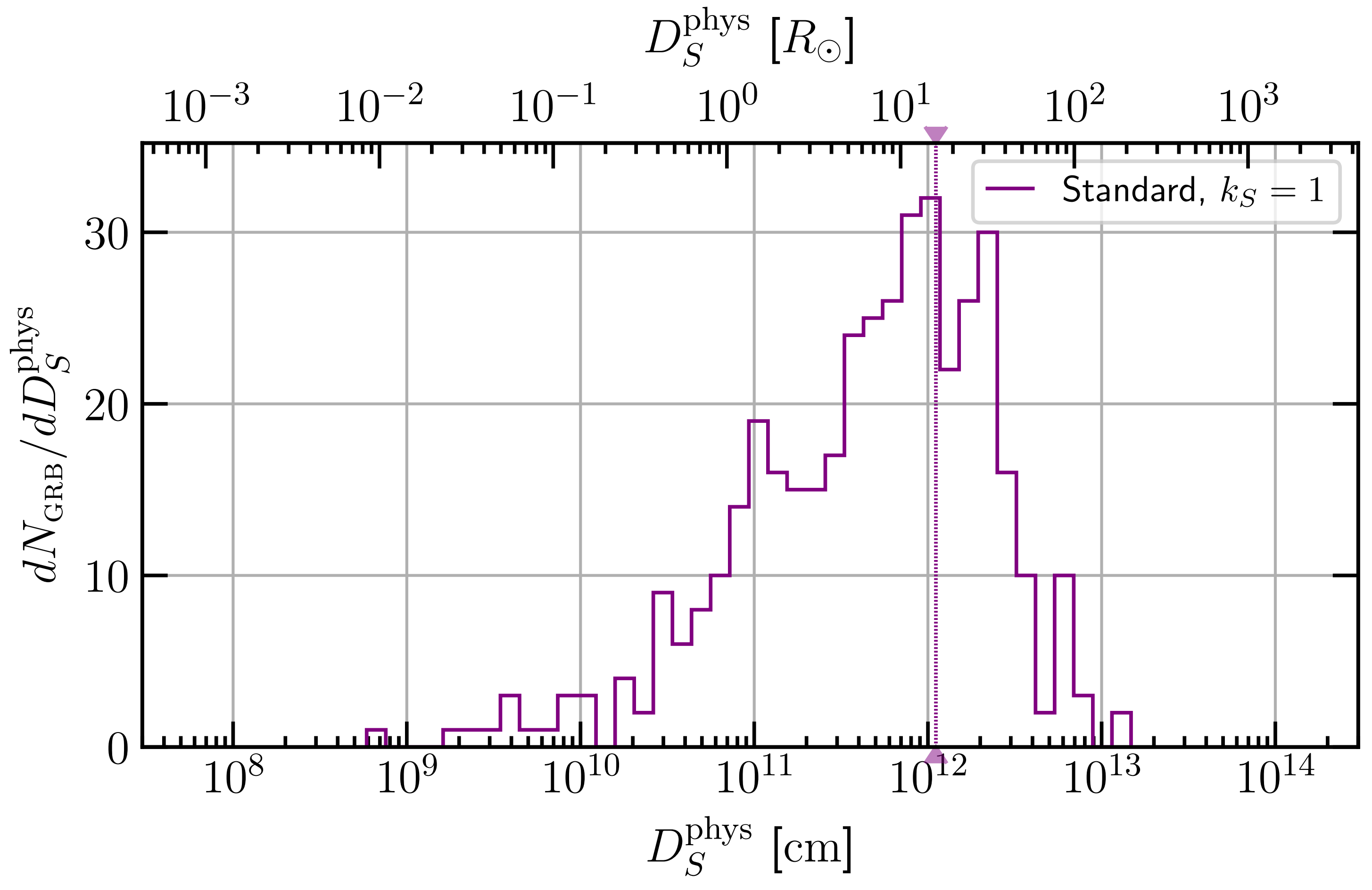

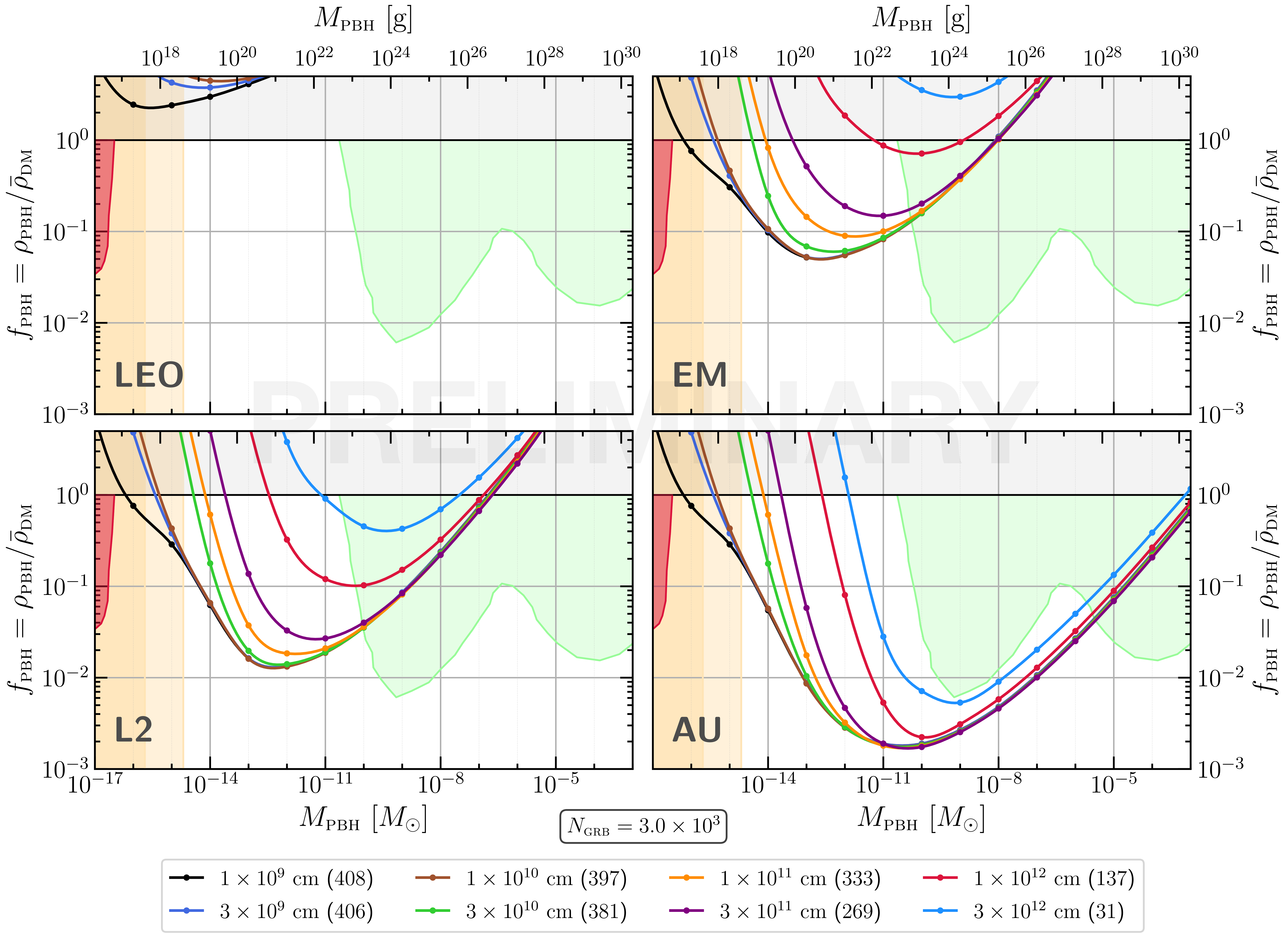

*markers are computed; lines are log-log cubic spline interpolants

Vary the background level

Note: not always $\propto \sqrt{f_b}$

Higher backgrounds once out of LEO?

Some x-ray detection backgrounds from HE particles hitting detector / spacecraft

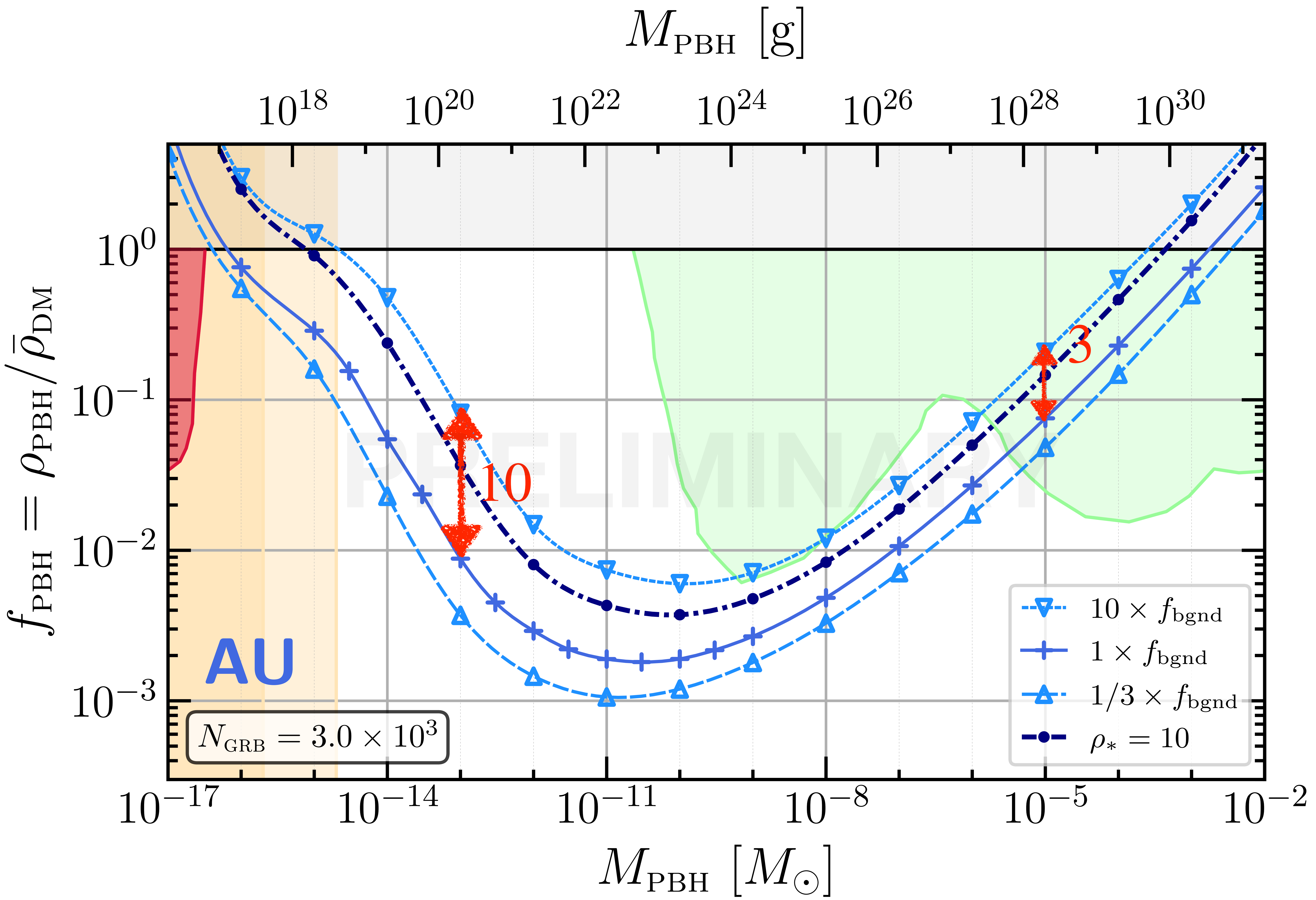

*markers are computed; lines are log-log cubic spline interpolants

Michael A. Fedderke [Perimeter]

Scalings

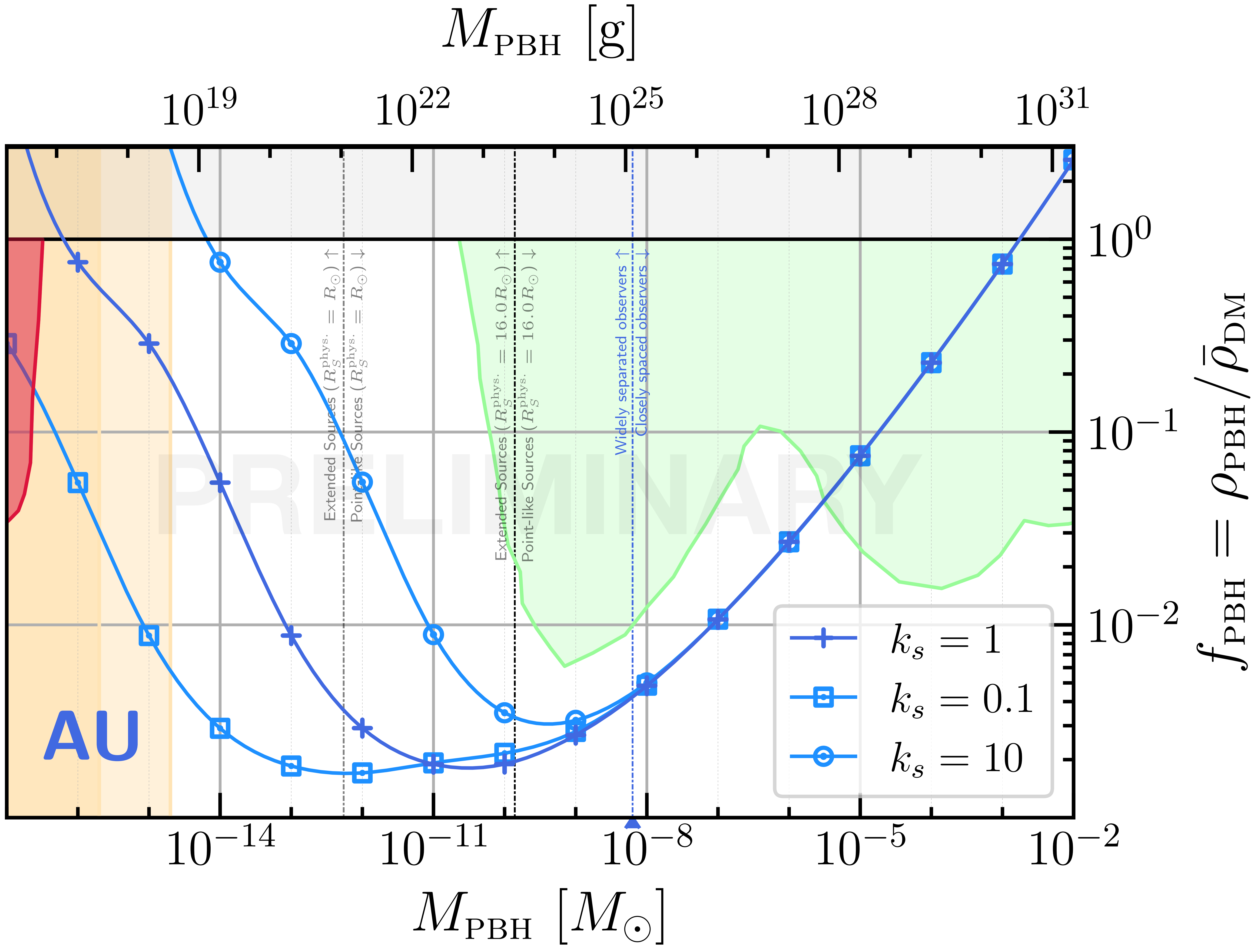

Michael A. Fedderke [Perimeter]

Scalings

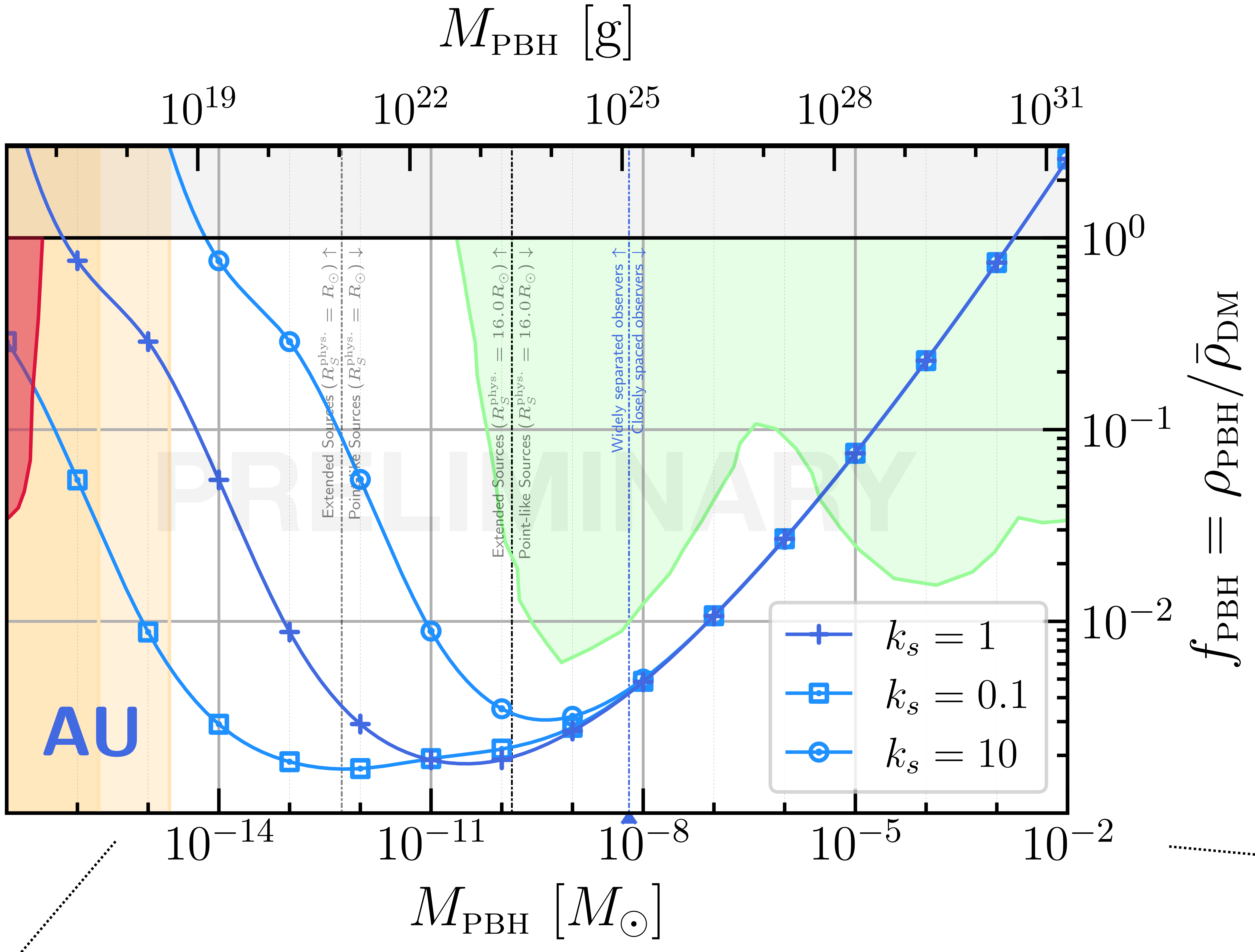

Michael A. Fedderke [Perimeter]

Scalings

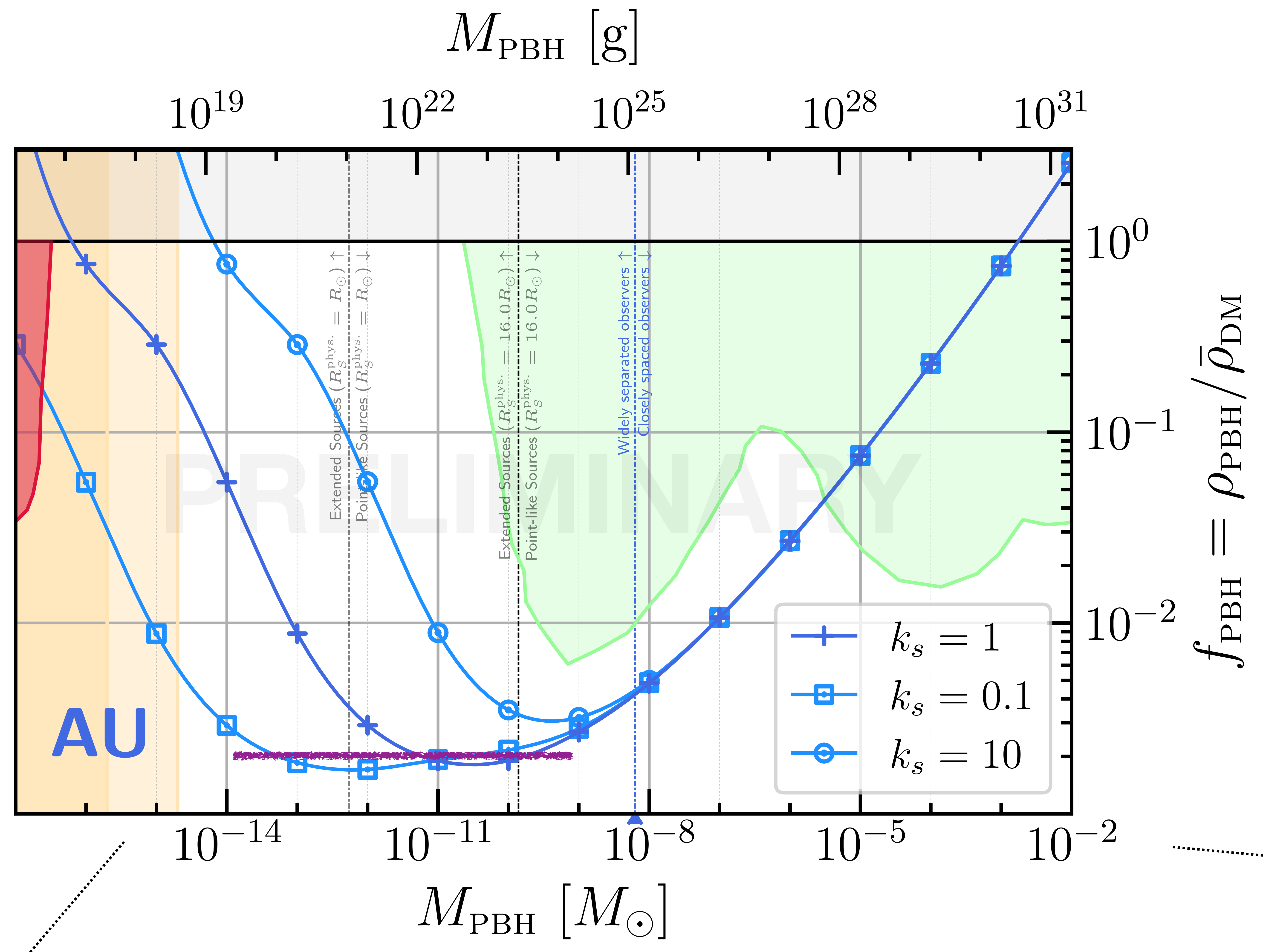

~POINT SOURCES, WIDELY SEPARATED OBSERVERS

Scalings

POINT SOURCES, CLOSELY SPACED OBSERVERS

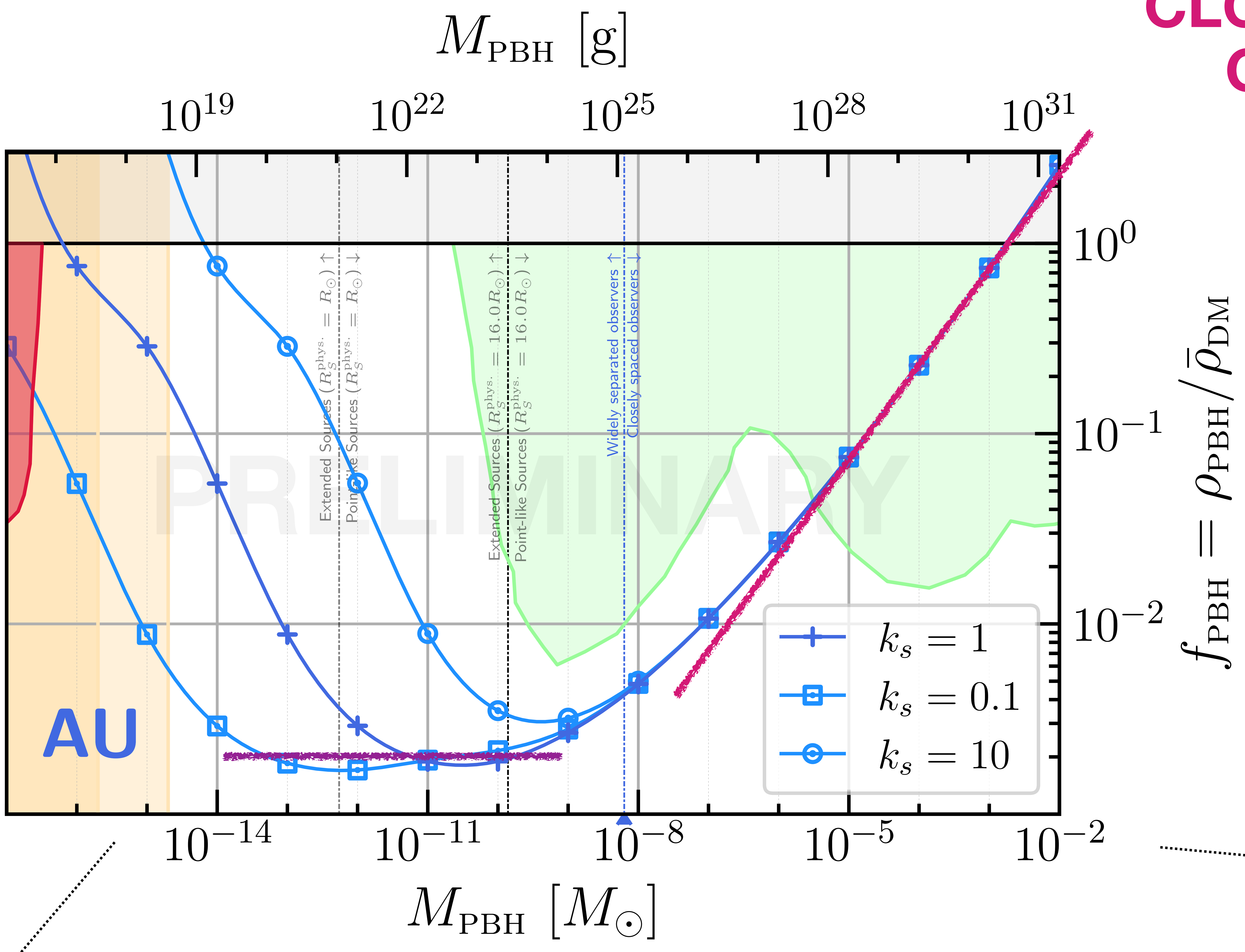

~POINT SOURCES, WIDELY SEPARATED OBSERVERS

Scalings

POINT SOURCES, CLOSELY SPACED OBSERVERS

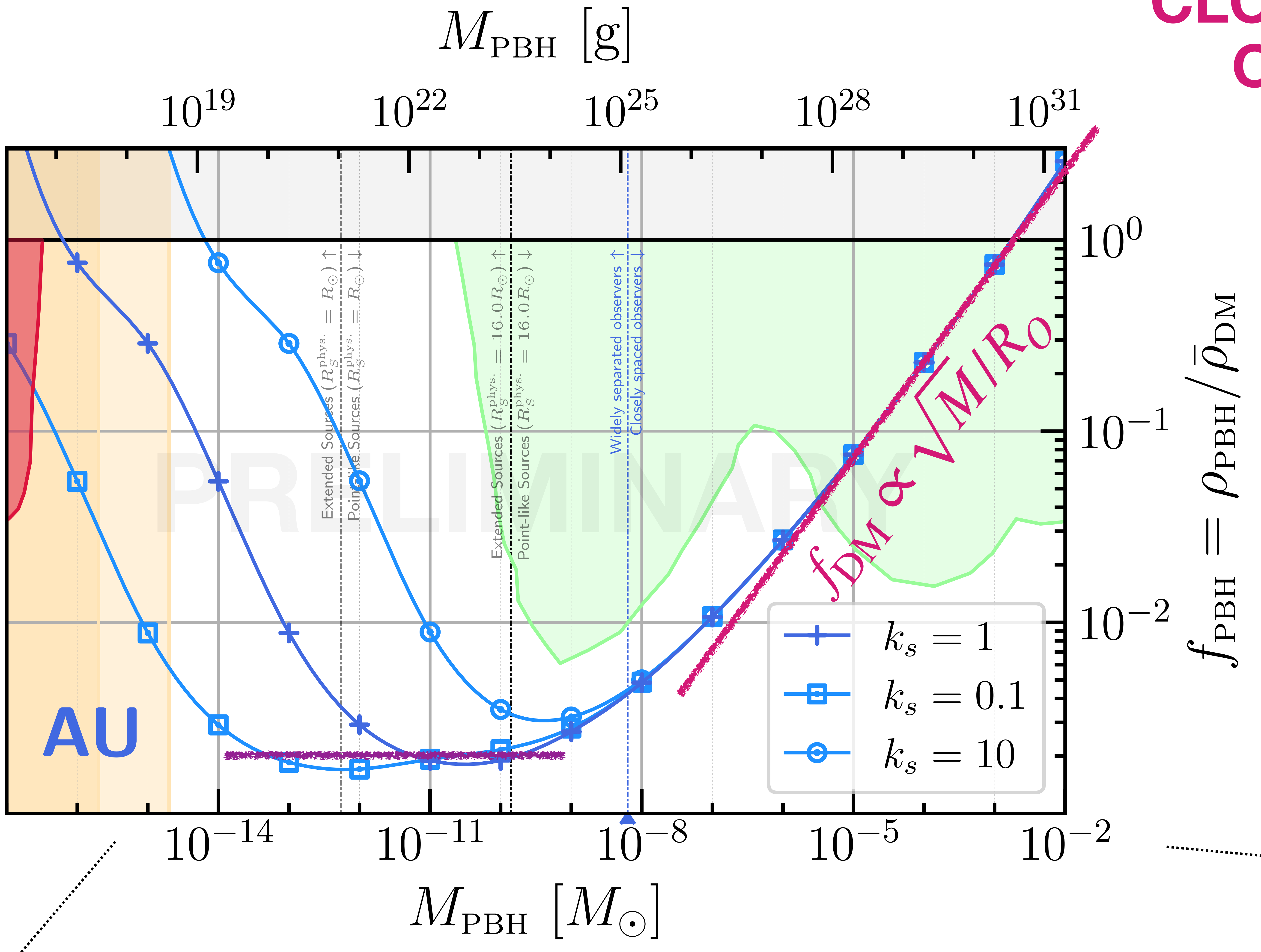

~POINT SOURCES, WIDELY SEPARATED OBSERVERS

Scalings

EXTENDED SOURCE, WIDELY SEPARATED OBSERVERS

POINT SOURCES, CLOSELY SPACED OBSERVERS

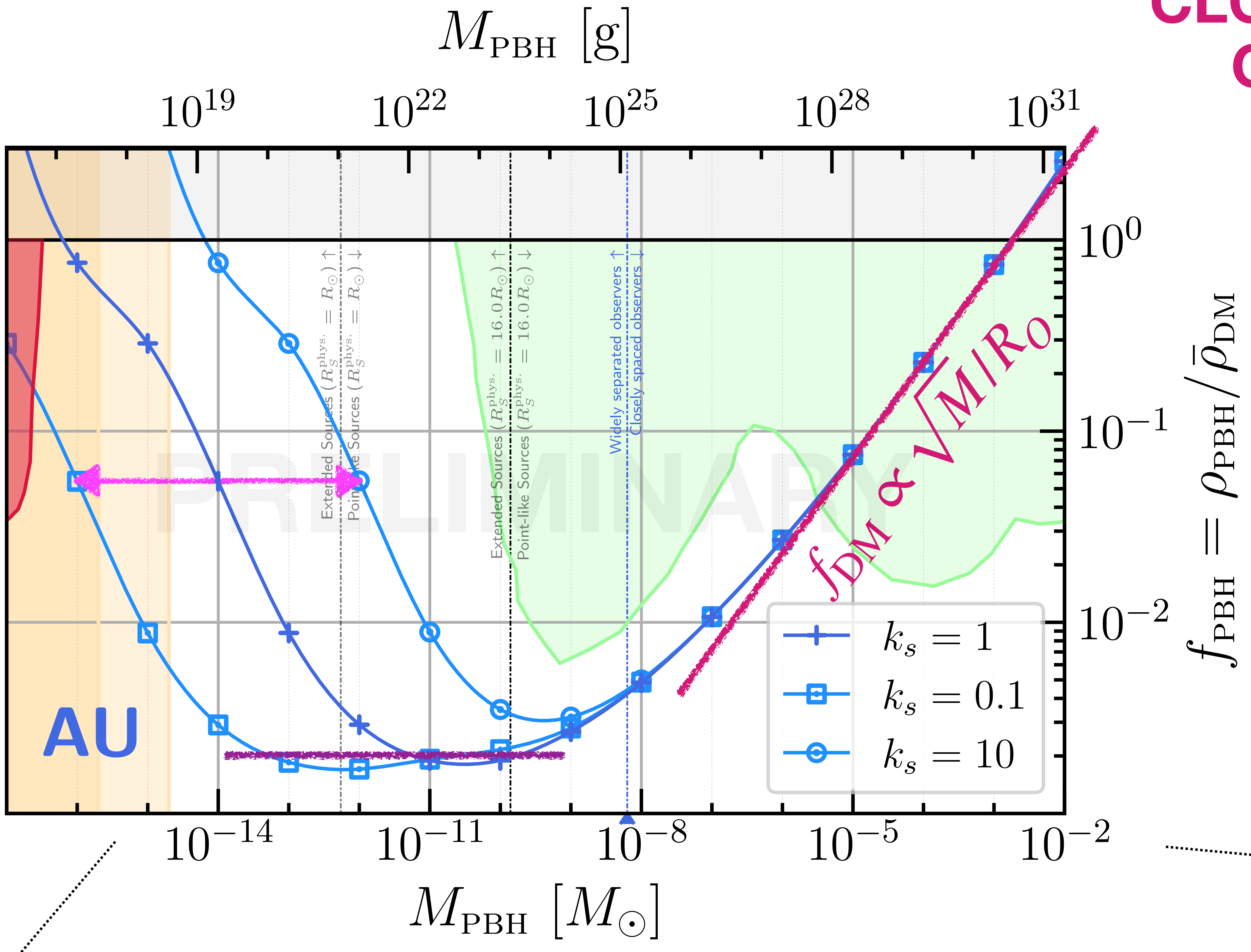

~POINT SOURCES, WIDELY SEPARATED OBSERVERS

Michael A. Fedderke [Perimeter]

Scalings

EXTENDED SOURCE, WIDELY SEPARATED OBSERVERS

POINT SOURCES, CLOSELY SPACED OBSERVERS

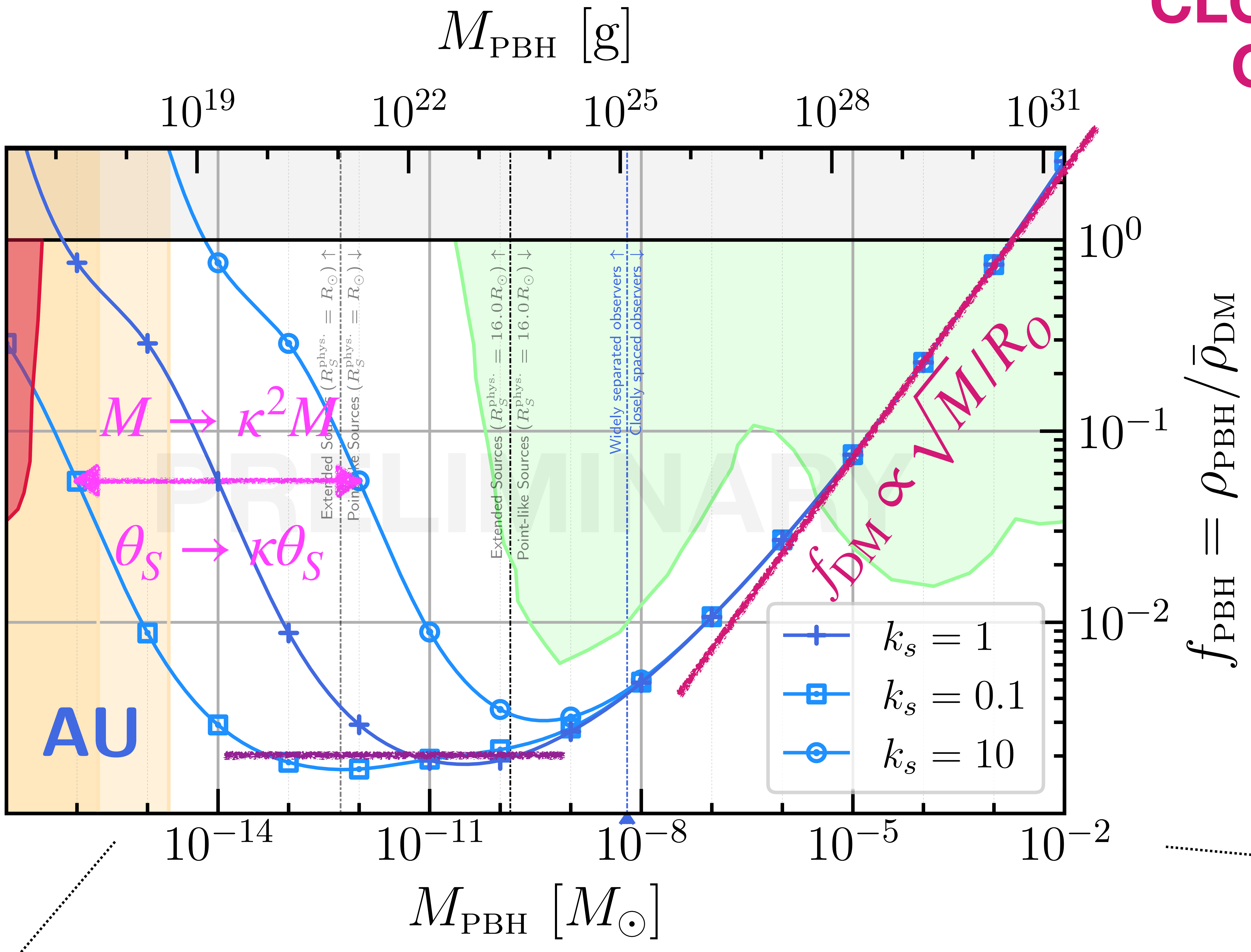

~POINT SOURCES, WIDELY SEPARATED OBSERVERS

Scalings

EXTENDED SOURCE, WIDELY SEPARATED OBSERVERS

POINT SOURCES, CLOSELY SPACED OBSERVERS

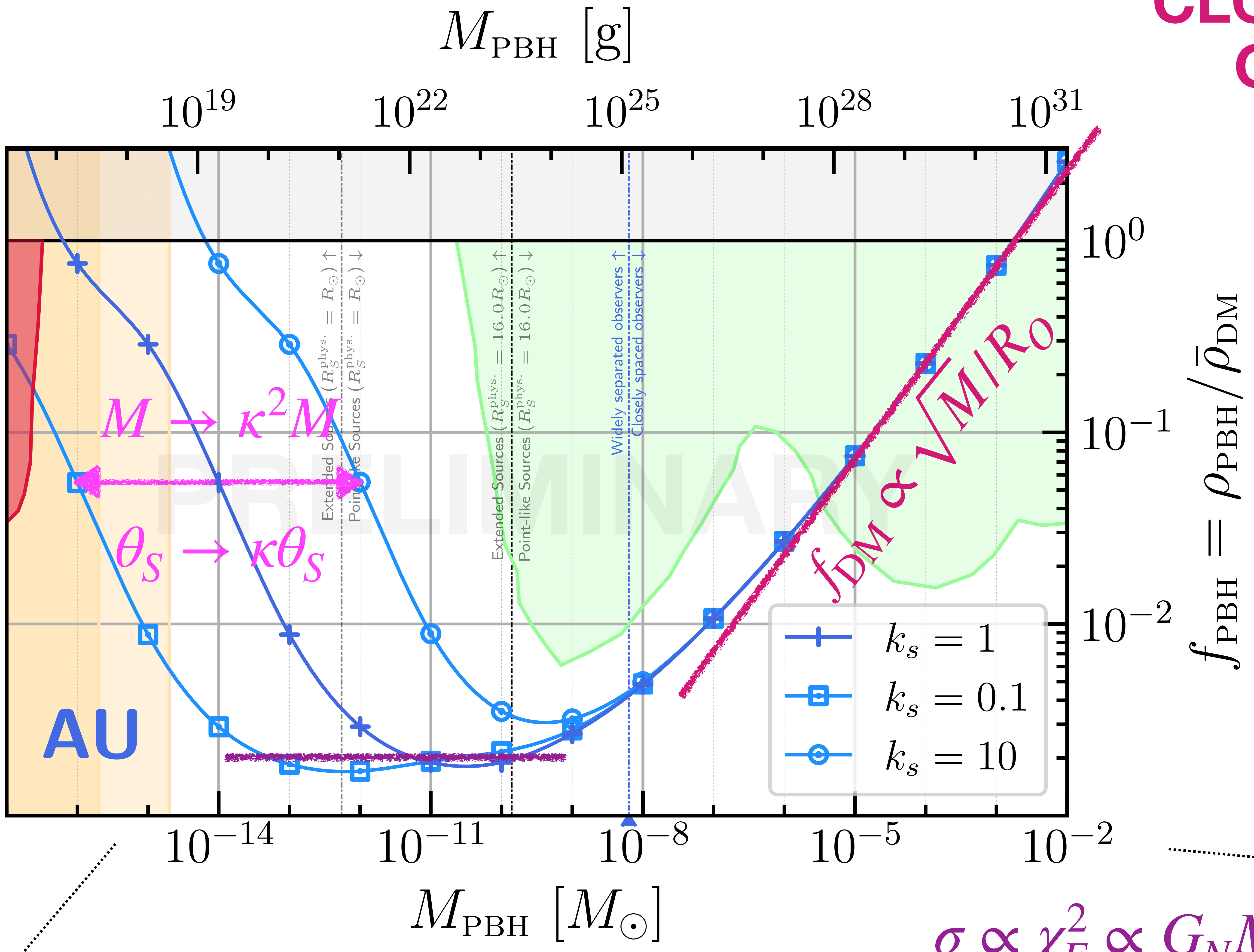

$\sigma \propto \chi_E^2 \propto G_N M \chi_L$

~POINT SOURCES, WIDELY SEPARATED OBSERVERS

Michael A. Fedderke [Perimeter]

Scalings

EXTENDED SOURCE, WIDELY SEPARATED OBSERVERS

POINT SOURCES, CLOSELY SPACED OBSERVERS

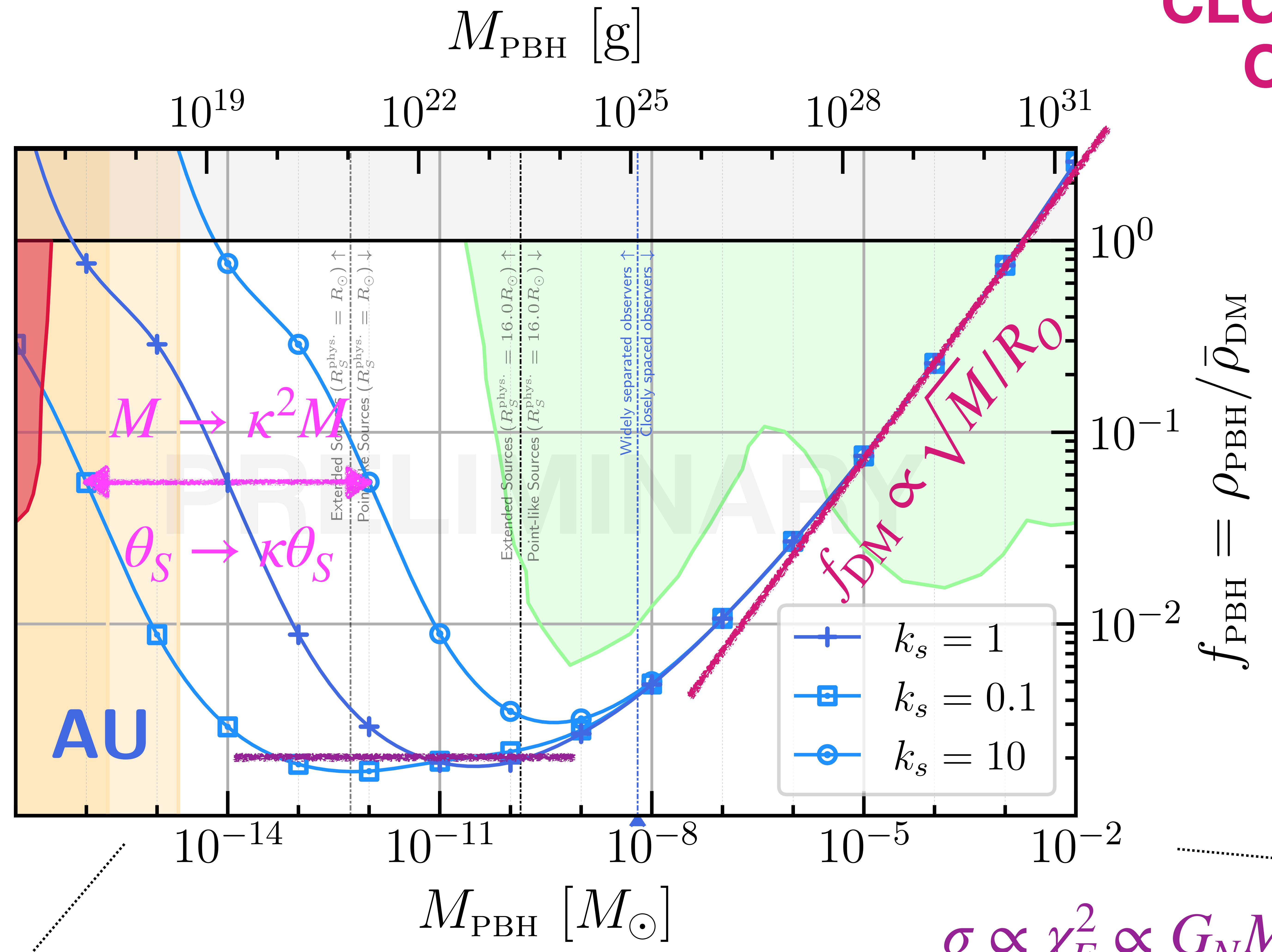

$$\sigma \propto \chi_E^2 \propto G_N M \chi_L$$

$$\mathscr{V} \propto G_N M \chi_S^2$$

~POINT SOURCES, WIDELY SEPARATED OBSERVERS

Scalings

EXTENDED SOURCE, WIDELY SEPARATED OBSERVERS

POINT SOURCES, CLOSELY SPACED OBSERVERS

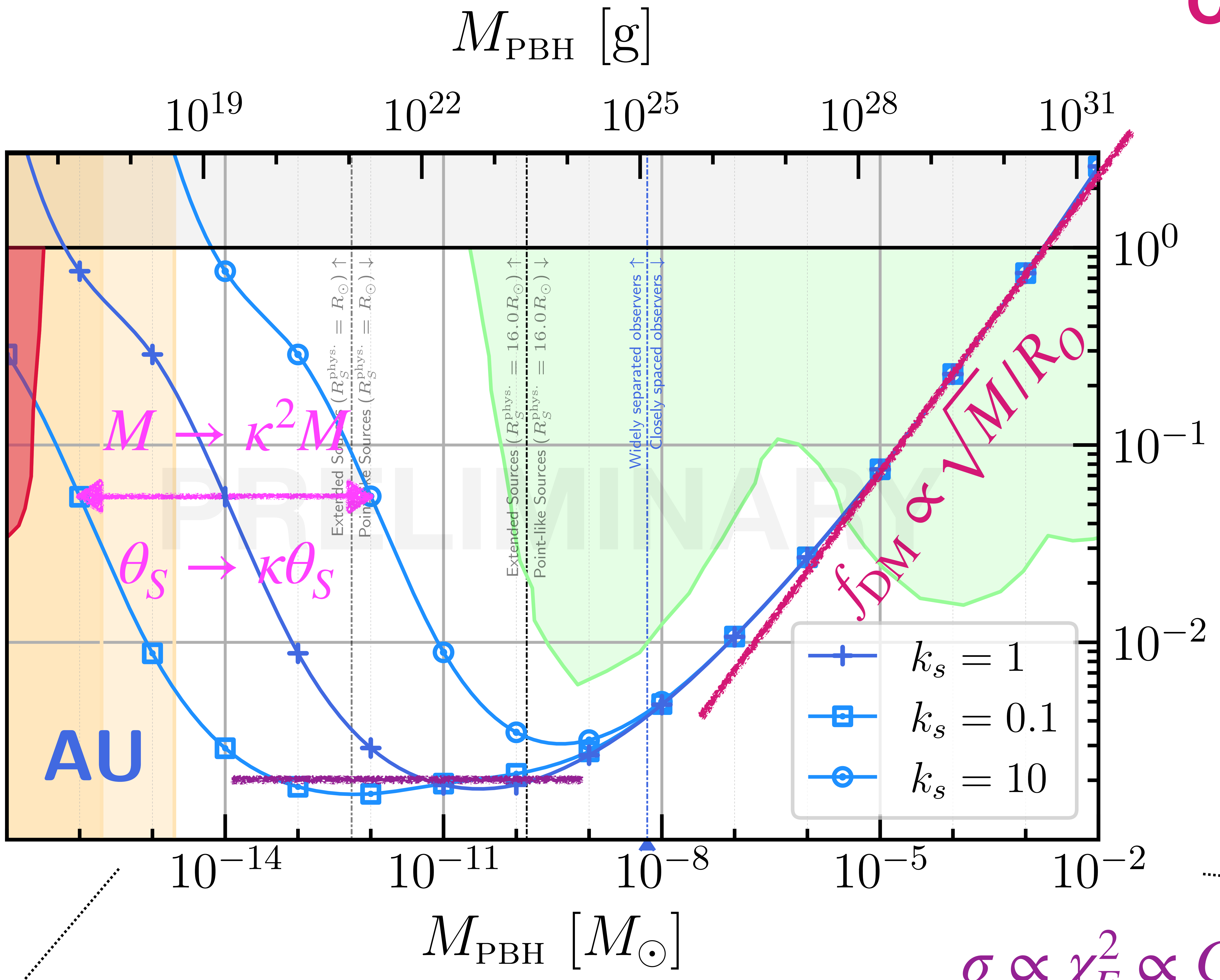

~POINT SOURCES, WIDELY SEPARATED OBSERVERS

$\sigma \propto \chi_E^2 \propto G_N M \chi_L$

$\mathscr{V} \propto G_N M \chi_S^2 \qquad f_{\rm DM}^{\rm limit} \propto \frac{M}{\bar{\mathscr{V}}} \propto M^0$

Michael A. Fedderke [Perimeter]

Scalings

Michael A. Fedderke [Perimeter]

Scalings

$$\Delta\mu \sim \bar{\mu}_1 - 1 \longrightarrow \frac{d\bar{\mu}}{dy}\Delta y \propto \frac{R_O}{\chi_E}(\bar{\mu}_1 - 1)$$

EXTENDED SOURCE, WIDELY SEPARATED OBSERVERS

POINT SOURCES, CLOSELY SPACED OBSERVERS

$$\sigma \propto R_O \chi_E \propto R_O\sqrt{G_N M \chi_L}$$

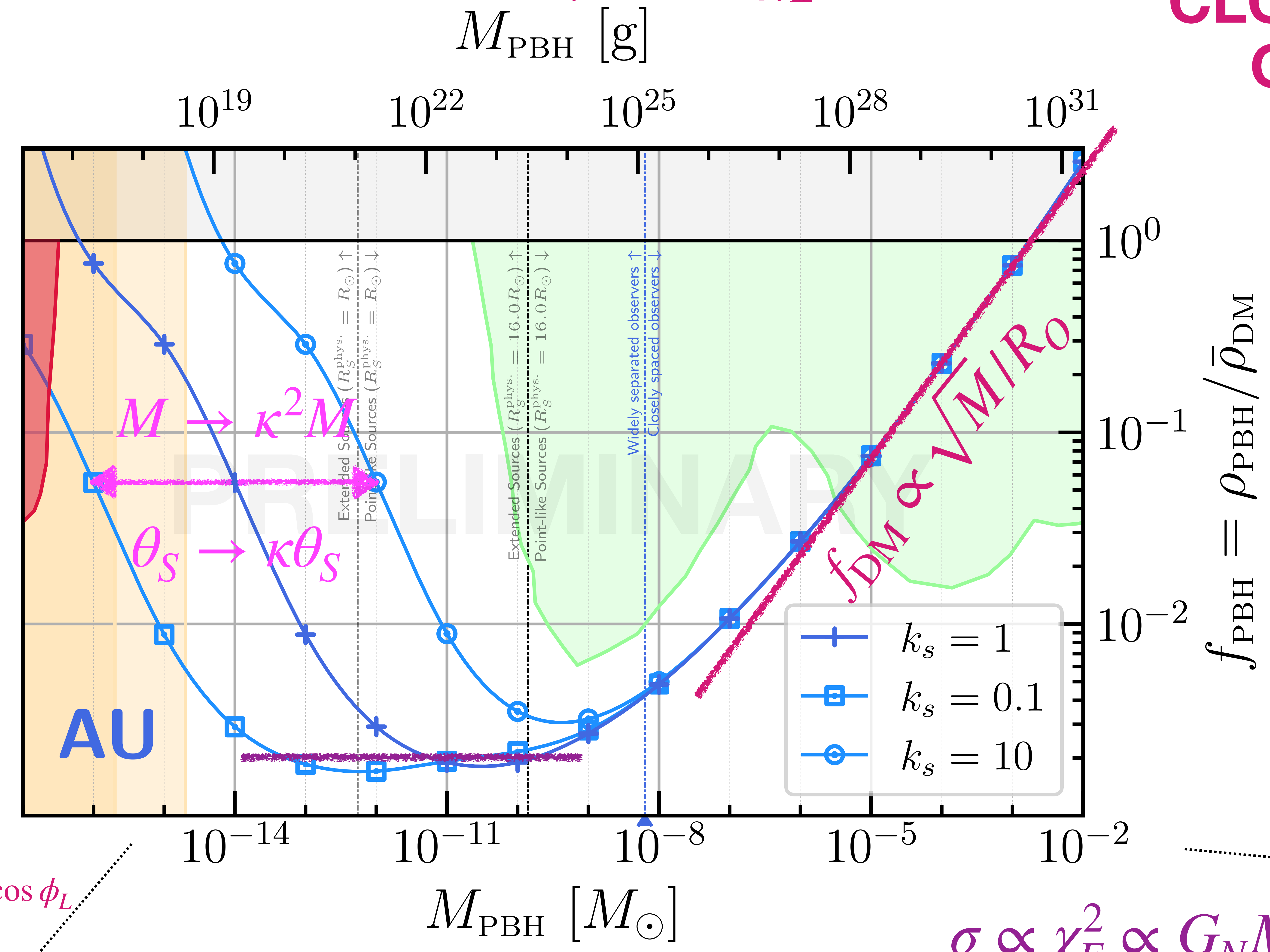

$$\bar{y}_i^2 = \left(\frac{\Delta\chi_\perp^L}{\chi_E^L}\right)^2 + \left(\frac{R_O/2}{\chi_E^O}\right)^2 \mp \frac{R_O}{\chi_E^O}\frac{\Delta\chi_\perp^L}{\chi_E^L}\cos\phi_L$$

~POINT SOURCES, WIDELY SEPARATED OBSERVERS

$$\sigma \propto \chi_E^2 \propto G_N M \chi_L$$

$$\mathscr{V} \propto G_N M \chi_S^2 \qquad f_{\rm DM}^{\rm limit} \propto \frac{M}{\bar{\mathscr{V}}} \propto M^0$$

Scalings

EXTENDED SOURCE, WIDELY SEPARATED OBSERVERS

POINT SOURCES, CLOSELY SPACED OBSERVERS

$$\sigma \propto R_O \chi_E$$

$$\propto R_O \sqrt{G_N M \chi_L}$$

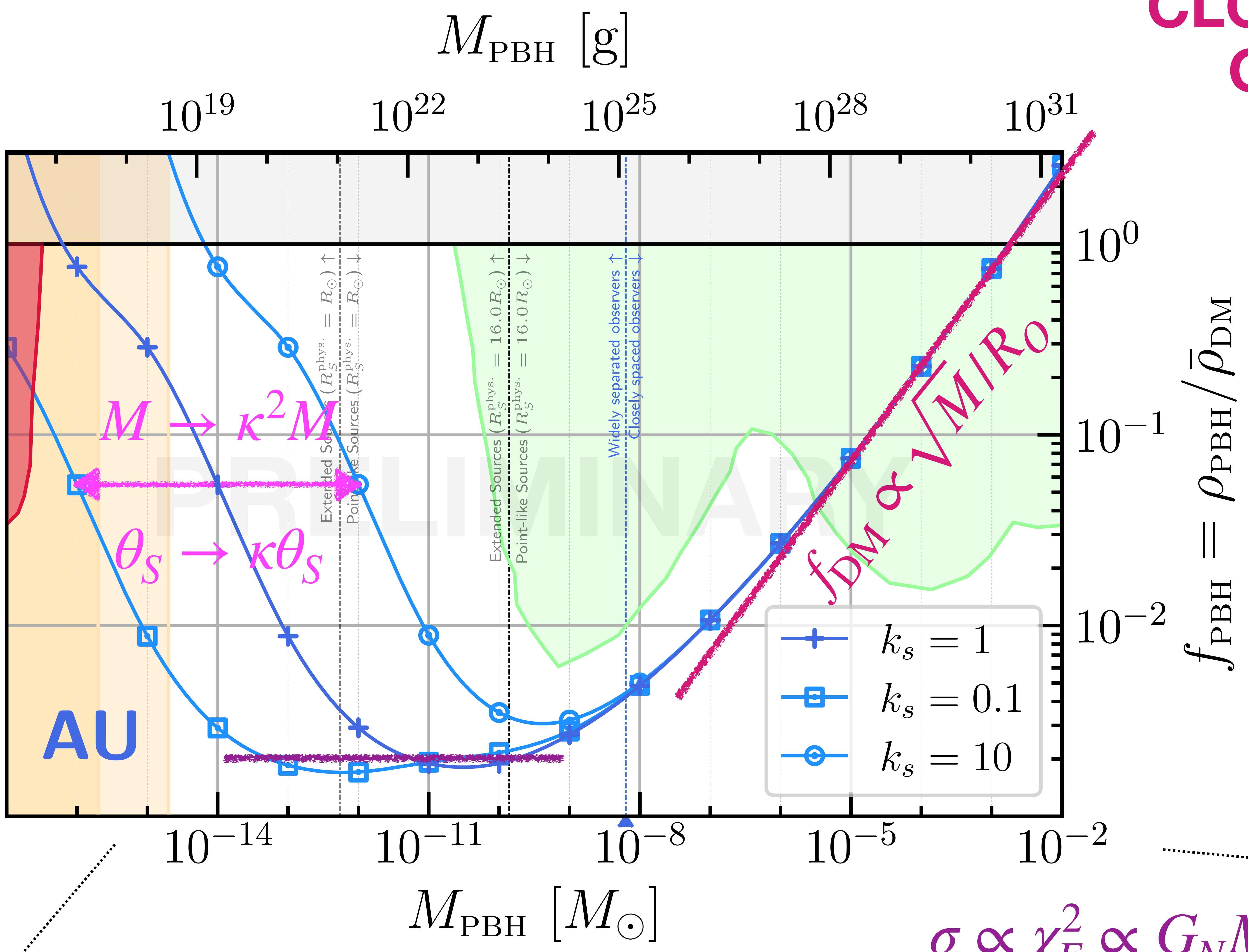

~POINT SOURCES, WIDELY SEPARATED OBSERVERS

$$\sigma \propto \chi_E^2 \propto G_N M \chi_L$$

$$\mathscr{V} \propto G_N M \chi_S^2 \qquad f_{\rm DM}^{\rm limit} \propto \frac{M}{\bar{\mathscr{V}}} \propto M^0$$

Michael A. Fedderke [Perimeter]

Scalings

EXTENDED SOURCE, WIDELY SEPARATED OBSERVERS

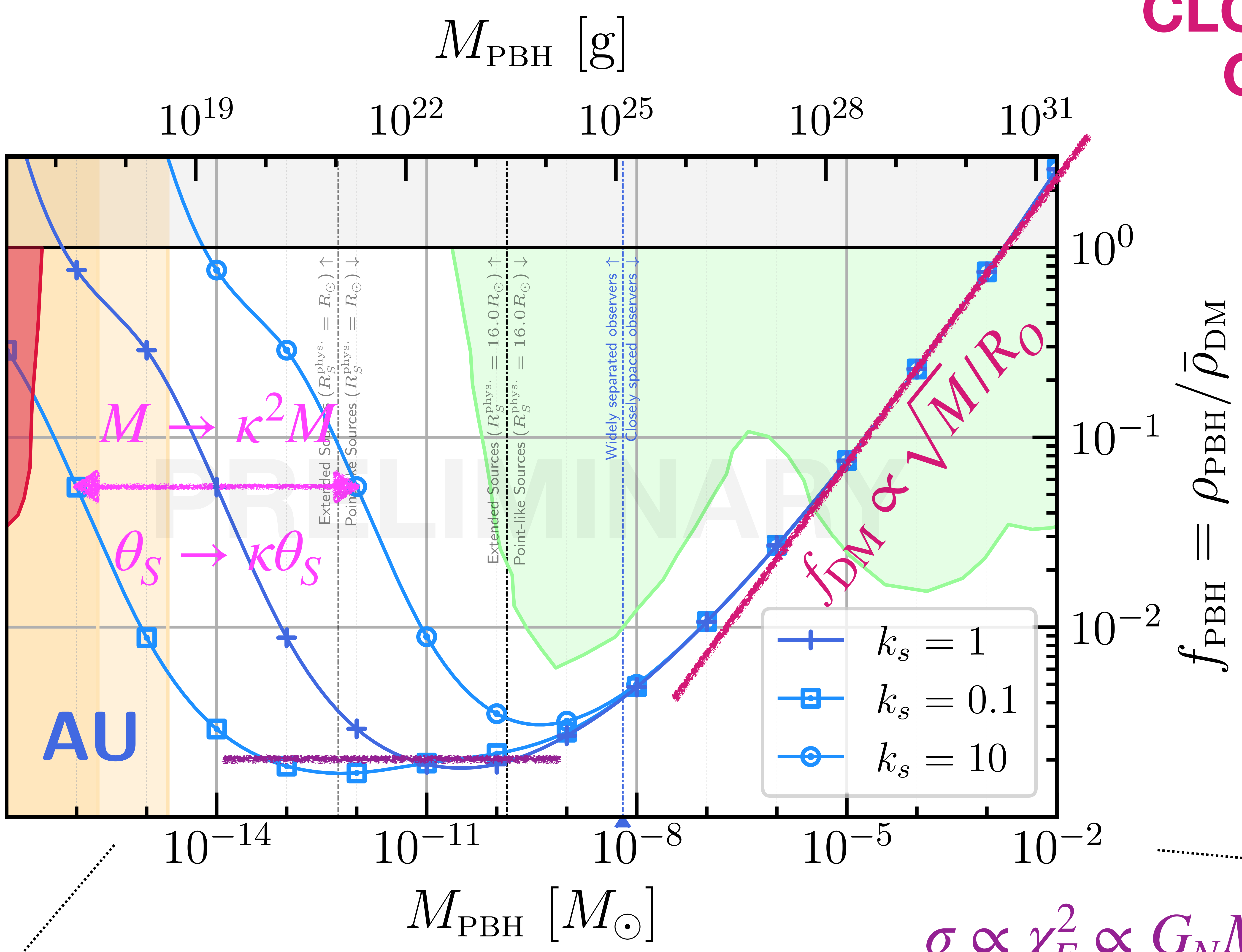

POINT SOURCES, CLOSELY SPACED OBSERVERS

$$\sigma \propto R_O \chi_E$$
$$\propto R_O \sqrt{G_N M \chi_L}$$
$$\mathscr{V} \propto R_O \sqrt{G_N M \chi_S^3}$$

~POINT SOURCES, WIDELY SEPARATED OBSERVERS

$$\sigma \propto \chi_E^2 \propto G_N M \chi_L$$
$$\mathscr{V} \propto G_N M \chi_S^2 \qquad f_{\rm DM}^{\rm limit} \propto \frac{M}{\bar{\mathscr{V}}} \propto M^0$$

Scalings

EXTENDED SOURCE, WIDELY SEPARATED OBSERVERS

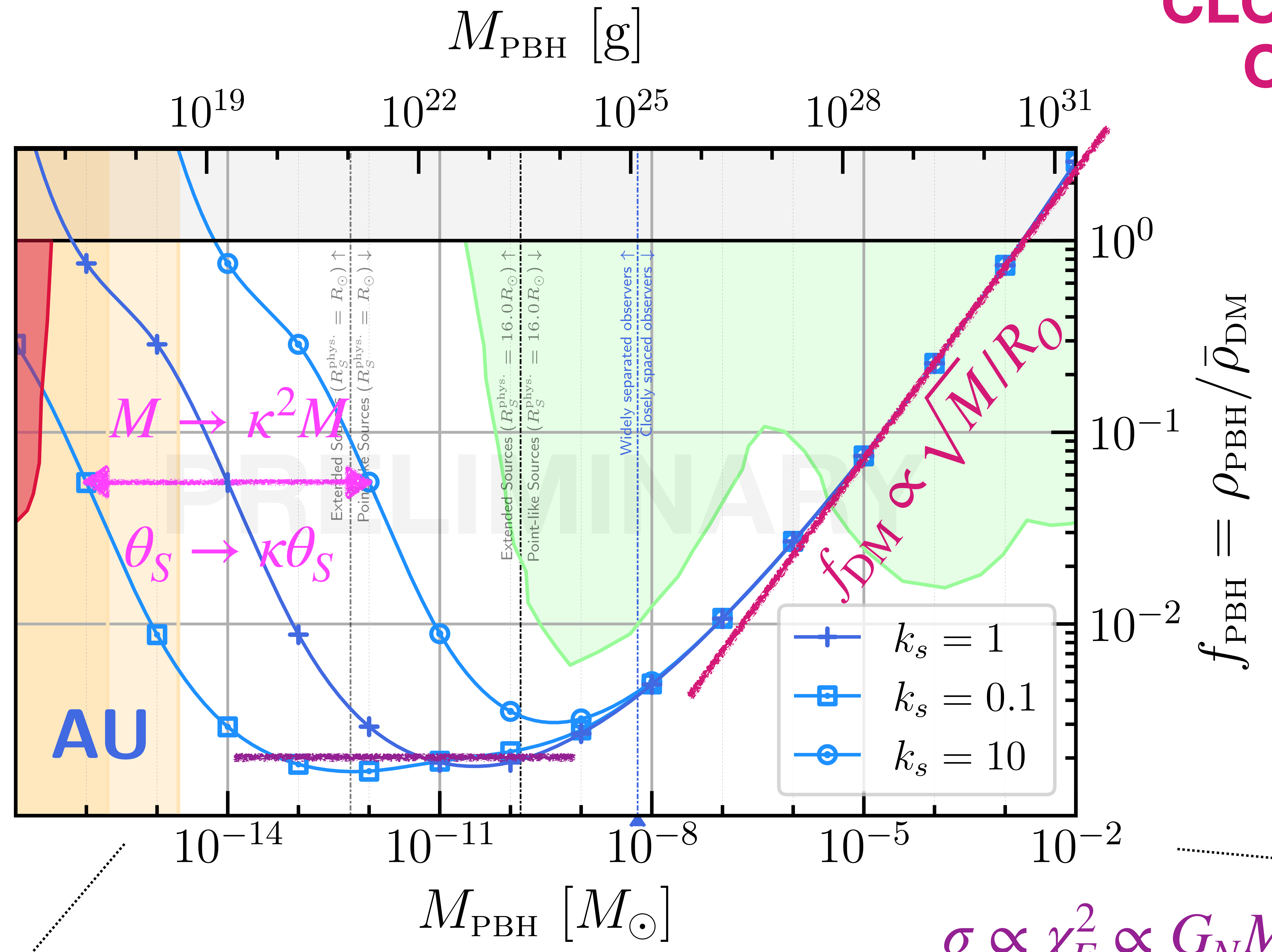

POINT SOURCES, CLOSELY SPACED OBSERVERS

$\sigma \propto R_O \chi_E$

$\propto R_O \sqrt{G_N M \chi_L}$

$\mathscr{V} \propto R_O \sqrt{G_N M \chi_S^3}$

$f_{\rm DM}^{\rm limit} \propto \frac{\sqrt{M}}{R_O}$

~POINT SOURCES, WIDELY SEPARATED OBSERVERS

$\sigma \propto \chi_E^2 \propto G_N M \chi_L$

$\mathscr{V} \propto G_N M \chi_S^2$ $\quad f_{\rm DM}^{\rm limit} \propto \frac{M}{\bar{\mathscr{V}}} \propto M^0$

Michael A. Fedderke [Perimeter]

Scalings

EXTENDED SOURCE, WIDELY SEPARATED OBSERVERS

POINT SOURCES, CLOSELY SPACED OBSERVERS

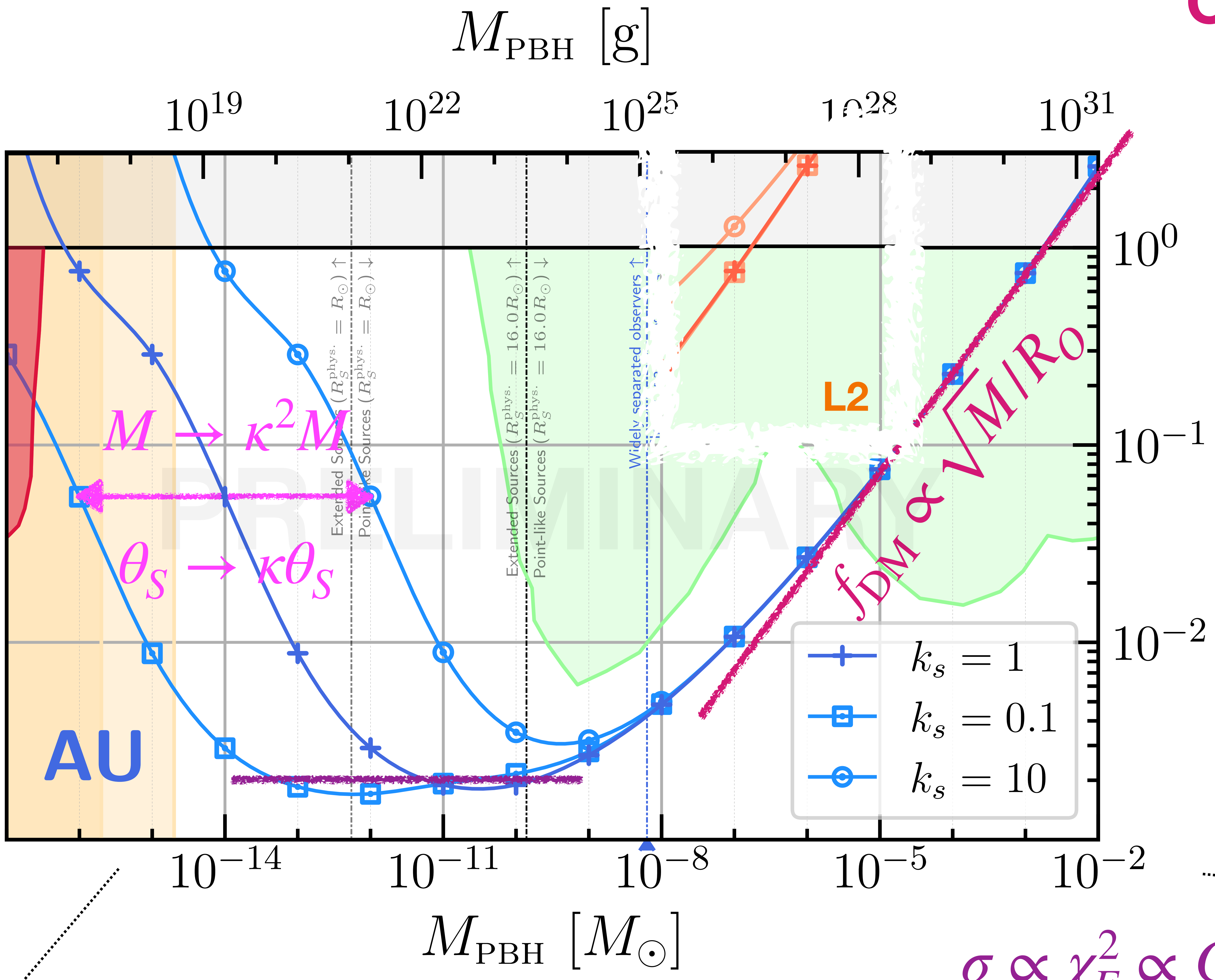

$\sigma \propto R_O \chi_E$

$\propto R_O \sqrt{G_N M \chi_L}$

$\mathscr{V} \propto R_O \sqrt{G_N M \chi_S^3}$

$f_{\rm DM}^{\rm limit} \propto \frac{\sqrt{M}}{R_O}$

$\sigma \propto \chi_E^2 \propto G_N M \chi_L$

$\mathscr{V} \propto G_N M \chi_S^2$ $\quad f_{\rm DM}^{\rm limit} \propto \frac{M}{\bar{\mathscr{V}}} \propto M^0$

~POINT SOURCES, WIDELY SEPARATED OBSERVERS

Michael A. Fedderke [Perimeter]

Scalings

$R_{L2} \sim 10^{-2}$AU

POINT SOURCES, CLOSELY SPACED OBSERVERS

EXTENDED SOURCE, WIDELY SEPARATED OBSERVERS

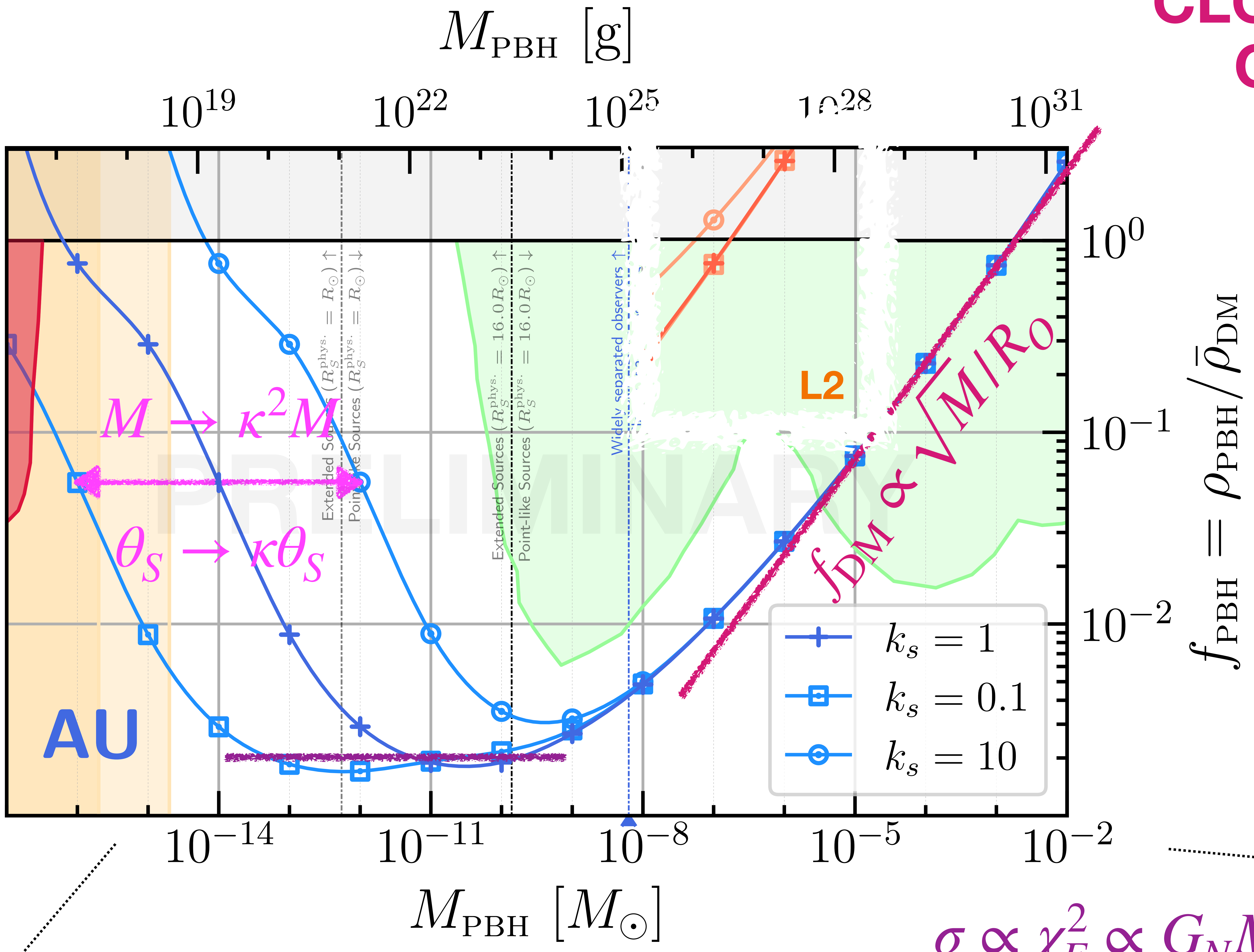

$\sigma \propto R_O \chi_E$

$\propto R_O\sqrt{G_N M \chi_L}$

$\mathscr{V} \propto R_O\sqrt{G_N M \chi_S^3}$

$f_{\rm DM}^{\rm limit} \propto \frac{\sqrt{M}}{R_O}$

~POINT SOURCES, WIDELY SEPARATED OBSERVERS

$\sigma \propto \chi_E^2 \propto G_N M \chi_L$

$\mathscr{V} \propto G_N M \chi_S^2$

$f_{\rm DM}^{\rm limit} \propto \frac{M}{\bar{\mathscr{V}}} \propto M^0$

Scalings

EXTENDED SOURCE, WIDELY SEPARATED OBSERVERS

$R_{L2} \sim 10^{-2}$AU

POINT SOURCES, CLOSELY SPACED OBSERVERS

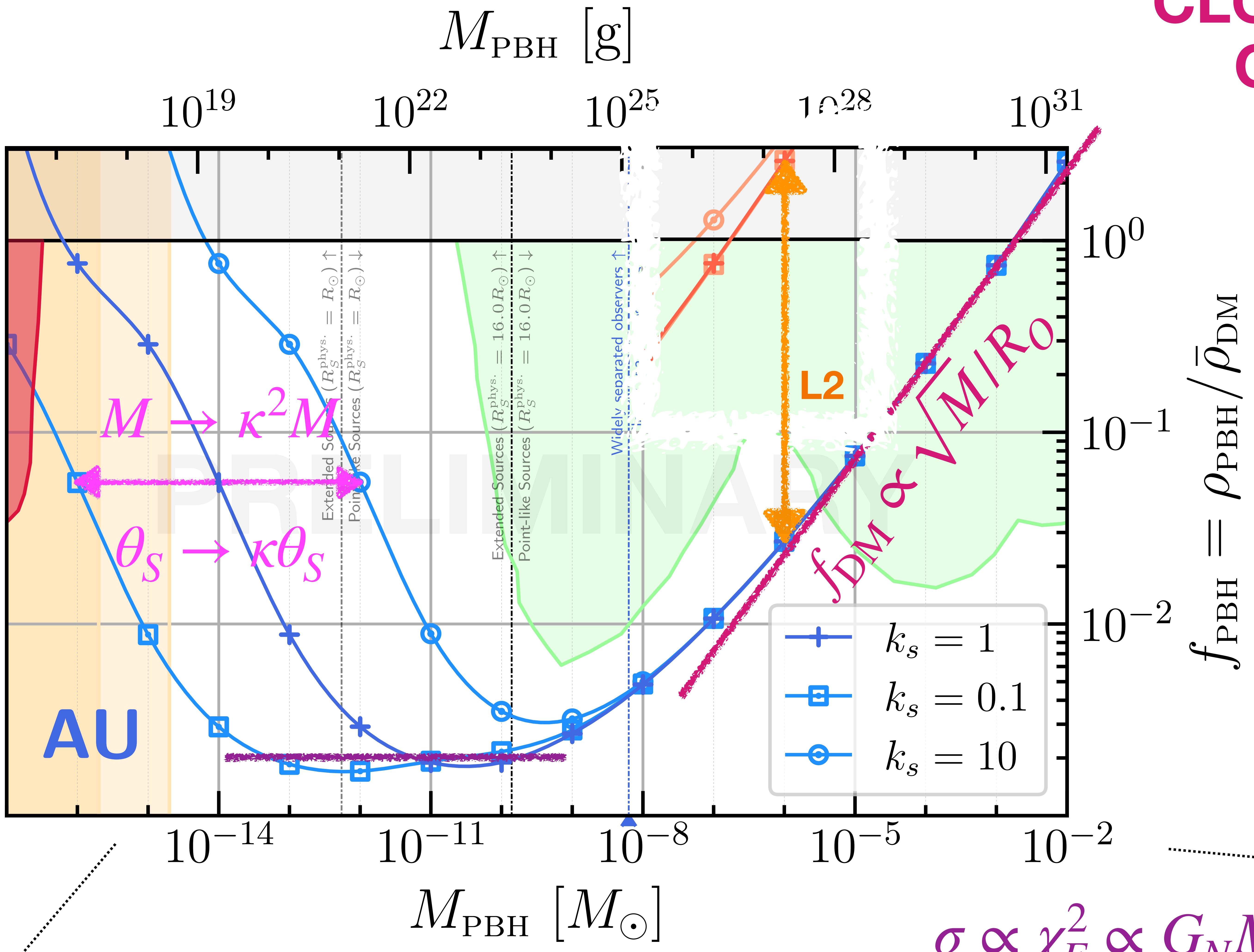

$\sigma \propto R_O \chi_E$

$\propto R_O \sqrt{G_N M \chi_L}$

$\mathscr{V} \propto R_O \sqrt{G_N M \chi_S^3}$

$f_{\rm DM}^{\rm limit} \propto \dfrac{\sqrt{M}}{R_O}$

~POINT SOURCES, WIDELY SEPARATED OBSERVERS

$\sigma \propto \chi_E^2 \propto G_N M \chi_L$

$\mathscr{V} \propto G_N M \chi_S^2 \qquad f_{\rm DM}^{\rm limit} \propto \dfrac{M}{\bar{\mathscr{V}}} \propto M^0$

Michael A. Fedderke [Perimeter]

Scalings

$R_{L2} \sim 10^{-2}$AU

EXTENDED SOURCE, WIDELY SEPARATED OBSERVERS

POINT SOURCES, CLOSELY SPACED OBSERVERS

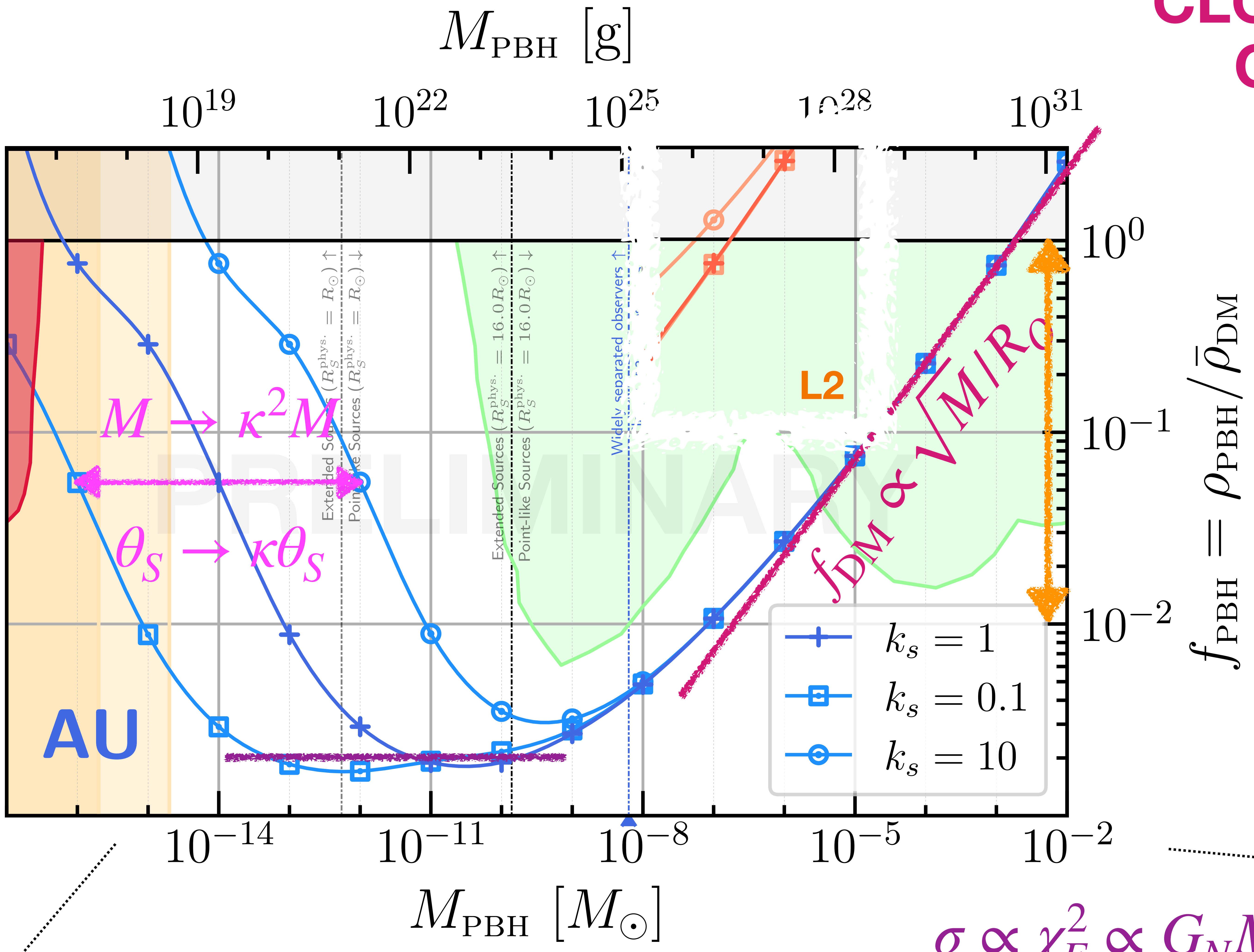

$\sigma \propto R_O \chi_E$

$\propto R_O \sqrt{G_N M \chi_L}$

$\mathscr{V} \propto R_O \sqrt{G_N M \chi_S^3}$

$f_{DM}^{\text{limit}} \propto \dfrac{\sqrt{M}}{R_O}$

$\sigma \propto \chi_E^2 \propto G_N M \chi_L$

$\mathscr{V} \propto G_N M \chi_S^2 \qquad f_{DM}^{\text{limit}} \propto \dfrac{M}{\bar{\mathscr{V}}} \propto M^0$

~POINT SOURCES, WIDELY SEPARATED OBSERVERS

Michael A. Fedderke [Perimeter]

Scalings

EXTENDED SOURCE, WIDELY SEPARATED OBSERVERS

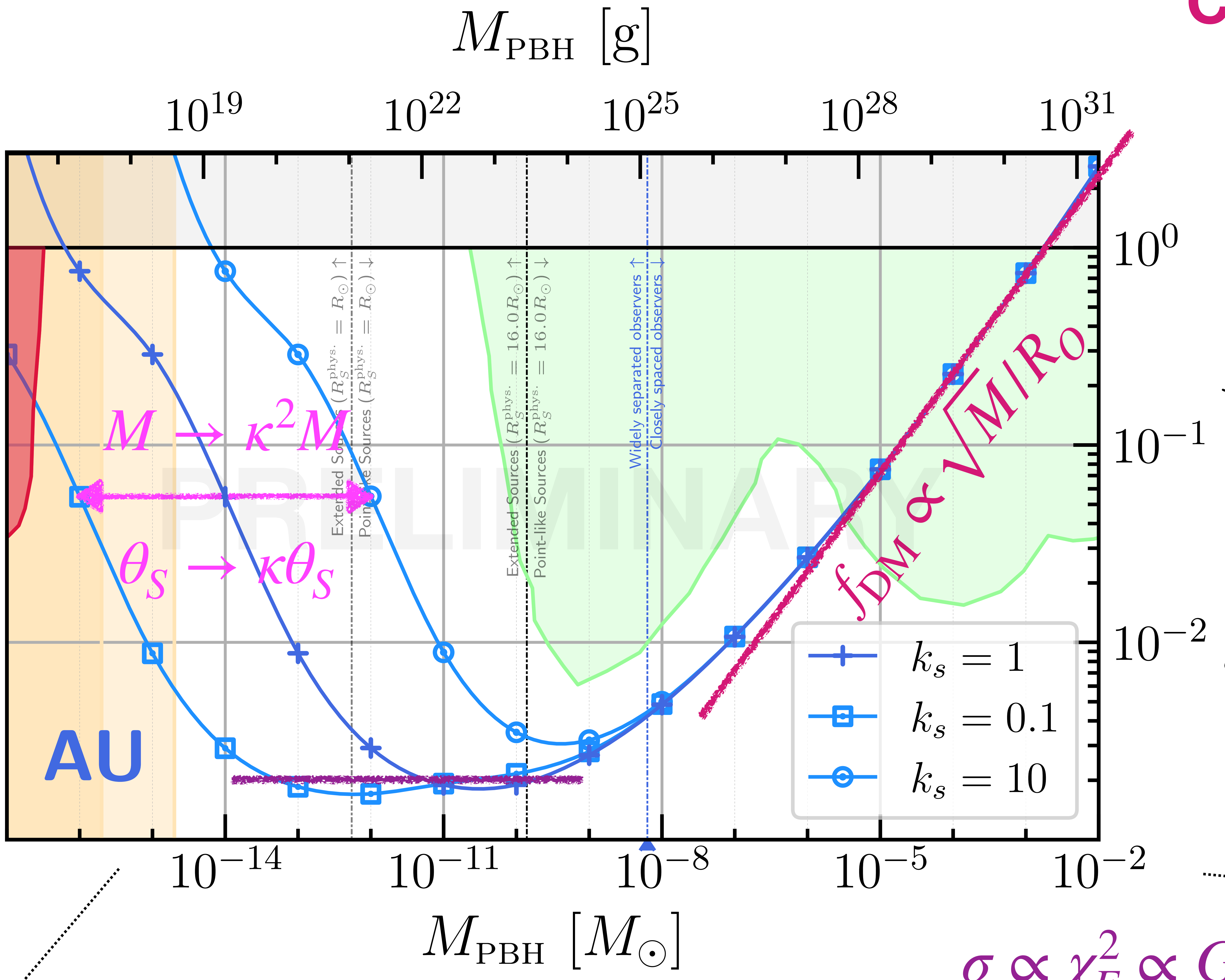

POINT SOURCES, CLOSELY SPACED OBSERVERS

$$\sigma \propto R_O \chi_E$$

$$\propto R_O \sqrt{G_N M \chi_L}$$

$$\mathscr{V} \propto R_O \sqrt{G_N M \chi_S^3}$$

$$f_{\rm DM}^{\rm limit} \propto \frac{\sqrt{M}}{R_O}$$

~POINT SOURCES, WIDELY SEPARATED OBSERVERS

$$\sigma \propto \chi_E^2 \propto G_N M \chi_L$$

$$\mathscr{V} \propto G_N M \chi_S^2 \qquad f_{\rm DM}^{\rm limit} \propto \frac{M}{\bar{\mathscr{V}}} \propto M^0$$

Michael A. Fedderke [Perimeter]

Scalings

EXTENDED SOURCE, WIDELY SEPARATED OBSERVERS

$$\mathscr{V} \propto \frac{(G_N M)^3}{\theta_S^4}$$

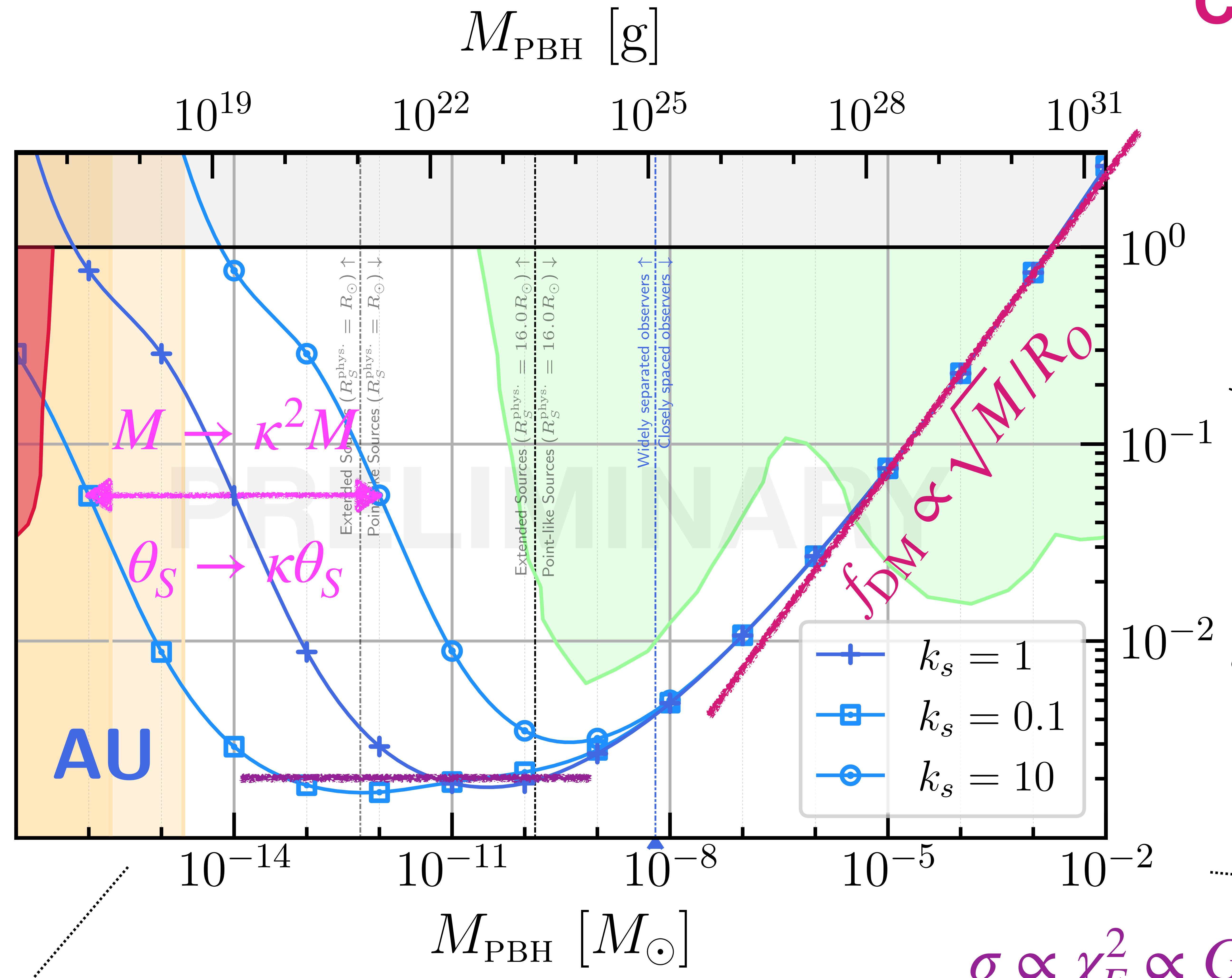

POINT SOURCES, CLOSELY SPACED OBSERVERS

$$\sigma \propto R_O \chi_E$$

$$\propto R_O \sqrt{G_N M \chi_L}$$

$$\mathscr{V} \propto R_O \sqrt{G_N M \chi_S^3}$$

$$f_{\rm DM}^{\rm limit} \propto \frac{\sqrt{M}}{R_O}$$

~POINT SOURCES, WIDELY SEPARATED OBSERVERS

$$\sigma \propto \chi_E^2 \propto G_N M \chi_L$$

$$\mathscr{V} \propto G_N M \chi_S^2 \qquad f_{\rm DM}^{\rm limit} \propto \frac{M}{\bar{\mathscr{V}}} \propto M^0$$

Michael A. Fedderke [Perimeter]

Scalings

EXTENDED SOURCE, WIDELY SEPARATED OBSERVERS

$$\mathscr{V} \propto \frac{(G_N M)^3}{\theta_S^4}$$

M-dependence of $f_{\rm DM}^{\rm limit}$ dominated by population distribution of θ_S

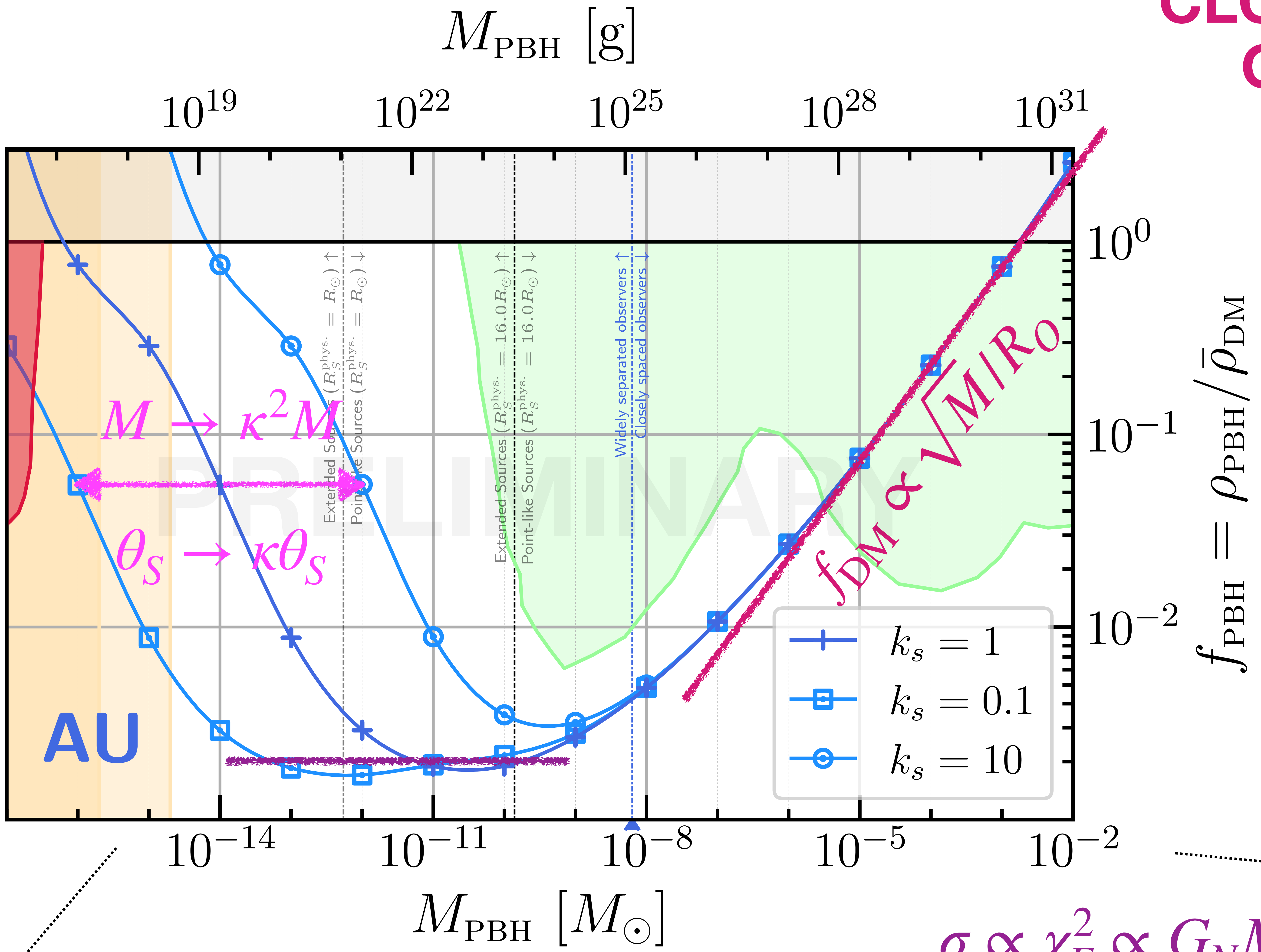

POINT SOURCES, CLOSELY SPACED OBSERVERS

$$\sigma \propto R_O \chi_E$$

$$\propto R_O \sqrt{G_N M \chi_L}$$

$$\mathscr{V} \propto R_O \sqrt{G_N M \chi_S^3}$$

$$f_{\rm DM}^{\rm limit} \propto \frac{\sqrt{M}}{R_O}$$

~POINT SOURCES, WIDELY SEPARATED OBSERVERS

$$\sigma \propto \chi_E^2 \propto G_N M \chi_L$$

$$\mathscr{V} \propto G_N M \chi_S^2 \qquad f_{\rm DM}^{\rm limit} \propto \frac{M}{\bar{\mathscr{V}}} \propto M^0$$

Michael A. Fedderke [Perimeter]

Scalings

$$\bar{\mathscr{V}} \sim (G_N M)^3 \sum_{i=1}^{\aleph} (\theta_S^i)^{-4} \sim (G_N M)^3 (\theta_S^{\min})^{-4} \sum_{i=1}^{\aleph} (\theta_S^{\min}/\theta_S^i)^4$$

EXTENDED SOURCE, WIDELY SEPARATED OBSERVERS

$$\mathscr{V} \propto \frac{(G_N M)^3}{\theta_S^4}$$

M-dependence of $f_{\rm DM}^{\rm limit}$ dominated by population distribution of θ_S

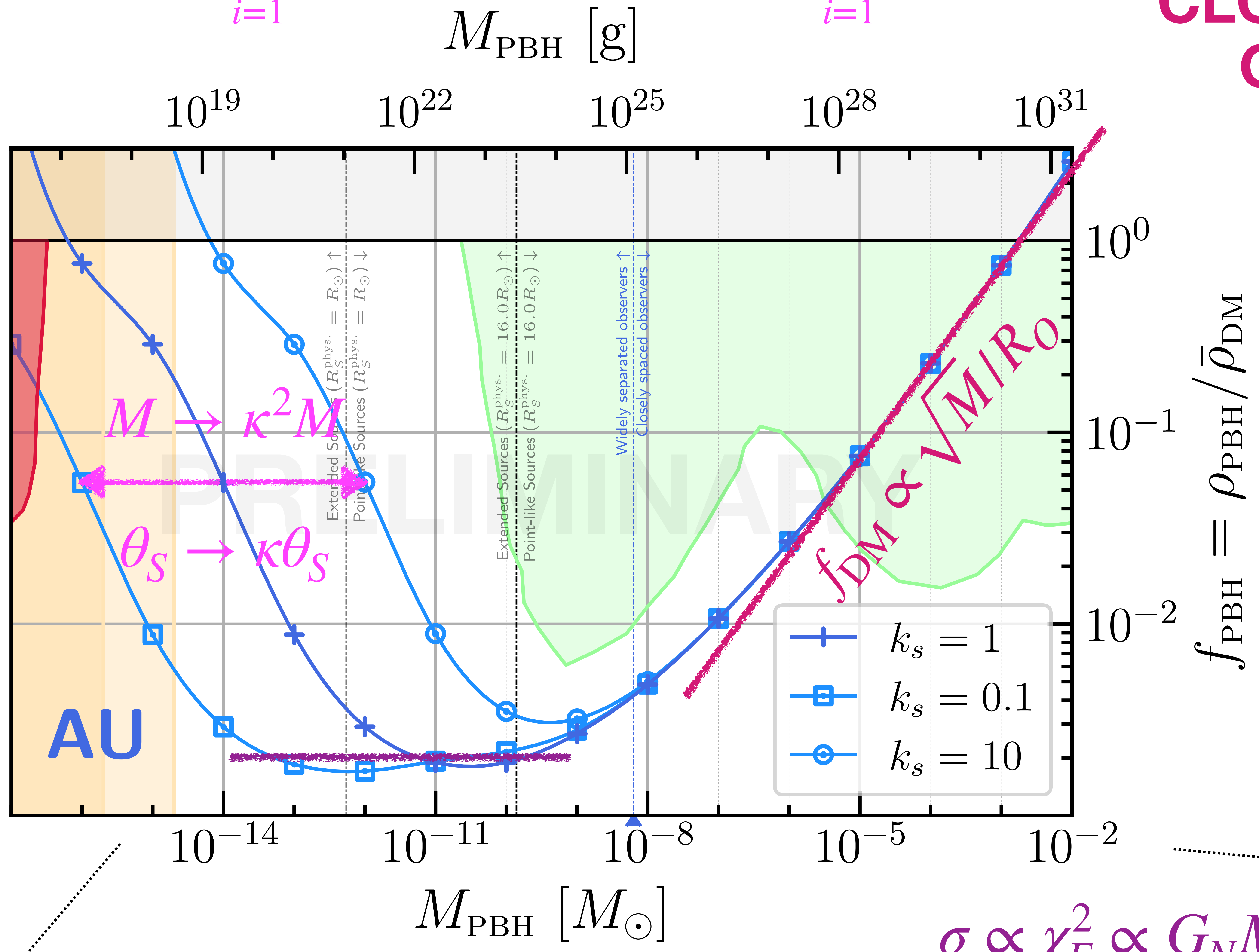

POINT SOURCES, CLOSELY SPACED OBSERVERS

$$\sigma \propto R_O \chi_E$$

$$\propto R_O \sqrt{G_N M \chi_L}$$

$$\mathscr{V} \propto R_O \sqrt{G_N M \chi_S^3}$$

$$f_{\rm DM}^{\rm limit} \propto \frac{\sqrt{M}}{R_O}$$

~POINT SOURCES, WIDELY SEPARATED OBSERVERS

$$\sigma \propto \chi_E^2 \propto G_N M \chi_L$$

$$\mathscr{V} \propto G_N M \chi_S^2 \qquad f_{\rm DM}^{\rm limit} \propto \frac{M}{\bar{\mathscr{V}}} \propto M^0$$

Michael A. Fedderke [Perimeter]

Scalings

$$\bar{\mathscr{V}} \sim (G_N M)^3 \sum_{i=1}^{\aleph} (\theta_S^i)^{-4} \sim (G_N M)^3 (\theta_S^{\min})^{-4} \sum_{i=1}^{\aleph} (\theta_S^{\min}/\theta_S^i)^4$$

EXTENDED SOURCE, WIDELY SEPARATED OBSERVERS

$$\mathscr{V} \propto \frac{(G_N M)^3}{\theta_S^4}$$

M-dependence of $f_{\rm DM}^{\rm limit}$ dominated by population distribution of θ_S

$$f_{\rm DM}^{\rm limit} \propto \frac{(\theta_S^{\min})^4}{M^2 \times N_S^{>}}$$

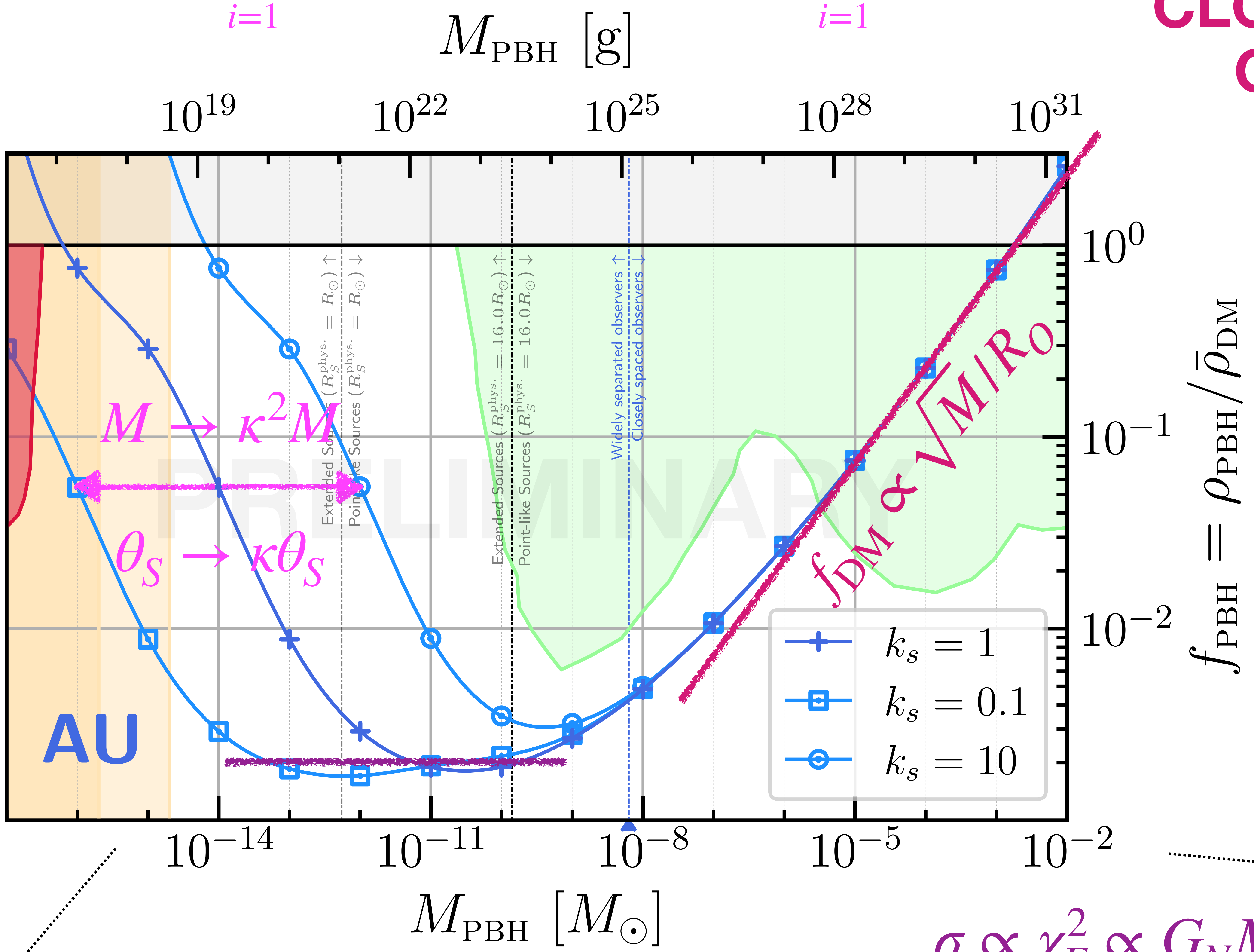

~POINT SOURCES, WIDELY SEPARATED OBSERVERS

POINT SOURCES, CLOSELY SPACED OBSERVERS

$$\sigma \propto R_O \chi_E$$

$$\propto R_O \sqrt{G_N M \chi_L}$$

$$\mathscr{V} \propto R_O \sqrt{G_N M \chi_S^3}$$

$$f_{\rm DM}^{\rm limit} \propto \frac{\sqrt{M}}{R_O}$$

$$\sigma \propto \chi_E^2 \propto G_N M \chi_L$$

$$\mathscr{V} \propto G_N M \chi_S^2 \qquad f_{\rm DM}^{\rm limit} \propto \frac{M}{\bar{\mathscr{V}}} \propto M^0$$

Michael A. Fedderke [Perimeter]

Scalings

$$\bar{\mathscr{V}} \sim (G_N M)^3 \sum_{i=1}^{\tilde{N}} (\theta_S^i)^{-4} \sim (G_N M)^3 (\theta_S^{\min})^{-4} \sum_{i=1}^{\tilde{N}} (\theta_S^{\min}/\theta_S^i)^4$$

EXTENDED SOURCE, WIDELY SEPARATED OBSERVERS

$$\mathscr{V} \propto \frac{(G_N M)^3}{\theta_S^4}$$

M-dependence of $f_{\rm DM}^{\rm limit}$ dominated by population distribution of θ_S

$$f_{\rm DM}^{\rm limit} \propto \frac{(\theta_S^{\min})^4}{M^2 \times N_S^{\gtrsim}}$$

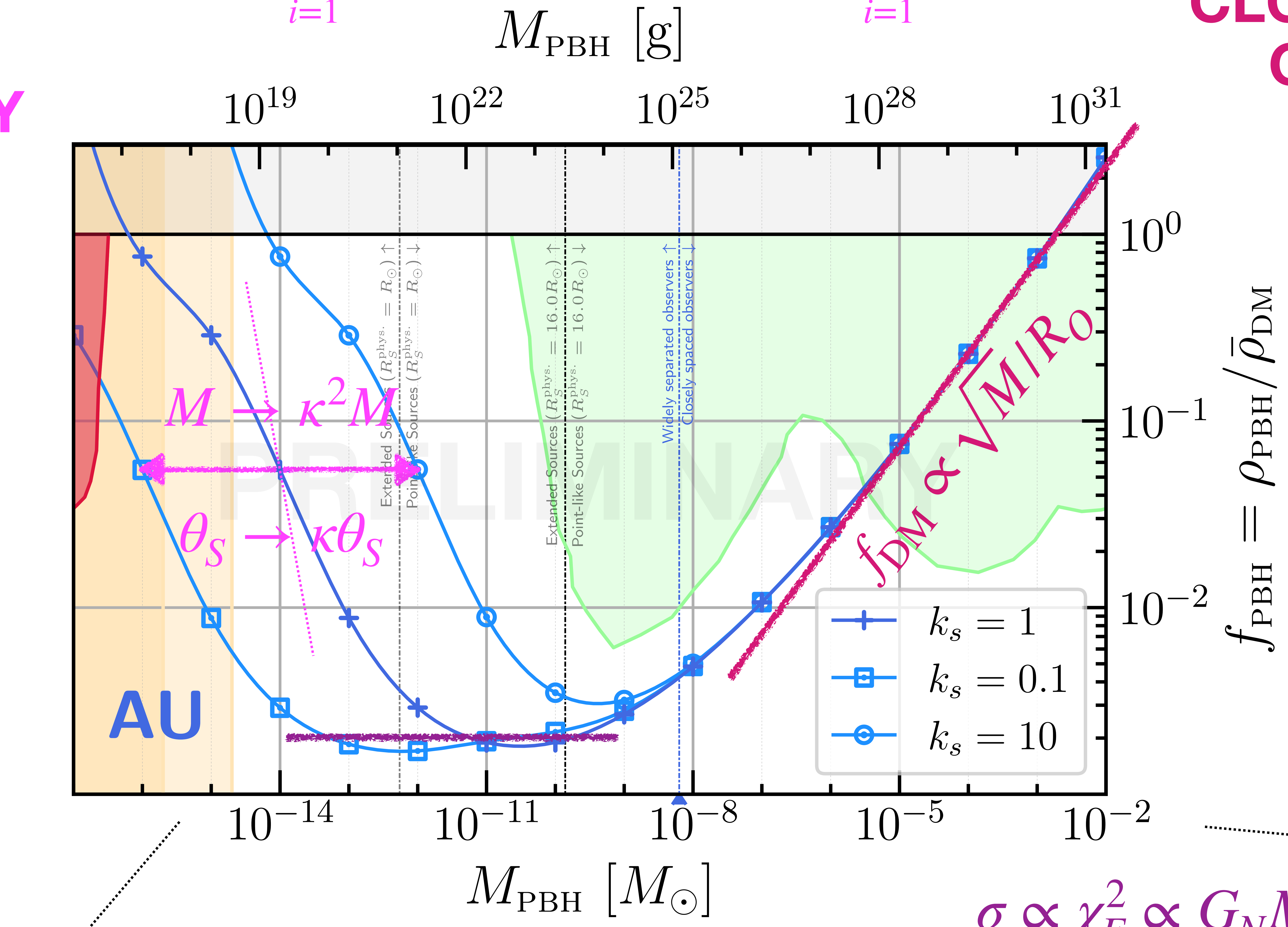

POINT SOURCES, CLOSELY SPACED OBSERVERS

$$\sigma \propto R_O \chi_E$$
$$\propto R_O \sqrt{G_N M \chi_L}$$

$$\mathscr{V} \propto R_O \sqrt{G_N M \chi_S^3}$$

$$f_{\rm DM}^{\rm limit} \propto \frac{\sqrt{M}}{R_O}$$

~POINT SOURCES, WIDELY SEPARATED OBSERVERS

$$\sigma \propto \chi_E^2 \propto G_N M \chi_L$$

$$\mathscr{V} \propto G_N M \chi_S^2 \qquad f_{\rm DM}^{\rm limit} \propto \frac{M}{\bar{\mathscr{V}}} \propto M^0$$

Minimum Variability Timescale

To find the observed minimum variability time scale for each GRB, we have used the method utilized by Bhat et al. (2012); Bhat (2013a,b), which searches for a characteristic time scale at which the variance ratios per bin width is minimum. The characteristic time scale is interpreted as an upper limit on the minimum variability time scale. This method incorporates the following steps: first, the time interval of the prompt emission is selected based on T_{90}; then, a background time interval of an equal duration is selected. Both the signal and the background intervals are used to derive differentials, which, in the next step, are used to calculate variances of the signal and the background. The ratios of the variances are calculated for different binnings in the range from 10^{-3} s up to $0.1 \times T_{90}$ using ten logarithmic bins per decade. The bin width at which the variance ratio divided by the bin width obtains its minimum value is interpreted as a minimum observed variability time scale, t_{var}, (e.g., see Figure 1 in Bhat 2013a). The resulting minimum variability time scales for the entire sample are listed in Table 1.

Barnacka, Loeb

[1408.1232]

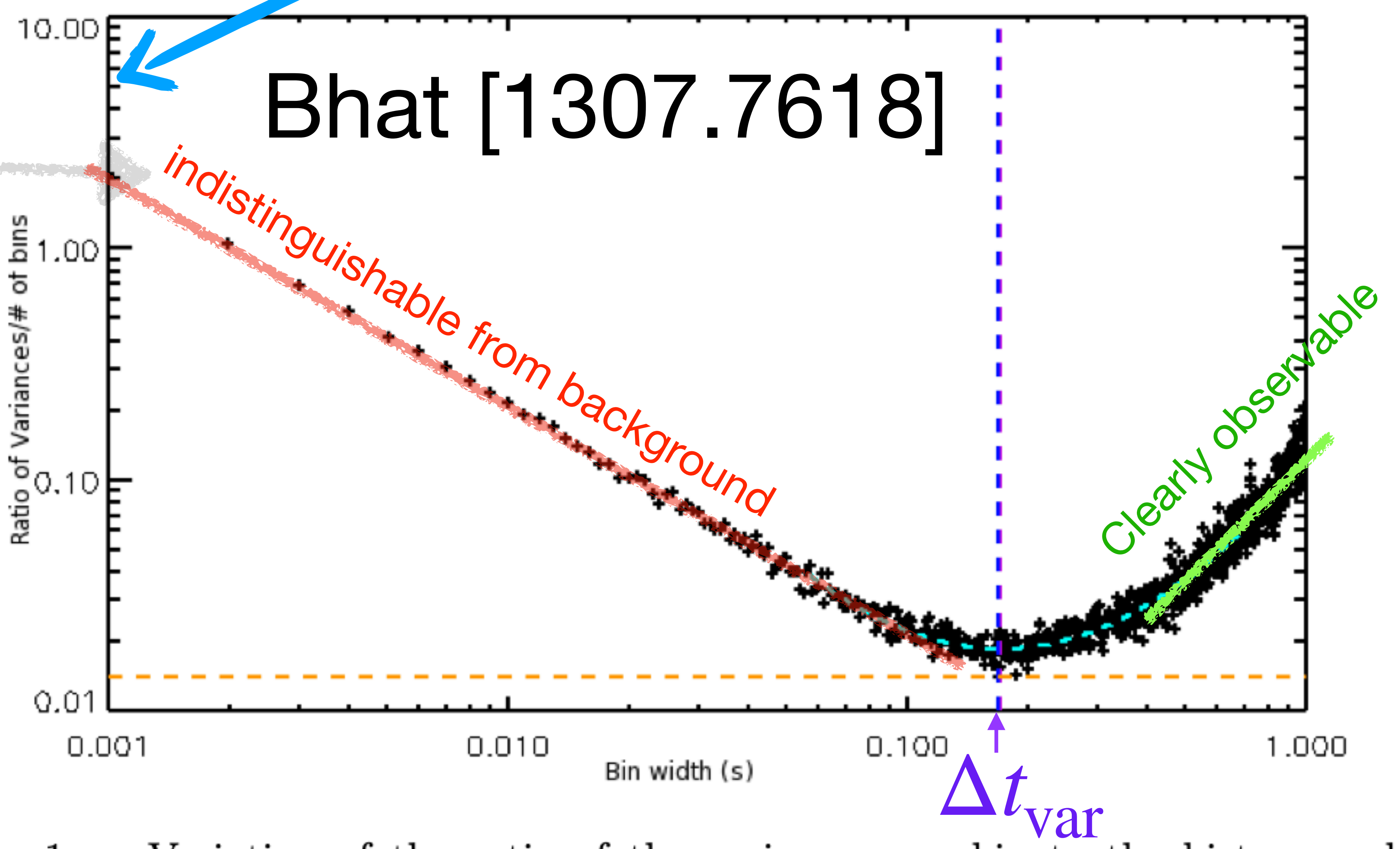

Figure 1: : Variation of the ratio of the variances per bin to the histogram bin-width. At very fine bin-widths the GRB signal is indistinguishable from background fluctuations and hence the ratio decreases monotonically with increasing bin-width. At larger bin-widths the signal is clearly visible from the background and hence the ratio per bin starts increasing. The bin-width at the turn over is defined as the minimum variability time scale where the bin-width is expected to be optimum. Cyan dashed line shows a fitted parabola around the minimum that has a minimum at a bin-width indicated by the vertical dashed line in blue.

Other issues?

Can “stuff” block a line of sight? (random asteroids, etc.)

How do you distinguish a positive signal?

Multiple lensing?

Axion Stars

More Axion Stars from Strings

Marco Gorghetto[a], Edward Hardy[b], and Giovanni Villadoro[c]

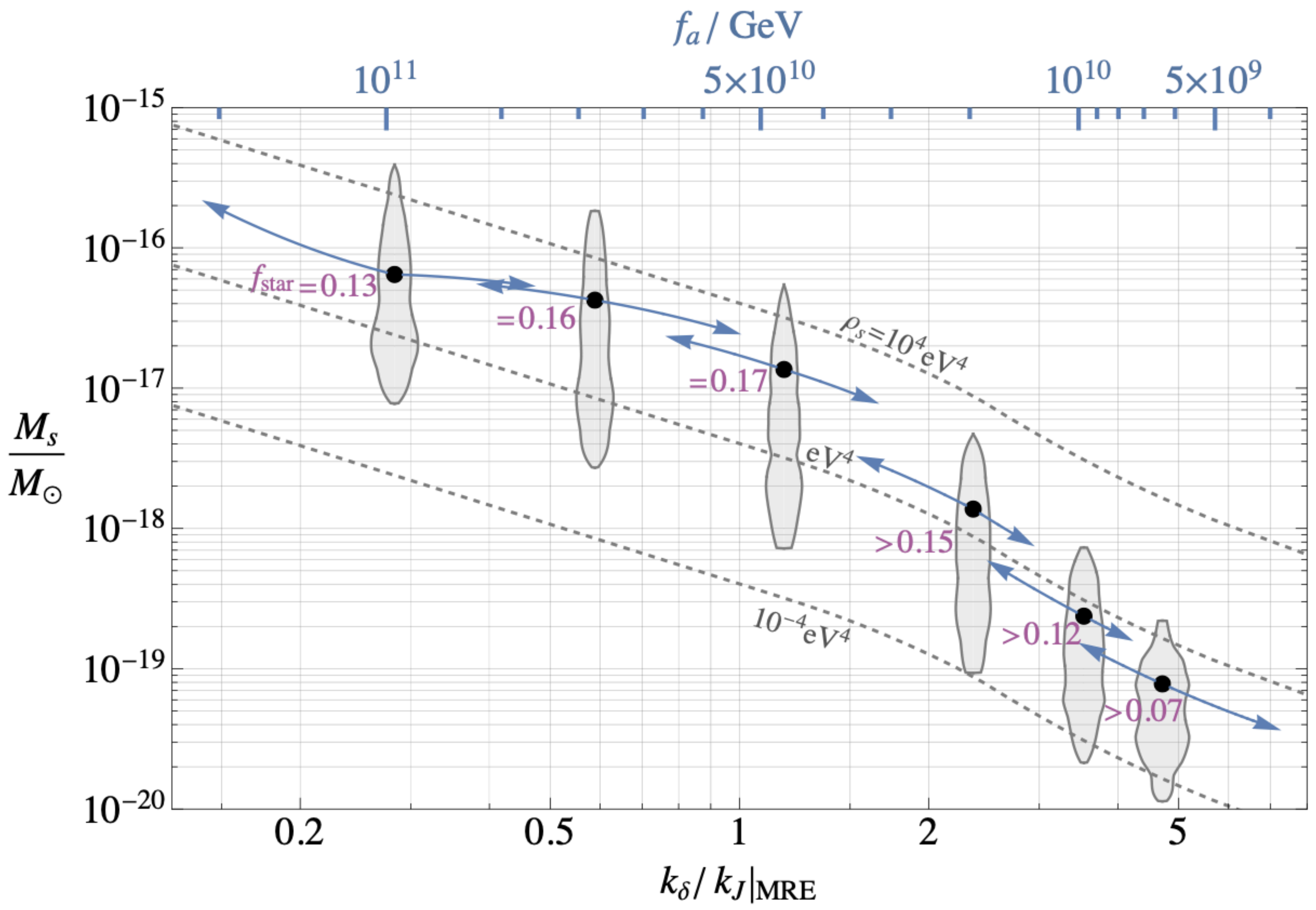

[2405.19389]

See also:
2305.01005
2406.09499